UNIVERSITÀ DEGLI STUDI DI NAPOLI "FEDERICO II"

Ph.D.
in
AGROBIOLOGY AND AGROCHEMISTRY
XXV Cycle

Chemical and biological characterization of phytotoxins produced by *Diplodia* species, fungi involved in forest plants diseases

Ph.D. dissertation by
Marco Masi

Tutor: Prof. Antonio Evidente
Co-tutor: Dr. Alessio Cimmino

2010-2013

TABLE OF CONTENTS

1. INTRODUCTION

1.1. Fungal phytotoxins

The diseases caused by fungal pathogens are one of the major problems for the agricultural production and the natural and forestry heritage. During the last forty years, the interest for these diseases and the associated fungi has assumed great importance due their social and economical impact. For this reason many fungi, isolated from infected plants, were grown *in vitro* in order to study their morphological characteristics, to establish a corrected taxonomic classification and to isolate and identify the phytotoxins produced.

Frequently, the appearance of symptoms and the evolution of the disease, observed at distal parts of the infection sites, suggest the involvement of translocable toxins in the disease process development. The chemical nature of these toxins was found to range from low molecular weight compounds, including all classes of natural products as terpenes, chromanones, butenolides, pyrones, macrolides, aromatic derivatives, aminoacids etc., to high molecular weight compounds such as proteins, glycoproteins and polysaccharides. From the biosynthetic point of view, they derive from the three most common ways of secondary metabolism. In particular, they can be produced by acetate pathway such as fatty acids and polyketides, by shikimato pathway, such as amino acids and aromatic phenylpropanones and by the mevalonate pathway such as terpenoids and steroids. Several studies have been conducted to understand the role of bioactive microbial metabolites in the pathogenesis processes and therefore to use them against specific diseases. As a result, many new phytotoxins, pesticides, fungicides, antibiotics, plant growth regulators, and mycotoxins have been previusly reported (Strobel, 1982; Graniti *et al.*, 1989; Ballio and Graniti, 1991; Tabacchi, 1994; Evidente, 1997; Evidente and Motta, 2001, 2002).

Phytotoxins are defined as microbial metabolites that are harmful to plants at very low concentrations. Most of the plant pathogenic fungi produce toxins *in vitro* culture and in their hosts. Frequently, these compounds play a role in the pathogenesis and produce some or even all of the disease symptoms observed in field. They are able to move from the site of their production to the surrounding tissues or are translocable within the plant vessels. The virulence of the plant pathogens may depend on their capability to synthesize one or more toxins. Only few phytotoxins are known to be host-specific toxins since they are more frequently phytotoxic for a broad range of plant species. In some cases, studies on their mode of action and their role as "*vivo*-toxins" have been also proved to be essential (Strobel, 1982; Graniti *et al.*, 1989; Ballio and Graniti, 1991; Evidente, 1997; Upadhyay and Mukerji, 1997, Evidente and Motta, 2001, 2002).

1.2. Fungi and phytotoxins involved in forest plants diseases

In recent years, numerous studies have been initiated in order to understand what are the microorganisms involved in forestal plants diseases and the role played by phytotoxins produced in the pathogenesis processes. In this field, Prof. Evidente's group studied the fungi and the phytotoxins associated with canker disease of the Italian cypress (*Cupressus sempervirens* L.), pine (*Pinus radiata*) decline, the cork oak (*Quercus suber* L.) decline, and the branch dieback of juniper (*Juniperus phoenicea* L.) which are plant diseases with noteworthy social and economical implications.

1.2.1. Fungi involved in canker disease of cypress (*Cupressus sempervirens* L.)

Cupressus sempervirens L., also known as Italian, Tuscan, or Mediterranean cypress is a species of cypress native to the Eastern Mediterranean region. This coniferous evergreen tree is very long-lived (some trees reported to be over 1000-years-old) but is

susceptible to cypress canker and can suffer extensive dieback where this disease is common. The fungi associated with canker disease of the Italian cypress (*Cupressus sempervirens* L.) and other species of *Cupressus* in the Mediterranean area are belonging to the genera *Diplodia*, *Pestalotiopsis*, *Seiridium* and *Sphaeropsis* (Grasso and Raddi, 1979; Graniti, 1985; Graniti and Frisullo, 1987; Solel *et al.*, 1987; Madar *et al.*, 1989; Madar *et al.*, 1991; Swart and Wingfield, 1991; Swart *et al.*, 1993; Graniti, 1998; Evidente and Motta, 2001; Evidente *et al.*, 2010a).

They are found to induce similar but different forms of canker with heavy loss of cypress plantation as forestry and ornamental heritage with consequent alteration of the typical landscape of some regions of Central Italy and other countries of the Mediterranean basin. The consequence of this disease is also very important for the economical point of view considering the noteworthy loss in the nursery industry and all the economy linked with the use of the precious cypress wood (Graniti, 1985).

Three species of *Seiridium*, namely *S. cardinale*, *S. cupressi* and *S. unicorne*, are associated with the canker diseases of cypress (*Cupressus sempervirens* L.).

The cypress canker caused by the imperfect fungus *S. cardinale* (Wag.) Sutt *et* Gibbs, firstly reported in the U.S.A. (Wagener, 1939), when introduced in Europe (Barthelet and Vinot, 1944) has become the major disease of the Mediterranean cypress and other species of *Cupressaceae*. The most noticeable symptom of *S. cardinale* canker is yellowing or browning of the foliage on one or more top or lateral branches (Photo 1). This discoloration may appear at any time of the year but is most likely to be seen during the spring. Disease development often continues until a considerable portion of the tree is killed. The causal fungus invades cypress and other hosts through wounds on the twigs and branch bases. Lens-shaped cankers on the twigs and branches appear as discolored areas on the bark. Resin often oozes from cracks on the surface of the cankers and flows down the

Photo 1. *Cupressus sempervirens* L. affected by *Seiridum cardinale* canker.

diseased branches or tree trunk. Fruiting bodies of the causal fungus *S. cardinale* appear on the canker face as small black dots (Hansen and Lewis, 1997).

A similar disease caused by strains of *S. cupressi* (Guba) Boesew. and *S. unicorne* Cooke *et* Ellis, although less serious, has spread in Greece (Kos) (Graniti, 1985; Xenopoulos, 1987) and Portugal (Graniti, 1985; Graniti and Frisullo, 1987). However, these fungi and the induced diseases occur in other parts of the world as well.

Diplodia cupressi A.J.L. Phillips & A. Alves (Alves *et al.*, 2006), previously recognized as *Diplodia pinea* f. sp. *cupressi* (syn. of *Sphaeropsis sapinea* f. sp. *cupressi*), *Diplodia mutila* and *Diplodia pinea* in cypress induce symtoms very similar to those produced by the three phytophatogenic *Seiridum* species (Photo 2), (Evidente *et al.*, 2010a). Several studies were carried out to investigate the phytopathogenic process induced by *Seiridium* spp. and *Diplodia* spp. in many *Cupressus* L. species as well as those of different strains of *Diplodia pinea* isolated from infected cypress tree in Italy.

1.2.2. Fungi involved in pine (*Pinus radiata* L.) decline

Pinus L. is the largest and most widespread genus, characteristic of many North temperate regions (except the plains), especially at lower altitudes, and in a few tropical regions, notably on mountain slopes. Pine decline is a complex disease resulting from the interactions of both biotic and abiotic stressors. More common than previously thought, this disease is often misdiagnosed as either little leaf disease or annosus root rot. Affected pines expressing declining symptoms can succumb within two to three years. Pine decline usually exists with trees that are over 35 years of age, but can exist in trees as young as 12-years-old (Langstrom *et al.*, 2001).

In 1998 and 1999 *Diplodia pinea*, also known as *Sphaeropsis sapinea* (Fr.) Dyko & Sutton, was repeatedly isolated in Sardinia from symptomatic samples taken in the upper

Photo 2. *Cupressus sempervirens* L. affected by *Diplodia cupressi* canker.

part of declining *Pinus radiata* L. plants. Observed symptoms mainly consisted of foliage chlorosis, drying of needles and cankers on branches (Photo 3). Following these observations, a monitoring program for *Pinus* spp. plantations in Sardinia, was started and *Diplodia pinea* was grown *in vitro* to evaluate the production of phytotoxic metabolites (Cabras *et al.*, 2006).

1.2.3. Fungi involved in cork oak (*Quercus suber* L.) decline

One of the most destructive of all tree root pathogens, the oomycete fungus *Phytophthora cinnamomi*, is associated with mortality and decline of cork and holm oaks in the Mediterranean region (Brasier, 1996). *P. cinnamomi* is a primary pathogen on a very wide range of trees and woody ornamentals worldwide, but is probably a native of the Papua New Guinea region. It is a soil borne microorganism that requires warm, wet soils to infect roots. Since 1900, it has caused major epidemics on native chestnuts in the United States and Europe, and now threatens the stability of entire forest and heath communities ecosystems in some parts of Australia. Together with drought, it may be a major predisposing factor in the Iberian oak decline (Brasier *et al*., 1993).

While root rot caused by *P. cinnamomi* has been regarded as a major factor in the decline of Iberian oaks, several fungi that cause cankers and diebacks also are considered to be important contributing factors (Luque *et al.*, 2001). The most common and important canker and dieback of the cork oak pathogen (*Quercus suber* L.) is considered to be *Diplodia corticola.* This latter is an endophytic fungus, widespread in Sardinian oak forests previously identified as *Diplodia mutila* Fr. apud Mont. (Franceschini *et al.*, 1999). The fungus can affect plants of different age, inducing symptoms very similar to those produced by tracheomycotic disease. When inoculated on stems of young cork oak plants, *D. corticola* induced a slight collapse and dark brown discoloration of the cortical tissues

Photo 3. *Pinus radiata* L. affected by *Diplodia pinea*.

around the inoculation site, a sudden wilting of the plant above it and subsequently a sprouting of the secondary shoots below it (Franceschini *et al.*, 2002). These symptoms suggested that this fungus produces phytotoxic metabolites (Evidente *et al*., 1997).

Another endophytic fungus involved in cork oak (*Quercus suber* L.) decline widespread in Sardinian oak forests is *Biscogniauxia mediterranea* (De Not.) O. Kuntze (Franceschini *et al*., 2002). This fungus can survive as an endophyte in all of the aerial organs of the oak plants, as well as being able to act as an opportunistic pathogen when the oaks suffer from prolonged periods of stress. The fungus induces discoloration of the woody tissues, dieback and stem and branch cankers, progressing to the appearance of characteristic black carbonaceous stromata on dead organs (Photo 4, Marras *et al*., 1995). These symptoms suggested that the fungus produced phytotoxic metabolites, as also observed for isolates of *Hypoxylon mammatum* (Wahlenberg) Miller, the causal agent of the poplar canker disease (Pinon and Manion, 1991).

1.2.4. Fungi involved in branch dieback of juniper (*Juniperus phoenicea* L.)

Phoenicean juniper (*Juniperus phoenicea* L.) is a typical juniper found throughout the Mediterranean region. In Sardinia (Italy), it grows mostly at low altitudes close to the coast and in particular on the small islands of the La Maddalena Archipelago, including Caprera Island (Camarda and Valsecchi, 2008).

Recently, a progressive dieback of shoots and branches of Phoenicean juniper trees has been observed in a natural area on Caprera Island (Linaldeddu *et al.*, 2011). Infected plants decline branch by branch and eventually die within one to two years. Following removal of the outer bark at the base of symptomatic twigs and branches, brown discoloration of wood and inner bark tissues was observed. Foliage on affected branches

Photo 4. *Quercus suber* L. affected by *Biscogniauxia mediterranea*.

discolors to shades of yellow, reddishbrown and finally brown. Leaves often remained attached for some time after branch death (Photo 5).

The causal agent of this severe outbreak was identified as *Diplodia africana* Damm & Crous by analysis of morphological features and DNA sequences of the Internal Transcribed Spacer (ITS) region and translation elongation factor 1-α gene (Linaldeddu *et al.*, 2011). *D. africana* was originally reported as an agent of wood necrosis on stone fruit trees in South Africa (Damm *et al.*, 2007). The symptoms detected on Phoenicean juniper in Sardinia were similar to those caused by *Diplodia mutila* Fr. on *Juniperus* spp. in the USA (Tisserat *et al.*, 1988; Flynn and Gleason, 1993; Stanosz and Moorman, 1997). However, it has been demonstrated, on the basis of morphological and molecular sequence data, that the juniper canker pathogen found in the USA and referred to as *D. mutila* is a distinct species named *Diplodia cupressi* A.J.L. Phillips & A. Alves (Alves *et al.,* 2006).

Diplodia africana differs from *D. cupressi* in conidia size, colony morphology and radial growth rate. In addition, both ITS and EF1-α sequences data clearly separate *D. africana* from *D. cupressi* and from any other *Diplodia* species. The symptoms caused by *D. cupressi* on *Juniperus* spp. in the USA and those caused by *D. africana* on *J. phoenicea* are similar. This observation and the lack of information on secondary metabolites produced by *D. africana*, suggested the examination of a highly virulent strain of this latter pathogen in order to evaluate its ability to produce *in vitro* phytotoxins potentially involved in the pathogenesis process.

1.2.5. *Seiridium* toxins

As previously described, three species of *Seiridium*, namely *S. cardinale*, *S. cupressi* and *S. unicorne*, are associated with the canker diseases of cypress (*Cupressus sempervirens* L.). Evaluation of the damage caused by strain of *Seiridium* to their host

Photo 5. Branch dieback of juniper (*Juniperus phoenicea* L.).

plant suggests that necrotic toxins are produced in the infected tissues and are possibly involved in the pathogenesis. For this reason, the three *Seiridum* species, isolated from infected plants, were studied to isolate and chemically and biologically characterize the phytotoxins they produce *in vitro.*

From the EtOAc extract of the *in vitro* culture filtrates of all three fungi, seven phytotoxic metabolites have been isolated. These toxins belong to different classes of organic compounds and proved to be four butenolides, named seiridin, *iso*-seiridin, 7'-hydroxyseiridin and 7'-hydroxy-*iso*-seiridin (**1**-**4**, Fig. 1), in addition to three sesquiterpenes, named seiricardines A, B and C (**5**-**7**, Fig. 1). Moreover, specific of *S. cupressi*, a 14-macrolide, named seiricuprolide (**8**, Fig. 1) and one aromatic *ortho*-dialdehyde, identified as cyclopaldic acid (**9**, Fig. 1), have been found. All the above phytotoxins were non-selective and induced symptoms on host plants which were very similar to those observed in naturally infected cypress trees.

The main phytotoxins produced by the three species of *Seiridium*, seiridin and *iso*-seiridin, (**1** and **2**, Fig.1), are disubstitued butenolides, characterized as 3-methyl-4-(6-hydroxyheptyl)-2-(5H)-furanone and its 4-(5-hydroxyheptyl) isomer, respectively (Evidente *et al.*, 1986; Sparapano *et al.*, 1986). **1** and **2** showed phytotoxic activity on host and non-host plants and antibacterial activity on *Pseudomonas* Mig and *Bacillus* Chon (Sparapano *et al.*, 1986).

Being possibly involved in the pathogenesis, the biological activity of these toxins was further investigated. The α,β-unsaturated-γ-lactone and the hydroxy heptyl side chain of seiridin and *iso*-seiridin were modified in order to obtain information on the structure-activity relationship. The effects of each compound on host and non-host plants (toxicity, electrolyte loss and seed germination) and their antimicrobial activity on bacteria were assayed and results showed that the integrity of the α,β-unsaturated-γ-lactone, and the

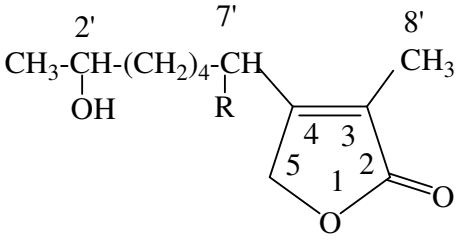

1 R=H; **3** R=OH

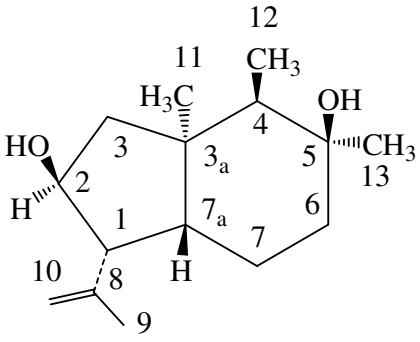

5

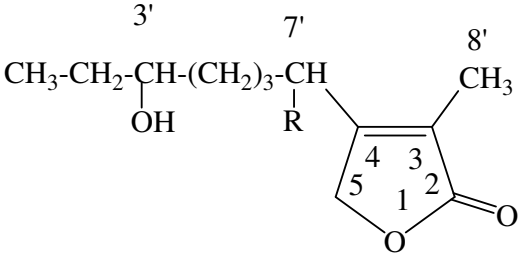

2 R=H; **4** R=OH

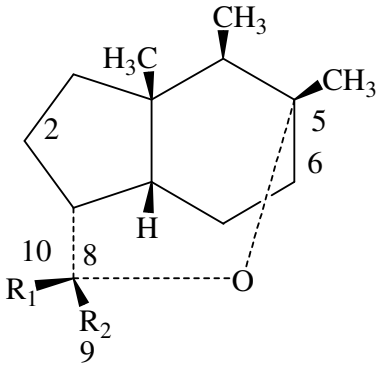

6 R_1=CH_3, R_2=CH_2OH

7 R_1=CH_2OH, R_2=CH_3

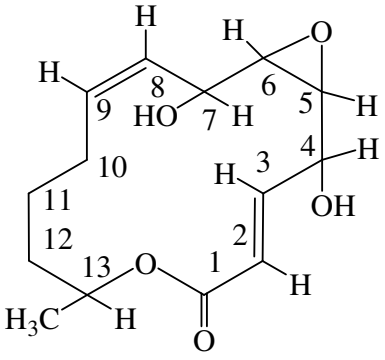

8

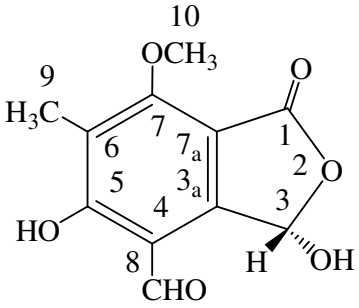

9

Figure 1. Structures of phytotoxins isolated from *Seiridium* spp. culture filtrates.

position and the presence of the hydroxy group in the heptyl side chain are important features for the biological activity of the two butenolides (Sparapano and Evidente, 1995a).

Other two new phytotoxic α,β-unsaturated butenolides, 7'-hydroxyseiridin and 7'-hydroxy-*iso*-seiridin (**3** and **4**, Fig. 1), have been isolated from culture filtrates of the three *Seiridium* spp. They are more polar and structurally related to seiridin and *iso*-seiridin from which differ for the presence of a further hydroxy group on the carbon of the side chain attached at the γ-lactone ring. The two new butenolides compared to **1** and **2** showed a lower phytotoxicity when assayed on host and non-host plants, as expected for the presence of a modified alkyl side chain at C-4 (Evidente and Sparapano, 1994).

From the culture filtrates of the above *Seiridium* species, other three structurally related metabolites, named seiricardines A, B and C (**5**, **6** and **7**, Fig. 1) were isolated (Ballio *et al.*, 1991; Evidente *et al.*, 1993). They were characterized as new cyclic sesquiterpenes containing the octahydro-1H-indene system, a carbon skeleton found in plant and microorganisms, including well known fungal metabolites showing phytotoxic and antifungal activity (Hikino *et al.*, 1966; Cole and Cox, 1981; Manitto, 1981; Turner and Aldridge, 1983). In particular, seiricardine A (**5**, Fig. 1) was identified as octahydro-1-isopropenyl-2,5-dihydroxy-3a,4,5-trimethyl-1H-indene. Seiricardines B and C (**6** and **7**, Fig. 1), proved to be two tricyclic sequiterpenes belonging to the same chemical class of **5**.

5, **6** and **7** showed phytotoxic activity when tested on host and non-host plants and antifungal activity on three test fungi (Ballio *et al.*, 1991; Evidente *et al.*, 1993)

Together with seiridins and seiricardins, a 14-macrolide named seiricuprolide and one aromatic ortho-dialdehyde, named cyclopaldic acid (**8** and **9**, Fig.1), were produced by *S. cupressi* only. Seiricuprolide, a new pentasubstituted 14-macrolide, was isolated in small amount from the culture filtrates of this strain (Ballio *et al.*, 1988; Graniti *et al.*, 1992). As a component of the mixture of fungal metabolites, **8** may contribute to the overall toxic

activity of the pathogen. In fact, macrolides are quite common as naturally occurring substances and some are biologically active (Dean, 1963; Richards and Hendrikson, 1964; Manitto, 1981). When assayed on host and non-host plants, **8** showed phytotoxic activity (Ballio *et al.*, 1988).

Structural investigation on the main phytotoxin produced *in vitro* in relatively high concentration by *S. cupressi* demonstrated that the substance was identical with cyclopaldic acid, an antibiotic known to be a metabolite of some species of *Penicillium*, *Aspergillus* and *Pestalotiopsis* (Achenbach *et al.*, 1982). In fact, the spectral (UV, IR, ^{1}H-NMR and EIMS) and the physical (m.p. and *Rf*) properties of the toxin (**9**, Fig. 1) were in excellent agreement with those reported in the literature for the fungal antibiotic (Achenbach *et al.*, 1982). **9** showed phytotoxic activity when tested on host and non-host plants and antifungal activity towards species of *Botrytis*, *Fusarium* and *Geotrichum*. Therefore, cyclopaldic acid was described as a non-selective fungal phytotoxin for the first time (Graniti *et al.*, 1992).

In order to investigate whether changes in the molecular structure of cyclopaldic acid might effect its biological activity, one structural isomer and six derivatives were prepared and assayed for toxicity on host and non-host plants, and for antifungal activity toward species of *Botrytis*, *Fusarium*, and *Geotrichum*. Toxicity for host and non-host plants of **9** derivatives having one or both aldehydic groups transformed, was less than that of **9**. Isocyclopaldic acid, **9** and, to a lesser extent, the monoacetylated, the phenylhydrazone and the hydrogenated derivatives of **9**, caused loss of electrolytes from cypress tissues. Isocyclopaldic acid, **9** and its monoacetyl derivative caused limited callus development of cypress tissue. Diacetylphenhylhydrazone of **9** enhanced the yield of cypress callus tissue. The antifungal activity showed by **9** toward the above cited species decreased in its derivatives (Sparapano and Evidente, 1995b).

1.2.6. *Diplodia* toxins

Several phytopathogenic fungi belonging to the genus *Diplodia* are involved in severe diseases of forestal trees as the canker disease of the Italian cypress (*Cupressus sempervirens* L.), the pine (*Pinus radiata*) and the cork oak (*Quercus suber* L.) decline. In recent years, these fungi have been extensively studied and many new phytotoxins, belonging to different classes of natural compounds, have been purified and identified from the *in vitro* culture of these pathogens.

1.2.6.1. *Diplodia pinea* toxins

Diplodia pinea (Desmaz.) J. Kickx f., also known as *Sphaeropsis sapinea* (Fr.) Dyko & Sutton, was repeatedly isolated in Sardinia from the upper part of declining *Pinus radiata* plants and in Apulia from infected trees of *Cupressus macrocarpa* and *Cupressus sempervirens* (Evidente *et al.*, 1999; Cabras *et al.*, 2006; Evidente *et al*., 2006a).

Two 5-substituted dihydrofuranones, named sapinofuranones A and B (**10** and **11**, Fig. 2), and a trisubstituted 2,4-pyridione, named sapinopyridione (**12,** Fig. 2) were isolated from liquid cultures of different strains of *Diplodia pinea* showing syntoms of cankers.

Compounds **10** and **11** were characterised, using spectroscopic methods, as two new 4-[(*2Z*,*4E*)-1-hydroxy-2,4-hexadienyl]butan-4-olides, which are epimers at C-5 of the side chain while **12** was characterized as 6-methyl-2-(2-methyl-1-oxobutyl)-1-oxa-5-azaspiro[2.5]oct-6-ene-4,8-dione. The chemical structure of **10** was also confirmed preparing the corresponding 5-*O*-acetyl derivative while the structure of compound **12** was supported by the preparation of three key derivatives (Evidente *et al.*, 1999; Evidente *et al.*, 2006a). The compounds **10** and **11** showed phytotoxicity when assayed on host plants such as cypress and pine trees and non-host plant such as tomato. The compound **12** showed

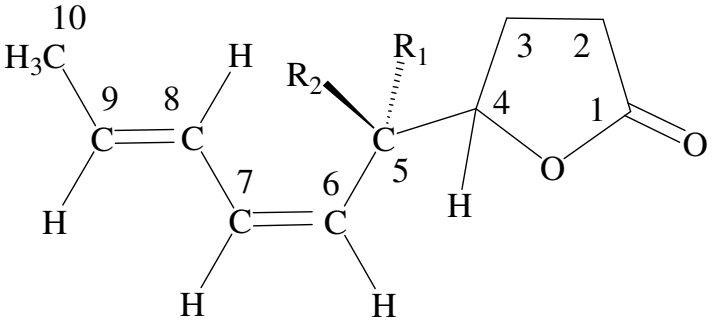

10 R_1=OH, R_2=H

11 R_1=H, R_2=OH

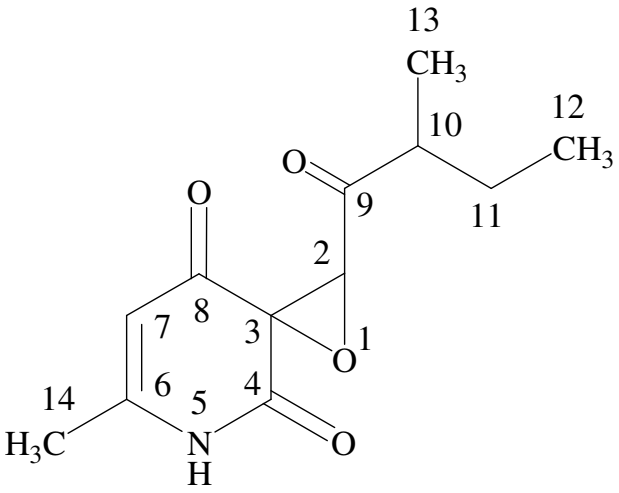

12

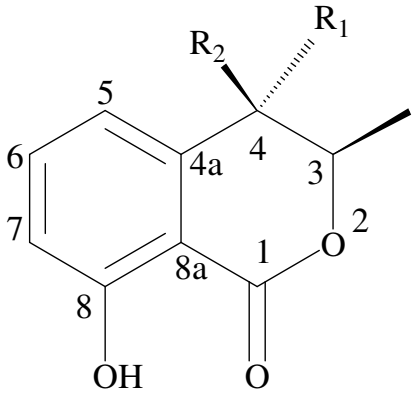

13 R_1=R_2=H

14 R_1=H, R_2=OH

15 R_1=OH, R_2=H

Figure 2. Structures of phytotoxins isolated from *Diplodia pinea* culture filtrates.

phytotoxic and antimycotic activities when tested on host plants and on three *Seiridium* species. The butanolide nature of **10** and **11** is rare in natural products (Turner and Aldridge, 1983). These compounds are closely related to butenolides and tetronic acids, which are well known as plant, fungal and lichen metabolites also exhibiting interesting biological activities (Dean, 1963). Among these, are the 3,4-dialkylbutenolides above cited and isolated from culture filtrates of three species of *Seiridium* spp. (Evidente *et al.*, 1986; Sparapano *et al.*, 1986; Evidente and Sparapano 1994).

Diplodia pinea was also isolated from wood of naturally infected adult plants of *P. radiata* from Sardinia. From the liquid culture of this strain, three metabolites were isolated and identified by their spectroscopic and optical properties as (*R*)-(-)-mellein and (3*R*,4*R*)-(-) and (3*R*,4*S*)-(-)-4-hydroxymellein (**13,** 1**4** and **15**, Fig. 2). Mellein and 4-hydroxymellein are 3,4-dihydroisocoumarins belonging to the family of pentaketide as well as related compounds with different substitution patterns on the phenyl moiety (Garson *et al*., 1984). Considering their relation with the ochratoxins group, potent mycotoxins isolated for the first time from *Aspergillus ochraceus* but also produced by other fungi genera including *Penicillium*, they were named ochracins (Cole and Cox, 1981). Mellein is a widely distributed dihydroisocoumarin derivative in fungi (Turner and Aldridge, 1983). When assayed for phytotoxic and antifungal activities on host and non-host plants and against some phytopathogenic fungi, the *R*-(-)-mellein showed significant activity while the other two 3,4-dihydroisocoumarins showed only a synergetic activity in both tests (Cabras *et al.*, 2006).

Synergistic interactions between secondary metabolites were already observed (Creppy *et al*., 2004; Carpinella *et al*., 2005), although little is known about the mechanisms underlying the synergistic or antagonistic interactions. This is the case of the phytotoxic lipodepsipeptides produced by *Pseudomonas fuscovaginea* in modulation of

plant plasma membrane H^+-ATPase (Batoko *et al*., 1997). Also the two phytotoxins produced by *Fusarium avenaceum* act in synergistic manner to cause necrotic lesions on detached knapweed (*Centurea maculosa*) leaves (Hershernhorn *et al*., 1992) as well as the phytotoxins produced by *Bursaphelenchus xylophilus*, when tested in combination for their toxicity on pine seedlings (Hachiro, 1988).

1.2.6.2. *Diplodia cupressi* toxins

Diplodia cupressi A.J.L Phillips & A. Alves, previously recognized as *Diplodia pinea* f. sp. *cupressi* (syn. *Sphaeropsis sapinea* f. sp. *cupressi*), was isolated from cortical tissues of infected cypress (*Cupressus sempervirens* L.) trees collected in Morocco and Italy (Sparapano *et al.* 2004; Alves *et al.* 2006).

From the *in vitro* cultures of this fungus were isolated six three- and tetra-cyclic unrearranged pimarane diterpenes named sphaeropsidines A-F (**16**, **17**, **18**, **19**, **20** and **21,** respectively, Fig. 3), two dimedone methyl ethers named sphaeropsidone and episphaeropsidone and their chlorinated derivatives named chlorosphaeropsidone and epichlorosphaeropsidone (**22**, **23**, **24** and **25**, respectively, Fig. 4), (Evidente *et al*., 1996, 1997, 1998, 2000, 2002, 2003a).

1.2.6.2.1. Sphaeropsidins A-F

The main toxin isolated from the *in vitro* culture of *D. cupressi*, called sphaeropsidin A (**16**, Fig. 3) and proved to be, by spectroscopic data, a 6α,6β,9α-trihydroxy-7-oxopimara-8(14),15-dien-20-oic acid 6β,20-lactone, was identical to a pimarane diterpenoid antibiotic previously isolated from some *Aspergillus* spp. (Ellestad *et al.*, 1972; Turner and Aldridge, 1983). This secondary metabolite showed phytotoxic activity on host and non-host plants and antimicrobial activities towards twelve fungal species. In

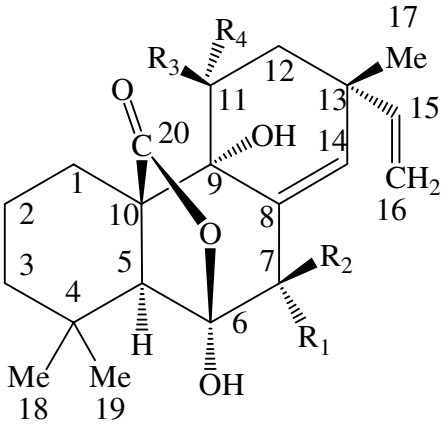

16 $R_1+R_2=O$, $R_3=R_4=H$

18 $R_1=R_3=R_4=H$, $R_2=OH$

19 $R_1+R_2=O$, $R_3=H$, $R_4=OH$

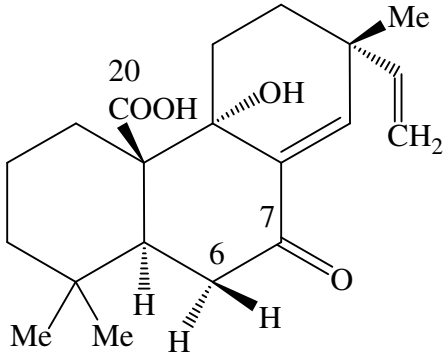

17

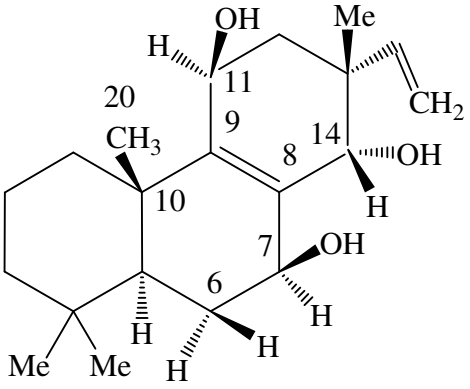

20

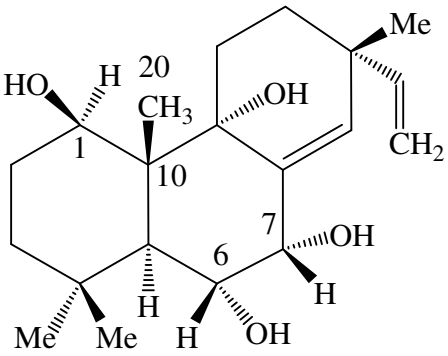

21

Figure 3. Structures of sphaerosidines A-F (**16**-**21**) isolated from *Diplodia cupressi* culture filtrates.

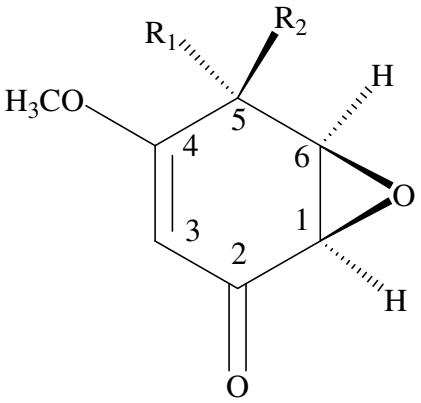

22 R_1=H, R_2=OH

23 R_1=OH, R_2=H

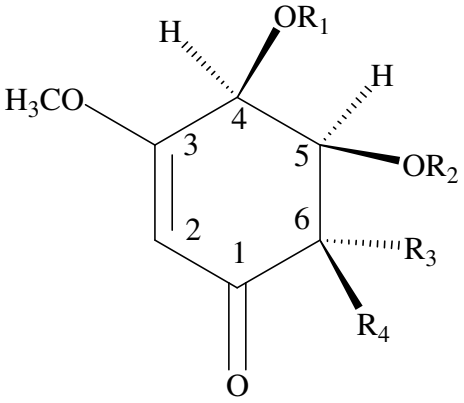

24 R_1=R_2=R_4=H, R_3=Cl

25 R_1=R_2=R_3=H, R_4=Cl

Figure 4. Structures of sphaeropsidones (**22** and **23**) and chlorosphaeropsidones (**24** and **25**) isolated from *Diplodia cupressi* culture filtrates.

particular, the fungistatic activity of sphaeropsidin A against *S. cardinale* and *S. cupress*i, fungi involved in canker disease of cypress as *Diplodia cupressi*, is sufficient to account for the antagonistic action of *Diplodia cupressi* against *Seiridium* species. If sphaeropsidin A is produced *in vivo* by the fungus, it can be postulated that *Diplodia cupressi* spreading along the stem or branches, may prevent the invasion of cortical tissue by *S. cardinal* or *S. cupressi* (Evidente *et al.*, 1996).

Other minor metabolites were found in the organic extract of *D. cupressi* culture filtrates. Two of them called sphaeropsidins B and C (**17** and **18**, Fig. 3), both structurally related to sphaeropsidin A (**16**), were isolated and chemically and biologically characterised. Sphaeropsidin B (**17**) proved to be a 6α,6β,9α,7β-tetrahydroxypimara-8(14),15-dien-20-oic acid 6β,20-lactone, the reduced derivative at C-7 of **16**. Sphaeropsidin C (**18**), characterized as 9α-hydroxy-7-oxopimara-8(14),15-dien-20-oic acid, proved to be a new tricyclic acid pimarane diterpene (Evidente *et al.*, 1997). Sphaeropsidin B (**17**) has been isolated for the first time as a metabolite of *D. cupressi* but previously isolated from *Aspergillus chevalieri* and labeled as LL-S491γ (McCrindle and Overton, 1969).

Assayed on host and non-host plants, like cypress and oak, **17** and **18** showed phytotoxic activity. In the antimicrobial assay, both compounds showed an inhibitory effect on mycelial growth of seven test fungi. These effects of both substances on two cypress pathogens *S. cardinale* and *S. cupressi* (as reported above for sphaeropsidin A) are promising for their potential use in the control of these two fungal pathogens of cypress in order to prevent early infections (Evidente *et al.*, 1997).

The sphaeropsidins A (**16**) and C (**18**) were also purified for the first time from the culture filtrates of *Diplodia mutila*, another fungus involved in the canker disease of *Cupressus sempervirens* L. (Evidente *et al.* 1997).

Another three minor metabolites were further isolated from the liquid culture filtrates of *D. cupressi* and named sphaeropsidines D, E and F (**19**, **20** and **21**, Fig. 3). Sphaeropsidin D (**19**), characterized as a 6α,6β,9α,11α-tetrahydroxy-7-oxopimara-8(14),15-dien-20-oic acid 6β,20-lactone, proved to be structurally related to sphaeropsidin A (**16**). Sphaeropsidin E (**20**) was characterized as a 7α,11β,14α-trihydroxypimara-8(9),15-diene while sphaeropsidin F (**21**) was characterized as a 1β,6α,7α,9α-tetrahydroxypimara-8(14),15-diene. **20** and **21** represent with **18** other fungal metabolites which differ from **16**, **17** and **19** due to the functionalities of the phenanthrene ring system (Evidente *et al.* 1996, 1997 and 2003a; McCrindle and Overton, 1969).

Sensitivity of various cypress to **19** and **20** has proved to be different. Sphaeropsidin D (**19**) showed phytotoxicity when assayed on *C. macrocarpa* while the other two cypress species, *C. sempervirens* and *C. arizonica*, were insensitive to **19**. When sphaeropsidin E (**20**) was assayed on twigs of the same cypress species, no phytotoxicity was recorded. Given the findings of Frisullo *et al.* (1997), who demonstrated that the artificial infection induced by the same strain of *D. cupressi* caused cortical canker and dieback on seedlings of *C. macrocarpa*, *C. sempervirens* and *C. arizonica*, it is possible to assume that the susceptibility of all three species tested did not correspond to their sensitivity to all the toxic metabolites produced by the pathogen (Evidente *et al.*, 2002).

When assayed on host plants, sphaeropsidin F (**21**) caused less severe symptoms compared with those caused by **16**. This confirms that the three cypress species had different grades of sensitivity towards the action of the toxin. As already demonstrated for rings B and C, the modification of the A ring changed the biological activity of the compound (Evidente *et al.*, 2003a). The occurrence of **19**, **20** and **21**, whether or not phytotoxic, may contributes to a better understanding if changes in the molecular structure

of **16** might affect its biological activity on host and non-host plants and its antifungal activity on plant pathogenic microorganisms (Evidente *et al*., 1996 and 1997).

1.2.6.2.2. Sphaeropsidones and chlorospheropsidones

The organic extract of the *in vitro* culture filtrates of *D. cupressi* contained other phytotoxic substances at lower concentration. Two of them appeared to be strictly related compounds more polar than sphaeropsidins, from which they were structurally different.

These compounds were characterized as two new phytotoxic dimedone methyl ethers and therefore named sphaeropsidone and episphaeropsidone (**22** and **23**, Fig.4). They proved to be two disubstituted 7-oxabicyclo[4.1.0]hept-3-en-2-ones, which are epimers at C-5 and closely related to other well known fungal metabolites as terremutin and panepoxydon (Miller, 1968; Fex and Wickberg, 1981), chaloxone, epoxydon, (+)-epiepoxidon and (+)-deoxyepiepoxidon (Nagasawa *et al.*, 1978). When assayed on host and non-host plants **22** and **23** showed phytotoxic activity. In a microbial assay, both compounds showed an inhibitory effect on the growth of five tested fungal species (Evidente *et al.*, 1998).

Besides the six sphaeropsidins A-F (**16**-2**1,** Fig.3), sphaeropsidone and episphaeropsidone (**22** and **23**) identified in the crude oily residue obtained by extraction of the culture filtrates of *D. cupressi*, other two more polar metabolites (**24** and **25**, Fig. 4) were isolated. The preliminary spectroscopic investigation on the two metabolites **24** and **25**, obtained as oily homogeneous compounds, revealed that their structures were closely related to those of the sphaeropsidones. On the basis of the spectroscopic data, they were characterized as two 6-chloro-4,5-dihydroxy-3-methoxycyclohex-2-en-1-ones epimers at C-6 and named chlorosphaeropsidone and epichlorosphaeropsidone (**24** and **25**). They contain a carbon skeleton also found in other closely related fungal metabolites (Miller,

1968; Sakamura *et al.*, 1975; Nagasawa *et al.*, 1978; Fex and Wickberg, 1981; Turner and Aldridge, 1983; Evidente *et al.*, 1998).

When assayed on three species of host *Cupressus* (*C. sempervirens*, *C. macrocarpa* and *C. arizonica*) and on non-host plant (tomato), the two chlorosphaeropsidones (**24** and **25**) showed no significant phytotoxicity in contrast with the marked symptoms induced by sphaeropsidone and episphaeropsidone (**22** and **23**).

The lack of phytotoxic activity by the two metabolites is probably due to the opening of the epoxy ring since it is well known that such ring is an important structural feature for the biological activity of those fungal metabolites that contain this part like some cytochalasins and trichothecens (Cole and Cox, 1981; Vurro *et al.*, 1997). An investigation into the structure-activity relationship of the sphaeropsidones and their derivatives, including the two chlorosphaeropsidones (**24** and **25**) might be a necessary step supporting the above reported observations.

Diplodia cupressi appears to be a good example of a phytopathogenic fungus which produces a number of toxins belonging to different families of natural products. This has already been observed as above reported for *Seiridium* spp., which also infects cypress (Evidente and Motta, 2001).

1.2.6.2.3. Structure-activity relationship studies among sphaeropsidins and some of their derivatives

In order to obtain information on the structure-activity relationship of sphaeropsidins, eight derivatives (**26–33,** Fig. 5) were prepared by chemical transformation of the functionalities present in the sphaeropsidins A, B and C (**16–18**). The aim of this work was to identify which structural features are essential for the biological activities of these

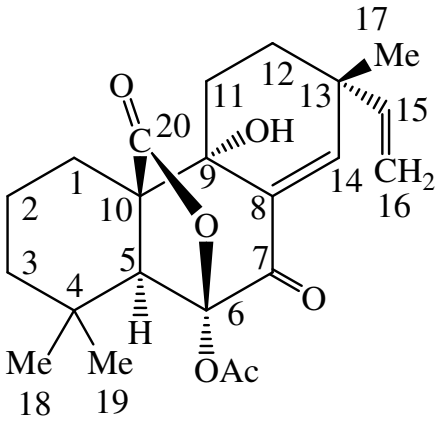

26

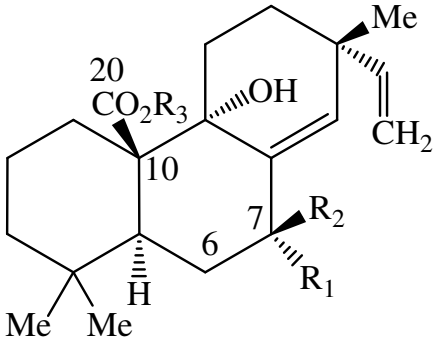

27 R_1=R_3=H, R_2=OH

28 R_1+R_2=O, R_3=Me

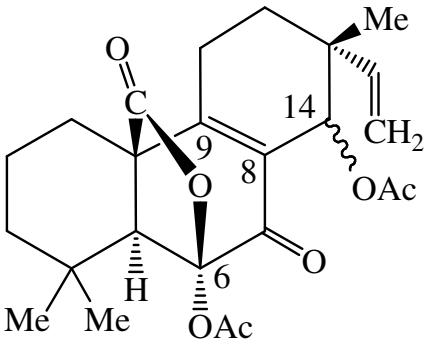

29

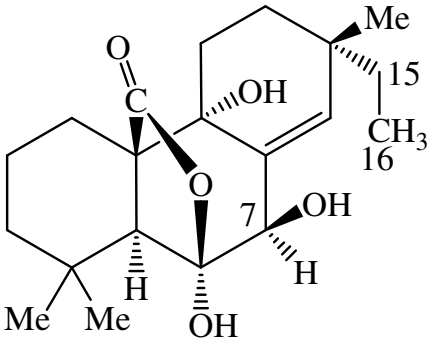

30

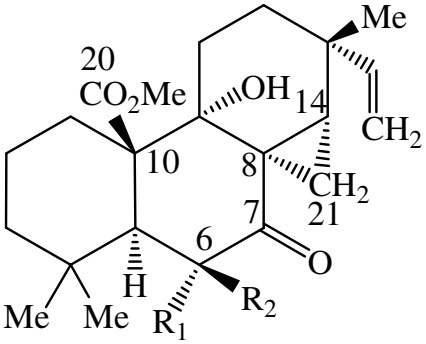

31 R_1+R_2=O

32 R_1=R_2=H

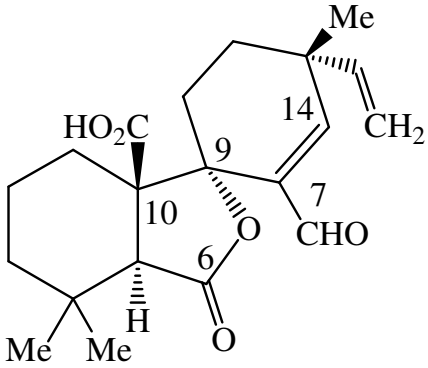

33

Figure 5. Structures of sphaeropsidins (**26**-**33**) derivatives.

compounds, in order to better understand their mechanism of action on plants, role in pathogenesis and potential antimycotic activity.

The phytotoxic and antifungal activity of eight sphaeropsidin derivatives was evaluated in comparison to the sphaeropsidins A (**16**), B (**17**), C (**18**), D (**19**) and E (**20**). Eight key derivatives were obtained by chemical transformations of **16**, **17** and **18.** The structural features of **16** and those of the other naturally-occurring sphaeropsidins **17**, **18**, **19** and **20** provide evidence for considering the latter as naturally modified analogues of **16**. In fact, sphaeropsidin B (**17**) differs from **16** for the presence of a secondary hydroxyl group at C-7 instead of a ketone group, whereas sphaeropsidin C (**18**) differs in the presence of a carboxylic and a methylene group at C-6 and the absence of an hemiketal lactone ring at C-10. Several structural modifications were observed when sphaeropsidins D and E (**19** and **20**) were compared to **16**. Sphaeropsidin D (**19**) showed the hydroxylation of C-11 as the only modification which was already observed in **20**, too. In fact, **20** showed modifications at the C-ring as the hydroxylation of both C-11 and C-14, the dehydroxylation of C-9 and the double bond shift from C(8)-C(14) to C(8)-C(9). Furthermore, **20** lack the hemiketal lactone ring, while a methylene and a methyl group are present at C-6 and C-10, respectively, as well as a secondary hydroxyl group at C-7; some of these structural modifications are already observed in **17** and in **18**.

By acetylation, sphaeropsidin A (**16**) was converted into the corresponding 6,*O*-acetylderivative (**26**, Fig. 5), which showed the modification of the hemiketal hydroxyl group at C-6 of the B-ring. 7,*O*-dihydrosphaeropsidin C (**27**, Fig. 5), was obtained by $NaBH_4$ reduction of **18** (Evidente *et al*., 1996). The methyl ester of sphaeropsidin C (**28**, Fig. 5), was obtained by reaction of **18** with diazomethane. 6-*O*-acetyl-14-*O*-acetyloxy-9-dehydroxy-$\Delta^{8,9}$-derivative **29** (Fig. 5), was obtained by reaction of sphaeropsidin A (**10**) with the Fritz and Schenk reagent (Fritz and Schenk, 1959). This compound showed a

modification of the hemiketal hydroxyl group at C-6 of the B-ring, together with the dehydroxylation at C-9 of the C-ring with the consequent shift of the double bond from C(8)-C(14) to C(8)-C(9) and the acetoxylation at C-14. Furthermore, the catalytic hydrogenation of **16** generated its 7,*O*,15,16-tetrahydroderivative (**30**, Fig. 5), which showed the saturation of the vinyl group at C-13 and the expected reduction of the carbonyl group at C-7 into a secondary hydroxyl group. By reaction with diazomethane, **16** was converted in the methyl ester (**31**, Fig. 5), which showed the opening of the hemiketal lactone producing the carbonyl group at C-6 and the carboxylic group at C-10 with the latter converted into the corresponding methyl ester. Compound **31** also showed, in agreement with literature data (Ellestad *et al.*, 1972) the formation of a cyclopropane ring between C-8 and C-14, due to the addition of the reactive methylene to the double bond previously located there. A cyclopropane ring formation was also observed in the derivative **32**, obtained from sphaeropsidin C (**18**) by reaction with diazomethane (Evidente *et al.*, 1997). This derivative also showed the methyl esterification of the carboxylic group present in sphaeropsidin C (**18**) at C-10 as already noted in **31**. As far as sphaeropsidin C (**18**) is concerned, the two derivatives **28** and **31** lacked the hemiketal lactone ring and displayed the presence of a methylene and a carboxylic group at C-6 and C-10 (which was converted into the corresponding methyl ester), respectively.

Sphaeropsidin B (**17**), in turn, was converted by sodium periodate oxidation into the derivative **33**, which showed marked modification of the B-ring, while the other two rings (A and C) appeared practically unaltered. In particular, the derivative **33** exhibited the opening of hemiketal lactone producing a carboxylic group at C-10, and the cleavage of the C(6)-C(7) bond. The C-6 was oxidized into a carboxylic group, which formed a γ-lactone with the hydroxyl group at C-9, while the carbonyl group at C-7 appeared as a formyl group conjugated with the C(8)-C(14) double bond.

Biological results were above reported in terms of phytotoxicity of sphaeropsidins A-E (**16**-**20,** Fig. 3). Also the sphaeropsidins derivatives (**26**-**33,** Fig. 5) were tested against three species of cypress and two non-host plants (tomato and mung bean). Compound **26** exhibited a phytotoxic activity similar to that given by **16** whereas derivative **27** affected only *C. macrocarpa* and *C. arizonica* and was ineffective on the two herbaceous plants. Derivatives **28**, **29**, **30**, **31**, **32** and **33** were non-toxic. The degree of phytotoxicity elicited by each compound permitted to establish some structure-activity relationships as well as to identify the structural features responsible for the biological activity. The reduction of the carbonyl group at C-7 to a secondary hydroxyl group (**17**) and the semi-reductive opening of the hemiketal lactone ring (**18**), did not reduce the bioactivity of these sphaeropsidins. The hydroxylation of C-11 (**19**) led to partial loss of activity. The dehydroxylation of C-9, which induces the shift of the double bond from C(8)-C(14) to C(8)-C(9) and the hydroxylation at C-14 of the C-ring (**20**), caused the loss of bioactivity. The acetylation of the hemiketal group at C-6 of the B-ring in **26** preserved its bioactivity whereas the reduction of the carbonyl group at C-7 into a secondary hydroxyl group (**27**) caused a complete loss of activity. This may be due to a synergistic effect with the other structural modifications already present in this latter derivative with respect to **16**. The dehydroxylation at C-9 of the C-ring, and the acetoxylation at C-14 together with concomitant acetylation of the hemiketal group at C-6 of the B-ring, caused the complete loss of activity for **29**. Furthermore, a complete loss of activity was observed for the saturation of the vinyl group at C-13 (**30**) or for the conversion of the C(8)-C(14) double bond into the corresponding cyclopropane ring observed in **31**, together with the opening of the hemiketal lactone ring and the consequent methyl esterification of the carboxylic group at C-10. The same structural modification was probably responsible for lacking of toxicity in compound **33**. Finally, it is interesting to note that modification in the B-ring

converted in a γ-lactone (derivative **33**) strongly reduced activity, suggesting that the perhydrophenanthrene arrangement of the carbon skeleton is essential for toxicity (Sparapano *et al.*, 2004).

The antimycotic activity of sphaeropsidins A-E (**16-20**) and their derivatives (**26–33**) was assessed on eight fungal species. The results showed that the activity of all derivatives referred to all tested fungi was lower than that of sphaeropsidins A-D (**16-19**).

On the basis of the results of this study, it can be inferred that the toxicity of **16**, **17**, **18** and **19** was associated with the presence of the double bond between C-8 and C-14 and probably also with that of the tertiary hydroxyl group at C-9. The sphaeropsidins **17**, **18** and **19**, structurally related to **16**, retained these features while sphaeropsidin E (**20**) did not. Moreover, **20** also differed from the other sphaeropsidins in the reduction of the carboxylic group at C-10 to a methyl group (Me-20). Derivatization of sphaeropsidins produced compounds lacking phytotoxic activity and with reduced antifungal activity. Modifications in the vinyl group at C-13 or in the tricyclic pimarane system, particularly in the C-ring, also reduced bioactivity, suggesting that both C-ring functionalities and spatial conformation are essential for activity (Sparapano *et al.*, 2004). Furthermore, the biological activity described previously of sphaeropsidin F (**21**), sucessively isolated from the culture filtrates of *D. cupress*i confirmed these results and also reflected an important role of ring A. Concerning the phytotoxic and antifungal behaviour of sphaeropsidins A-E (**16-20**) and their derivatives (**26–33**), it can be speculated that the integrity of the tricyclic pimarane system, the preservation of the double bond C(8)-C(14), the tertiary hydroxyl group at C-9, the vinyl group at C-13**,** the carboxylic group at C-10 and integrity of the A ring endow these compounds with phytotoxicity to host and non-host plants and with activity against certain plant pathogenic fungi (Sparapano *et al.*, 2004).

The antimycotic activity of sphaeropsidins A-E (**16-20**) may help in the saprophytic survival of sphaeropsidin-producing fungi in their natural habitat, or when they live as parasites within plant tissues. If sphaeropsidins A-E were really produced *in vivo* by the fungus, it is possible to postulate that infective growth of *D. cupressi* along the stem or branches of cypress may prevent the concomitant invasion of the bark by *S. cardinale, S. cupressi* and *S. unicorne.* Actually, the fungistatic activity of **16**-**20** against the *Seiridium* species infecting cypress can support a possible antagonistic action of *D. cupressi* and this result could be applied to prevent early infections of *Seiridium* canker disease of cypress.

1.2.6.2.4. Potential antibacterial activity of sphaeropsidins against several rice bacterial pathogens

While the phytotoxic activity on host and non host plants and the antifungal activity of sphaeropsidins A-F (**16**-**21**, Fig. 3) and some their hemisyntetic derivatives (**26**-**33**, Fig. 5) against phythopathogenic fungi have been extensively studied, no antibacterial activity and only a preliminary anticancer activity hase been reported (Wang et al., 2011).

Sphaeropsidins are structurally related to oryzalexins A-D and momilactones A and B, phytoalexins produced by rice (*Oryza sativa* L.) consequently to the attack of *Pyricularia oryzae,* the causal agent of rice blast disease (Cartwright *et al.*, 1977). They are compounds with potential application in the control of plant diseases (Cartwright *et al.*, 1977; Akatsuka *et al.*, 1983, 1985; Kono *et al.*, 1984). In fact, it has been demonstrated that the phytoalexins had inhibitory activity against spore germination and germ tube of the rice fungal pathogen *P. oryzae* (Cartwright *et al.*, 1977). Studies on the mode of action of oryzalexin D were also carried out (Sekido and Akatsuka, 1987).

Every year, fungal and bacterial diseases cause damage to crops and lead to severe economic losses in rice production. Among the pathogens associated with rice

diseases, *Xanthomonas oryzae* pv. *oryzae (Xoo)* is the causal agent of bacterial blight. This disease is one of the most serious bacterial diseases in many of the rice-growing region of the world together with the bacterial leaf streak induced by *Xanthomonas oryzae* pv. *oryzicola* (Xu *et al.*, 2010). The most common method to control these diseases is the application of bacteriocides and in particular bismerthiazol (Ren *et al.*, 1993; Xue, 2002). However, *Xoo* can develop resistance to this compound, as was observed for streptomycin, the antibiotic introduced for crop protection in 1955 for controlling plant diseases caused by Gram-negative bacteria. Other important bacterial pathogens of rice are *Pseudomonas fuscovaginae* responsible of sheath brown root and grain rot, and *Burkholderia glumae*, the causal agents of sheath rot and seedling rot (Batoko *et al.*, 1997; Shen and Zhou, 2002; Wang *et al.*, 1998). The symptoms induced also depend on the rice growth stage (Ham *et al.*, 2011; Mano and Morisaki, 2008). Currently, there are few control methods available for bacterial rice diseases, including chemical and biological methods and the use of resistant cultivars and lines (Ham *et al.*, 2011).

The use of synthetic agrochemicals in the control of plant microbial pathogens, carries the risk of causing unacceptable environmental damage such as ill effects on soil health, health hazard to humans, toxicity to useful non-target animals and environmental pollution (Roy and Dureja, 1998). The use of natural products could be an alternative way to reduce this risk and consequently the interest on their possible application in biocontrol has recently increased. As the oryzalexins and momilactones, the sphaeropsidins A-F (**16**-**21**) belong to the pimaradiene diterpene group and for this reason might be interesting to investigate the potential antibacterial activity of these phytotoxins against several rice bacterial pathogens and identify which structural features are essential for this biological activity.

1.2.6.3. *Diplodia corticola* toxins

Diplodia corticola anamorph of *Botryosphaeria corticola* Phillips Alves et Luque, previously identified as *Diplodia mutila* Fr. apud Mont., was isolated from stems of infected cork oak (*Q. suber* L.) trees in Sardinia (Evidente *et al.*, 2003b). The organic extract obtained from culture filtrates of *D. corticola* was purified and different phytotoxic compounds were isolated. The main metabolite, named diplopyrone (**34**, Fig. 6), proved to be a 6-(1-hydroxyethyl)-2,4a,6,8a-tetrahydropyran[3,2-*b*]pyran-2-one (Evidente *et al.*, 2003b). Diplopyrone showed phytotoxic activity when assayed on host and non-host plants (Evidente *et al.*, 2003b). Pyran-2-ones (α-pyrones), are a group of naturally occurring compounds which are widely distributed in nature as plant, animal, marine organism and microbial metabolites, most with interesting biological activity (Dean, 1963; Thomson, 1985; Moreno-Monas and Pleixats 1992) and the total synthesis of some of them has been achieved. Other secondary metabolites containing the pyran-2-one moiety are produced by fungi belonging to several genera including *Alternaria*, *Aspergillus*, *Fusarium* and *Trichoderma*, and exhibit antibiotic, antifungal, cytotoxic, neurotoxic, and phytotoxic activities (Dickinson, 1993).

The organic extract obtained from culture filtrates of *D. corticola* was further purified to isolate, beside diplopyrone (**34**), other minor metabolites. In fact, also sphaeropsidins A-C (**16**-**18**) and sapinofuranone B (**11**) were successively isolated (Evidente *et al*., 2006b). These metabolites, as above reported, were already described as fungal phytotoxins produced by *D. cupressi* and *D. pinea* phytopathogenic to cypress (*Cupressus sempervirens* L.) and conifers, respectively. Furthermore, from the same organic extract, the (*S*,*S*)-enantiomer of sapinofuranone B, which was isolated previously from *Acremonium strictum,* a saprophytic fungus commonly found in soil and plant

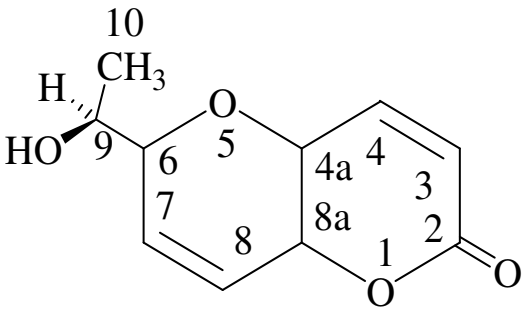

34

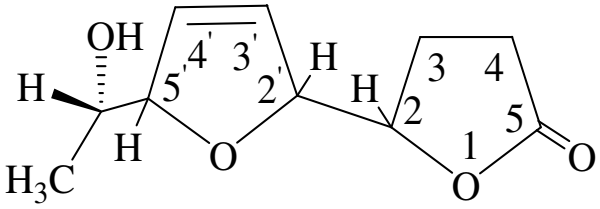

35

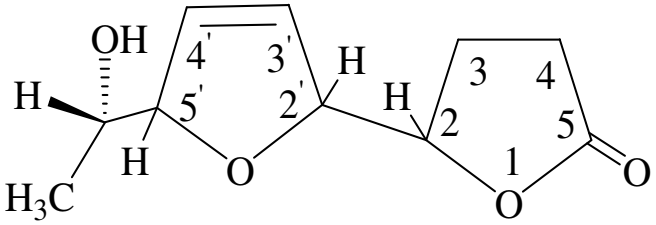

36

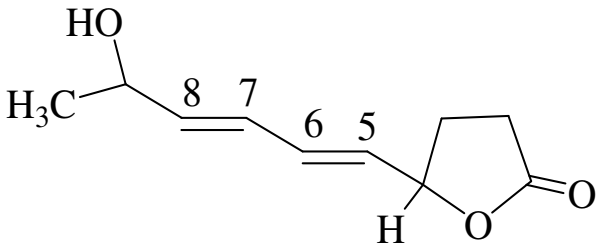

37

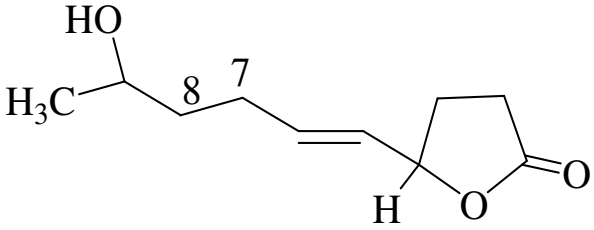

38

Figure 6. Structures of phytotoxins isolated from *Diplodia corticola* culture filtrates.

surfaces (Clough *et al.*, 2000), and (3*S*,4*R*)-*trans*- and (3*R*,4*R*)-*cis*-hydroxymelleins (Aldridge *et al*., 1971; Cole and Cox 1981; Devys and Barbier 1992) were isolated.

Further investigation among the most polar fungal metabolites allowed to isolate other two new metabolites obtained as homogeneous oils, which were named diplobifuranylones A and B (**35** and **36**, Fig. 6) and proved to be two diastereomeric 5'-(1-hydroxyethyl)-3,4,2',5'-tetrahydro-2*H*-[2,2']bifuranyl-5-ones (Evidente *et al.*, 2006b).

Diplobifuranylones A and B, assayed on non-host plants (tomato), showed no signs of phytotoxicity. Lethality tests for the compounds **35** and **36** on larvae of brine shrimps (*Artemia salina*) were run in order to detect potential cytotoxicity on cancer cell line. Both compounds were inactive against *A. salina* even when being sampled at the highest concentration tested (Evidente *et al.*, 2006b). The lack of phytotoxicity observed by testing diplobifuranylones A (**35**) and B (**36**) on non-host tomato plants compared to the strong activity recorded for the structurally related sapinofuranones A and B on host (cypress and pine) and non-host plant (tomato), can be explained by the structural modification of the 1-hydroxy-2,4-hexadienyl side chain at C-4, which in **35** and **36** is converted into a *trans*-and *cis*-2,5-disubstituted-2,5-dihydrofuran ring, while the γ-lactone residues remain unaltered.

Bisfuranoids are a polyketide group of naturally occurring compounds that are broadly distributed in nature essentially as microbial metabolites produced by different fungal species such as *Aspergillus*, *Bipolaris*, *Cercospora*, *Chaetomium*, *Dothistroma*, *Farrowia* and *Monocillium*. Most of these substances showed important biological activities such as aflatoxins (Turner and Aldridge, 1983). These natural compounds have two furan rings joined through one side while bisfuranyls, as **35** and **36** in which the furan rings are joined through a bond, are only known as synthetic compounds (Brown *et al*.,

2000; Behr *et al*., 2004). Diplobifuranylones A (**35**) and B (**36**) represent the first example of monosubstituted natural bifuranyls joined through a bond.

Further purification of the same organic extract yielded two metabolites as homogeneous oils resistant to crystallization, named diplofuranones A and B (**37** and **38**, Fig. 6) and proved to be the 4-[(1*E*,3*E*)-5-hydroxyhexadienyl]butan-4-olide and its corresponding 3,4-dihydro side chain derivative (Evidente *et al.*, 2007) . Diplofuranone A (**37**), when assayed on non-host tomato plants, did not show phytotoxic activity whereas the phytotoxicity of diplofuranone B (**38**) was not assessed due to the lacking of sufficient amount of this fungal metabolite. This inactivity was not surprising as **38**, in respect to the phytotoxic sapinofuranones A and B (**10** and **11**, Fig. 2), had a marked modification of the 1-hydro-2,4-hexadienyl side chain at C-4, which reveals its importance in phytotoxicity.

1.2.7. *Biscogniauxia* toxins

Biscogniauxia mediterranea is one of the fungi involved in the cork oak (*Quercus suber* L.) decline. A strain of *B. mediterranea* was isolated from stems of infected cork oak (*Q. suber*) trees in Sardinia. From the crude oily residue obtained by extraction of the culture filtrates of the fungus, three phytotoxic metabolites were isolated: the previously described 5-methylmellein (**39**, Fig. 7) (Maddau *et al*., 2002), and two other metabolites, the most polar of which was identified by means of its spectroscopic properties as phenylacetic acid (**40**, Fig. 7), a low molecular weight acid, isolated for the first time as a toxic metabolite from this fungus. The third metabolite which is the main toxin was called biscopyran (**41,** Fig. 7) and characterized as a 2-methoxy-1-[7-(2-methoxy-but-2-enoyl)-3,4,5,6-tetramethyl-2H,7H-pyrano[2,3-b]pyran-2-yl]-but-2-en-1-one. When assayed on host and non-host plants, **40** and **41** showed phytotoxic activity (Evidente *et al.*, 2005).

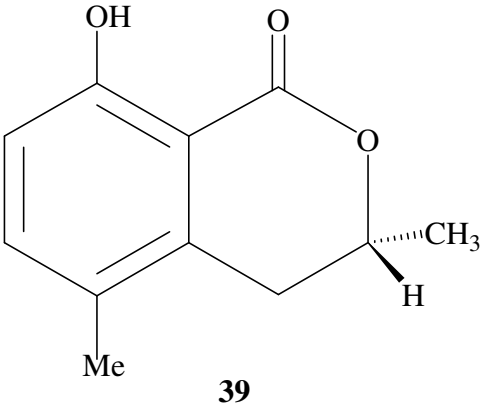

39

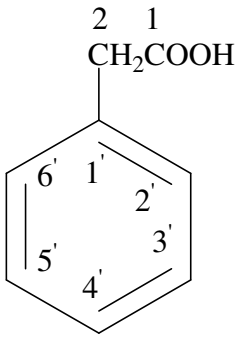

40

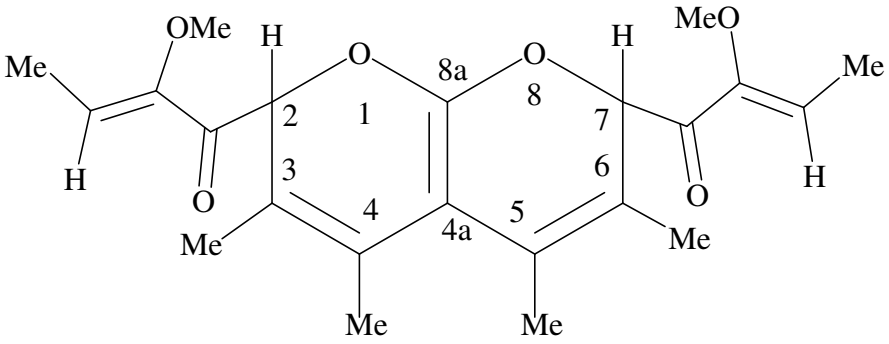

41

Figure 7. Structures of phytotoxins isolated from *Biscogniauxia mediterranea* culture filtrates.

The biscopyran belongs to the family of pyranopyrans, which are well known as synthetic intermediate compounds, but few of them are known as natural compounds (Kozikowski and Lee, 1990; Leeuwenburgh *et al*., 1997; Grotenbreg *et al*., 2004).

Isolation of phenylacetic acid as a phytotoxin was not unexpected since it was previously reported as a fungal phytotoxic metabolite produced by *Rhizoctonia* spp. (Turner and Aldridge, 1983). Furthermore, low molecular weight acids like namely β-nitropropionic (Evidente *et al*., 1992), oxalic (Noyes and Hancock, 1981), fumaric (Mirocha 1961) and 3-methylthiopropionic (Scala *et al*., 1996) acids, were previously described as toxins produced by both phytopathogenic fungi and bacteria.

The isolation of 5-methylmellein from *B. mediterranea* was also not unexpected as this is the most frequent dihydroisocoumarin isolated from Ascomycetes belonging to different genera (see *Entonaema*, *Hypoxylon*, *Xylaria*, *Resillinia*, *Poronia*, *Podosodaria*, *Hycocopra*, *Daldinia*, *Nummularia*, *Kretzschmaria*, *Camillea* and *Penzigia*) of the Xylariaceae family, which have also been shown to produce toxic metabolites with different chemical structures such as cytochalasins, naphthelene derivatives, butyrolactones, succinic acid derivatives, chromanones and diketopiperazines. Several studies have been carried out to use the distribution of such secondary metabolites in conjunction with traditional taxonomic characters in an attempt to develop a better understanding of natural relationships within the family (Anderson and Edwards 1983; Whalley and Edwards, 1995; Stadler *et al*., 2001). Chemical data indicate that there are at least two major divisions within the family and on the basis of production of 5-methylmellein, *B. mediterranea* was grouped together with *Hypoxylon*, *Daldinia*, *Camillea*, *Entonaema* genera (Whalley and Edwards, 1995). Furthermore, the phenylacetic acid and biscopyran are specifically biosynthesized by *B. mediterranea*, and although a

polyketide origin could be hypothesized for biscopyran as for dihydroisocoumarins (Turner and Aldridge 1983), they could be used as exclusive metabolite profiles to recognize the fungus producer.

2. OBJECTIVES

The aim of the present thesis was the chemical and biological characterization of the phytotoxins produced by *Diplodia africana* and *Diplodia cupressi*, two fungi involved in forest plants diseases, in order to understand the role of these metabolites in the phatogenesis process and therefore to use them as natural products with potential applications in agriculture and medicine. The steps proposed to achieve this goal are summarized in the following points:

- Isolation and characterization, using spectroscopic technique and chemical methods, of the phytotoxic metabolites produced *in vitro* by *Diplodia africana*, the causal agent of branch dieback on *Juniperus phoenicea* L.

- Isolation of sphaeropsidones and sphaeropsidins, phytotoxic metabolites produced *in vitro* by the fungus *Diplodia cupressi*, the causal agent of canker disease of cypress in the Mediterranean area.

- Hemisynthesis of some sphaeropsidones derivatives to use in a structure-activity relationship study for the evaluation of their phytotoxic and antifungal activities against five fungal species belonging to the genus *Phytophthora,* destructive pathogens of forest trees and shrubs.

-Hemisynthesis of some sphaeropsidins derivatives to use in a structure-activity relationship study for the evaluation of their antibacterial activity toward *Xantomonas oryzae* pv. *oryzae*, *Burkholderia glumae* and *Pseudomonas fuscovaginae*, three causal agents of severe rice diseases.

3. MATERIALS AND METHODS

3.1. Fungi

The fungal strain of *Diplodia africana* was originally isolated from symptomatic branch of Phoenicean juniper collected from a natural area on Caprera Island (Italy). The fungus was identified on the basis of morphological characters and analysis of Internal Transcribed Spacer (ITS) rDNA and EF1-α gene sequence (Linaldeddu *et al.*, 2011). Pure cultures were maintained on potato-dextrose-agar (PDA, Fluka, Sigma-Aldrich Chemic GmbH, Buchs, Switzerland) and stored at 4°C in the collection of the "Dipartimento di Protezione delle Piante", Università di Sassari, Italy, as DA1. Representative sequences of the isolate DA1 (ITS: accession number JF302648; EF1-α: accession number JN157807) were deposited in GenBank.

Diplodia cupressi strain 261.85 CBS used in this study was purchased from Centraalbureau voor Schimmelcultures of Baarn (Netherland), and deposited in the collection of the "Dipartimento di Protezione delle Piante", Università di Sassari, Sassari, Italy.

3.2. Bacteria

Xanthomonas oryzae pv. *oryzae* XKK.12, was isolated in Kerala, India (Ferluga *et al.*, 2007). *Burkholderia glumae* AU6208, clinical isolate highly virulent to rice, and *Pseudomonas fuscovaginae* UPB0736 were isolated in Madagascar (Devescovi *et al.*, 2007; Mattiuzzo *et al.*, 2011). The three bacterial strains, used in this study, were deposited in the collection of the "International Centre for Genetic Engineering and Biotechnology", Area Science Park, Padriciano, Trieste, Italy.

3.3. General Procedures

Optical rotations were measured in $CHCl_3$ solution on a Jasco P-1010 digital polarimeter. IR spectra were recorded as glassy film on a Perkin-Elmer Spectrum One FT-IR spectrometer and UV spectra was taken in MeCN solution on a Perkin-Elmer Lambda 25 UV/Vis spectrophotometer.

^{1}H- and ^{13}C-NMR spectra were recorded at 600, 400 and 150 MHz, respectively in $CDCl_3$ on Bruker spectrometers unless otherwise noted. The same solvent was used as internal standard. Carbon multiplicities were determined by DEPT (Distortionless Enhancement by Polarization Transfer) spectra (Berger and Braun, 2004). DEPT, COSY-45 (Correlation Spectroscopy), HSQC (Heteronuclear Single Quantum Coherence spectroscopy), HMBC (Heteronuclear Multiple-Bond Vorrelation spectroscopy) and NOESY (Nuclear Overhauser Effect spectroscopy) experiments (Berger and Braun, 2004) were performed using Bruker microprograms. Chemical shifts are in δ (ppm).

Coupling constants (*J*) are in Hertz. The following symbols were used: s: singlet; br s: broad singlet; d: doublet; dd: double doublet; ddd: doublet of double doublet; t: triplet; q: quartet; m: multiplet.

HR EI (High Resolution Electron Impact) and HR ESI MS (High Resolution Electrospray Ionisation Mass Spectroscopy) spectra were recorded at 70 eV on QP 5050 Shimadzu, on Waters Micromass Q-TOF Micro and on Agilent 1100 coupled to a JOEL AccuTOF (JMS-T100LC) instruments, respectively.

Analytical and preparative TLC were performed on silica gel (Merck, Kieselgel 60 F_{254}, 0.25 and 0.50 mm, respectively) or reversed phase (Whatman, KC18 F_{254}, 0.20 mm) plates; the spots were visualized by exposure to UV light or by spraying previously with

10% H_2SO_4 in methanol and then with 5% phosphomolybdic acid in ethanol, followed by heating at 110 °C for 10 min.

Column chromatography was performed with silica gel (Merck, Kieselgel 60, 0.063-0.200 mm).

X-ray data collection was performed at 173 K on a Bruker-Nonius kappa CCD diffractometer equipped with graphite monochromated MoKα radiation (λ = 0.71073 Å, φ scans and ω scans to fill the asymmetric unit).

4. EXPERIMENTAL

4.1. Production, extraction and purification of phytotoxins from *Diplodia africana* culture filtrates

The fungus *Diplodia africana* was grown in 2 l Erlenmeyer flasks containing 400 ml of M1D medium (pH 5.7). Each flask was seeded with 5 ml of a mycelia suspension and then incubated at 25°C for 4 weeks in darkness. The culture filtrates (12 l) were acidified to pH 4 with 2 M HCl and extracted with EtOAc (4 x 3 l), (Scheme 1, Pag. 68). The organic extracts were combined, dried with Na_2SO_4 and evaporated under reduced pressure to give a brown-red oil residue (6.0 g), having a high phytotoxic activity. This latter was chromatographed on a silica gel column eluted with $CHCl_3$-*i*-PrOH (93:7) affording 8 groups of homogeneous fractions, of which groups 3-6 showed phytotoxic activity. The residue (48.5 mg) of group 3 was further purified by preparative TLC eluted with EtOAc-*n*-hexane (6:4) producing six bands. The second and the third of them (8.2 and 7.4 mg, respectively) were independently purified by analytical TLC eluted with $CHCl_3$-*i*-PrOH (97:3) to give afritoxinones A and B (**42** and **43,** Fig. 8, Pag. 70, R_f 0.60 and 0.68, 5.6 and 4.8 mg, respectively) as homogeneous oils. The residue (90.7 mg) of fraction 4 of the first column was further purified by preparative TLC eluted with $CHCl_3$-*i*-PrOH (97:3) to give sphaeropsidin A (**16**, Fig. 3, Pag. 26, R_f 0.35, 4.6 mg) as homogeneous compound and a mixture of fluorescent metabolites. These latter were purified by reversed phase TLC eluted with H_2O-EtOH (6:4) to give *R*-(-)-mellein, (3*R*,4*R*)-4-hydroxymellein and (3*R*,4*S*)-4-hydroxymellein (**13-15**, Fig. 2, Pag. 23, R_f 0.65, 0.70 and 0.75, 4.1, 45.6 and 3.9 mg, respectively) as homogeneous compounds. The residues of fraction 5 and 6 (0.7 g and 1.4 g, respectively) of the same column were combined and further chromatographed on a silica gel column eluted with EtOAc-*n*-

hexane (9:1) affording 5 groups of homogeneous fractions. The residue (298.2 mg) of the fraction 2 gave episphaeropsidone (**23**, Fig. 4, Pag. 27, R_f 0.48) as homogeneous oil. The residue (376.7 mg) of the fraction 3, containing the main metabolite, was further purified by silica gel column to give oxysporone (**44**, Fig. 8, R_f 0.40, 356.7 mg) as homogeneous oil.

4.1.1. Afritoxinone A (42)

Afritoxinone A, obtained as homogeneous oil had: IR ν_{max} 1781, 1660 cm^{-1}; UV λ_{max} nm (log ε) 210 (3.3); ^1H and ^{13}C NMR spectra: see Table 1 (Pag. 78); HR ESIMS (+) *m/z*: 209.1036 [calcd. for $C_8H_{10}KO_4$ 209.1052, M + K]$^+$, 193.0489 [calcd. for $C_8H_{10}NaO_4$ 193.0477, M + Na]$^+$, 171.0657 [calcd. for $C_8H_{11}O_4$ 171.0667, M + H]$^+$.

4.1.2. Afritoxinone B (43)

Afritoxinone B, obtained as homogeneous oil had: IR ν_{max} 1788, 1651 cm^{-1}; UV λ_{max} nm (log ε) 211 (3.26); ^1H and ^{13}C NMR spectra: see Table 1; ESIMS (+) *m/z*: 209 [M + K]$^+$, 193 [M + Na]$^+$, 171 [M + H]$^+$.

4.1.3. Oxysporone (44)

Oxysporone, obtained as homogeneous oil had: $[\alpha]^{25}_D$ +365 (*c* 0.5); IR ν_{max} 3390, 1788, 1651 cm^{-1}; UV λ_{max} nm (log ε) 209 (3.40) (Venkatatasubbaiah *et al.*, 1991): IR^{film} cm^{-1}: 3350 (*br*) 1785 (*s*) (γ-lactone) 1645 (-HC=CH-O-); UV λ_{max} nm (ε): 211 (2000) ^1H and ^{13}C NMR spectra were very similar to those reported in literature (Adegosan and Alo, 1979) except for the assignment in the ^{13}C NMR spectrum of the carbon at C-5 and C-7 at δ 40.6 and 28.1. ESIMS (+) *m/z*: 179 [M + Na]$^+$, 157 [M + H]$^+$.

4.2. Production, extraction and purification of sphaeropsidones and sphaeropsidins A-C from *Diplodia cupressi* culture filtrates

The fungus *Diplodia africana* was grown in 2 l Erlenmeyer flasks containing 400 ml of modified Czapek medium supplemented with 2% corn meal (pH 5.7). Each flask was seeded with 5 ml of a mycelia suspension, and then incubated at 25 °C for 4 weeks in darkness. The culture filtrates (15 l) were acidified and extracted with EtOAc as previously reported (Evidente *et al.*, 1998). The organic extract, obtained as a brown-red oil (9.2 g), having an high phytotoxic activity, was chromatographed on a silica gel column eluted with $CHCl_3$-*i*-PrOH (19:1) affording nine groups of homogeneous fractions (Scheme 2, Pag. 101). The residue of the second fraction (2.4 g) was crystallized from EtOAc-*n*-hexane (1:5) yielding sphaeropsidin A (**16**, Fig. 3, Pag. 26, R_f 0.65, 1.6 g). The residue left from the mother liquors and the residue of the third fraction of the first column were combined (970 mg) and further purified by combination of column chromatography and preparative TLC eluted with $CHCl_3$-*i*-PrOH (9:1) to give a further amount of **16** (300 mg, for a total of 126.6 mg/l), sphaeropsidin B (**17**, Fig. 3, R_f 0.50, 120 mg, 8 mg/l) and sphaeropsidin C (**18**, Fig. 3, R_f 0.43, 63 mg, 4.2 mg/l). The residue (3.6 g) of fractions 4-7 were combined and further purified by silica gel column, eluted with $CHCl_3$-*i*-PrOH (9:1), yielding six groups of homogeneous fractions. The residue of fraction 3 was crystallized from EtOAc-*n*-hexane (1:5) yielding sphaeropsidone (**22**, Fig. 5, Pag. 32, R_f 0.40, 2.3 g, 153.3 mg/l) as white needles. The mother liquors were further purified by silica gel CC, eluted with petroleum ether-acetone (7:3), affording episphaeropsidone (**23**, Fig. 5, R_f 0.53, 725 mg, 48.3 mg/l) as homogeneous oil. The residue (775.5 mg) of fraction 8 from the first column containing two more polar metabolites (R_f 0.21 and 0.14) was purified by silica gel CC, eluted with $CHCl_3$-*i*-PrOH (9:1) to afford five groups of homogeneous fractions. The residues (150 mg and 102.4 mg) of fractions 3 and 4 were independently purified by two

further steps of preparative TLC on silica gel, using $CHCl_3$-*i*-PrOH (9:1) and petroleum ether-acetone (7:3) to give chlorosphaeropsidone and epichlorosphaeropsidone (**24** and **25**, Fig. 5, 80 and 57 mg, 5.3 and 3.8 mg/l, respectively) as homogeneous oils. Sphaeropsidone (**22**, Fig. 5) was than re-crystallized from $CHCl_3$-benzene (1:1) to obtain white crystals suitable for single crystal X-ray analysis.

4.3. X-ray diffraction study of sphaeropsidone

As reported above, white block shaped single crystals of sphaeropsidone **22** were obtained by slow evaporation of $CHCl_3$-benzene solution at room temperature. Cell parameters were obtained from a least-squares fit of the θ angles of 109 reflections in the range $5.235° \leq \theta \leq 20.272°$. A semiempirical absorption correction (multi-scan, SADABS) was applied. The structure was solved by direct methods and anisotropically refined by the full matrix least-squares method on F^2 against all independent measured reflections (SHELXS97 and SHELXL97 programs; Sheldrick, 2008). The positions of hydroxyl H atoms were determined from difference Fourier maps and refined according to a riding model, all other H atoms were placed in calculated positions and allowed to ride on carrier atoms [C-H in the range 0.95 – 1.00 Å ; $U_{iso}(H) = 1.2U_{eq}$ (C methine or aromatic), $U_{iso}(H) = 1.5U_{eq}$(C methyl) of the attached atom]. Crystals resulted twinned by 180° rotation around *a* axis and TWIN 1 0 0 0 -1 0 0 0 -1 instruction of SHELXL97 program was used in the refinement. In the absence of any significant anomalous scattering, the absolute configuration was set by reference to previous studies (Mennucci *et al.*, 2007). The final refinement converged to R1 = 0.0433, wR2 = 0.0821 for 2759 observed reflections having $I > 2\sigma(I)$. Minimum and maximum residual electronic density was –0.170 and 0.159 e/Å^3. Crystal data and structure refinement details are reported in Table 2 (Tuzi *et al.*, 2012).

Crystallographic data for the structure have been deposited with the Cambridge Crystallographic Data Centre as supplementary pubblication number CCDC 794356. These data can be obtained free of charge at www.ccdc.cam.ac.uk/conts/retrieving.html.

4.4. Preparation of sphaeropsidones derivatives

4.4.1. 5-*O*-Acetylsphaeropsidone and 2,4,5-triacetoxyanisole (45 and 46)

To sphaeropsidone (**22**, 21.2 mg), dissolved in pyridine (240 μl) was added under stirring Ac_2O (240 μl). The reaction was carried out at 80° for 30 min. The reaction was stopped by addition of MeOH and evaporation of the mixture by an N_2 stream. The residual crude oil was purified by preparative TLC eluted with EtOAc-*n*-hexane (6:4) to yield both derivative **45** and **46** (Scheme 3, Pag. 112, 7.9 and 11.4 mg, respectively) as homogeneous compounds.

Derivative **45** had: $[\alpha]_D^{25}$ - 20.7 (*c* 0.2); IR ν_{max} 1747, 1668, 1616 cm^{-1}; UV λ_{max} nm (log ε) 251 (3.81); ^{1}H NMR, δ 5.96 (1H, d, *J* = 3.1 Hz, H-5), 5.31 (1H, d, *J* = 1.6 Hz, H-3), 3.77 (1H, dd, *J* = 3.9 and 3.1 Hz, H-6), 3.72 (3H, s, OMe), 3.51 (dd, *J* = 3.9 and 1.6 Hz, H-1), 2.24 (3H, s, MeCO). EIMS (rel. int) *m/z*: 198 $[M]^+$ (10), 156 $[M\text{-}CH_2CO]^+$ (50), 141 $[M\text{-}CH_2CO\text{-}Me]^+$ (17), 127 $[M\text{-}CH_2CO\text{-}HCO]^+$ (75), 113 $[M\text{-}CH_2CO\text{-}Me\text{-}CO]^+$ (24), 111 (88), 69 (100).

Derivative **46** had: IR ν_{max} 1769 cm^{-1}; UV λ_{max} nm (log ε) 277 (3.42), 222 (shoulder); ^{1}H NMR, δ 6.94 and 6.79 (1H each, *s*, H-3 and H-6), 3.80 (3H, s, OMe), 2.29, 2.28 and 2.25 (3H each, s, three MeCO); ^{13}C NMR, δ 168.3, 168.1 and 168.0 (s, three C=O), 149.2 (*s*, C-5), 139.9, 137.0 and 134.8 (s, C-1, C-2, and C-4), 117.8 (d, C-3), 107.4 (d, C-6) 56.3 (q, MeO), 20.5 (q, three MeCO). EIMS (rel. int) *m/z*: 282 $[M]^+$ (34), 267 [M-

Me]$^+$ (10), 240 [M-CH_2CO]$^+$ (54), 198 [M-2xCH_2CO]$^+$ (81), 156 [M-3xCH_2CO]$^+$ (100), 141 [M-3xCH_2CO-Me]$^+$ (94), 127 [M-3xCH_2CO-HCO]$^+$ (28), 113 [M-3xCH_2CO-Me-CO]$^+$ (15), 69 (25), 43 (44).

4.4.2. 5,*O*-Didehydrosphaeropsidone (47)

Sphaeropsidone (**22,** 15.3 mg) was dissolved in dry CH_2Cl_2 (300 µl) and oxidized with MnO_2 (15 mg) under stirring at room temperature. After 1 h the starting compound was completely converted and the reaction stopped by filtration. The residue was washed with a small volume of CH_2Cl_2, which then was evaporated under reduced pressure. The oily residue (12.5 mg) was purified by preparative TLC eluted with $CHCl_3$-*i*-PrOH (9:1) to give the derivative **47** (Scheme 3, Pag. 112) as homogeneous solid (9.3 mg): $[\alpha]_D^{25}$ -94.8 (*c* 0.2); IR ν_{max} 1713, 1668, 1598 cm^{-1}; UV λ_{max} nm (log ε) 291 (3.38), 229 (shoulder). ^{1}H NMR, δ 5.77 (1H, d, *J* = 1.8 Hz, H-3) , 3.86 (1H, d, *J* = 3.6 Hz, H-6), 3.80 (1H, dd, *J* = 3.6 and 1.8 Hz, H-1), 3.78 (3H, s, OMe). ESIMS (+) *m/z*: 193 [M + K]$^+$, 177 [M + Na]$^+$, 155 [M + H]$^+$.

4.4.3. 6-Bromo-4,5-dihydroxy-3-methoxycycloex-2-enone (48)

Sphaeropsidone (**22**, 15 mg) dissolved in dry THF (1.5 ml) was treated with a solution of 0.4 M Li_2NiBr_4 in dry THF (1.5 ml) prepared according to Dawe *et al.*, 1984. The reaction was performed at room temperature with stirring in the dark. After 30 min **22** was completely transformed and the reaction was stopped by addition of phosphate buffer at pH = 7.5 (15 ml). The aqueous solution was extracted with CH_2Cl_2 (3 x 30 ml). The organic extracts were combined, washed with H_2O, dried (Na_2SO_4), and evaporated under reduced pressure to give a crude residue. This latter was purified by preparative TLC eluted with $CHCl_3$-*i*-PrOH (9:1) to give **48** (Scheme 3, Pag. 112) as a homogenous compound (13 mg): $[\alpha]_D^{25}$ + 44.8 (*c* 0.2); IR ν_{max} 3392 1653, 1599 cm^{-1}. UV λ_{max} nm (log

ε) 253 (3.08) nm. ^{1}H NMR, δ 5.46 (1H, s, H-3), 4.74 (1H, d, *J* =3.5 Hz, H-5) , 4.54 (1H, d, *J* = 6.0 Hz, H-1), 4.32 (1H, dd, *J* = 6.0 and 3.5 Hz, H-6), 3.72 (3H, s, OMe). ^{13}C NMR ($CDCl_3$+MeOH-d_4, 1:10 v/v) δ 191.0 (s, C-2), 174.3 (s, C-4), 99.2 (d, C-3), 72.1 (d, C-6), 67.1 (d, C-5), 56.6 (q, OMe), 49.7 (d, C-1). EIMS *m/z*: (%): 238 $[M+2]^+$ (0.4), 236 $[M]^+$ (0.5), 220 $[M+2-H_2O]^+$ (3.9), 218 $[M-H_2O]^+$ (4.2) 156 $[M-HBr]^+$ (13), 139 $[M-HBr-OH]^+$ (83), 114 $[M-HBr-OH-Me]^+$ (100), 86 (29), 58 (64), 43 (72).

4.4.4. 2,*O*-Dihydrosphaeropsidone (49)

Sphaeropsidone (**22**, 30 mg) in MeOH (15 ml) was reduced with $NaBH_4$ (30 mg) under stirring at room temperature for 30 min. The mixture was neutralized with 0.1 M HCl, extracted with CH_2Cl_2 (3 x 30 ml) and dried (Na_2SO_4). The oily residue was purified by preparative TLC eluted with $CHCl_3$-*i*-PrOH (9:1) to give the derivative **49** (Scheme 3, Pag. 112) as a white needles (28.2 mg). Derivative **49** had: $[\alpha]_D^{25}$ + 50.2 (*c* 0.5); IR ν_{max} 3392, 1668 cm^{-1}; UV λ_{max} nm (log ε) < 220. ^{1}H NMR, δ 4.55 (br d, *J* = 11.0 Hz, H-2), 4.50 (br s, H-3), 4.42 (br s, H-5), 3.64 (dd, *J* = 3.5 and 3.1 Hz, H-6), 3.60 (br s, H-1), 3.59 (s, OMe), 2.54 (d, *J* = 4.4 Hz, HO-C(5)), 1.89 (d, *J* = 11 Hz, HO-C(2)). ^{13}C NMR δ 153.0 (s, C-4), 95.0 (d, C-3), 65.6 (d, C-2), 65.0 (d, C-5), 54.9 (each d, C-1 and C-6), 54.8 (s, OMe). ESIMS (+) *m/z*: 197 $[M + K]^+$, 181 $[M + Na]^+$, 159 $[M + H]^+$.

4.4.5. 2,4-Dihydroxy-5-metoxycycloexanone (50)

Sphaeropsidone (**22**, 20 mg), dissolved in MeOH (1.5 ml), was added to a presaturated suspension of Pd (10% on charcoal) in MeOH (1.5 ml). Hydrogenation was carried out at room temperature and atmospheric pressure with continuous stirring. After 2 h, the reaction was stopped by filtration and the clear solution evaporated under an N_2

stream. The residue was purified by preparative TLC eluted with $CHCl_3$-*i*-PrOH (9:1) to yield derivative **50** (Scheme 3, Pag. 112, 8.3 mg) as a homogeneous compound.

Derivative **50** had: $[\alpha]_D^{25}$ + 42 (*c* 0.2); IR ν_{max} 3392, 1709 cm^{-1}; UV λ_{max} nm (log ε) < 220. ^{1}H NMR, δ 4.20 (br s, H-5), 4.04 (br s, H-1), 3.71 (dd, *J* = 4.8 and 4.0 Hz, H-4), 3.42 (3H, *s*, OMe), 2.78 (br d, *J* = 14.5, H-6A), 2.75 (br d, *J* = 14.5 Hz, H-6B), 2.62 (dd, *J* = 14.5 and 4.8 Hz, H-3A), 2.55 (br d, *J* = 14.5 and 4.0 Hz, H-3B). ^{13}C NMR, δ 205.7 (s, C-2), 79.8 (d, C-4), 70.3 (d, C-1), 60.6 (d, C-5), 57.3 (q, OMe), 46.2 (t, C-6), 41.7 (t, C-3). ESIMS (+) *m/z*: 199 $[M + K]^+$, 183 $[M + Na]^+$, 161 $[M + H]^+$.

4.4.6. 5-*O*-Acetylepisphaeropsidone and 4,5,6-triacetoxy-3-methoxycyclohex-2-enone (51 and 52)

To episphaeropsidone (**23,** 50 mg), dissolved in Ac_2O (2.5 ml), was added under stirring NaOAc (50 mg). The reaction was carried out at 80°C for 30 min. The reaction was cooled at room temperature and stopped by addition of H_2O. The mixture was extracted with EtOAc (3 x 20 ml). The organic extracts were combined, dried (Na_2SO_4) and evaporated under vacuum. The residual crude oil was purified by preparative TLC eluted with EtOAc-*n*-hexane (6:4) to yield derivatives **51** and **52** (Scheme 4, Pag. 113, 4.6 and 33.2 mg, respectively) as homogeneous compounds.

Derivative **51** had: $[\alpha]_D^{25}$ - 20.7 (*c* 0.2); IR ν_{max} 1746, 1667, 1621 cm^{-1}; UV λ_{max} nm (log ε) 252 (4.14). ^{1}H NMR, δ: 5.91 (1H, dt, *J* = 1.5 and 0.5 Hz, H-5), 5.36 (1H, d, *J* = 1.5 Hz, H-3), 3.71 (3H, s, OMe), 3.62 (1H, dd, *J* = 3.5 and 1.5 Hz, H-6), 3.44 (ddd, *J* = 3.5, 1.5 and 0.5 Hz, H-1), 2.17 (3H, s, MeCO). ESIMS (+) *m/z*: 237 $[M + K]^+$, 221 $[M + Na]^+$, 199 $[M + H]^+$.

Derivative **52** had: $[\alpha]_D^{25}$ - 40.6 (*c* 0.2); IR ν_{max} 1752, 1681, 1608 cm^{-1}; UV λ_{max} nm (log ε) 289 (3.01), 244 (4.11). ^{1}H NMR, δ 5.91 (dd, *J* = 11.3 and 2.7 Hz, H-6), 5.52 (d,

J = 2.7 Hz, H-5), 5.43 (d, *J* = 11.3, H-1), 5.30 (s, H-3), 3.77 (3H, s, OMe), 2.17, 2.12 and 2.07 (3H each, s, three MeCO); ESIMS (+) *m/z*: 339 $[M+ K]^+$, 323 $[M + Na]^+$, 301 $[M + H]^+$.

4.5. Preparation of sphaeropsidins A-C derivatives

The 6,*O*-acetyl (**26**, Fig. 5, Pag. 32), 7,*O*,15,16-tetrahydro (**30**, Fig. 5), 6-*O*-acetyl-14-acetoxy-9-dehydroxy-$\Delta^{8,9}$ (**29**, Fig. 5) and methyl ester cyclopropyl derivative (**32**, Fig. 5) of sphaeropsidin A (**16**, Fig. 3, Pag. 26), as well as the oxidized derivative of sphaeropsidin B (**33**, Fig. 5) and the methyl ester of sphaeropsdin C (**28**, Fig. 5) were prepared according to the procedures previously reported (Sparapano *et al.*, 2004). The 7-*O*-dihydro derivative (**27**, Fig. 5) of **18** was prepared as previously reported (Evidente *et al.*, 1997).

4.5.1. 7,*O*-Methylen and 7,*O*-methylen-9-*O*-methyl-sphaeropsidin A methyl ester (54 and 53)

An ethereal solution of CH_2N_2 was added to a solution of **16** (150 mg) in MeOH (15 ml) to obtain a persistent yellow colour. The reaction was carried out at room temperature with contineus stirring and was stopped after 24 h by evaporation under an N_2 stream. The crude residue (130 mg) was purified by preparative TLC eluted with *n*-hexane-EtOAc (7:3) to give 100 mg of the 8,14-methylensphaeropsidin A methyl ester (**32,** Fig. 5), and the two new derivatives **53** and **54** (Scheme 5, Pag. 160; 7.4 and 9.6 mg, respectively) as homogeneous compounds.

Derivative **53** had: IR ν_{max} 1730, 1634 cm^{-1}; UV λ_{max} nm (log ε) < 220 nm; ^1H NMR: see Table 3; ESIMS, *m/z*: 425 $[M+K]^+$, 411 $[M+Na]^+$. EIMS *m/z*: (%): 388 $[M]^+$ (1), 374 $[M-CH_2]^+$ (9), 356 $[M-CH_3OH]^+$ (28), 342 $[M-CH_2-CH_3OH]^+$ (13).

Derivative **54**: IR ν_{max}, 3383, 1730, 1633 cm^{-1}; UV λ_{max} nm (log ε) < 220 nm; ^1H NMR: see Table 3; ESIMS, *m/z*: 413 $[M+K]^+$, 397 $[M+Na]^+$, 375 $[M+H]^+$.

4.5.2. 14-Methyl-7,*O*-didehydro-sphaeropsidin B and sphaeropsidin B methyl ester (56 and 55)

An ethereal solution of CH_2N_2 was added to a solution of **17** (20 mg) in MeOH (1.5 ml) to obtain a persistent yellow colour. The reaction was carried out at room temperature with continuous stirring and was stopped after 4 h by evaporation under an N_2 stream. The crude residue (16 mg) was purified by preparative TLC eluted with petroleum ether-Me_2CO (8:2) to give derivative **55** and **56** (Scheme 5, Pag. 160; 8.1 and 6.3 mg, respectively) as homogeneous compounds.

Derivative **55** had: IR ν_{max}, 3461, 1726, 1665 cm^{-1}, UV λ_{max} nm (log ε): 265 (1.72); ^1H NMR: see Table 3 (Pag. 170); ESIMS, *m/z*: 385 $[M+Na]^+$, 363 $[M+H]^+$.

Derivative **56** had: IR ν_{max}, 3445, 1715, 1623 cm^{-1}, UV λ_{max} nm (log ε): 281 (3.20); ^1H NMR: see Table 3 (Pag. 170); ESIMS, *m/z*: 413 $[M+K]^+$, 397 $[M+Na]^+$, 375 $[M+H]^+$.

4.5.3. 15,16-Dihydrosphaeropsidin A (57)

Sphaeropsidin A (**16**, 40 mg) dissolved in MeOH (1.5 ml) was added to a presaturated suspension of PtO_2 in MeOH (1.5 ml). Hydrogenation was carried out at room temperature and atmospheric pressure with continuous stirring. After 15 h, the reaction was stopped by filtration, and the clear solution evaporated under reduced pressure. The residue was purified by preparative TLC eluted with $CHCl_3$-i-PrOH (9:1) to yield 19.8 mg of 7,*O*,15,16-tetrahydrosphaeropsidin A (**30,** Fig. 5 and Scheme 5, Pag. 32 and 160), already described (Sparapano *et al.*, 2004) and 12.5 mg of 15,16-dihydroderivative of sphaeropsidin A (**57,** Scheme 5) obtained as a homogeneous solid.

Derivative **57** had: $[\alpha]_D^{25}$ = +22.1 (*c* 0.2). IR: ν_{max}: 3405, 1733, 1684, 1620 cm^{-1}. UV (MeOH) λ_{max} nm (log ε) 239 (3.58). ^{1}H NMR, δ: 6.84 (1H, br s, H-14), 3.65 (1H, br s, OH), 2.71 (1H, s, H-5), 2.23 (1H, d, *J* = 8.0 Hz, H-1), 1.82–1.35 (9H, m, H-10 , H_2-2, H_2-3, H_2-11, H_2-12), 1.52 and 1.41 (3H each, s, Me-18 and Me-19), 1.36 (2H, q, *J* = 7.5 Hz, H_2-15), 1.19 (3H, s, Me-17), 0.88 (3H, t, *J* = 6.8 Hz, Me-16). ESIMS (positive) *m/z*: 387 $[M+K]^+$, 371$[M+Na]^+$, 349 $[M+H]^+$.

4.5.4. 7-*O*-Acetyl-7,*O*,15,16-tetrahydrosphaeropsidin A (58)

To 7,*O*,15,16-tetraydrosphaeropsidin A (**30**, Fig. 5, Pag. 32, 15.6 mg) dissolved in pyridine (200 µl) Ac_2O (200 µl) was added under stirring. The reaction was carried out at 25 °C for 3 h and then stopped by the addition of MeOH and evaporation of the mixture by a N_2 stream. The residual crude oil was purified by preparative TLC eluted with petroleum ether-EtOAc (8:2), to yield derivative **58** (Scheme 5, Pag. 160, 10 mg) as an homogeneous solid.

Derivative **58** had: $[\alpha]_D^{25}$ = + 41.8 (*c* 0.2). IR: ν_{max}: 3444, 1737 cm^{-1}. UV λ_{max} nm (log ε) < 220. ^{1}H NMR, δ: 5.54 (1H, d, *J* = 1.6, H-14), 5.24 (1H, br s, H-7), 3.86 (1H, br s, OH), 2.66 (1H, s, H-5), 2.12 (1H, br d, *J* = 7.8, H-1), 2.28 (3H, s, MeCO), 1.92 (1H, td, *J* = 14.3 and 3.8 Hz, H-12), 1.62 (1H, dt, J = 14.3 and 3.8 Hz, H-12'), 1.57 –1.26 (5H, m, H-10, H_2-2, H_2-3) 1.36 (2H, q, *J* = 7.5 Hz, H_2-15), 1.28 (1H, br d, *J* = 8.4 Hz, H-11), 0.88 (1H, m, H-11'), 1.19 (3H, s, Me-18), 1.12 (3H, s, Me-19), 0.86 (3H, s, Me-17), 0.79 (3H, t, *J* = 7.5 Hz, Me-16). ESIMS (positive) *m/z*: 431$[M+K]^+$, 415 $[M+Na]^+$, 393 $[M+H]^+$.

4.5.5. 7-*O*-Acetylsphaeropsidin B (59)

To sphaeropsidin B (**17,** Fig. 3, Pag. 26,10 mg) dissolved in pyridine (100 µl) Ac_2O (100 µl) was added under stirring. The reaction was carried out at 25 °C for 4 h and was

stopped by the addition of MeOH and evaporation of the mixture by a N_2 stream. The residual crude oil was purified by preparative TLC eluted with petroleum ether-EtOAc (8:2)) to yield derivative **59** (Scheme 5, Pag. 160, 8.2 mg) as a homogeneous solid.

Derivative **59** had: $[\alpha]_D^{25}$ = +72.5 (*c* 0.2). IR: ν_{max}: 3413, 1749, 1713, 1626 cm^{-1}. UV λ_{max} nm (log ε) < 220 nm; ^{1}H NMR, δ: 5.77 (1H, dd, *J* = 17.5 and 10.5 Hz, H-15), 5.55 (1H, s, H-7), 5.35 (1H, br s, H-14), 4.96 (1H, dd, *J* = 10.5, 1.5 Hz, H-16), 4.93 (1H, dd *J* = 17.5 and 1.5 Hz, H-16'), 3.63 (1H, br s, OH), 2.71 (1H, s, H-5), 2.27 (3H, s, MeCO), 2.14 (1H, br d, *J* = 8.0 Hz, H-1), 2.00 (1H, td, *J* = 14.1 and 3.8 Hz, H-12), 1.69 (1H, dt, *J* = 14.1 and 3.8 Hz, H-12'), 1.66–1.15 (7H, m, H-10, H_2-2, H_2-3 and H_2-11), 1.18 (3H, s, Me-18), 1.12 (3H, s, Me-19), 0.97 (3H, s, Me-17). ESIMS (positive) *m/z*: 429 $[M+K]^+$, 413 $[M+Na]^+$, 391 $[M+H]^+$.

4.6. Biological assays

4.6.1. Leaf puncture assays of afritoxinones A and B and oxysporone

Tomato (*Lycopersicon esculentum* L. var. Marmande), holm oak (*Quercus ilex* L.) and cork oak (*Q. suber* L.) leaves were utilized for this assay. Afritoxinones A and B and oxysporone (**42**-**44**, Fig. 8, Pag. 70) were dissolved in MeOH and then brought up to the assay concentrations with distilled water (the final content of MeOH was 4%). Each compound was assayed at 1.0, 0.5, 0.25 and 0.1 mg/ml. The test solutions (20 µl) were applied on the axial side of leaves that had previously been needle punctured. Droplets (20 µl) of MeOH in distilled water (4%) were applied on leaves as control. Each treatment was repeated three times. The leaves were then kept in a moist chamber to prevent the droplets from drying. Leaves were observed daily and scored for symptoms after 1 week. The effect of the toxins on the leaves, consisting in necrotic spots surrounding the puncture, were

observed up to 21 days. Lesions were estimated using APS Assess 2.0 software (Lamari, 2002) following the tutorials in the user's manual. The lesion size was expressed in mm^2.

4.6.2. Plant cutting assays of afritoxinones A and B and oxysporone

Afritoxinones A and B and oxysporone (**42-44**, Fig.8, Pag. 70) were tested for phytotoxicity using excised twigs of *Juniperus phoenicea* L. For the experiments, the apical part of the twigs, approximately 10 cm long, were used. The cuttings were taken from 3-year-old seedlings of *Juniperus phoenicea* L. grown in the greenhouse at 25°C. Pure substance were assayed at 0.2, 0.1 and 0.05 mg/ml. The toxicity of these solutions was evaluated by placing the test plant parts in the assay solution (2 ml) and then transferring them to distilled water. Symptoms were visually evaluated up to 30 days.

The phytotoxicity of compounds (**42-44**) was also tested on tomato cuttings taken from 21-day-old seedlings. Cuttings were placed in the test solutions (3 ml) for 48 h and then transferred to distilled water. The substances were assayed at 0.2, 0.1 and 0.05 mg/ml. Symptoms were visually evaluated up to 7 days.

4.6.3. Leaf puncture assays of sphaeropsidones and their derivatives

Tomato (*Lycopersicon esculentum* L. var. Marmande), young cork oak (*Quercus suber*), holm oak (*Q. ilex* L.), and red oak (*Q. rubra* L.) leaves were utilized for this assay. The compounds **22**-**25** (Fig. 4, Pag. 27) and **45**-**52** (Scheme 3 and 4, Pag. 112 and 113) were dissolved in MeOH and then brought up to the assay concentrations with distilled H_2O (the final content of MeOH was 4%). Each compound was assayed at 0.4 mg/ml. The test solutions (20 µl) were applied on the axial side of leaves that had previously been needle punctured. Droplets (20 µl) of MeOH in distilled H_2O (4%) were applied on leaves as control. Each treatment was repeated three times. The leaves were then kept in a moist

chamber to prevent the droplets from drying. Leaves were observed daily and scored for symptoms after 1 week The effect of the toxins on the leaves, consisting in necrotic spots surrounding the puncture, were observed up to 15 days.

4.6.4. Tomato cutting assays of sphaeropsidones and their derivatives

The compounds **22**-**25** (Fig. 4) and **45**-**52** (Scheme 3 and 4) were assayed at four different concentration (0.1, 0.05, 0.025 and 0.01 mg/ml) on tomato cuttings taken from 21-day-old seedling. Cuttings were placed in the test solutions (3 ml) for 48 h and then transferred to distilled water. Symptoms were visually evaluated up to 7 days.

4.6.5. Antifungal assays of sphaeropsidones and their derivatives

Sphaeropsidones (**22**-**23,** Fig. 4), their natural analogues **24** and **25** (Fig. 4) and derivatives **45**-**52** (Scheme 3 and 4) were tested on five fungal species, listed in Table 4, belonging to the genus *Phytophthora* to evaluate their antifungal properties. The antifungal activity was evaluated on carrot-agar (CA) as inhibition of the mycelial radial growth. In brief, mycelial plugs (6-mm diameter) were cut from the margin of actively growing 4-day old colonies using a flamed cork borer. One plug was placed in the center of a 9-cm diameter Petri dish with the mycelia in contact with the medium. Twenty µl of the test solution at a concentration of 200 µg/plug was applied on top of each plug. As required, highly toxic compounds were tested again at concentrations of 100 and 50 µg/plug. The controls were obtained by applying 20 µl of MeOH. The solvent was evaporated in a laminar flow cabinet and the plates were incubated at 20 °C for 4-7 days depending on the fungal species. The antifungal activity of the compounds was also compared with metalaxyl-M (mefenoxam; p.a. 43.88%; Syngenta), a synthetic fungicide to which the oomycetes are sensitive. Colony diameters were measured in two perpendicular directions

for all treatments. Each treatment consisted of three replicates and the experiment was repeated twice.

4.6.6. Antibacterial assays of sphaeropsidins and their derivatives

Sphaeropsidin A, its natural analogues sphaeropsidins B and C (**16**-**18**, Fig. 3, Pag. 26) and their derivatives (**26-30** and **32-33**, Fig. 5, Pag. 32; **53-58**, Scheme 5, Pag. 160) were tested, at a concentration range of 0.5-6.0 10^{-3} M against three major bacterial pathogens of rice, *Xanthomonas oryzae* pv. *oryzae* XKK.12, *Burkholderia glumae* AU6208 and *Pseudomonas fuscovaginae* UPB0736. The bacterial isolates, were grown overnight at 30°C in PY, King's Medium, and Luria-Bertani (LB) media, respectively (King *et al.*, 1954; Ferluga *et al.*, 2007). Each culture was mixed with PSA, KB, and LB top agar (0.75% w/v agar) at 45°C, respectively, with a ratio of 50 µl of culture and 10 ml on top agar, and poured on top of LB Petri dishes. One hundred µl wells were obtained on Petri dishes by using part of plastic tips put on the LB agar before pouring the top agar. As soon as the top agar was solidified, 25 or 100 µg of different compounds were pipetted into the wells. The negative control was represented by 50 µl of DMSO, as this solvent was used to re-suspend the compounds. The Petri dishes were incubated at 30°C for 1-2 days or until the growth in the top agar was evident. The inhibition of growth around the wells was measured in mm. The effect of sphaeropsidins and their derivatives on growth of *Xanthomonas oryzae* pv *oryzae* was estimated also in liquid cultures, measuring both the optical density at 600 nm and the colony forming units per ml (CFU/ml) of cultures grown with and without the different compounds. Ten ml of PY medium with and without the addition of 50 µg/ml (0.5-1.5 10^{-4} M) of different compounds was inoculated with an overnight culture of *Xoo* at a dilution rate estimated to give an initial OD_{600} of 0.4. Samples were taken after 6 and 24 h from the inoculation and the OD_{600} and CFU/ml were

measured. The experiments were repeated three times and the standard deviation calculated. In order to estimate the bactericidal activity of compound **16**, 100 µl of culture at time 0 and after 24 h were taken, washed twice with medium PY, and plated at different dilution rate to measure the CFU/ml.

4.6.7. Anticancer assays of sphaeropsidins and their derivatives

The natural sphaeropsidins A-C (**16**-**18**) and the hemisynthetic derivatives (**26**-**30**, **32**-**33** and **53**-**59**, Fig. 5 and Scheme 5, respectively) were assayed for their *in vitro* anticancer activities against five human and one mouse cancer cell lines.

4.6.7.1. Determining the IC_{50} *in vitro* growth-inhibitory concentrations

The overall growth level of the cancer cell lines was determined using the colorimetric MTT (3-[4,5-dimethylthiazol-2yl])-diphenyl tetrazolium bromide) assay, as previously detailed (van Goietsenoven *et al.*, 2010). The assessment of cell population growth by means of the MTT colorimetric assay is based on the ability of living cells to reduce the yellow product MTT to a blue product, formazan, by a reduction reaction that occurs in the mitochondria. The number of living cells after 72 h of culture in the presence (or absence: control) of the various compounds is directly proportional to the intensity of the blue, which is quantitatively measured by spectrophotometry (Biorad Model 680XR) at a 570 nm wavelength (with a reference of 630 nm). Each experiment was carried out in six replicates. The cell lines were incubated for 24 h in 96-microwell plates (at a concentration of 10,000 to 40,000 cells/ml culture medium depending on the cell type) to ensure adequate plating prior to cell growth determination. The cells were cultured in RPMI media supplemented with 10% heat-inactivated fetal calf serum. All culture media were supplemented with 4 mM glutamine, 100 µg/ml gentamicin, and penicillin-streptomycin (200 U/ml and 200 µg/ml). Five human and one

mouse cancer cell lines were used. The five human cancer cell lines include the OE21 esophageal cancer (obtained from the European Collection of Cell Culture (ECACC) code 96062201), the A549 non-small-cell lung cancer (obtained from the Deutsche Sammlung von Mikroorganismen und Zellkulturen (DSMZ) code ACC107), the SKMEL-28 melanoma (obtained from the American Type Culture Collection (ATCC) code HTB-72), the Hs683 oligodendroglioma (obtained from ATCC code HTB-138) and the U373 glioblastoma (obtained from ECACC code 89081403) cell lines, whereas the mouse cancer cell line relates to the B16F10 melanoma (obtained from the ATCC code CRL-6475). The positive control includes cisplatin, carboplatin, VP16 (etoposide) and temozolomide.

4.6.7.2. Videomicroscopy

The effects of **16** on cell morphology, proliferation and death have been evaluated by means of videomicroscopy as detailed elsewere (Delbrouck *et al*., 2002). The experiment was conducted once in triplicate with the human SKMEL-28 and mouse B16F10 melanoma cell lines. The compound has been applied at 0 h for a 72 h period of observation at its IC_{50} concentration determined by the colorimetric MTT experiment 1, i.e. 7 μM in the SKMEL-28 and 3 μM in the B16F10 cells, respectively.

5. RESULTS AND DISCUSSION

5.1. Purification and chemical characterization of phytotoxins from *Diplodia africana* culture filtrates

The fungus *Diplodia africana* was identified as the causal agent of a progressive dieback of shoots and branches of Phoenicean juniper (*Juniperus phoenicea* L.) in Sardinia. The lack of information on secondary metabolites produced by *D. africana*, suggested the examination of a highly virulent strain of this latter pathogen in order to evaluate its ability to produce *in vitro* phytotoxins potentially involved in the pathogenesis process. For this reason the fungus was grown in liquid cultures and the organic extract, showing a high phytotoxic activity was purified by a combination of CC and TLC (normal and reverse phase) as detailed in the Experimental section (Scheme 1). The main metabolites (29.7 and 24.8 mg/l, respectively) were isolated from the most polar fraction and identified as episphaeropsidone (**23**, Fig. 4, Pag. 27) and oxysporone (**44**, Fig. 8, Pag. 70). The spectroscopic (^{1}H and ^{13}C NMR and ESIMS) and physical ($[\alpha]_D^{25}$) data of episphaeropsidone (**23**, Fig. 4) were identical to those previously reported (Evidente *et al.*, 1998). Also oxysporone (**44**, Fig. 8) is a known fungal phytotoxin and its ^{1}H-NMR (Fig. 9) as well as the other spectroscopic (^{13}C NMR and ESIMS) and physical ($[\alpha]_D^{25}$) data were identical to those previously reported (Adesogan and Alo, 1979; Nagata and Ando, 1989; Venkatassubbaiah *et al.*, 1991). High resolution NMR spectra allowed the reassignment of the ^{13}C-NMR (Fig. 10) chemical shifts at C-5 and C-7 of **44** which must be practically reversed and now proposed at δ 40.6 and 21.8 on the basis of the couplings observed in the 2D ^{1}H and ^{13}C NMR spectra (COSY, HSQC and HMBC, Fig. 11-13, respectively). Furthermore, its ESI MS spectrum (Fig.14) showed the sodium cluster and the pseudomolecular ion at *m/z* 179 $[M + Na]^+$ and 157 $[M + H]^+$, respectively.

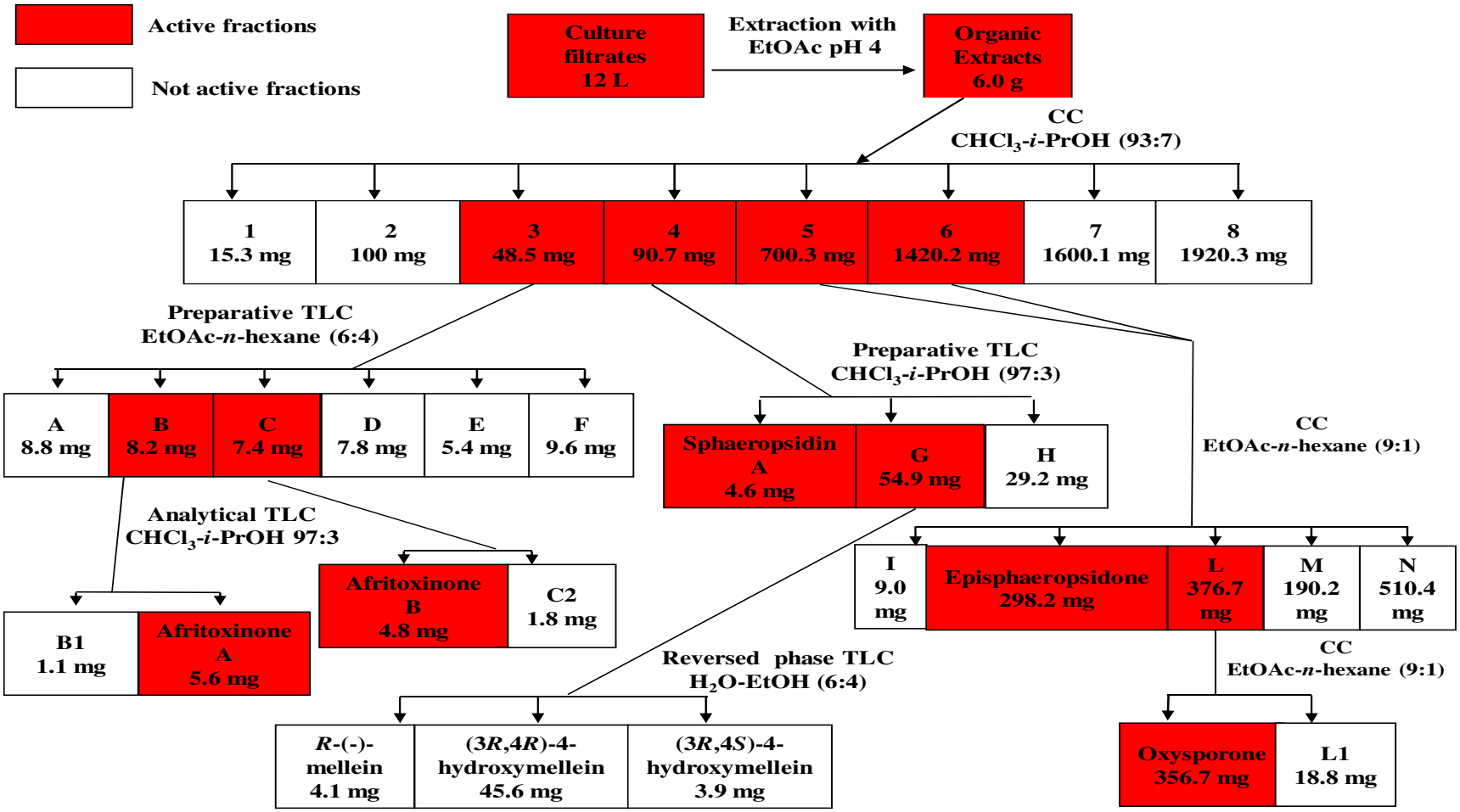

Scheme 1. Extraction and purification of *Diplodia africana* culture filtrates.

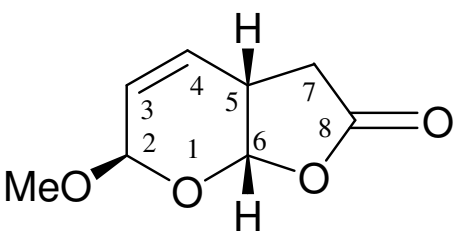

42

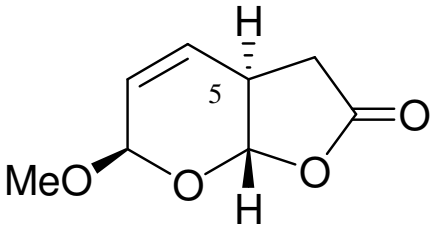

43

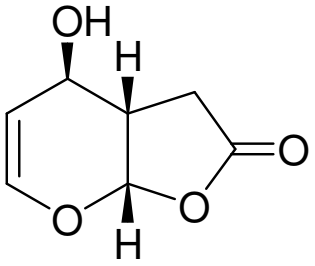

44

Figure 8. Structures of afritoxinones A and B (**42** and **43**) and oxysporone (**44**).

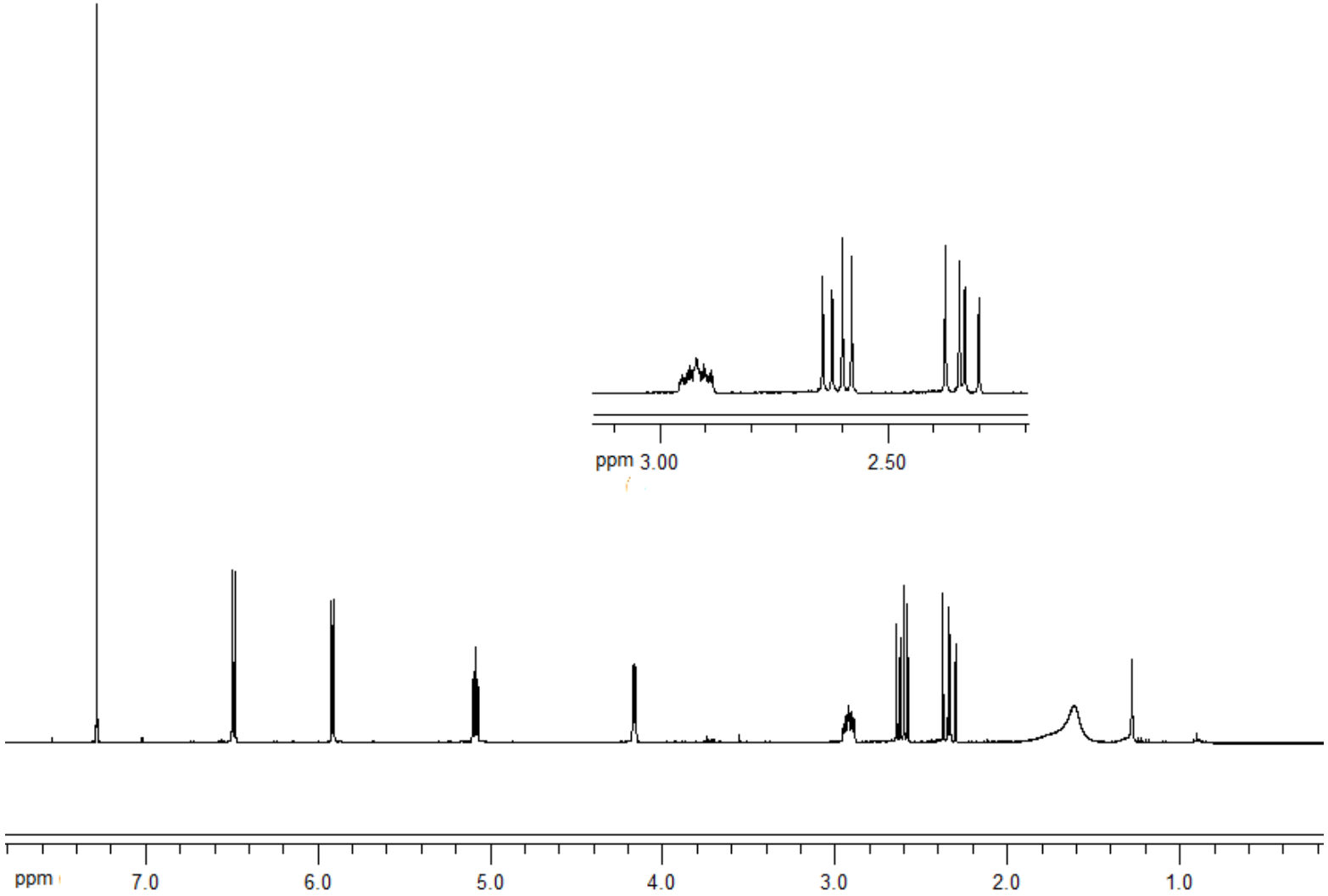

Figure 9. ^{1}H NMR spectrum of oxysporone (**44**), isolated from *D. africana* liquid culture, recorded in $CDCl_3$ at 600 MHz.

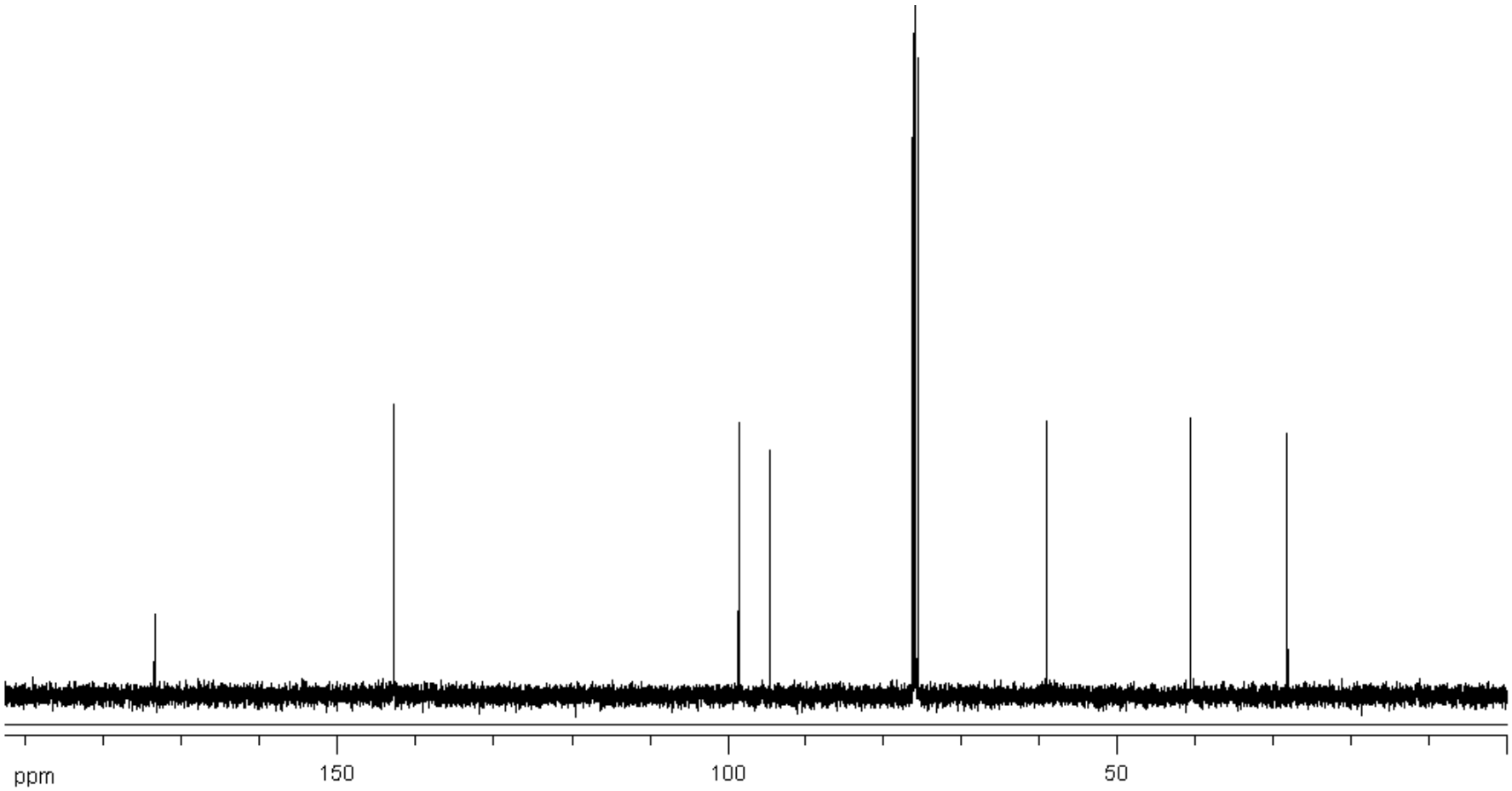

Figure 10. ^{13}C NMR spectrum of oxysporone (**44**), isolated from *D. africana* liquid culture, recorded in $CDCl_3$ at 150 MHz.

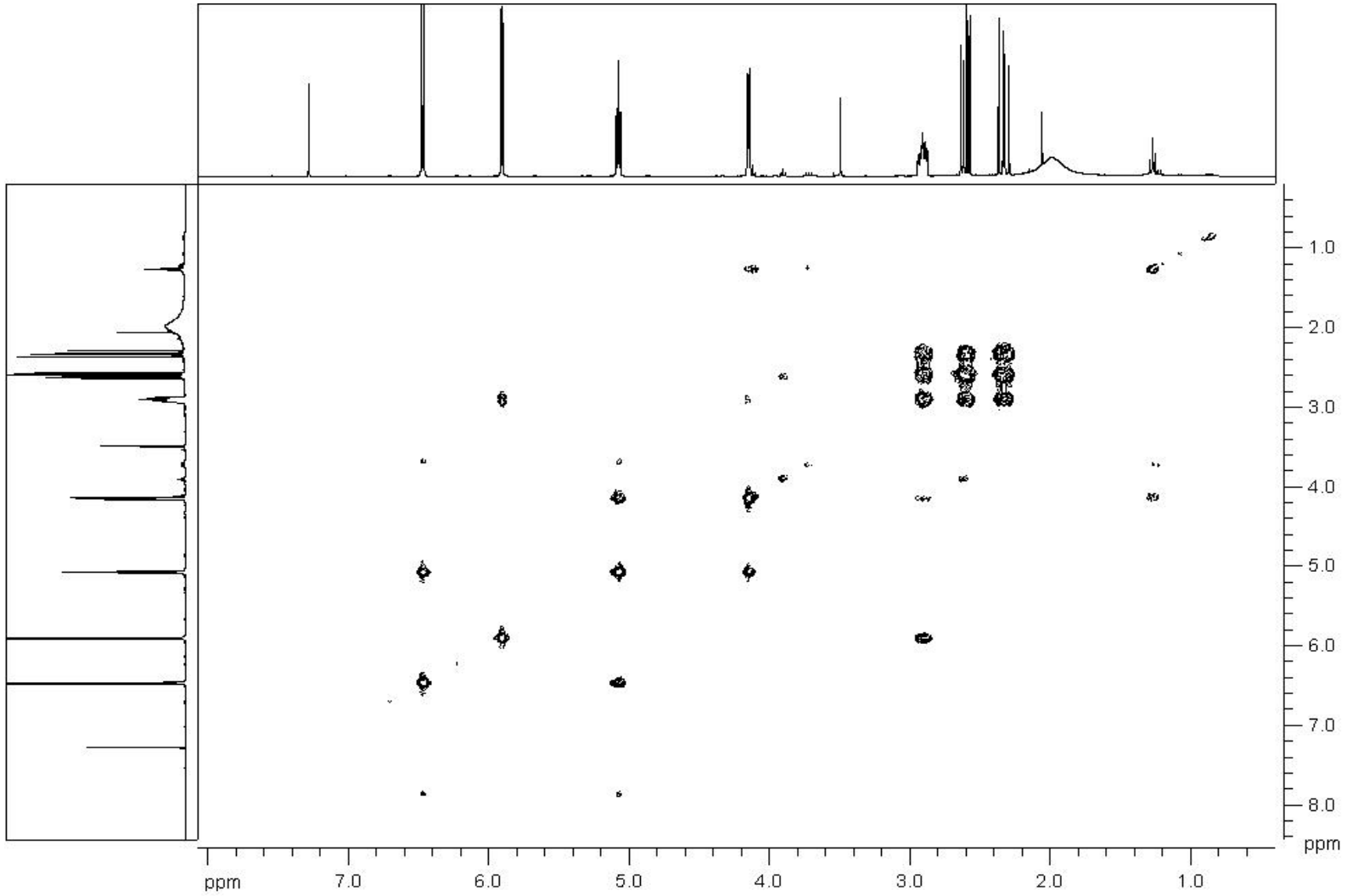

Figure 11. COSY spectrum of oxysporone (**44**), isolated from *D. africana* liquid culture, recorded in $CDCl_3$ at 600 MHz.

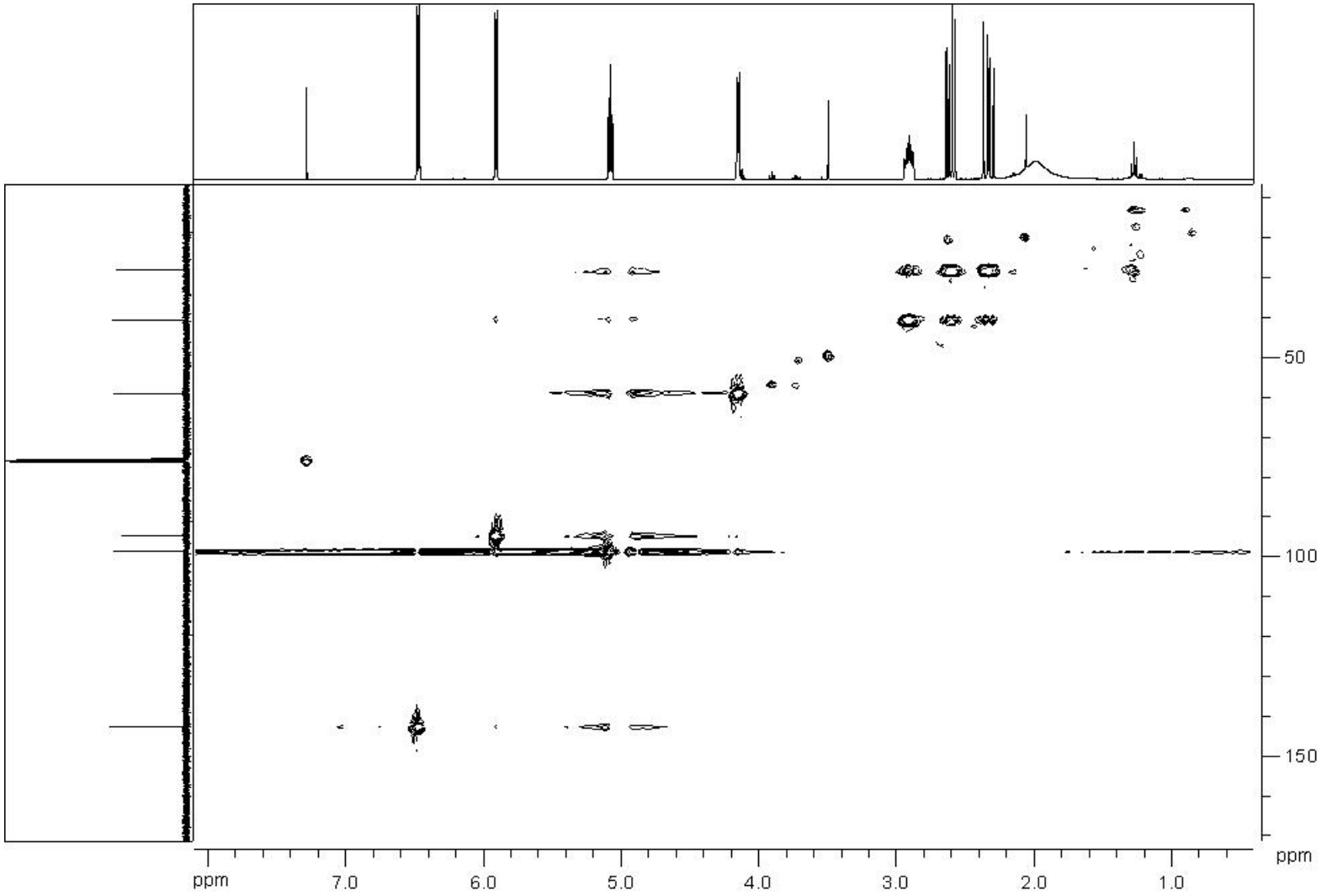

Figure 12. HSQC spectrum of oxysporone (**44)**, isolated from *D. africana* liquid culture, recorded in $CDCl_3$ at 600 MHz.

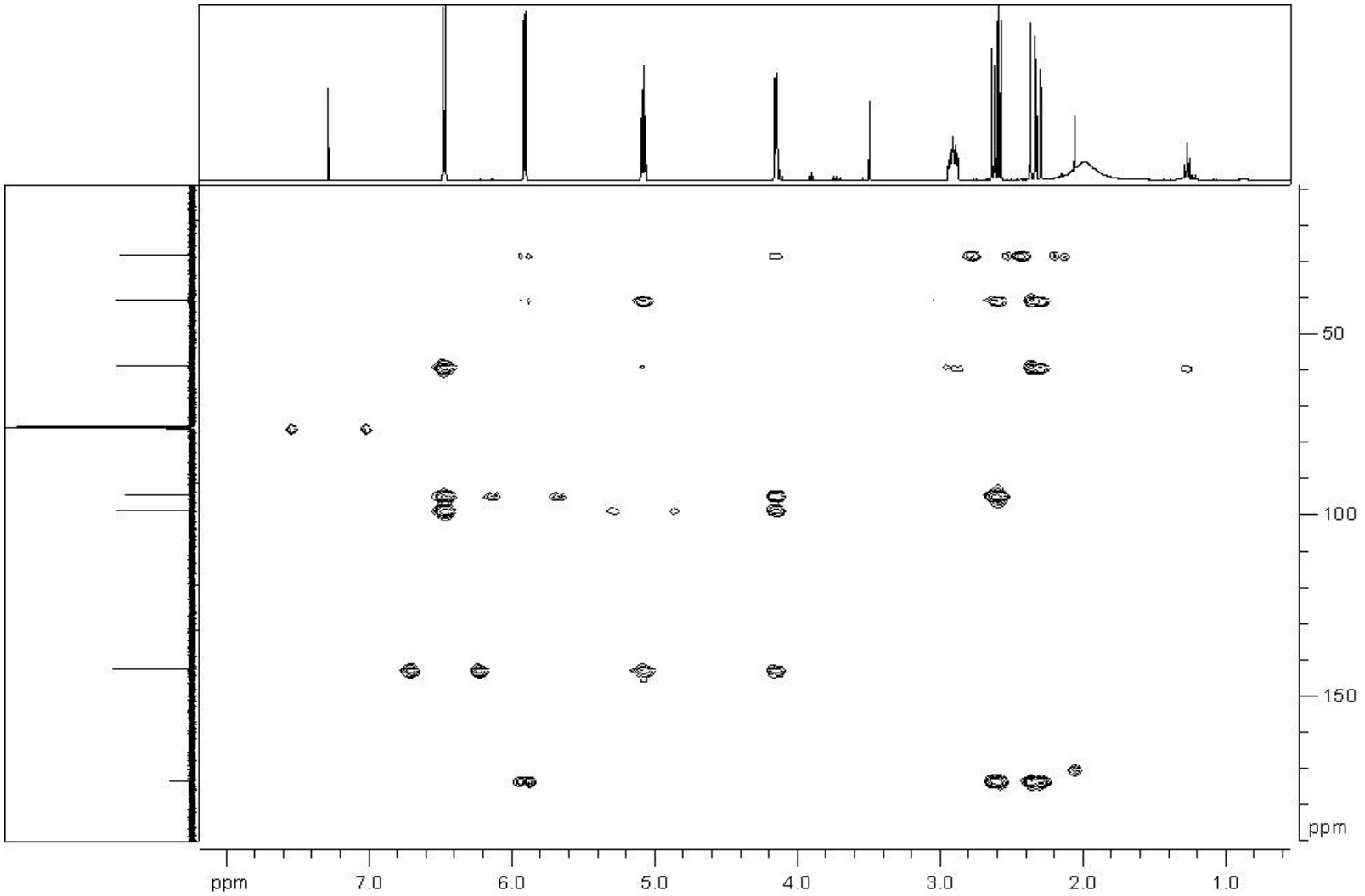

Figure 13. HMBC spectrum of oxysporone (**44)**, isolated from *D. cupressi* liquid culture, recorded in $CDCl_3$ at 600 MHz.

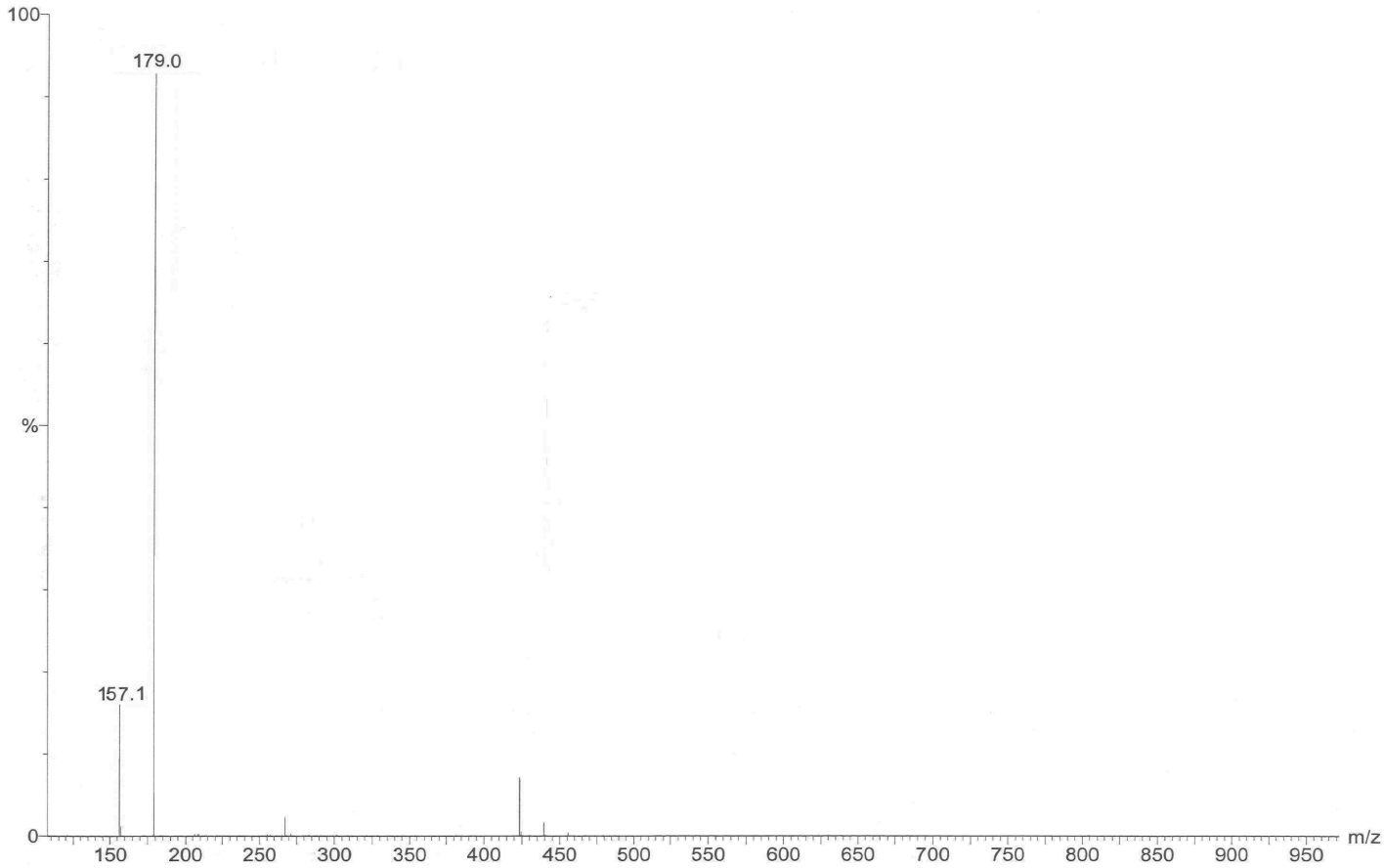

Figure 14. ESI MS spectrum of oxysporone (**44**), isolated from *D. africana* liquid culture, recorded in positive modality.

From the intermediate column fractions, sphaeropsidin A (**16**, Fig. 3, Pag. 26, 0.38 mg/l), *R*-(-)-mellein, (3*R*,4*R*)-4-hydroxymellein and (3*R*,4*S*)-4-hydroxymellein (**13-15**, Fig. 2, Pag. 23, 0.34, 3.8 and 0.32 mg/l, respectively) were isolated. **13**-**16** are also well known fungal phytotoxins identified by their physical ($[\alpha]_D^{25}$) and spectroscopic (^1H and ^{13}C NMR and ESIMS) data which were in agreement with those previously reported (Evidente *et al.*, 1996; Evidente *et al.*, 2010b).

From the relative less polar fractions of the initial column, other two homogeneous phytotoxic metabolites (0.47 and 0.40 mg/l, respectively) were isolated as new natural occurring compounds, which were named afritoxinones A and B (**42** and **43**, Fig. 8, Pag. 70).

Preliminary ^1H and ^{13}C NMR investigation showed that afritoxinones A and B (**42** and **43**, Fig. 8) were closely related themselves and with oxysporone (**44**, Fig.8).

Afritoxinone A (**42**) had a molecular formula of $C_8H_{10}O_4$ as deduced from its HR ESI MS, with the same 4 unsaturations of oxysporone and therefore consistent with the presence of a bicyclic carbon skeleton showing a suitable substituted dihydropyran ring joined with a disubstituted furanone. Its IR spectrum (Fig. 15) showed an absorption band typical of the furanone carbonyl as well as the band typical of a disubstituted olefinic group probably located into the dihydropyran ring (Nakanishi and Solomon, 1977). Its ^1H NMR spectrum (Table 1 and Fig. 16) showed a doublet (J = 6.4 Hz) of the proton (H-2) of the secondary oxygenated pyran ring at δ 5.98 being also bonded to a methoxy group, which resonating as a singlet at δ 3.52. H-2 in the COSY spectrum (Fig. 17) (Berger and Braun, 2004) coupled with the adjacent proton (H-3) of the 1,2-disubstituted *cis*-double bond appearing as a doublet of doublets (J = 10.3 and 6.4 Hz) at the typical chemical shift value of δ 5.99. This in turn coupled with the broad doublet of doublets (J = 10.3 and 2.9 Hz) of the other olefinic proton (H-4) at δ 6.06 (Pretsch *et al.*, 2000). H-4 was also long-

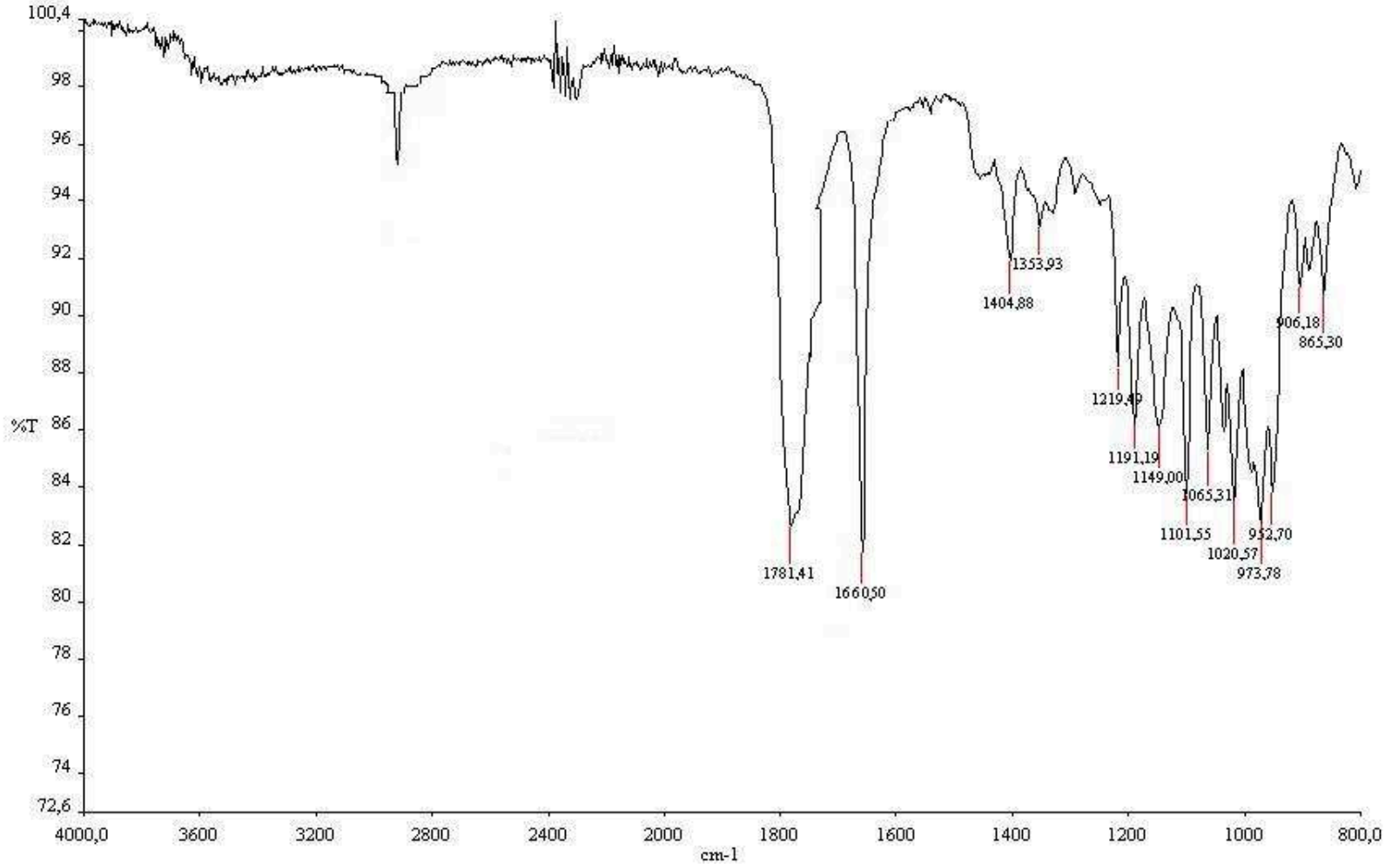

Figure 15. IR spectrum of afritoxinone A (**42**), isolated from *D. africana* liquid culture, recorded as glassy film.

Table 1. ^{1}H, ^{13}C NMR, HMBC and NOESY data of afritoxinones A and B (**42**-**43**).

Position	**42**			**43**		
	δC m[c]	δH	HMBC	δC m[c]	δH	HMBC
2	98.0 *d*	5.98 *d* (*J* = 6.4 Hz)	H-6	95.7 *d*	5.90 *d* (*J* = 4.5 Hz)	H-3, H-4,H-6,OMe
3	126.6 *d*	5.99 *dd* (*J* = 10.3 and 6.4 Hz)		126.9 *d*	5.96 *dd* (*J* = 10.1 and 4.5 Hz)	
4	125.8 *d*	6.06 *br dd* (*J* =10.3 and 2.9 Hz)	H-7A	126.3 *d*	5.91 *br dd* (*J* = 10.1 and 2.3 Hz)	H-6, H_2-7
5	31.3 *d*	3.21 *m*	H-3	34.1 *d*	2.92 *br dd* (*J* = 9.5 and 9.0 Hz)	H-3, H-4, H_2-7
6	93.3 *d*	5.09 *br d* (*J* = 2.9 Hz)	H-2, OMe	95.9 *d*	5.07 *d* (*J* = 2.3 Hz)	H_2-7
7	34.6 *t*	2.90 *dd* (*J* = 17.7 and 10.0 Hz) 2.54 *dd* (*J* = 17.7 and 5.0 Hz)	H-4	32.5 *t*	2.70 *dd* (*J* = 17.3 and 9.0 Hz) 2.40 *dd* (*J* = 17.3 and 9.5 Hz)	H-5
8	173.0 *s*		H-7A	174.9 *s*		H-4, H_2-7
OMe	54.4 *q*	3.52 *s*		56.2 *q*	3.52 *s*	H-6

NOESY			
42		**43**	
Irradiated	Observed	Irradiated	Observed
H-2	OMe	H-3	H-5
H-3	H-5, H_2-7	H-4	H-6
H-4	H-6	H-5	H-3, H_2-7
H-6	H-4, H-5, OMe	H-6	H-4, OMe
H-5	H-3, H-6, H_2-7	H-7A	H-7B
H-7A	H-7B		

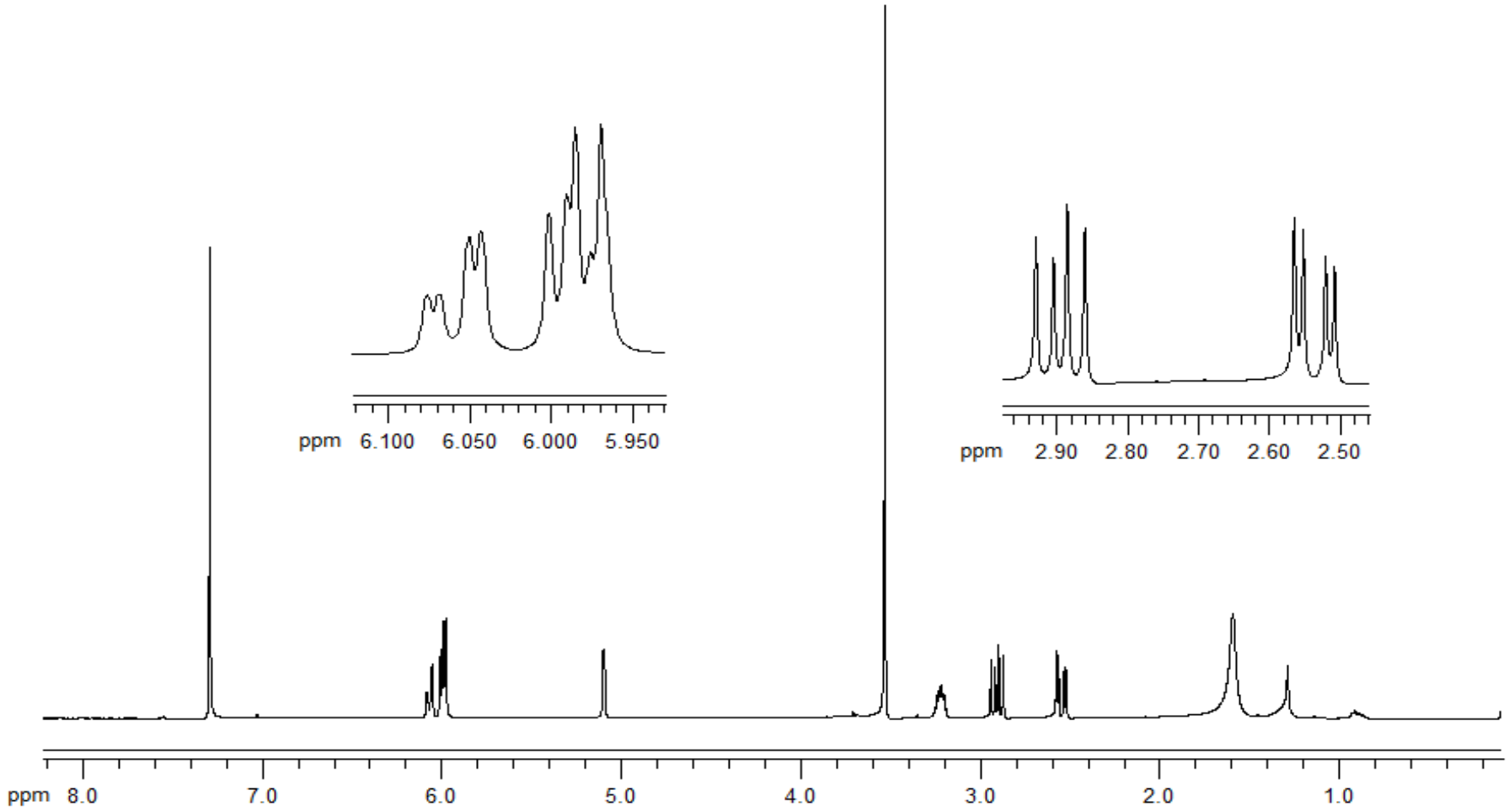

Figure 16. ^{1}H NMR spectrum of afritoxinone A (**42**), isolated from *D. africana* liquid culture, recorded in $CDCl_3$ at 600 MHz.

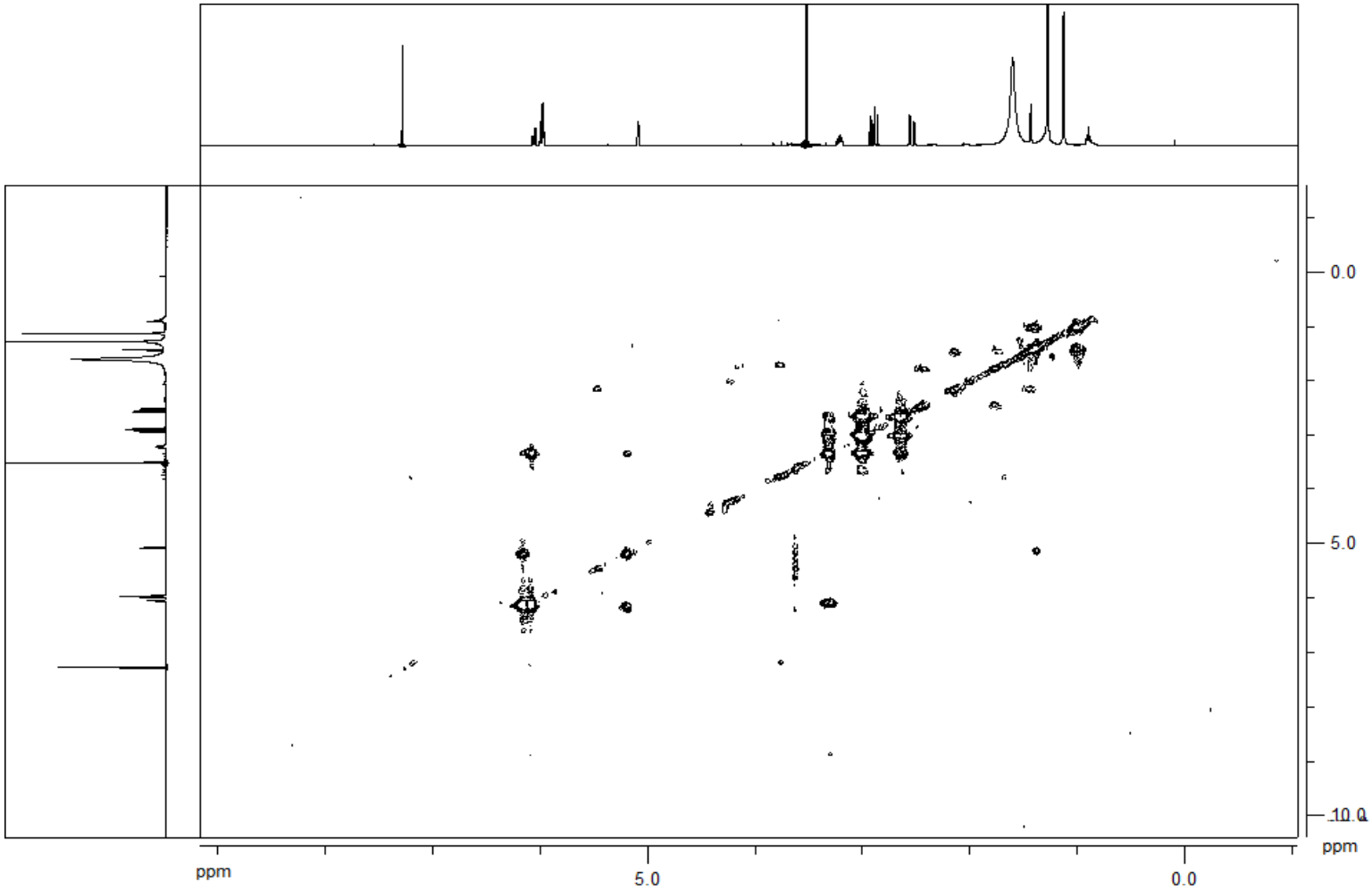

Figure 17. COSY spectrum of afritoxinone A (**42**), isolated from *D. africana* liquid culture, recorded in $CDCl_3$ at 600 MHz.

range coupled (J = 2.9 Hz) with the proton (H-6) of one on the bridgehead carbon (C-6) of the junction between the two rings, resonating as a broad doublet (J = 2.9) at δ 5.09, and lesser extended (J<1 Hz) with H-5 . The couplings over four or more bonds are often observed in condensed alicyclic compounds. Such long-range couplings are particularly significant if the arrangement of the bonds between the two protons is w-shaped (Pretsch *et al.*, 2000). This is the arrangement observed in afritoxinone A between the proton H-4 and H-6 as deduced by an investigation of its Dreiding model. H-5, which is bonded to the other bridgehead carbon (C-5), resonated as a multiplet at δ 3.21 being also coupled with the adjacent protons of the methylene group (CH_2-7) of the furanone ring appearing as expected as two double doublets (J = 17.7 and 10.0 and 17.7 and 5.0 Hz) at δ 2.90 and 2.54, respectively (Pretsch *et al.*, 2000). All these couplings constants were confirmed through ^{1}H double resonance experiments carried out on afritoxinone A and were also in agreement with the values reported for the same proton system ($J_{4',7'}$= 3.1, $J_{2'A,2'B}$ = 17.7, $J_{2'A,3'}$ =10.0 and $J_{2'B,3'}$ = 4.3 Hz) for the upward moiety of pestalotine A. Pestalotines A and B (**60** and **61**, Fig. 18) 4-oxo-4H-pyran-3-acetic acid and 6-hydroxymulosin, are two γ-lactonic phytotoxins which were isolated from *Pestalotiopsis* sp. HC02, a fungus residing in *Chondracis rosee* gut (Zhang *et al.*, 2008). The presence of these two joined partial structures (dihydropyran and a furanone ring) was confirmed by the data of the ^{13}C NMR spectrum (Fig. 19) whose protonated carbons were assigned on the basis of the coupling observed in the HSQC spectrum (Fig. 20) (Berger and Braun, 2004) and reported in Table 1. The carbonyl of the furanone ring appeared at the typical chemical shift of δ 173.0, as well as the secondary carbons of the 1,2-disubstituted olefinic and the methoxy groups, observed at δ 126.6, 125.8 and 54.4 (C-3, C-4 and OMe) (Breitmaier and Voelter, 1987). Finally, the methoxylated secondary carbons of the dihydropyran ring, the two bridge head

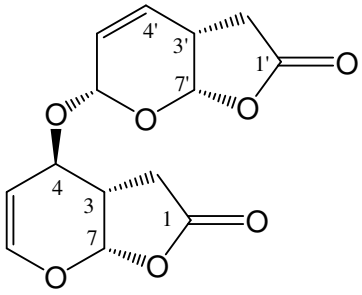

60

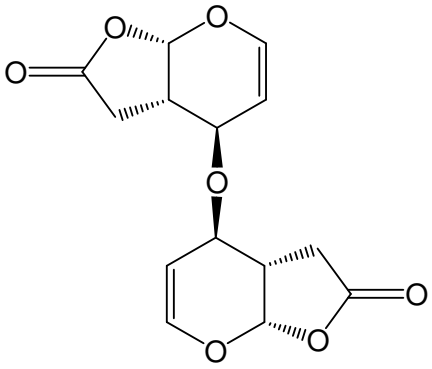

61

Figure 18. Structures of pestalotines A and B (**60** and **61**).

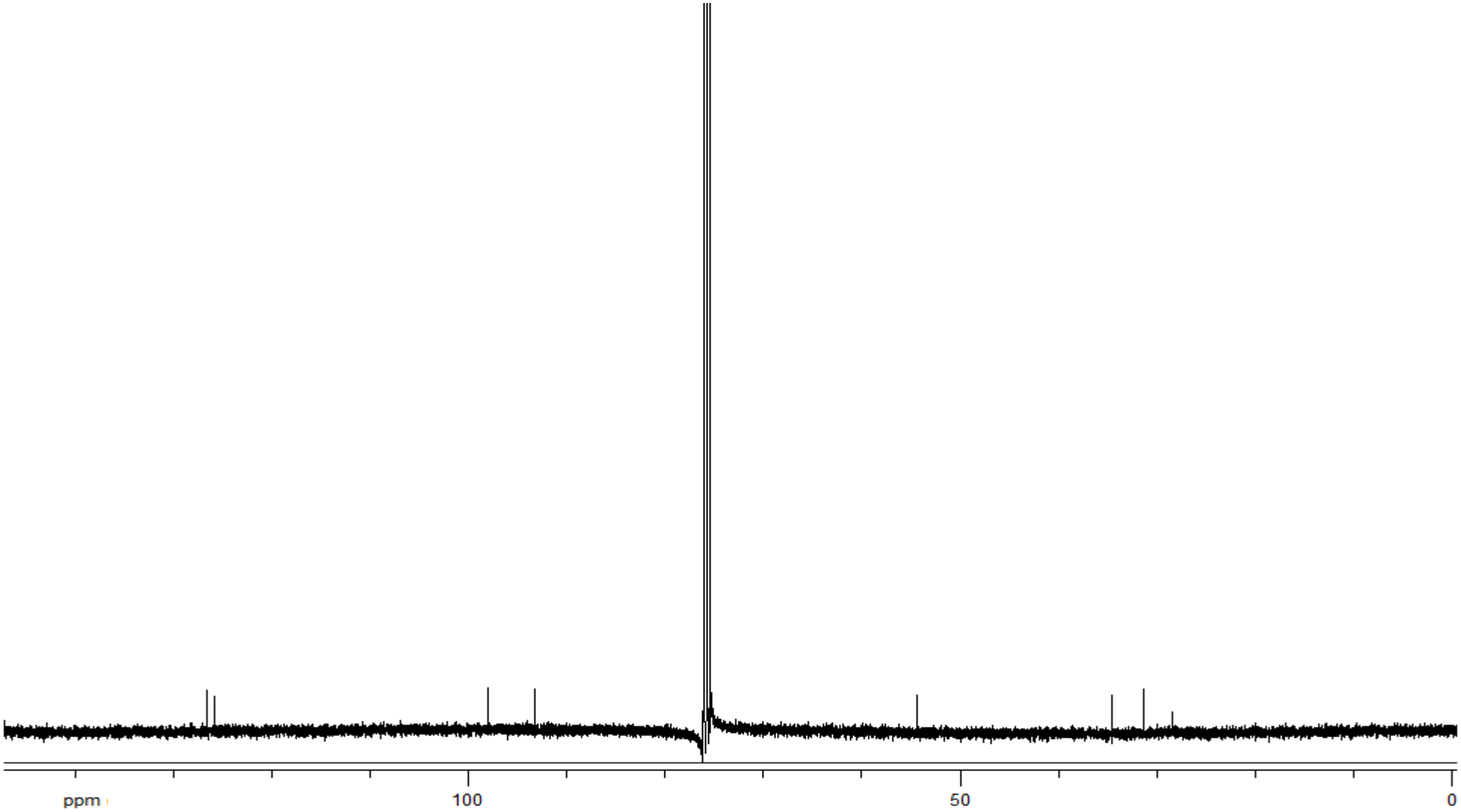

Figure 19. ^{13}C NMR spectrum of afritoxinone A (**42**), isolated from *D. cupressi* liquid culture, recorded in $CDCl_3$ at 150 MHz.

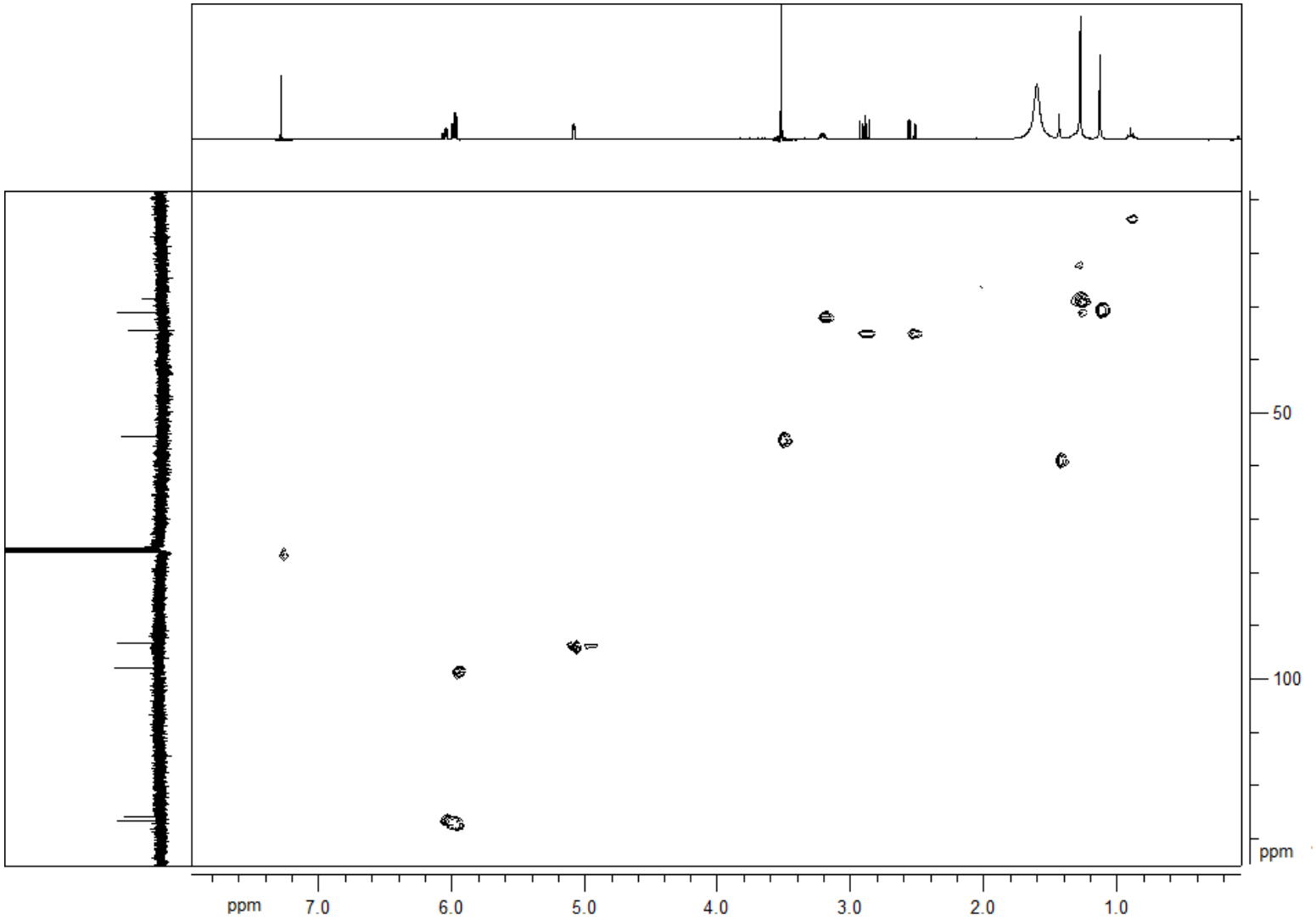

Figure 20. HSQC spectrum of afritoxinone A (**42**), isolated from *D.africana* liquid culture, recorded in $CDCl_3$ at 600 MHz.

carbons of the junction of the two rings and the furanone methylene carbon resonated at δ 98.0, 93.3, 31.3 and 34.7 (C-2, C-6, C-5 and C-7), (Breitmaier and Voelter, 1987). On the basis of these results afritoxinone A can be formulated as 6-methoxy-3a,7a-dihydro-3*H*,6*H*-furo[2,3-b]pyran-2-one. The structure assigned to afritoxinone A (**42**) was supported by the several long range couplings observed in its HMBC spectrum (Fig. 21) (Berger and Braun, 2004). As expected the carbonyl furanone and the olefinic carbon C-4 coupled with H-7A, while the methylene carbon C-7 coupled with H-4. The bridgehead carbons C-5 and C-6 coupled with H-3 and H-2 and OMe, respectively, while C-2 coupled with H-6. The structure assigned to afritoxinone A was further supported by the data of its ESI MS (Fig. 22) spectrum which showed the potassium and sodium clusters and the pseudomolecular ion at *m/z* 209 $[M+K]^+$, 193 $[M+Na]^+$, 171 $[M+H]^+$, respectively.

A *cis*-stereochemistry between the dihydropyran and the furanone ring was assigned by comparing the coupling constants between the protons (H-5 and H-6) of the bridgehead carbons and those of H-5 with the adjacent furanone methylene group H_2C-7 with those above reported for the upward part of pestalotine A (**60**, Fig. 18) as the relative configurations of both pestalotines A and B (**60** and **61**, Fig. 18) were assigned on the basis of NOESY correlations and a 3D structure generated by computer modelling (Zhang *et al.*, 2008). Therefore, a *cis*-stereochemistry between the dihydropyran and furanone ring was assigned to afritoxinone A (**42,** Fig. 8). This stereochemistry, already observed in pestalotine A and oxysporone, was also supported by the couplings observed in the NOESY spectrum (Fig. 23) of **42** (Berger and Braun, 2004) (Table 2). Beside the couplings observed between H-5 and H_2-7 and between these two latter protons themselves, other couplings were recorded between H-2 and OMe, H-3 and H-5. Particularly significant appeared to be the coupling observed between H-5 with H-6 and

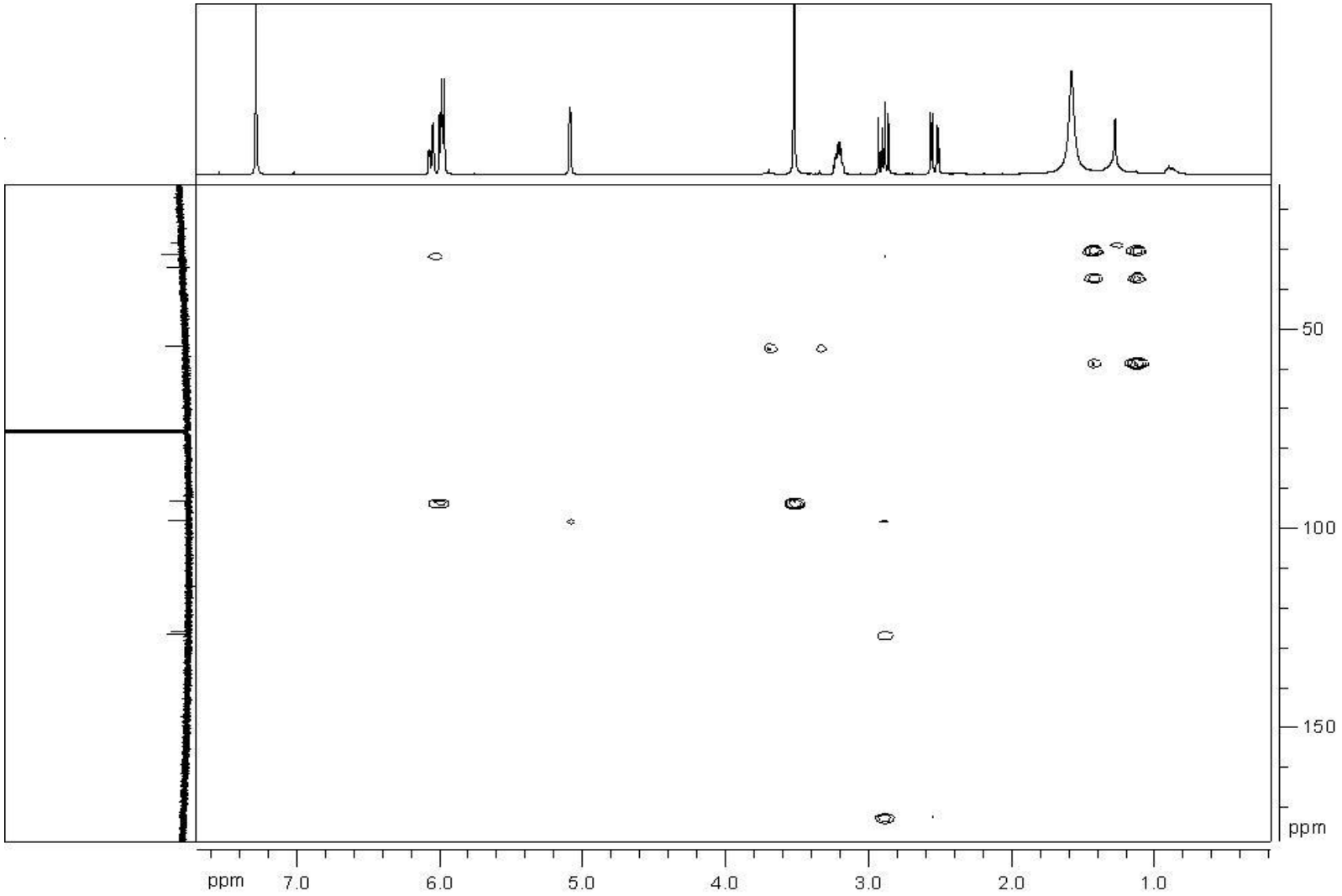

Figure 21. HMBC spectrum of afritoxinone A (**42**), isolated from *D. africana* liquid culture, recorded in $CDCl_3$ at 600 MHz.

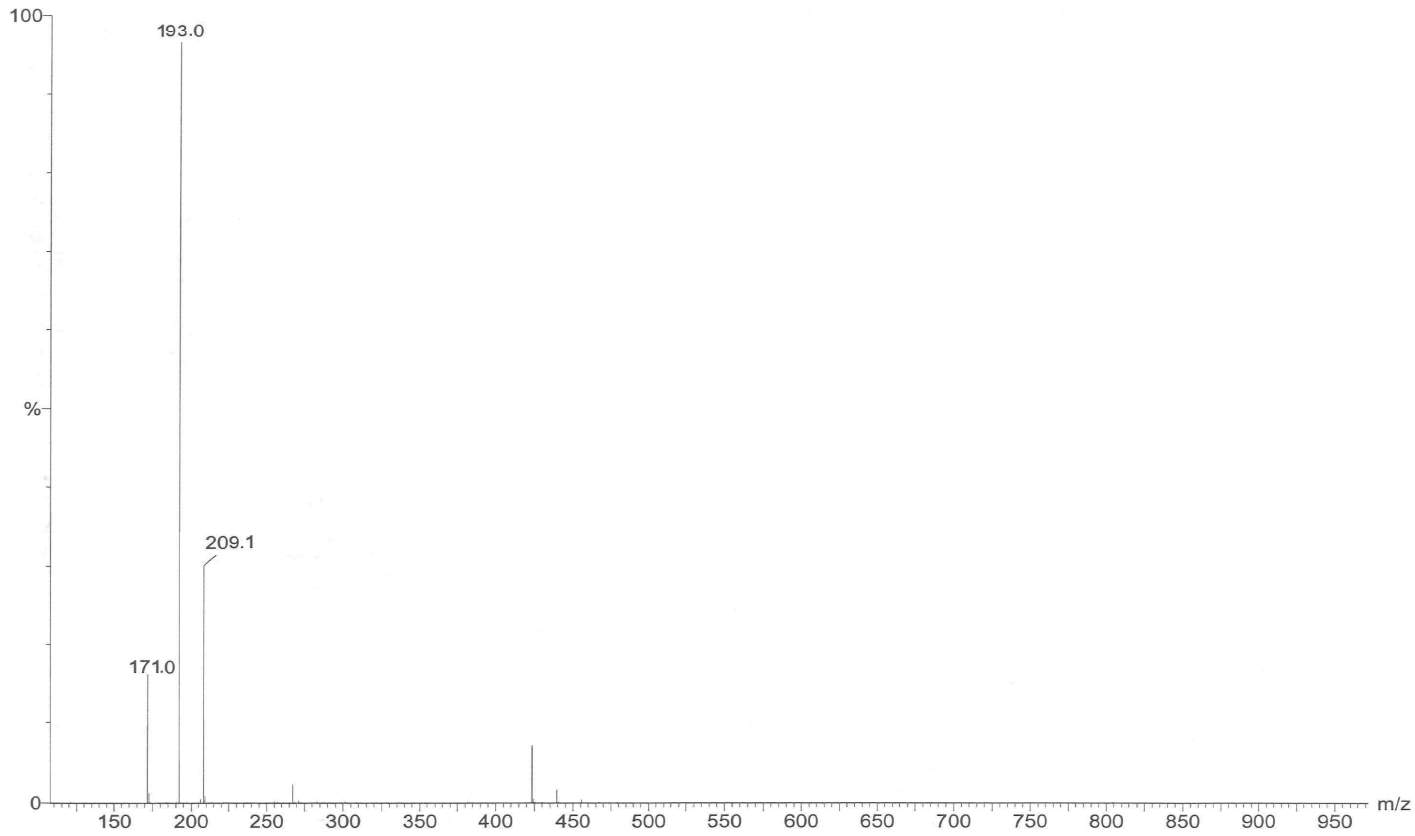

Figure 22. ESI MS spectrum of afritoxinone A (**42**), isolated from *D. africana* liquid culture, recorded in positive modality.

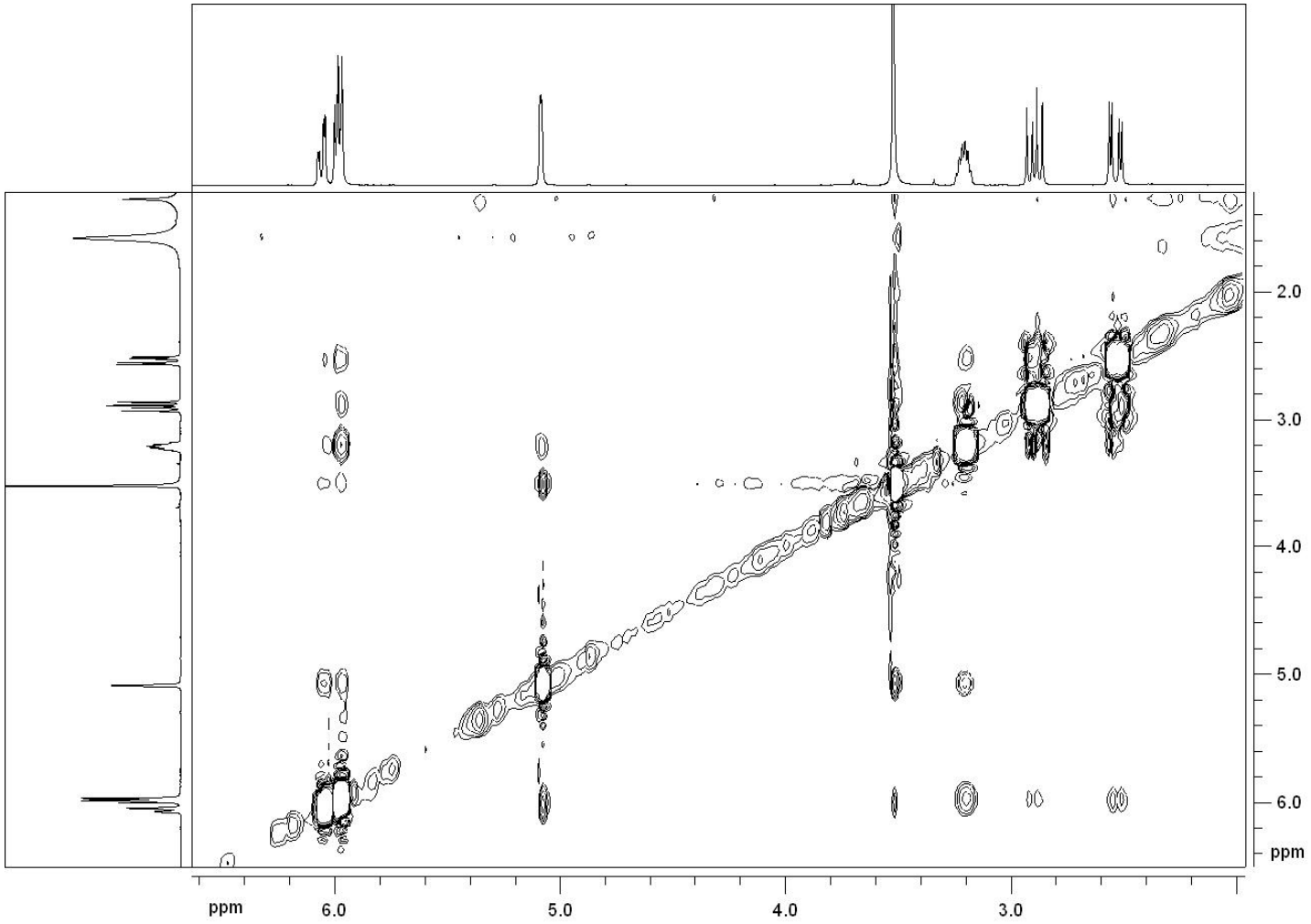

Figure 23. NOESY spectrum of afritoxinone A (**42**), isolated from *D. africana* liquid culture, recorded in $CDCl_3$ at 600 MHz.

those between H-6 with H-4 and OMe. The last one also allowed to assign the relative stereochemistry at C-2 as depicted in **42**. So, on the basis of these data, afritoxinone A can be formulated as (3a*S**,6*R**,7a*S*)-6-methoxy-3a,7a-dihydro-3*H*,6*H*-furo[2,3-b]pyran-2-one, which was consistent with an inspection of a Dreiding model of **42**.

Afritoxinone B (**43**, Fig. 8) gave the same molecular formula $C_8H_{10}O_4$, deduced from its HR ESI MS spectrum. The IR (Fig. 24) and ^{13}C NMR (Fig. 25 and Table 1) spectra were very similar to those of **42**. The ^{1}H NMR spectrum (Fig. 26 and Table 1) of afritoxinone B showed substantial differences compared to that of afritoxinone A suggesting that **43** could be a stereoisomer of **42**. In fact, this latter spectrum differed from that of **42** for the couplings between H-6, which resonated as a sharp doublet (J = 2.3) at δ 5.07, and H-5, which appeared as a broad doublet of doublets (J = 9.5 and 9.0 Hz) at δ 2.92, a chemical shift significantly different from that proton had in **42**. H-5 also differently coupled with the two protons of the furanone methylene group (H_2-7), which resonated both as doublet of doublets (J = 17.7 and 9.0 and 17.7 and 9.5 Hz) at δ 2.70 and 2.40, respectively. Also the chemical shifts of H-4, H_2C-7 are significantly different from those observed in **42** for the same protons. On the basis of these results **43** appeared to be the *trans*-stereoisomer of **42**.

Several long-range couplings (Table 1) were observed in its HMBC spectrum (Fig. 27) and in particular those between the carbonyl furanone with H-4 and H_2C-7, C-4 with H-6 and H_2C-7, C-2 with H-3, H-4 and OMe, C-5 with H-3, H-4 and H_2C-7 and C-7 with H-5. This structure was also supported by the data observed in its HSQC spectrum (Fig. 28).

The structure assigned to afritoxinone B was further supported by the data of its ESI MS (Fig. 29) spectrum which showed the potassium and sodium clusters and the pseudomolecular ion at *m/z* 209 $[M+K]^+$, 193 $[M+Na]^+$, 171 $[M+H]^+$, respectively.

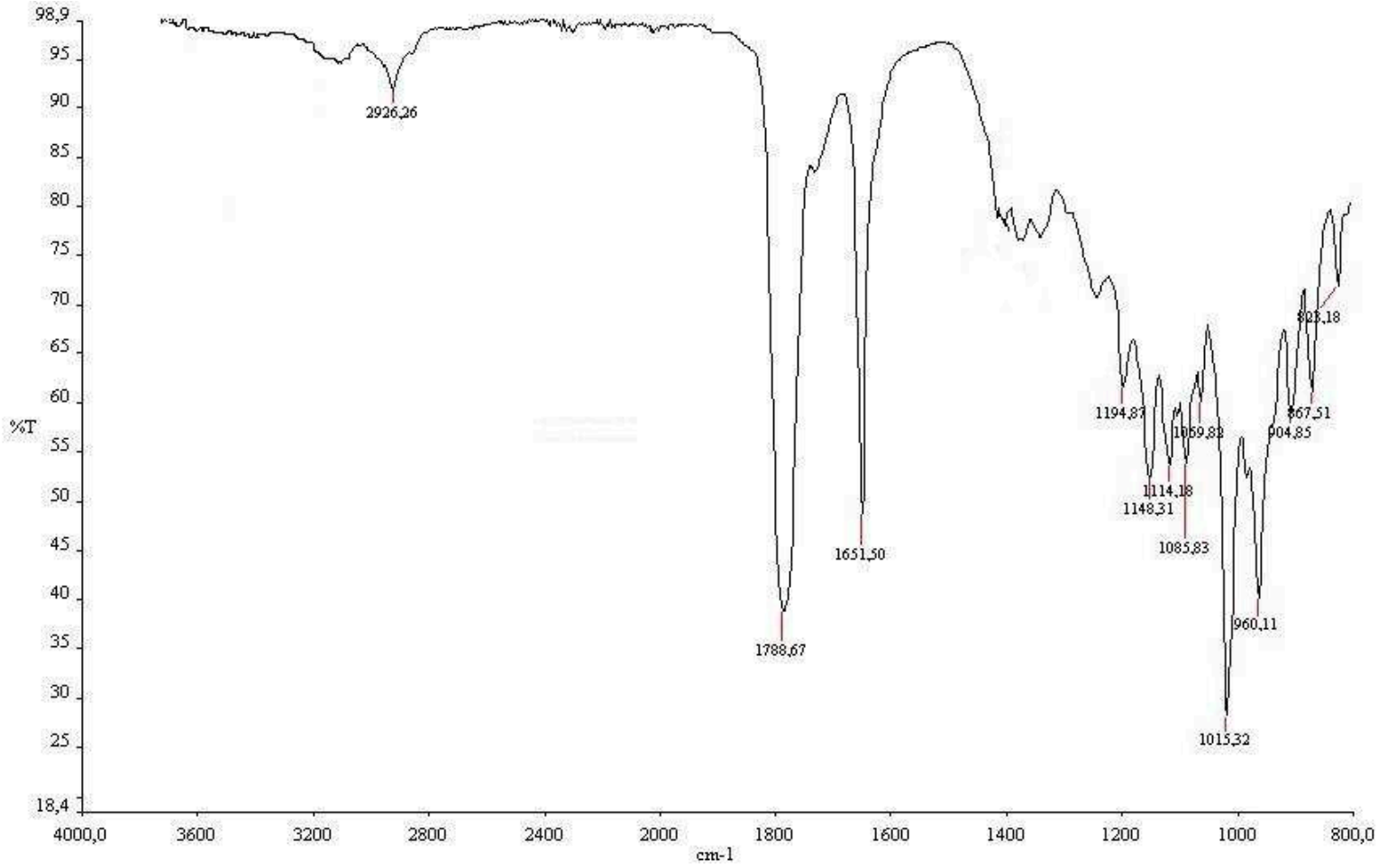

Figure 24. IR spectrum of afritoxinone B (**43**), isolated from *D. africana* liquid culture, recorded as glassy film.

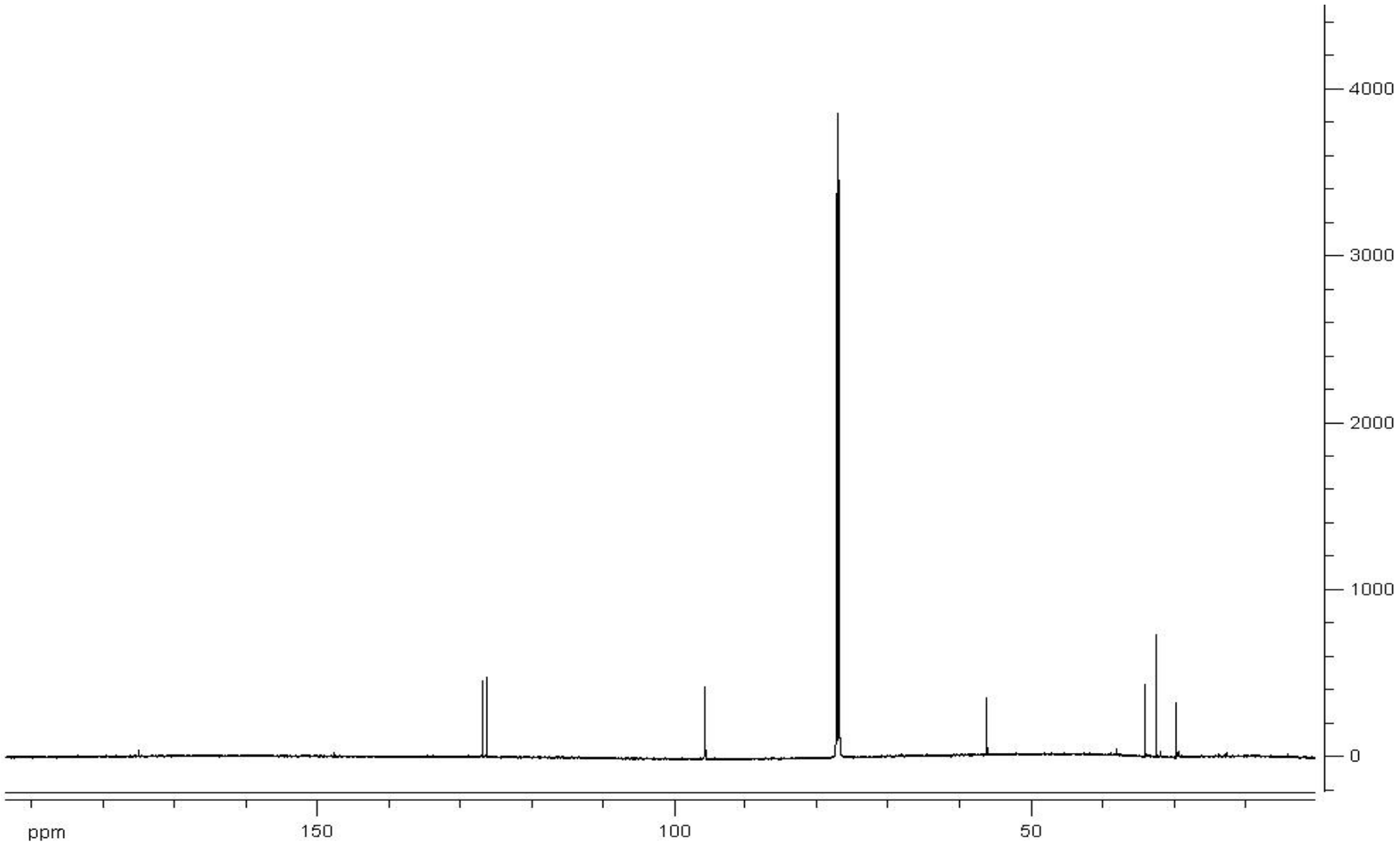

Figure 25. ^{13}C NMR spectrum of afritoxinone B (**43**), isolated from *D. africana* liquid culture, recorded in $CDCl_3$ at 600 MHz.

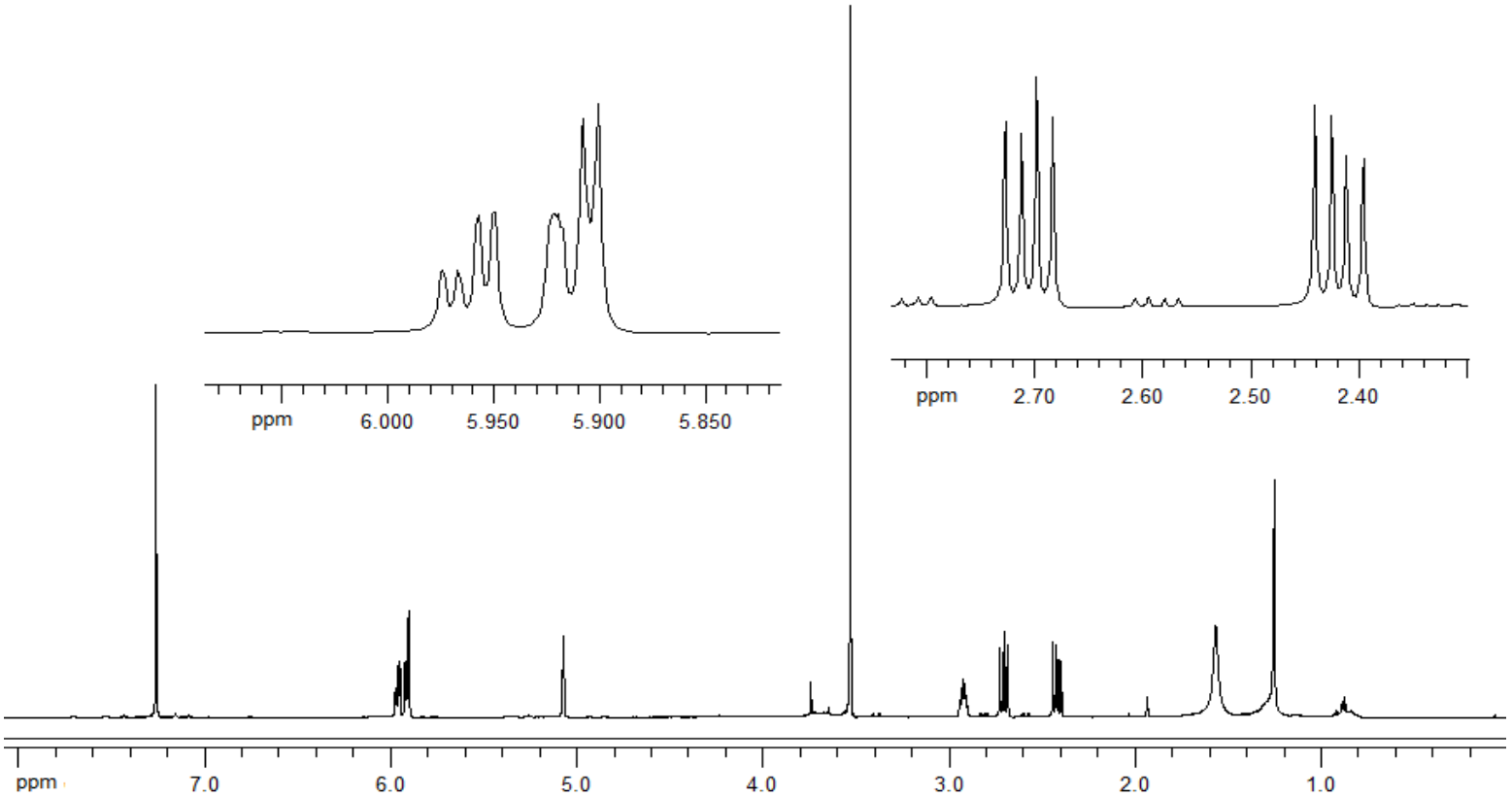

Figure 26. ^{1}H NMR spectrum of afritoxinone B (**43**), isolated from *D. africana* liquid culture, recorded in $CDCl_3$ at 600 MHz.

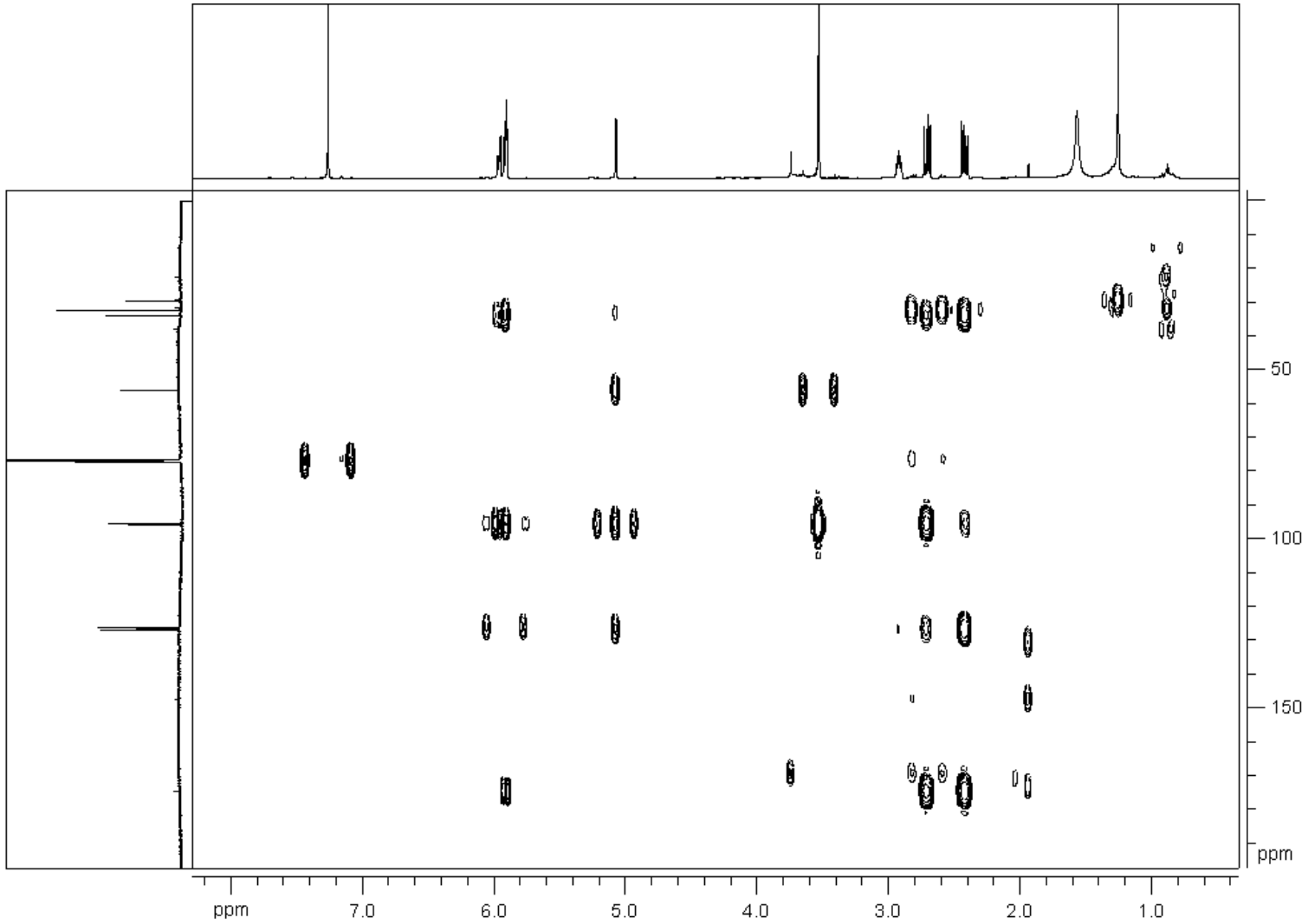

Figure 27. HMBC spectrum of afritoxinone B (**43**), isolated from *D. cupressi* liquid culture, recorded in $CDCl_3$ at 600 MHz.

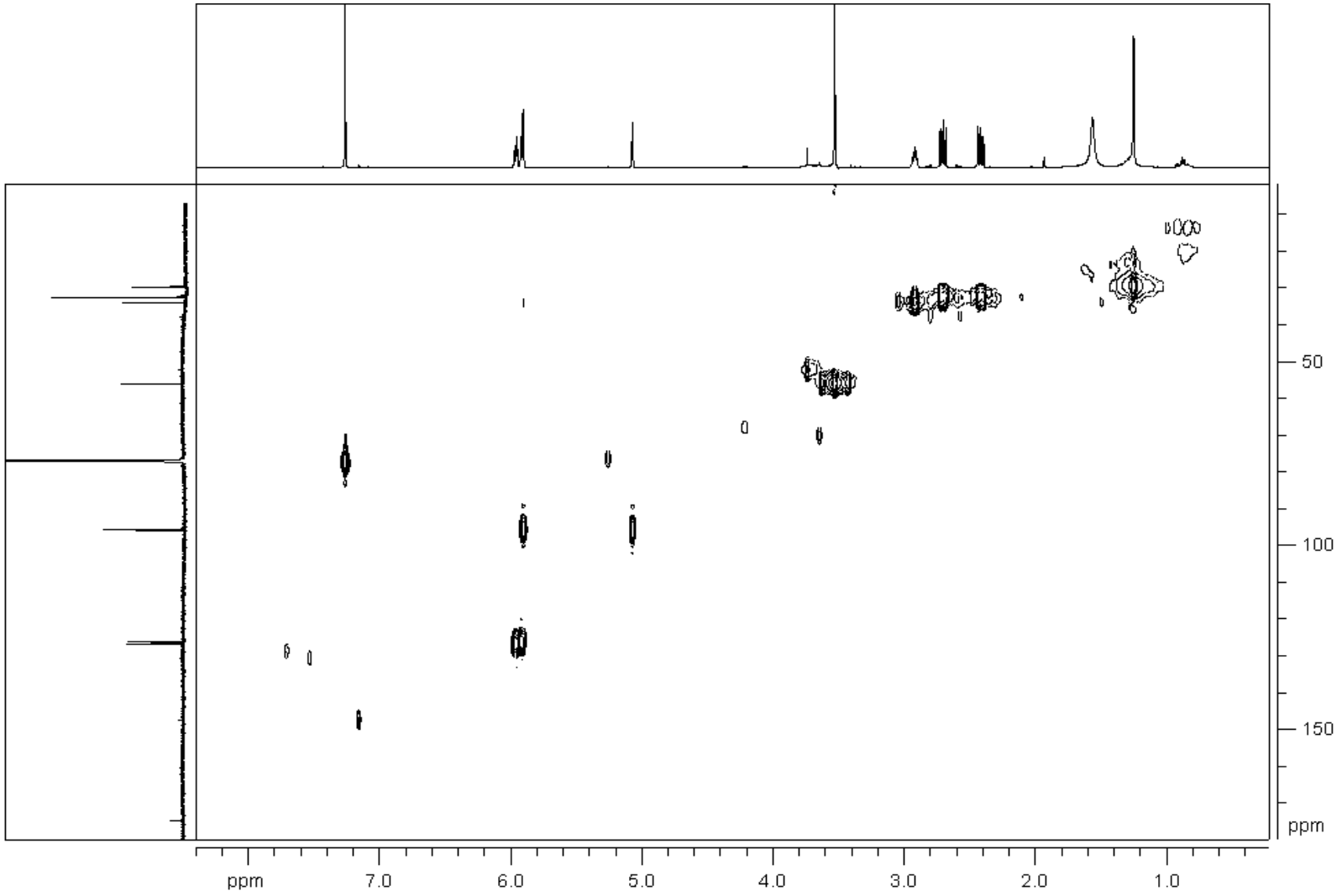

Figure 28. HSQC spectrum of afritoxinone B (**43**), isolated from *D. africana* liquid culture, recorded in $CDCl_3$ at 600 MHz.

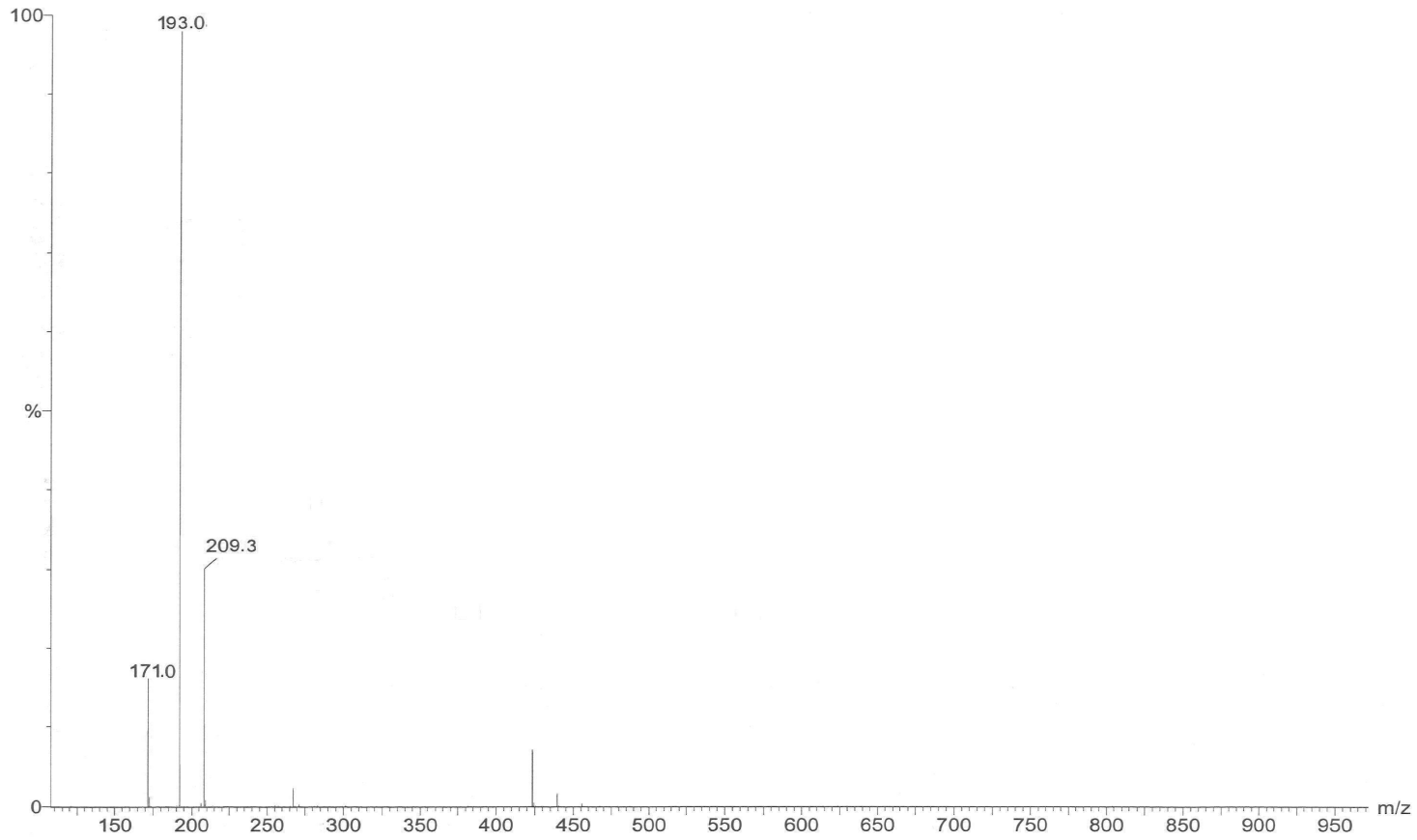

Figure 29. ESI MS spectrum of afritoxinone B (**43**), isolated from *D. africana* liquid culture, recorded in positive modality.

Finally, the *trans*-stereochemistry between the two rings assigned to **43** was supported by the couplings observed in the NOESY spectrum (Fig. 30 and Table 1). In fact, the coupling between H-6 and H-5 observed in **42** was significantly absent, while H-5 always coupled with H-3 and with the protons of H_2C-7, which were also themselves coupled. Furthermore H-4 coupled with H-6 and this latter with OMe. This latter coupling also allowed to assign the relative stereochemistry at C-2, which is the same of that in **42**. So that afritoxinone B could be formulated as (3a*R**,6*R**,7a*S*)-6-methoxy-3a,7a-dihydro-3*H*,6*H*-furo[2,3-b]pyran-2-one which was consistent with an inspection of a Dreiding model of **43**. Although furanones and pyrones are widely diffused as natural occurring compounds (Turner and Aldridge, 1983), dihydrofuropyranones and closed related compounds appear to be rarely isolated as natural compounds. Among them 3,7-dimethyl-*2H*-furo[2,3-*c*]pyran-2-one is reported as active agent in plant-derived smoke which promote the germination of a variety of wild species (Flematti *et al*., 2007; Trinh *et al.*, 2010), and alboatrin isolated as a phytotoxic metabolite from liquid culture of *Verticillium alboatrum* (Biswas *et al*., 2008). Instead, dihydrofuropyranones were frequently reported as synthones, intermediates or end-products in the total synthesis of different class of organic compounds (Tezuka *et al.*, 1972; Cakir and Mead, 2004; Biswas *et al.*, 2008).

5.2. Phytotoxic activity of afritoxinones A and B and oxysporone

The phytotoxic activity of afritoxinones A and B and oxysporone (**42**-**44**, Fig. 8) was investigated through leaf puncture assays on non-host plants and cutting assays on host and non-host plants. In all bioassays oxysporone (**44**) appeared to be the most active metabolite. In the leaf-puncture assay, the phytotoxicity was evaluated for holm oak, cork oak and tomato leaves. The toxicity data (Fig. 31) showed that oxysporone (**44**) had

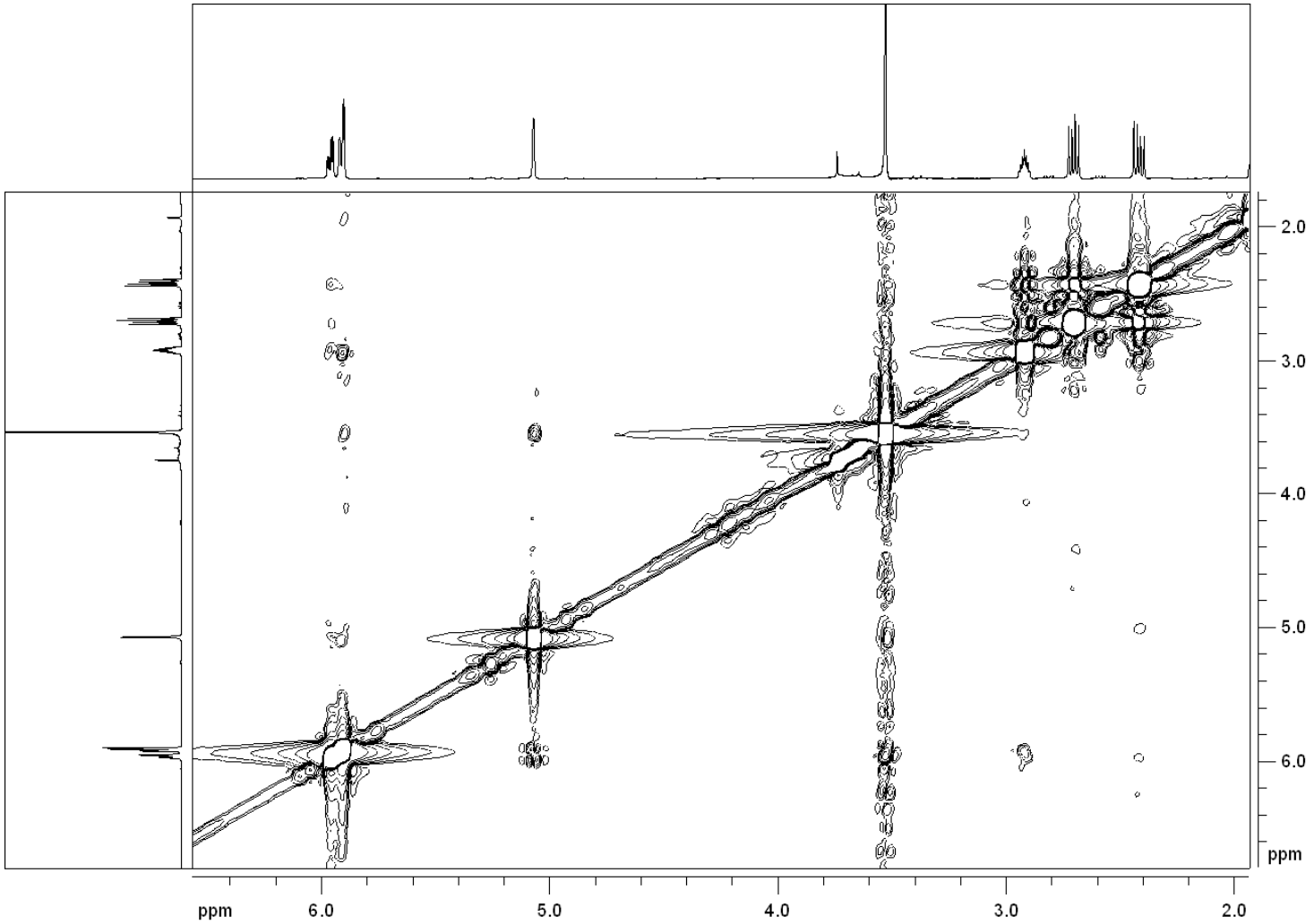

Figure 30. NOESY spectrum of afritoxinone B (**43**), isolated from *D. africana* liquid culture, recorded in $CDCl_3$ at 600 MHz.

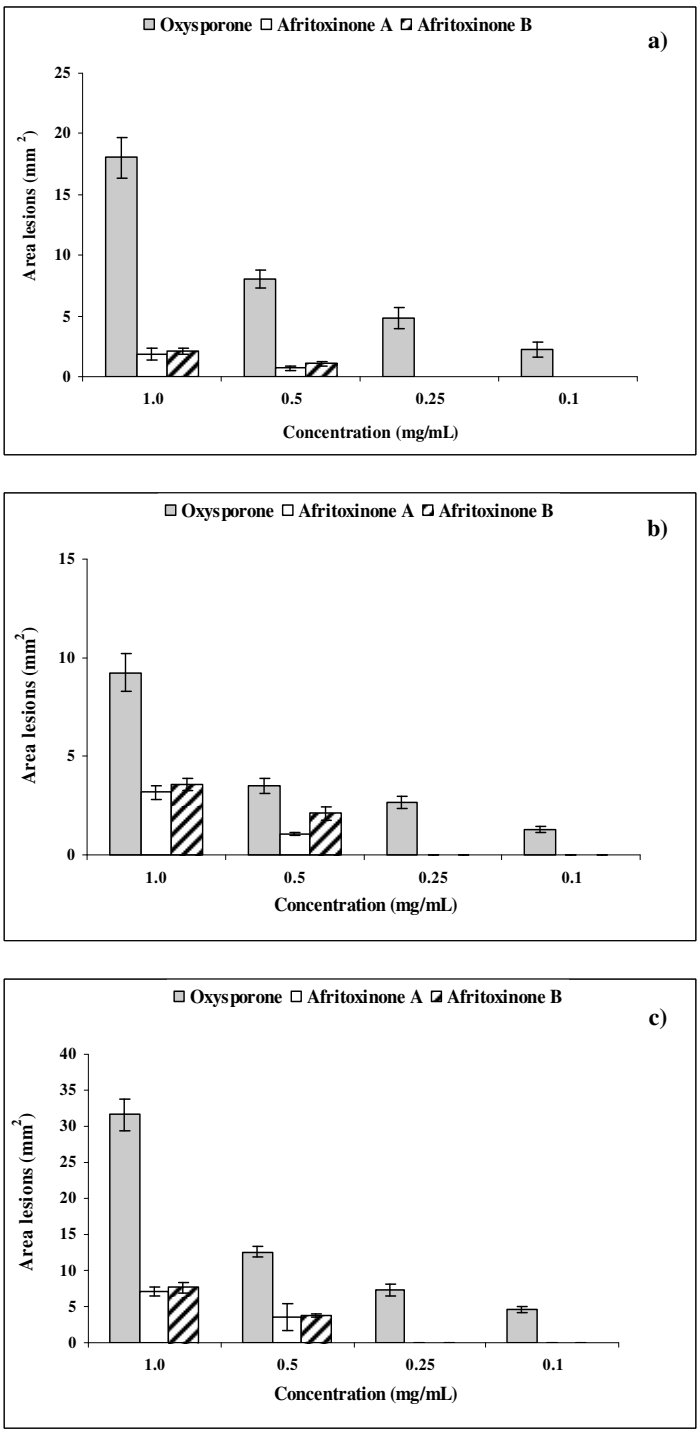

Figure 31. Phytotoxicity of oxysporone (**44**), afritoxinone A and B (**42** and **43**) evaluated on three plant species: a) holm oak; b) cork oak; c) tomato.

remarkable toxicity at a range of concentrations from 0.1 to 1 mg/ml, causing necrotic lesions (necrosis area ranging from ~ 2 to 30 mm^2) to leaves of all species tested.

A markedly decrease of activity was observed for afritoxinones A and B at the concentration of 1.0 and 0.5 mg/ml. At these latter concentrations, **42** and **43** showed similar activity on leaves of all species tested. At the lower doses of 0.25 and 0.1 mg/ml both compounds were no phytotoxic.

In the cutting bioassay, the phytotoxicity was evaluated for tomato (*Lycopersicon esculentum* L. var. Marmande) and *Juniperus phoenicea* L. twigs. In the tomato cuttings bioassay, oxysporone (**44**) was shown to be phytotoxic. The cuttings treated with 0.2 and 0.1 mg/ml oxysporone (**44)** showed complete wilting within 48 h from the application. Symptoms of phytotoxicity (stewing on stem) were also observed with this compound at the lowest concentration tested of 0.05 mg/ml. Neither **42** and **43** demonstrated phytotoxic activity even at the highest concentration.

When tested on excised twigs of *Juniperus phoenicea* L., oxysporone (**44**) caused yellowing and browning on leaves and twig dieback at 0.2 and 0.1 mg/ml. No symptoms were observed at the lowest concentration used after 30 days from the treatment. Symptoms induced by oxysporone were similar to those observed in the field. The reproduction of many of the disease symptoms by oxysporone would give evidence of the role of toxin as a pathogenicity or virulence factor. These results highlight a significant decrease of phytotoxic activity for compounds **42** and **43** in comparison with **44**. As the γ-lactone is present in all three compounds (**42**-**44**), the decrease of phytotoxicity observed testing **42** and **43** is probably due to the modification of the functionalities of their dihydropyran ring. In fact, both afritoxinones A and B, in respect to oxysporone, showed the methoxylation of C-2 with consequent shift of the double bond from C(2)-C(3) to C(3)-C(4) and the dehydroxylation of C-4. However, as checked by inspection of the Dreiding

models of **42** and **43** compared to that of **44**, these modifications do not determine a different stereochemistry of the dihydropyran ring.

The effect on the phytotoxic activity of modification of the ring junction as well as that of the γ-lactone ring should be investigated by preparing suitable oxysporone derivatives.

5.3. Purification and identification of sphaeropsidones and sphaeropsidins A-C from *Diplodia cupressi* culture filtrate

As previously described, sphaeropsidone and episphaeropsidone (**22** and **23**, Fig. 4, Pag. 27) were isolated for the first time, but only in a limited amount, from the culture filtrates of *D. cupressi* a fungus involved in canker disease of cypress (*Cupressus sempervirens* L.), (Evidente *et al.*, 1998). Recently, a new strain of *D. cupressi* obtained from the Centraalbureau voor Schimmelcultures (CBS), was examinated and appeared to be a good producer of both **22** and **23**. This latter strain was used in this study to obtain adequate amounts of **22** and **23** (Fig. 4) and sphaeropsidins A-C (**16-18**, Fig. 3, Pag. 26) to investigate their biological activities. The fungus was grown in liquid cultures and the organic extract, showing a high phytotoxic activity was purified by a combination of CC and TLC as detailed in the Experimental part (Sheme 2, Pag.101). The main metabolite **22** (153.3 mg/l) was crystallized from EtOAc-*n*-hexane (1:5) obtaining white needles. The mother liquors of crystallization were further purified obtaining **23** (48.3 mg/l) as a homogeneous oil. From the most polar fraction, chlorosphaeropsidone and epichlorosphaeropsidone (**24** and **25**, Fig. 5, Pag. 32, 5.3 and 3.8 mg/l, respectively) were isolated as homogeneous oils. The ^{1}H NMR spectra of sphaeropsidone **22** and episphaeropsidone **23** (Fig. 32a and 32b, respectively) as well as the other spectroscopic

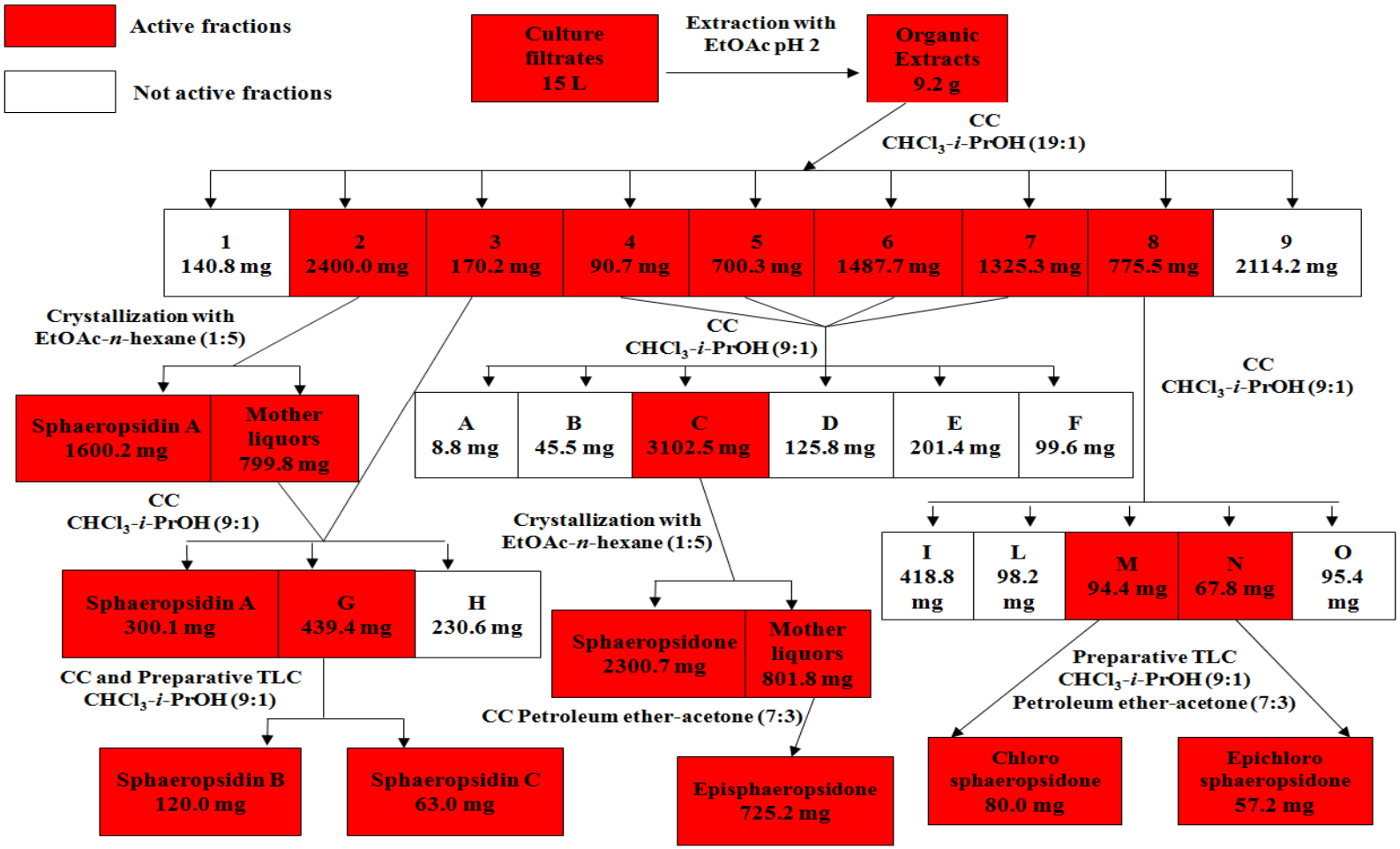

Scheme 2. Extraction and purification of *Diplodia cupressi* culture filtrates.

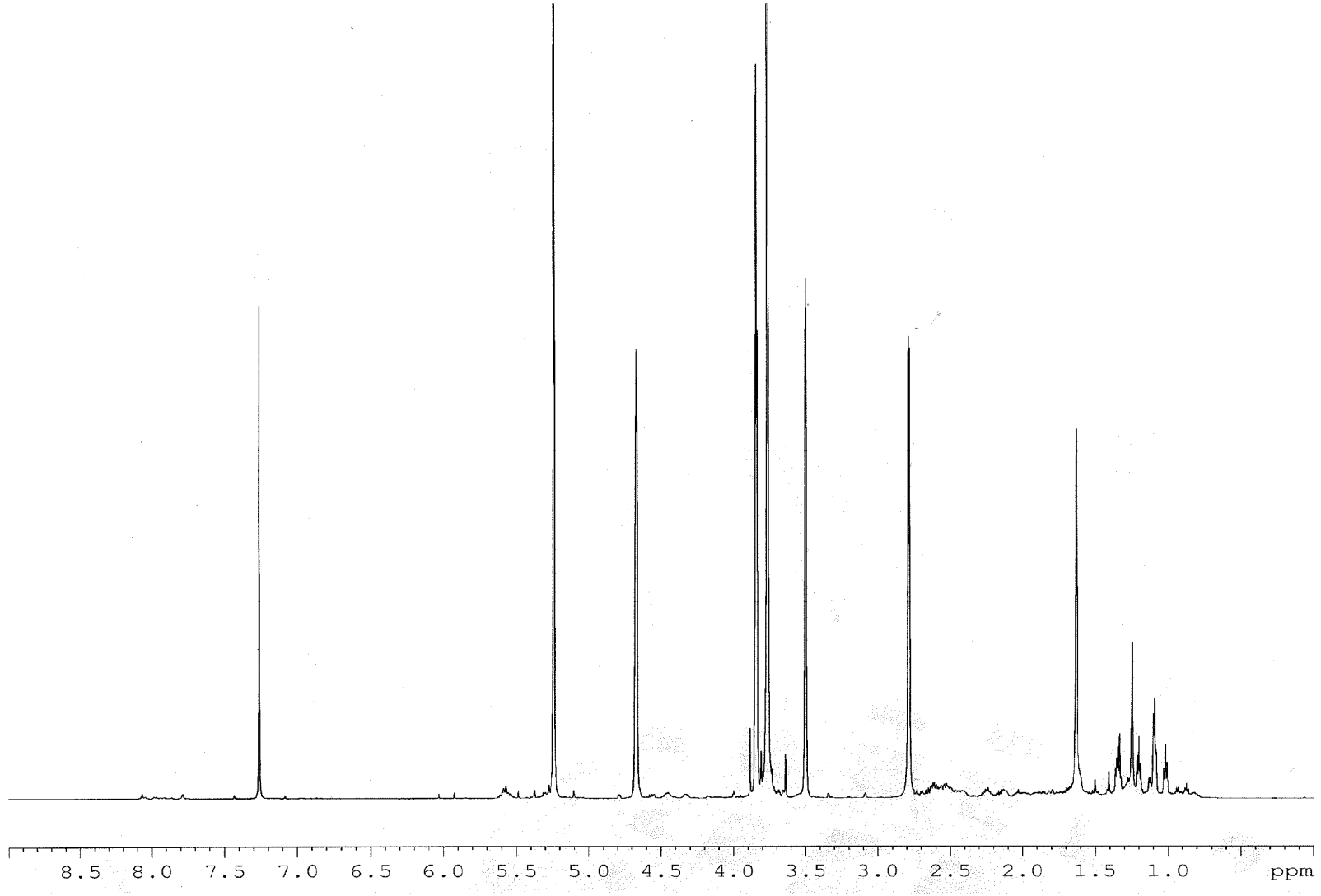

Figure 32a. ^{1}H NMR spectrum of sphaeropsidone (**22**), isolated from *D. cupressi* liquid culture, recorded in $CDCl_3$ at 400 MHz.

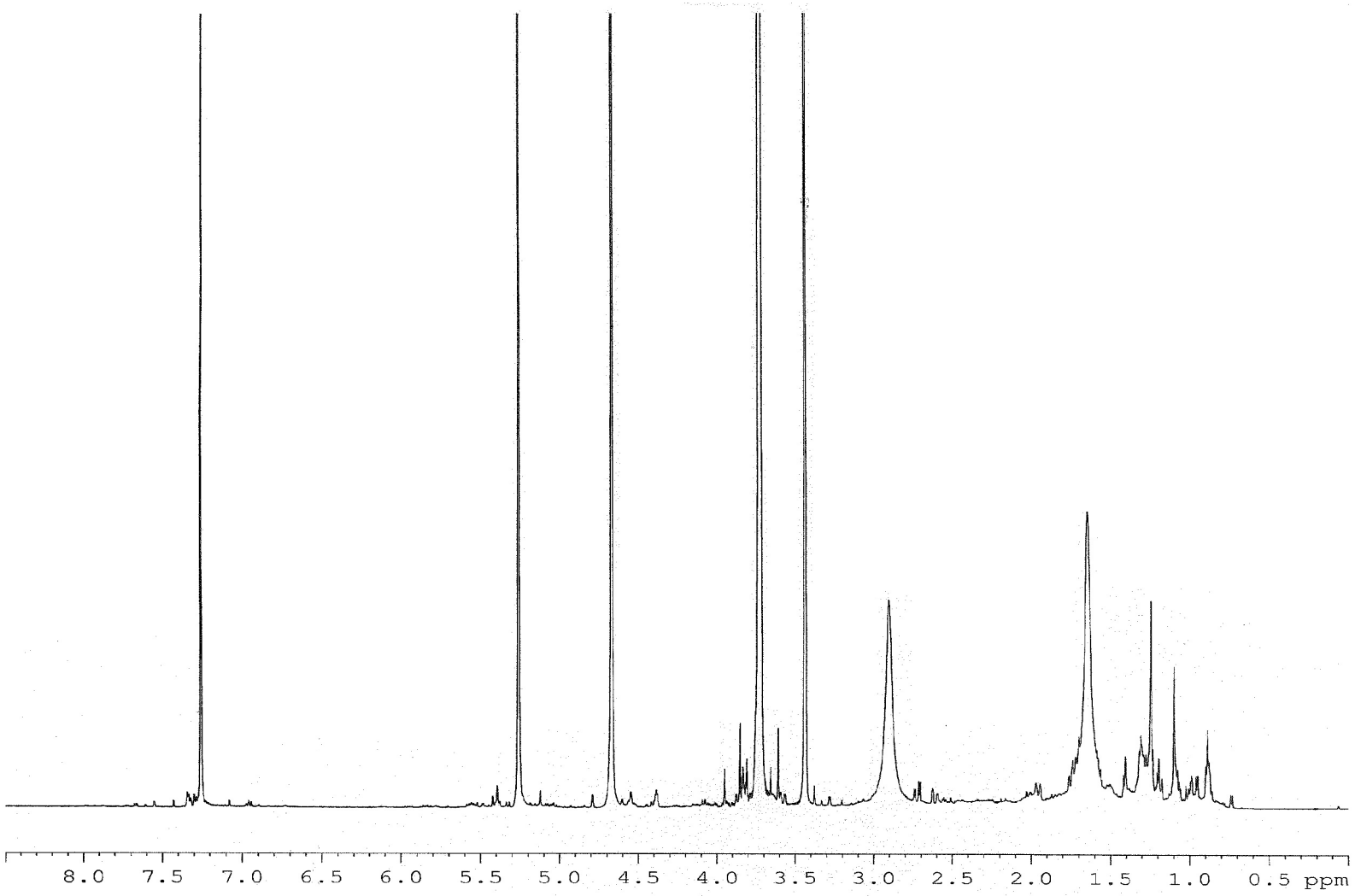

Figure 32b. ^{1}H NMR spectrum of episphaeropsidone (**23**), isolated from *D. cupressi* liquid culture, recorded in $CDCl_3$ at 400 MHz.

(^{13}C NMR and ESIMS) and physical ($[\alpha]_D^{25}$) data of both compounds were identical to those previously reported (Evidente *et al.*, 1998). From the less polar fractions sphaeropsidins A-C (**16-18**, Fig. 3, 126.6, 8 and 4.2 mg/l, respectively) were isolated. **16** was crystallized from EtOAc-*n*-hexane (1:5) obtaining colorless needles. The ^{1}H-NMR spectra of **16**, **17** (Fig. 33a and 33b, respectively) and **18,** as well as the other spectroscopic (^{13}C NMR and ESIMS) and physical ($[\alpha]_D^{25}$) data of these compounds were identical to those previously reported (Evidente *et al.*, 1996 and 1997).

5.4. X-ray structural analysis of sphaeropsidone

The availability of large amount of sphaeropsidone (**22**, Fig. 5) allowed its easy crystallization for an X-ray structural analysis to assign the relative and absolute stereochemistry of sphaeropsidones. White needles of **22** were re-crystallized from $CHCl_3$-benzene (1:1) to obtain crystals suitable for single crystal X-ray analysis. An ORTEP (Farrugia, 1997) view of sphaeropsidone **22** is shown in Fig. 34, selected bond lengths, bond angles and torsion angles are reported in Table 2.Compound **22** crystallize in $P2_1$ space group with two independent molecules in the asymmetric unit (A and B) with slightly different conformations and joined by intermolecular OH···O=C hydrogen bond (Fig. 34). Bond lengths and angles in **22** are in the normal range and in agreement with similar compounds (Allen *et al.*, 1987; Carreno *et al.*, 2007). In the six-membered ring, the geometry around C2, C3 and C4 confirms the presence of the cycloexene double bond and of the ketone group (C3-C4 = 1.338(6), 1.337(6)Å, C2-O1 = 1.220(6), 1.222(6) Å for A and B). The shortness of C1-C6 bond length reflects the strain due to the epoxide ring (C1-C6 = 1.456(6), 1.459(6) Å for A and B). As already found (Fex and Wickberg, 1981; Kis *et al.*, 1970;), the cycloexene ring adopts a very flat boat conformation with C2 and C5

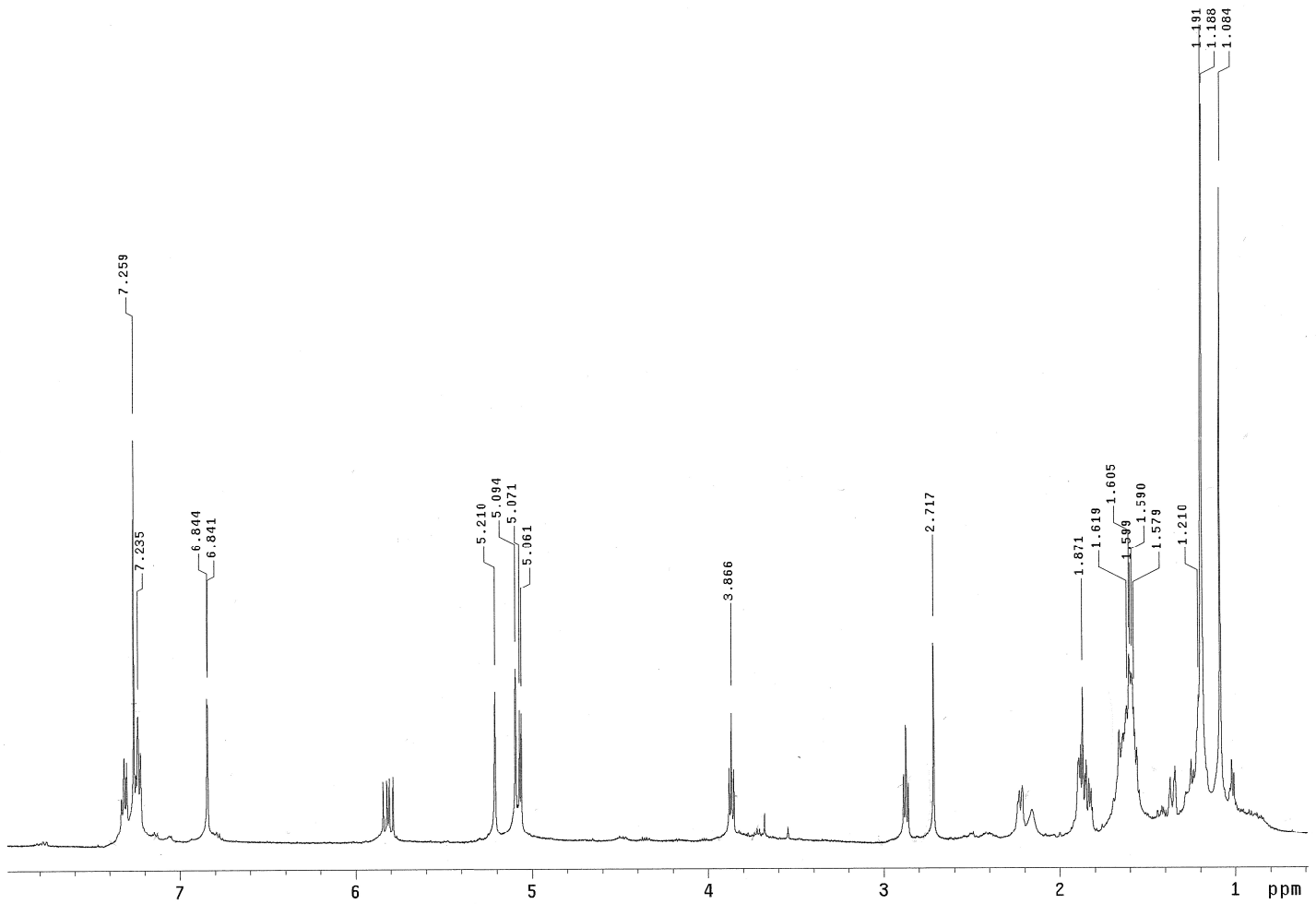

Figure 33a. ^{1}H NMR spectrum of sphaeropsidin A (**16**), isolated from *D. cupressi* liquid culture, recorded in $CDCl_3$ at 600 MHz.

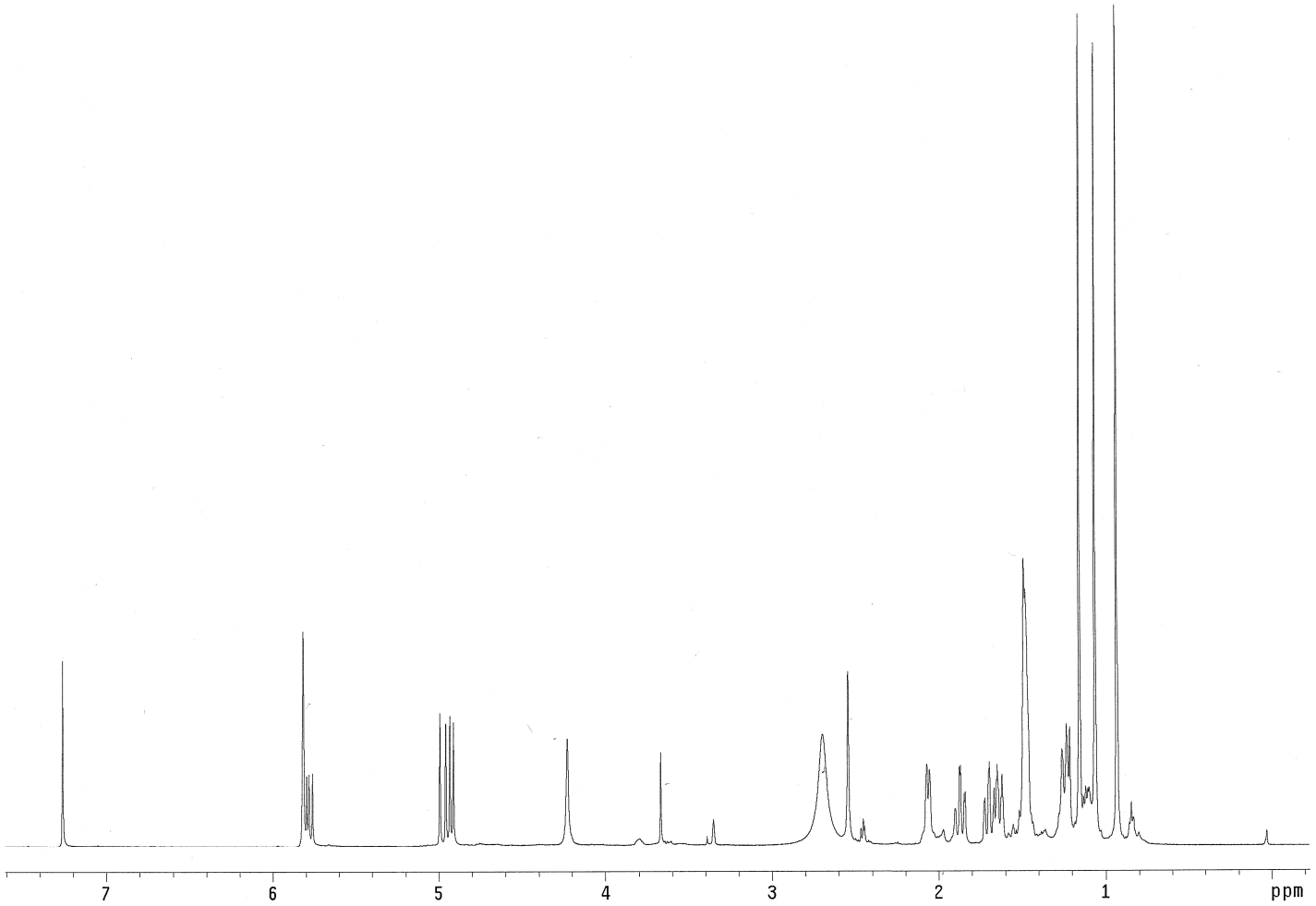

Figure 33b. ^{1}H NMR spectrum of sphaeropsidin B (**17**), isolated from *D. cupressi* liquid culture, recorded in $CDCl_3$ at 600 MHz.

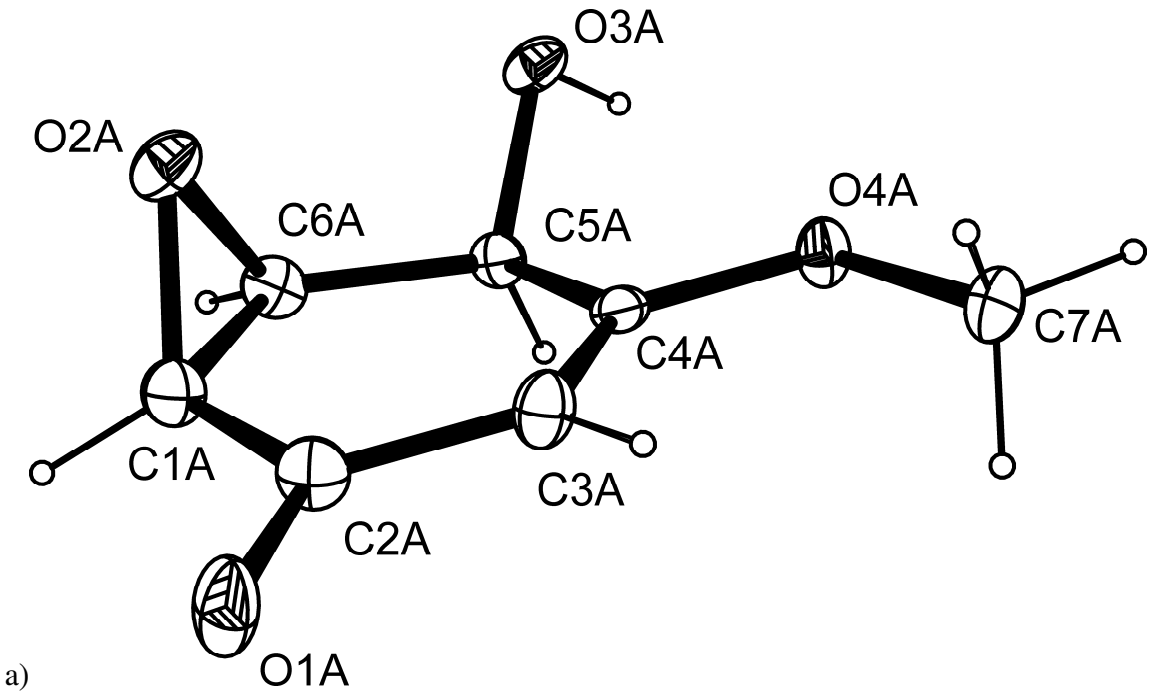

a)

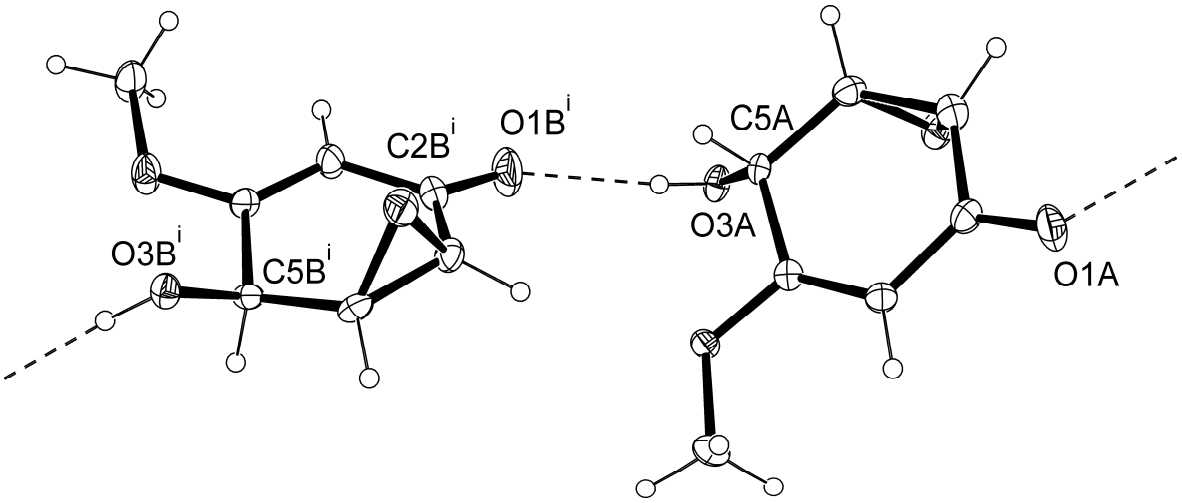

b)

Figure 34. a) ORTEP view of sphaeropsidone (**22**) and b) intermolecular OH···O=C head-to-tail hydrogen bonding pattern between the two independent molecules A and B of sphaeropsidone (**22**).

Table 2. Crystal data and structure refinement details for sphaeropsidone (**22**).

Chemical formula	$C_7H_8O_4$
Formula weight	156.13
Temperature, K	173(2)
Radiation, wavelength, Å	Mo Kα, 0.71073
Crystal system	Monoclinic
Space group	$P2_1$
a , Å	4.1280(6)
b , Å	13.161(2)
c , Å	13.333(3)
β , deg	90.14(1)
V , Å^3	724.4(2)
Z, D_{calc} , Mg/m^3	4, 1.432
Absorption coefficient, mm^{-1}	0.119
Theta range, deg	3.06 - 27.48
Reflections collected / unique	4603 / 2759 [R(int) = 0.0381]
Data / restraints / parameters	2759 / 1 / 201
Final R indices , [I>2σ (I)]	R1 = 0.0433, wR2 = 0.0821
R indices (all data)	R1 = 0.0916, wR2 = 0.0944
Largest diff.peack and hole, e/Å^3	0.159 and -0.170
CCDC deposition number	794356

atoms flipping away from oxirane oxygen atom. In fact, the maximum deviation from least square plane C1/C3/C4/C6 is 0.003(3) Å for A and B, C2 and C5 distances from the least square plane are 0.008(3) and 0.007(3) Å for A [0.008(3) and 0.008(29) Å for B]. The methoxy group is quite in plane with cycloexenone ring with the methyl group pointing towards the vinyl hydrogen atom. The hydroxyl group and the epoxide ring are mutually *cis* positioned and the absolute configuration at C1,C5,C6 was assigned as 1*S*,5*R*,6*S* on the basis of a previous theoretical study (Mennucci *et al.*, 2007). In the same study, a high energy barrier was found to prevent the free rotation of OH group and in the most stable conformer, the oxirane O atom was involved as acceptor in intramolecular OH···O hydrogen bond. As a consequence, the *anti* arrangement of hydrogen atoms in H-O-C-H fragment was observed. At variance with these results, no intramolecular hydrogen bonds are found in **22** (Fig. 34).The OH group is, in fact, involved in a strong intermolecular hydrogen bond with the carbonyl oxygen atom of an adjacent molecule, while the oxirane O atom is involved only in weak CH···O intermolecular interactions (Table 2). As can be observed in Fig. 35, a roughly eclipsed conformation of H-O3-C5-H fragment is observed. In the crystal packing the molecules are head-to-tail joined through strong intermolecular OH···O=C hydrogen bonds. In this way, infinite linear chains of molecules having $C_2^2(14)$ graph set symbol (Bernstein *et al.*, 1995) and running along [0 0 1] direction are formed (Fig. 35). The infinite chains of molecules are arranged into layers that roughly lie in (0 1 1) plane. In this way a stacking of layers of molecules in [1 0 0] direction is obtained. Only weak CH···O intermolecular interactions are found between the adjacent layers (Fig. 35). These data confirmed the structure and abosolute stereochemistry previously assigned as 1*S*,5*R*,6*S* to (-)-spheropsidone and 1*S*,5*S*,6*S* to (-)-epispheropsidone by application of the time-dependent density functional theory (TDDFT) calculation of the optical rotation (Mennucci *et al.*, 2007).

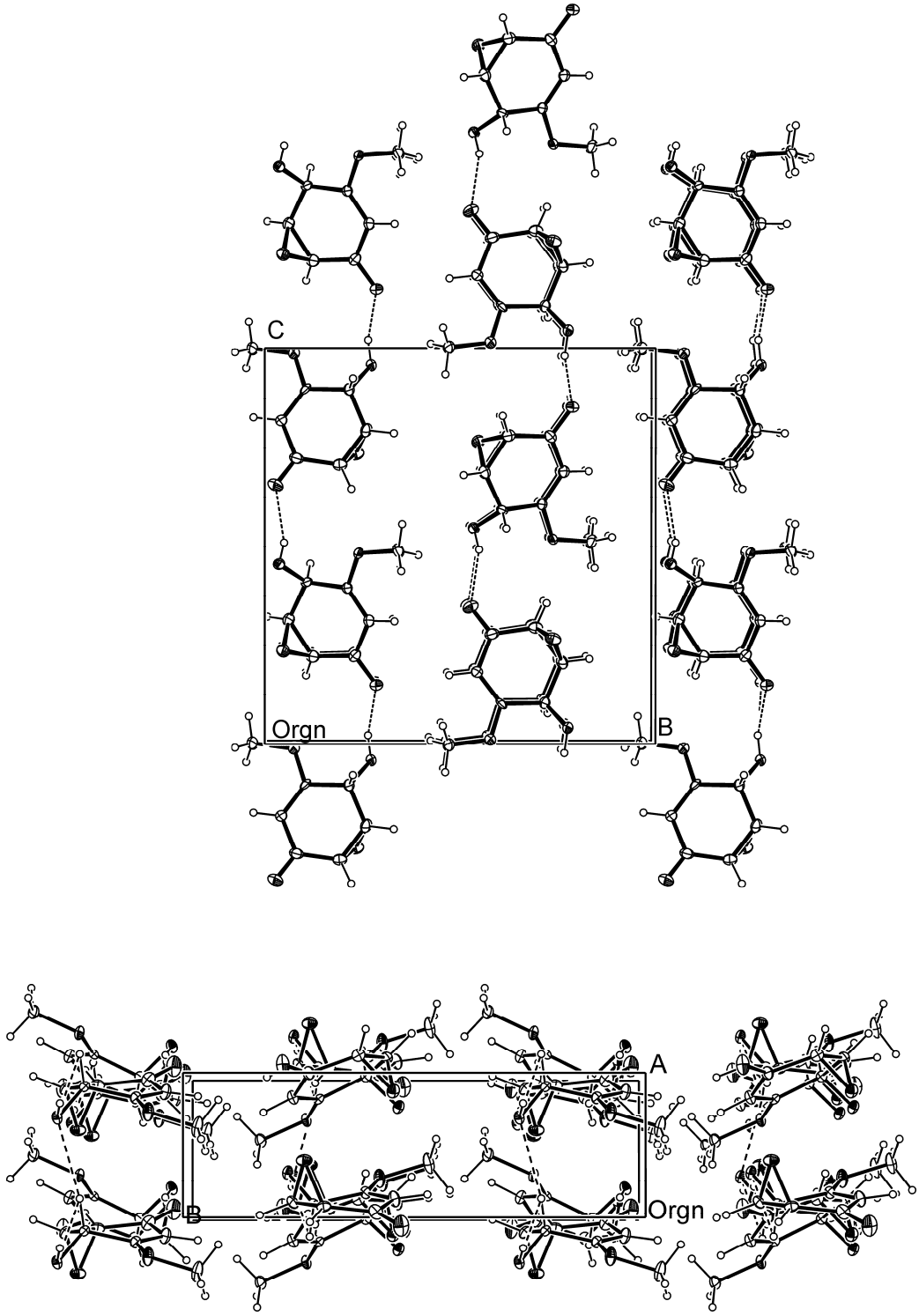

Figure 35. Crystal packing viewed along *a* and *c* axes of sphaeropsidone (**22**).

5.5. Hemisynthesis and chemical characterization of sphaeropsidones derivatives

To investigate the phytotoxic and antifungal activities of sphaeropsidones with a structure-activity relationship study, eight derivatives (**45**–**52**, Scheme 3 and 4) were prepared by chemical transformation of the functionalities present in **22** and **23** as detailed in the Experimental part. The aim was to identify which structural features essential for the biological activities of these compounds, in order not only to understand their mechanism of action on plants and their true role in pathogenesis, but also to generate new compounds with potential application in agriculture.

The structural features of **22** and those of the naturally-occurring episphaeropsidone (**23**) provide evidence for considering the latter as a naturally modified analogue of **22**.

The structures assigned to the new derivatives of sphaeropsidones (**45-50**) and episphaeropsidones (**51** and **22**) were determined by comparing their UV, IR, ^{1}H and ^{13}C NMR, and EI or ESI MS spectra with those of **22** and **23**, respectively. In particular, the structures assigned to derivatives **49** and **50** were also supported by the couplings observed in their COSY, HSQC, HMBC and NOESY spectra.

By acetylation, sphaeropsidone (**22**) was converted into the corresponding 5-*O*-acetylderivative (**45**, Scheme 3), and into the 2,4,5-triacetylanisole (**46**, Scheme 3).

The IR spectrum (Fig. 36) of **45,** compared with **22**, showed the very typical bands of the acetyl group and that of the ester group (Nakanishi and Solomon, 1977) but also the significant lack of the characteristic band of hydroxyl groups. As expected, the UV spectrum (Fig. 37) had the same absorption maximum at 251 nm of **22** (Scott, 1964). These data supported the presence of the acetyl group that was confirmed by the ^{1}H NMR spectrum. In fact, this latter showed the singlet of MeCO at δ 2.24 and the downfield shift ($\Delta\delta$: 1.29) of the proton H-5 resonating as doublet at δ 5.96 (Pretsch *et al.*, 2000). The HREI MS spectrum of **45** showed the molecular ion at *m/z* 198 $[M]^{+}$ and the significant

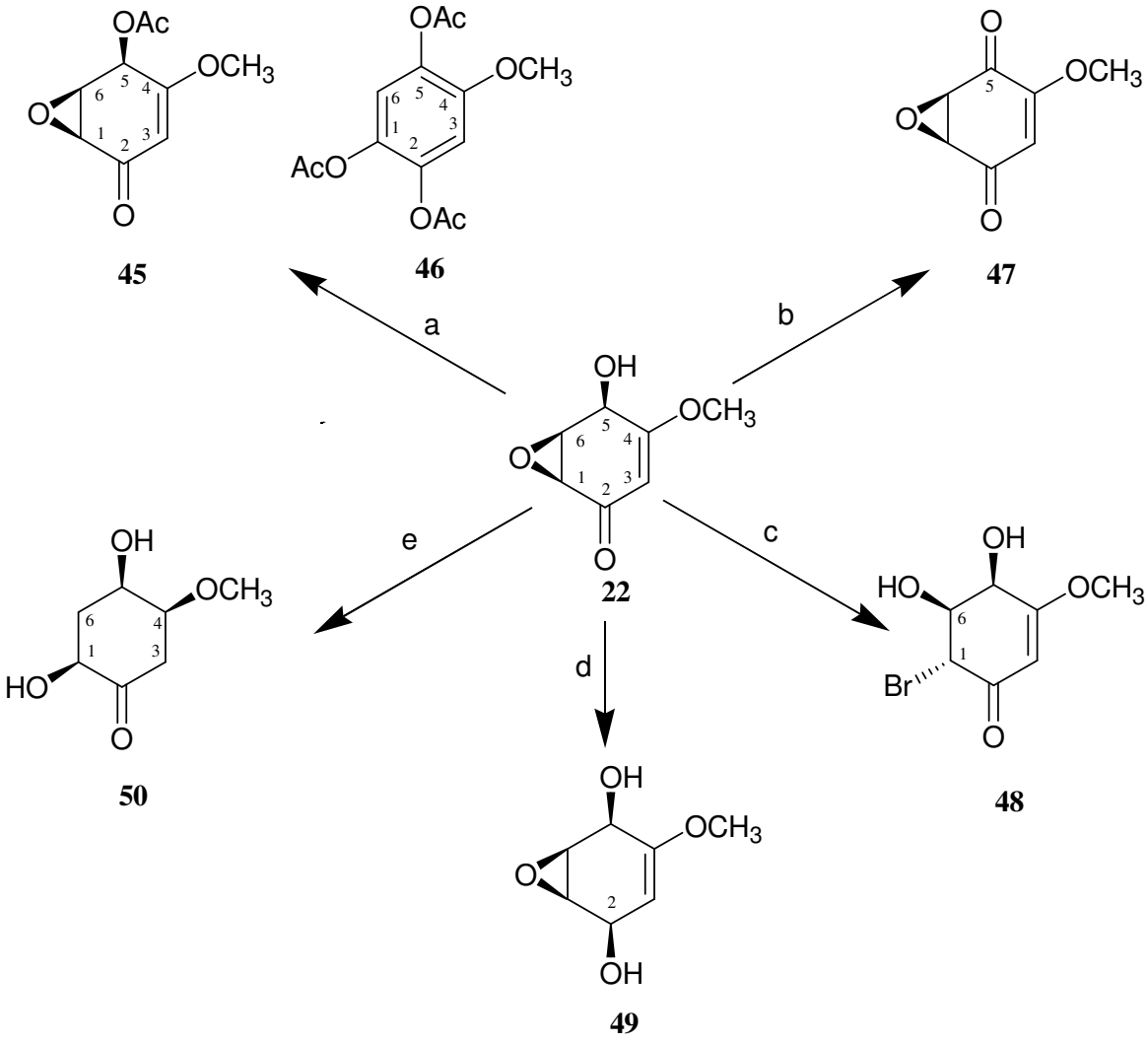

[a]Reagents and conditions: (a) Ac_2O, pyridine, 80 °C, 30 min; (b) MnO_2, CH_2Cl_2, rt, 1 h; (c) Li_2NiBr_4, THF, rt, 30 min; (d) $NaBH_4$, MeOH, rt, 30 min; (e) H_2, Pd 10%, MeOH, rt, 2 h.

Scheme 3. Hemisynthesis of sphaeropsidone derivatives (**45**-**50**).[a]

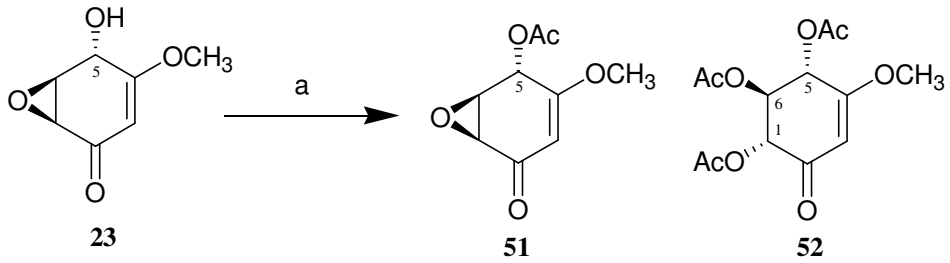

23 **51** **52**

[a]Reagents and conditions: (a) Ac_2O, NaOAc, 80 °C, 30 min.

Scheme 4. Hemisynthesis of episphaeropsidone derivatives (**51**-**52**).[a]

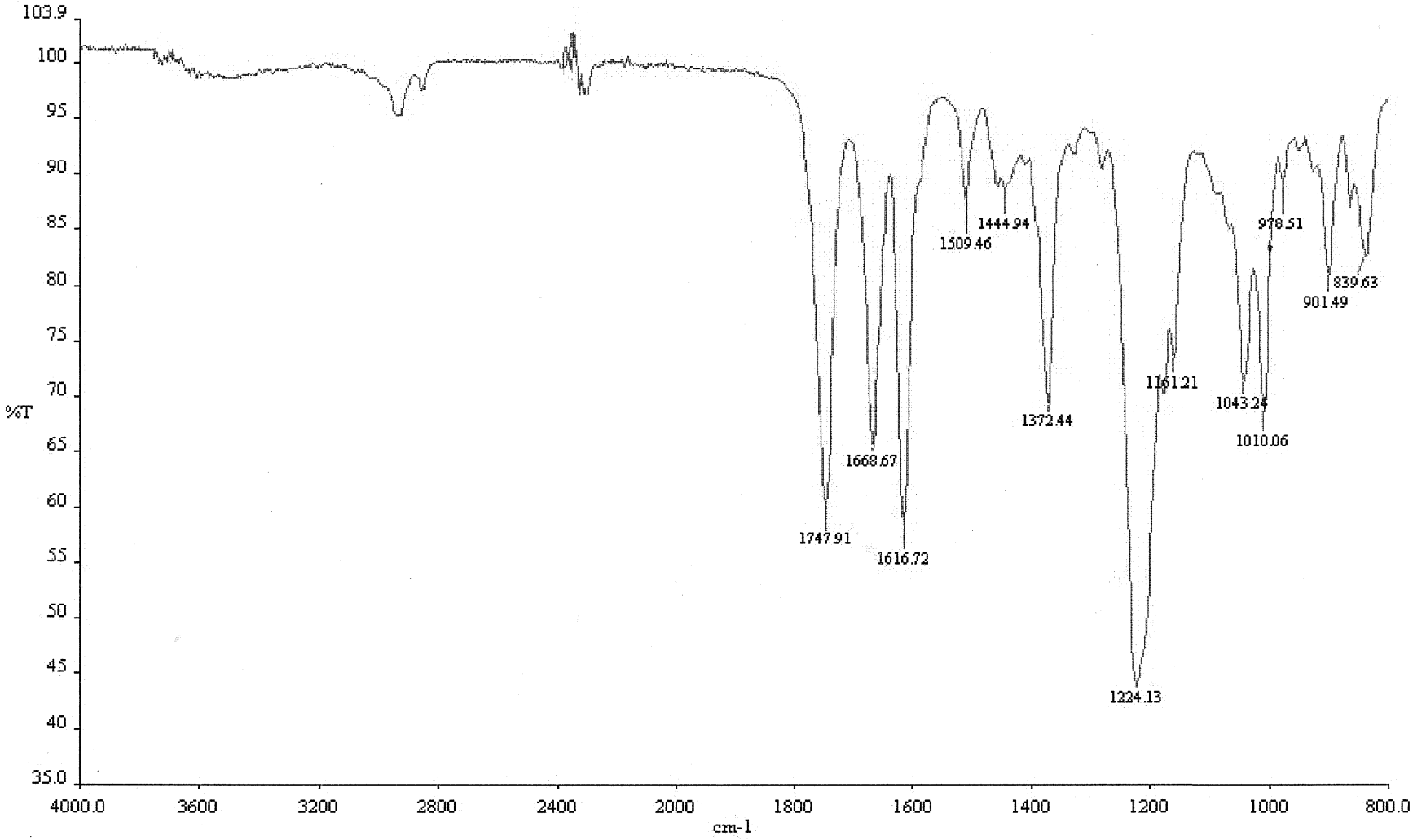

Figure 36. IR spectrum of 5-*O*-acetylsphaeropsidone (**45**), recorded as glassy film.

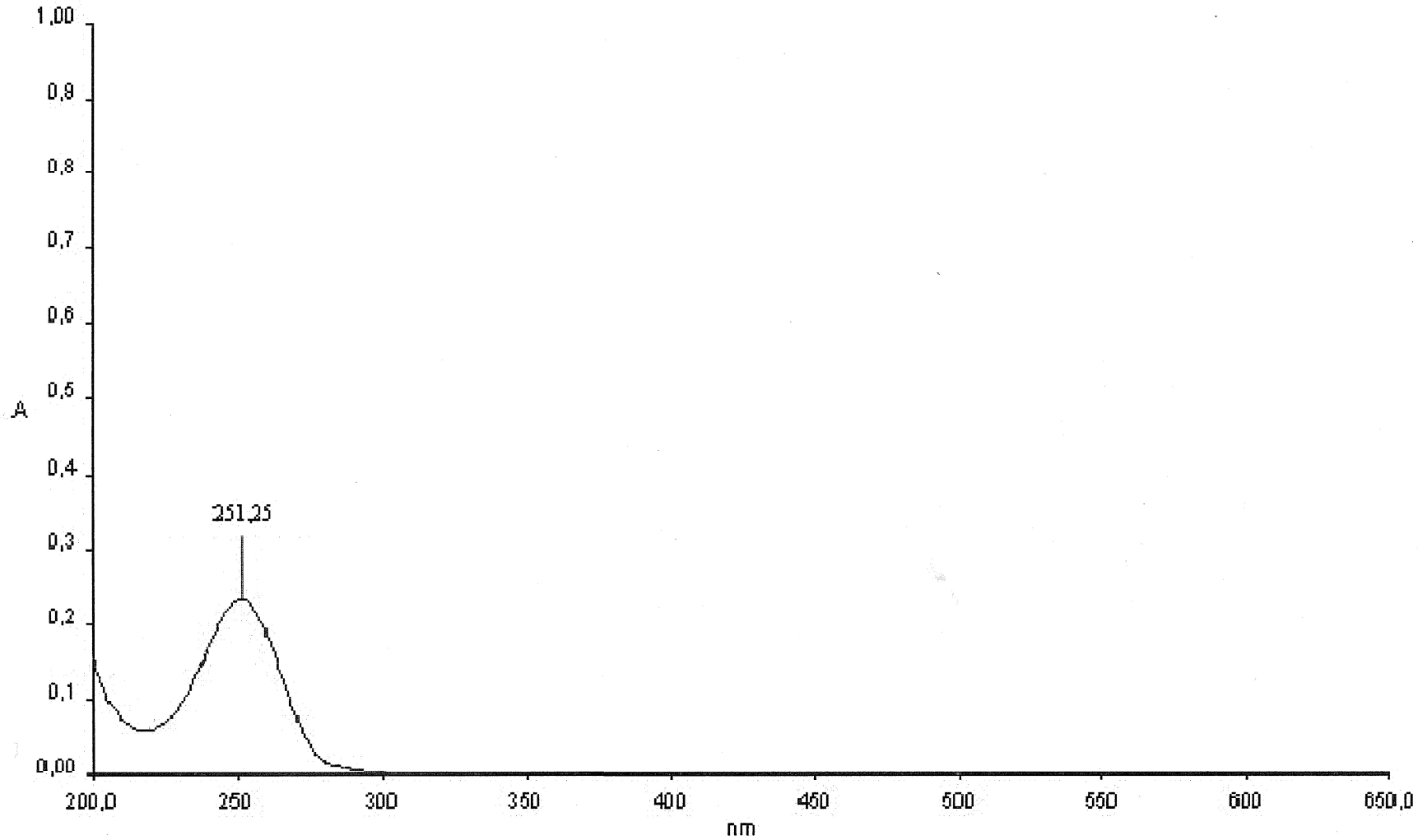

Figure 37. UV spectrum of 5-*O*-acetylsphaeropsidone (**45**), recorded in MeCN solution.

ions generated by consecutive losses of CH_2CO, Me, and CO residues at *m/z* 156, 141 and 113. The ion at *m/z* 156, by the alternative loss of HCO, produced the ion at *m/z* 127.

46 showed strong structural modification relative to **22**, with the acetylation of the same hydroxy group at C-5 of **45** but also the aromatisation of the cyclohexenone. The IR spectrum of **46** (Fig. 38), compared to **45**, showed only one band for the carbonyls of the three acetyl groups, the typical band of an aromatic residue and three bands of the ester groups. The UV spectrum (Fig. 39) showed a typical adsorption maximum of a suitable substituted aromatic ring. The ^{1}H NMR spectrum showed the typical system of two meta-coupled protons of a 1,2,4,5 tetrasubstituted aromatic ring at δ 6.94 and 6.79; the presence of four singlets, one of the expected methoxy group at δ 3.80 and three of the acetyl groups at δ 2.29, 2.28 and 2.25. The EI MS spectrum of **46** showed the molecular ion at *m/z* 282 $[M]^+$ which, by consecutive loss of 3 CH_2CO residues followed by Me and CO residues generate the ions at *m/z* 240, 198, 156, 141 and 113. The ion at *m/z* 156, by the alternative loss of HCO, produced the ion at *m/z* 127.

The allylic hydroxy group at C-5 was oxidised with activated MnO_2 (Scheme 3) yielding the corresponding 1,4-dione derivative (**47**) in which the cyclohexene ring lost conformational flexibility having only the epoxy oxygen projecting from the plane. The ESI MS spectrum of **47** (Fig. 40) showed the potassium and sodium clusters and the pseudomolecular ions at *m/z* 193, 177 and 155. The IR spectrum (Figure 41) of **47**, compared to **22,** showed a further α-β unsaturated ketone group and the lack of the hydroxy group band. The UV spectrum showed the typical absorption of an α-β unsaturated dienone system. The ^{1}H NMR spectrum (Fig. 42) of **47**, compared to **22**, showed the lack of the proton (H-5) of the secondary idroxylated carbon (C-5) while the proton H-6 resonated as singlet at δ 3.86.

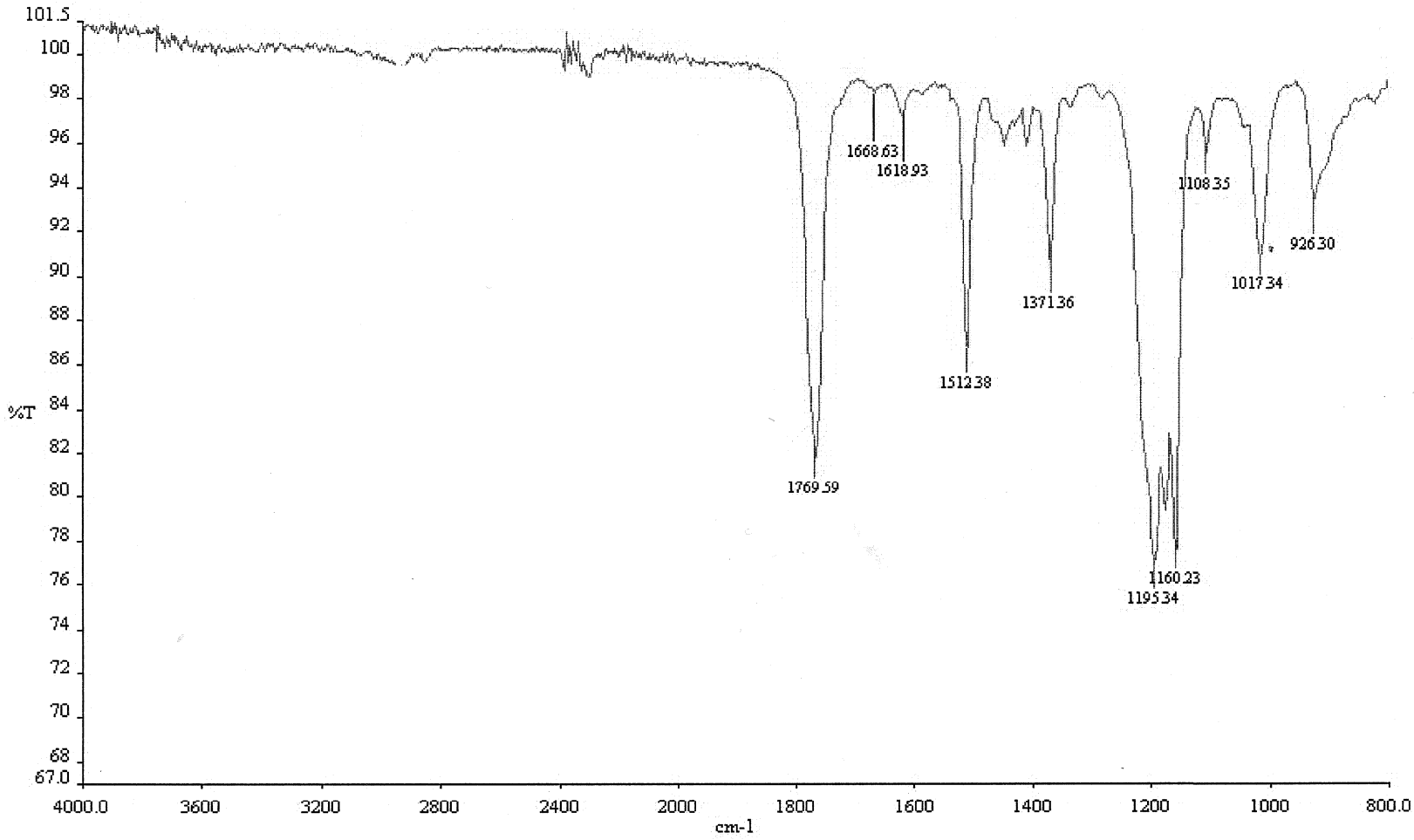

Figure 38. IR spectrum of 2,4,5-triacetylanisole (**46**), recorded as glassy film.

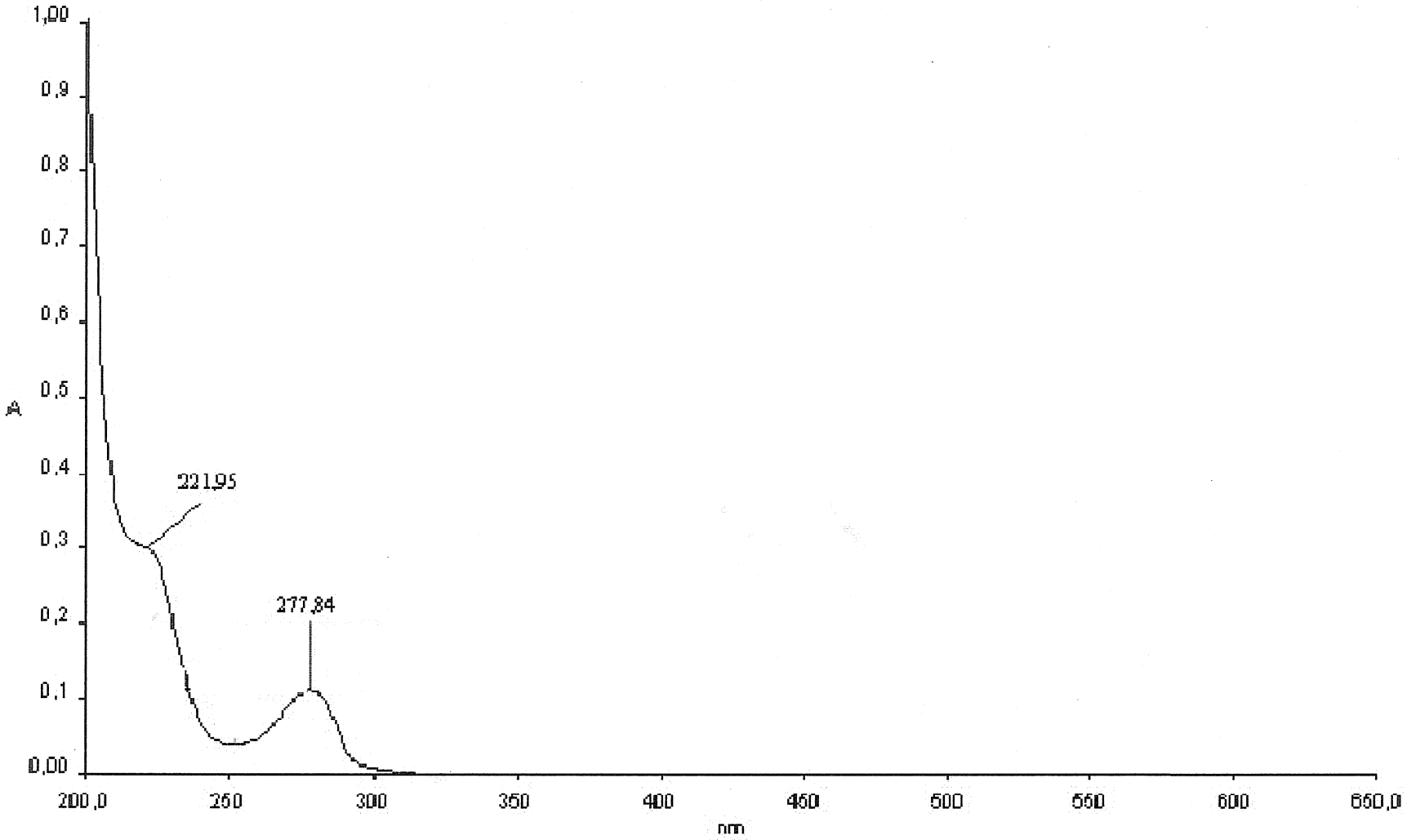

Figure 39. UV spectrum of 2,4,5-triacetylanisole (**46**), recorded in MeCN solution.

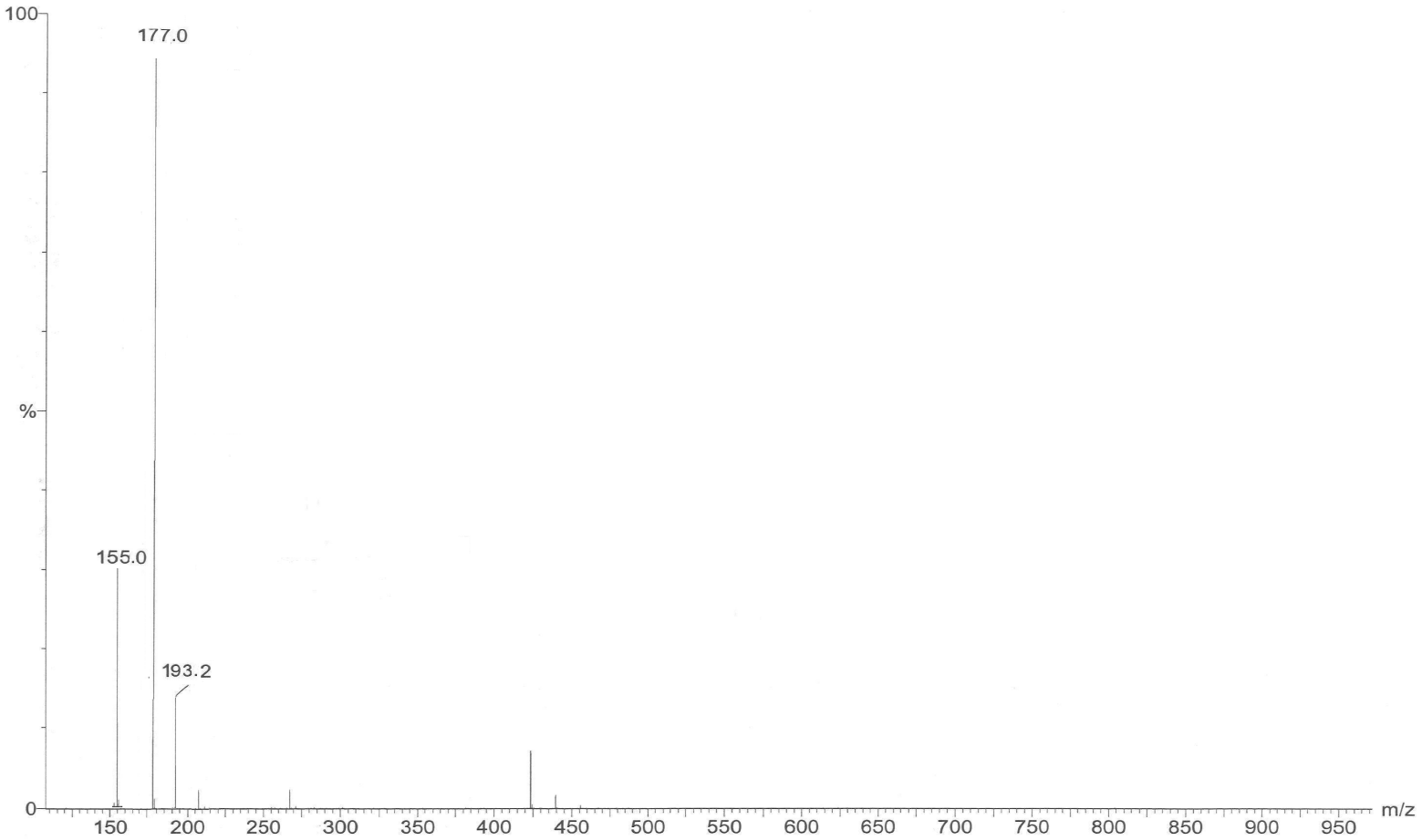

Figure 40. ESI MS spectrum of 5,*O*-didehydrosphaeropsidone (**47**), recorded in positive modality.

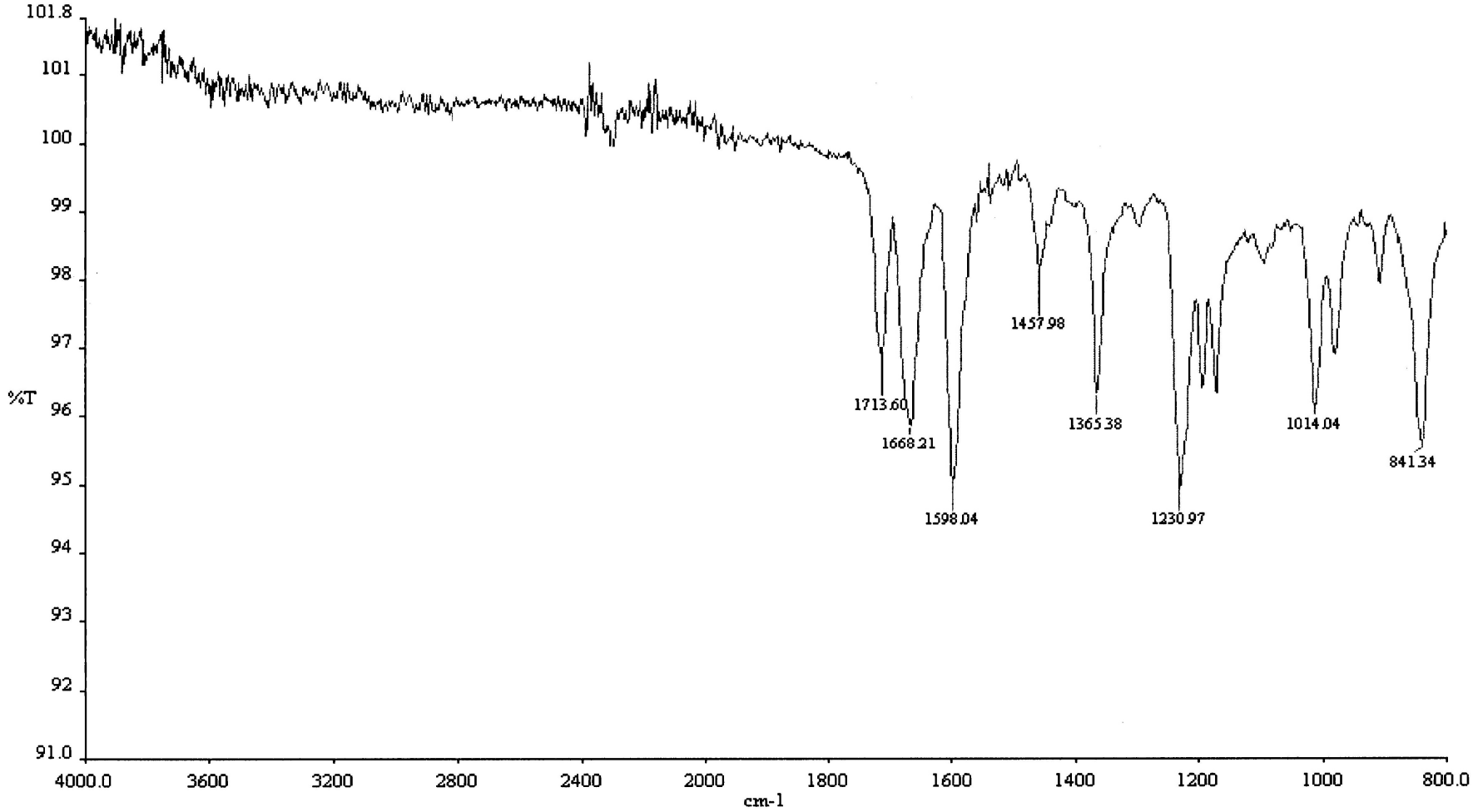

Figure 41. IR spectrum of 5,*O*-didehydrosphaeropsidone (**47**), recorded as glassy film.

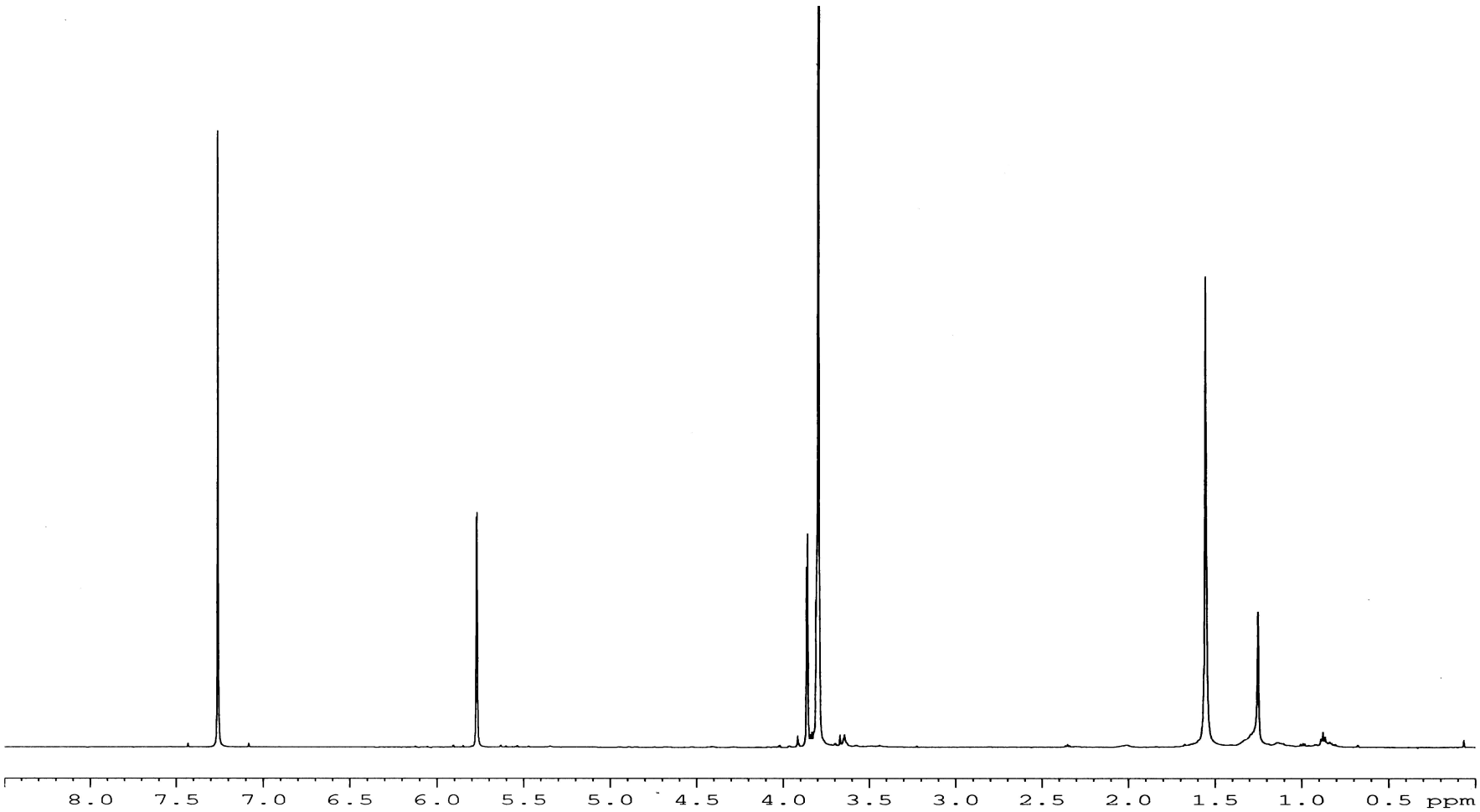

Figure 42. ^{1}H NMR spectrum of 5,*O*-didehydrosphaeropsidone (**47**), recorded in $CDCl_3$ at 600 MHz.

The stereoselective epoxy ring opening that converted **22** into the corresponding bromohydrin (**48**, Scheme 3), was performed with dilithium tetrabromonickelate, a source of "soft" bromide, which also provide a "hard" but mild electrophile (i.e. Li^+), (Dawe et al., 1984). As expected, the IR (Fig. 43) and the UV (Fig. 44) spectra of **48** were very similar to those of **22**. The ^1H NMR spectrum (Fig. 45), compared to that of **22**, showed the significant downfield shifts of H-5 and H-6 ($\Delta\delta$: 1.06 and 0.82) resonating as doublet and double doublet at δ 4.54 and 4.32. The EI MS spectrum showed the typical pattern of bromurated and not bromurated ions. In fact were observed the couple of ions at *m/z* 238 and 236 due to the $[M+2]^+$ and $[M]^+$, which by loss of H_2O generated the couple of ions at 220 and 218 respectively. Furthermore the molecular ion by successive losses of HBr, OH and Me residues, produced the ions at *m/z* 156, 139 and 114. The stereochemistry of the bromohydrin **48** was deduced by the coupling constants measured in its ^1H NMR spectrum and by its agreement with the mechanism of reaction which provide the nucleophilic attack of bromide at the less hindered C-1 and from the α-side opposite to the epoxy ring (Dawe *et al.*, 1984). Consequently, the bromohydrin **48** assumes a half-chair conformation with the C-6 hydroxy group assuming a β-orientation. The values of 6.0 and 3.5 Hz measured in the ^1H NMR spectrum (Fig. 45) for the coupling constants between H-6 with H-1 and H-5, respectively, justify the location of H-1 β-pseudoaxial, H-5 α-pseudoaxial, and H-6 α-pseudoequatorial (Pretsch *et al.*, 2000). This configuration is also in agreement with a Dreiding model of **48**.

Reduction with $NaBH_4$ (Scheme 3) converted **22** into the corresponding 1,4-diol derivative (**49**), which differed from sphaeropsidone only by the reduction of the α,β-unsaturated carbonyl group with consequent increase of the cyclohexene ring flexibility.

The ESI MS spectrum (Fig. 46) of **49** showed the potassium and sodium clusters and the pseudomolecular ions at *m/z* 197, 181 and 159. The IR spectrum (Fig. 47), compared to

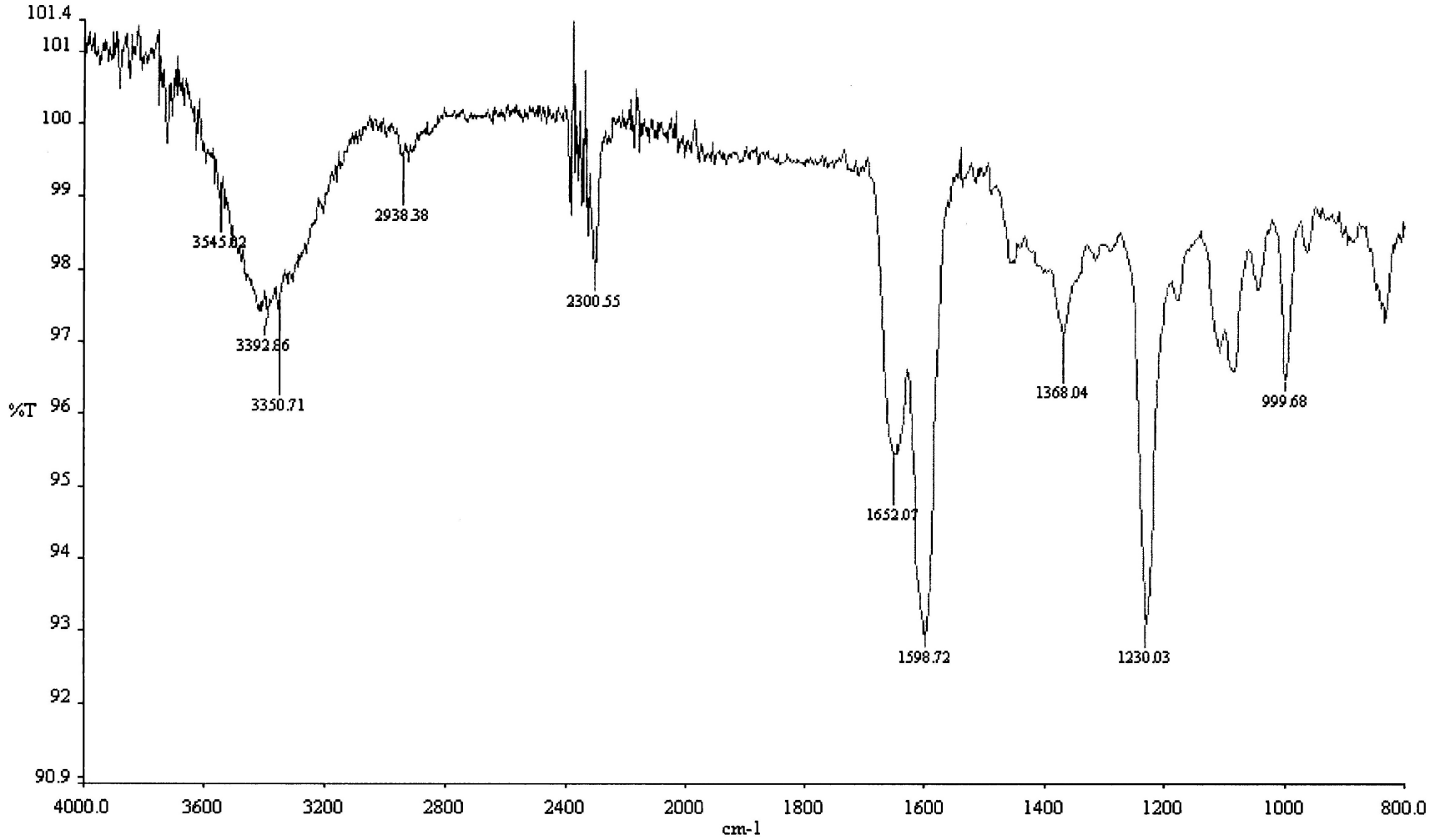

Figure 43. IR spectrum of 6-bromo-4,5-dihydroxy-3-methoxycycloex-2-enone (**48**), recorded as glassy film.

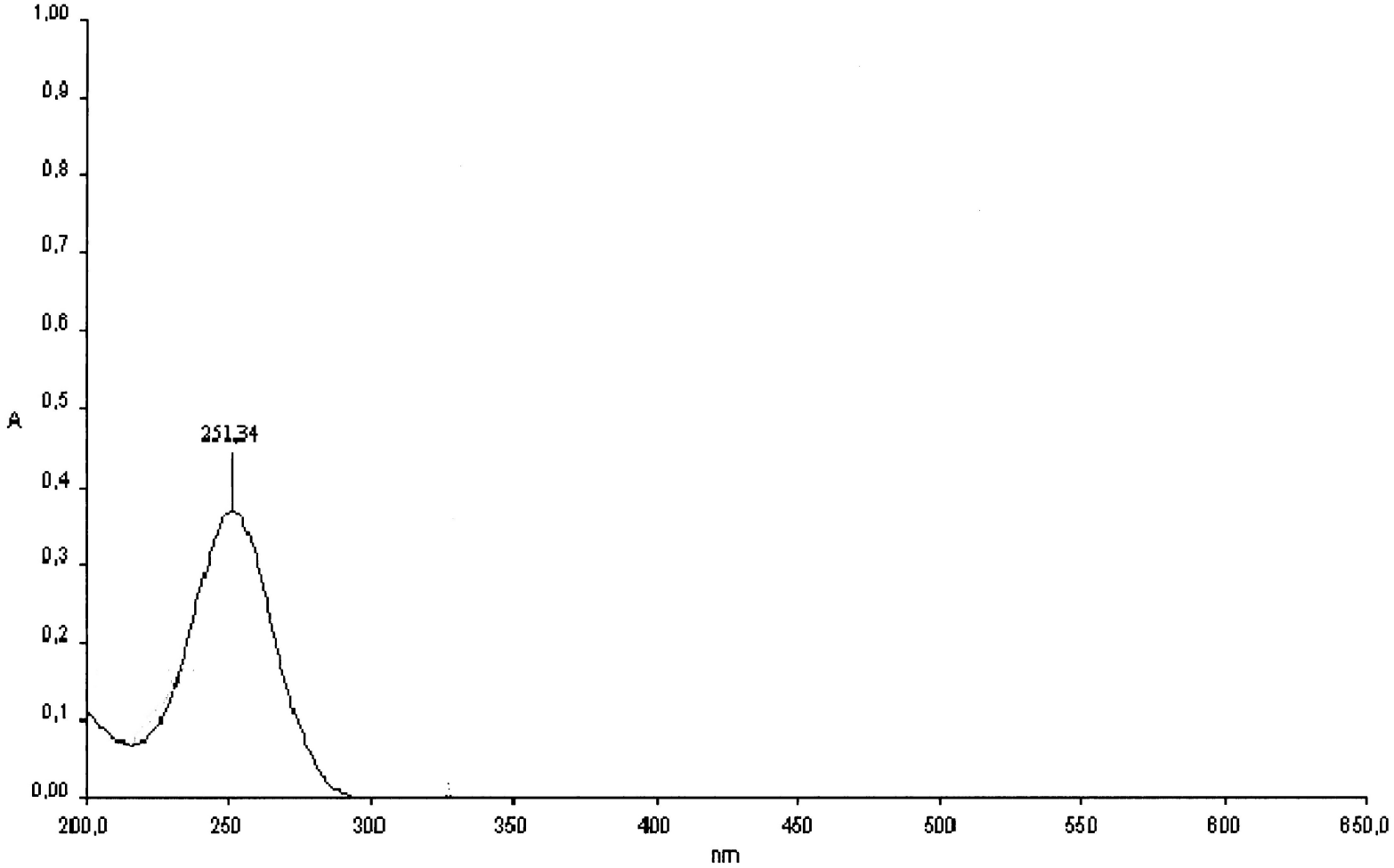

Figure 44. UV spectrum of 6-bromo-4,5-dihydroxy-3-methoxycycloex-2-enone (**48**), recorded in MeCN solution.

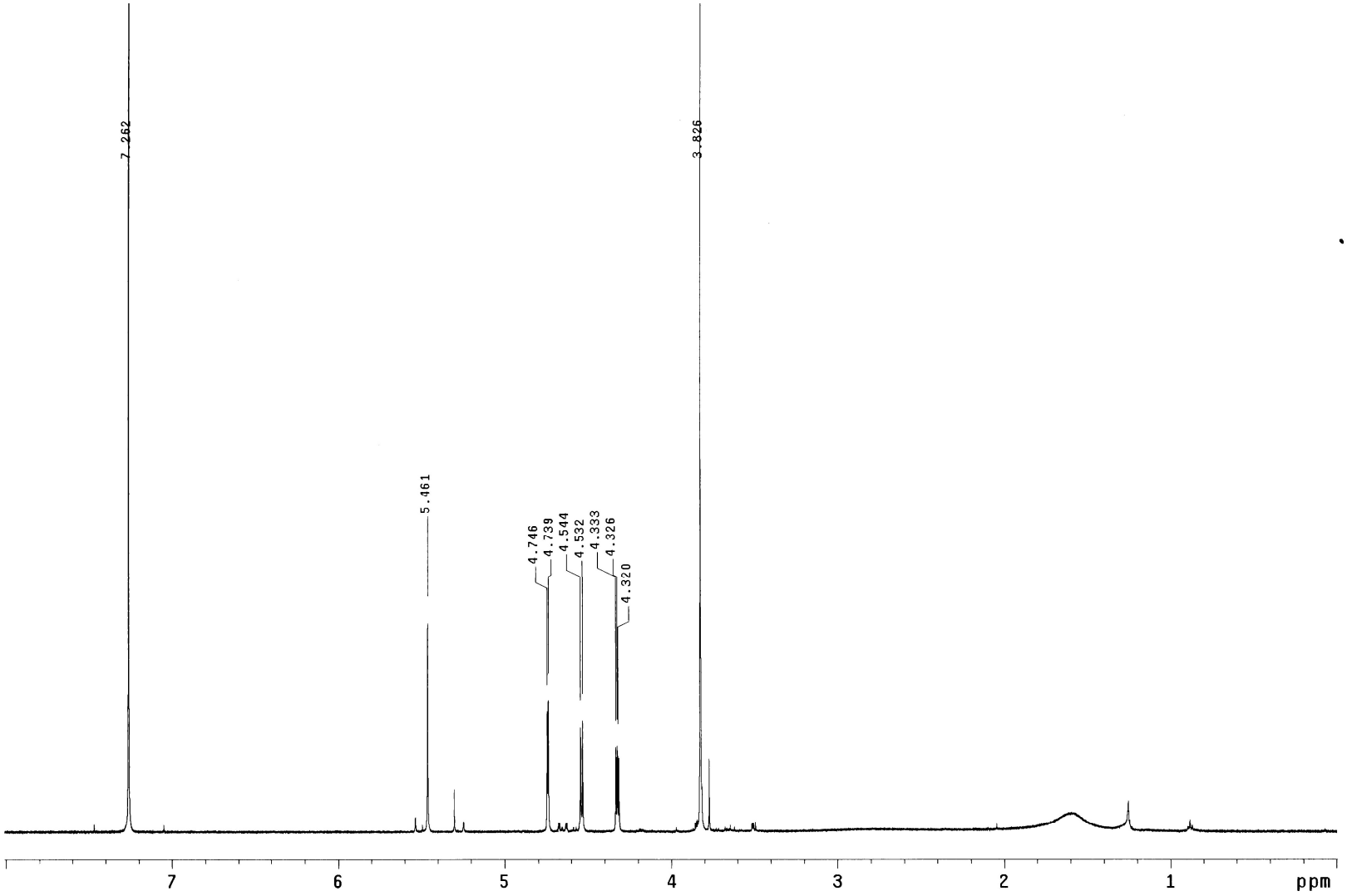

Figure 45. ^{1}H NMR spectrum of 6-bromo-4,5-dihydroxy-3-methoxycycloex-2-enone (**48**), recorded in $CDCl_3$ at 600 MHz.

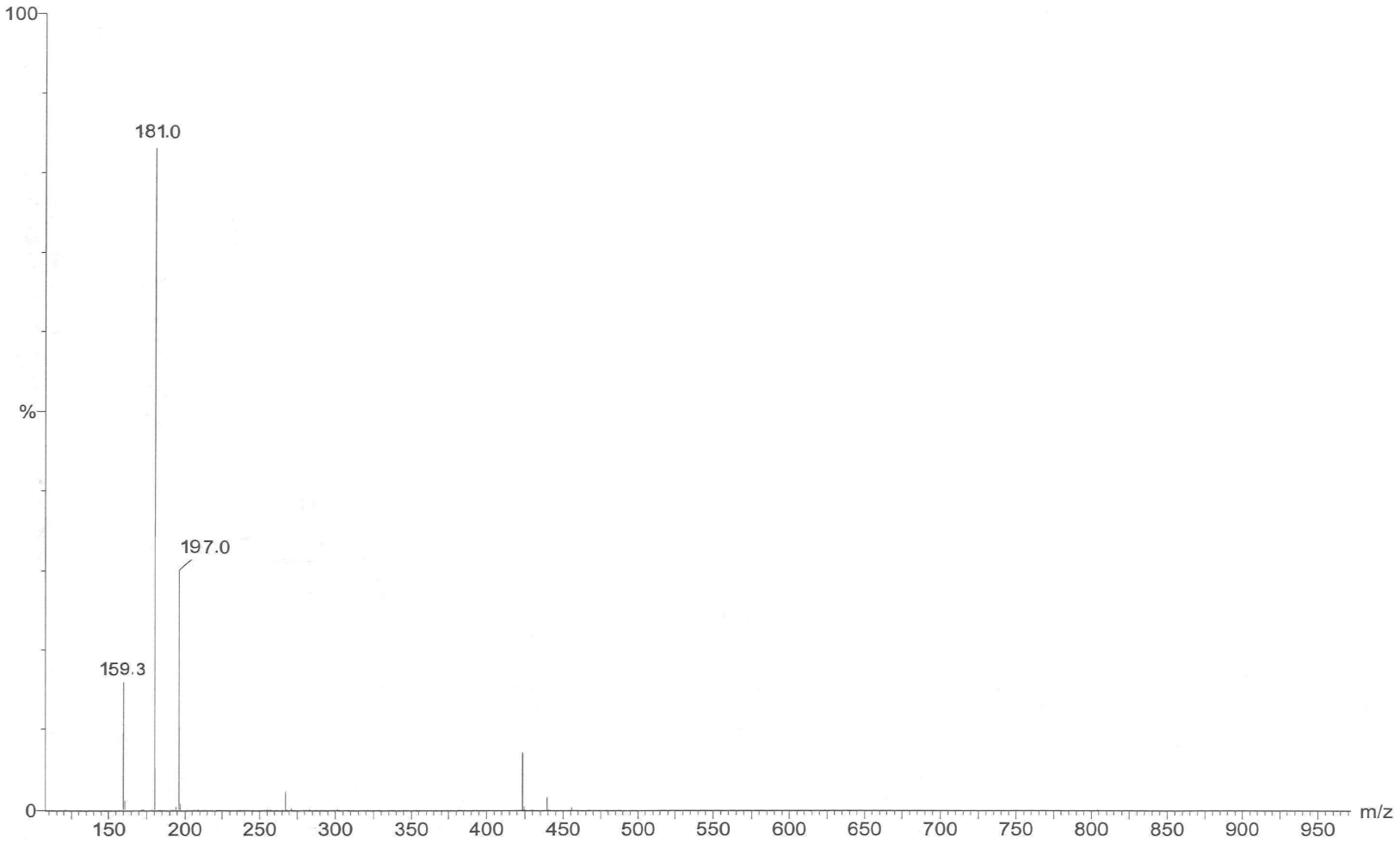

Figure 46. ESI MS spectrum of 2,*O*-dihydrosphaeropsidone (**49**), recorded in positive modality.

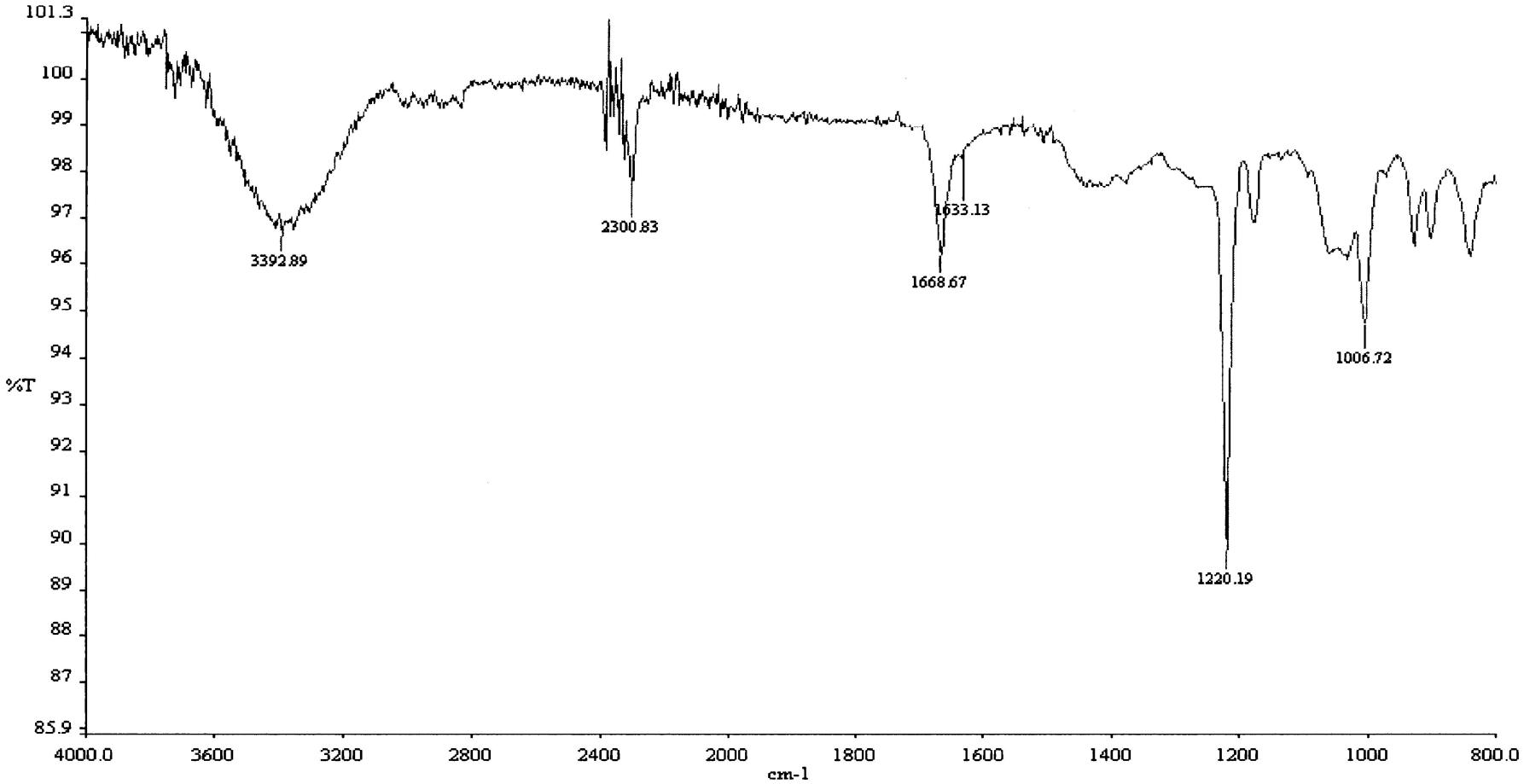

Figure 47. IR spectrum of 2,*O*-dihydrosphaeropsidone (**49**), recorded as glassy film.

22, differed for the lack of the carbonyl group band as well as the UV spectrum showed an end adsorption for the lack of the α-β unsaturated ketone group. The ^{1}H NMR spectrum (Fig. 48), compared to **22**, differed essentially for the appearance of the proton of a further secondary hydroxylated carbon (C-2) which resonated as doublet at δ 4.55, and for the upfield shift (Δδ: 0.7) of H-3 appearing as broad singlet at δ 4.50. The structure of this derivative was confirmed by NMR studies (^{13}C, COSY, HSQC, HMBC and NOESY, Fig. 49-53, respectively). The C-2 stereochemistry was deduced by the coupling observed in the ^{1}H-NMR and NOESY spectra. In particular, the value of 3.5 and 3.1 Hz for the coupling of H-6 with both H-1 and H-5, respectively, as expected, were similar to those observed in **22**. The small constant (J<1 Hz) observed for the coupling between H-1 and H-2 showed an H-2 α-pseudoaxial and its geminal hydroxy group β-pseudoequatorial orientation (Pretsch *et al.*, 2000). This stereochemistry at C-2 is also in agreement with the mechanism of reduction, with the nucleophilic attack of $NaBH_4$ at this carbon at the less hindered α-side opposite to the epoxy ring. The configuration at C-2 was also confirmed by the absence of a coupling between H-1 and H-2 in the NOESY spectrum (Fig. 53), while, as expected, a clear effect was observed between the methoxy group and H-3, and by an inspection of a Dreiding model of **49**.

The catalytic hydrogenation of **22** (Scheme 3) produced a tetrahydro derivative (**50**). The ESI MS spectrum of **50** (Fig. 54) showed the potassium and sodium clusters and the pseudomolecular ion at *m/z* 199, 183 and 161. The IR spectrum (Fig. 55), compared to that of **22**, differed essentially for the lack of the olefinic band while the UV spectrum showed an end adsorption. The ^{1}H NMR spectrum (Fig. 56) showed the appearance of the proton H-4 of a further secondary hydroxilated carbon (C-4) resonating as double doublet at δ 3.71, the downfield shift (Δδ: 0.56) of H-1 resonating as singlet at δ 4.04. The presence of two broad doublets at δ 2.78 and 2.75 due to C-6 H_2 and two double doublets

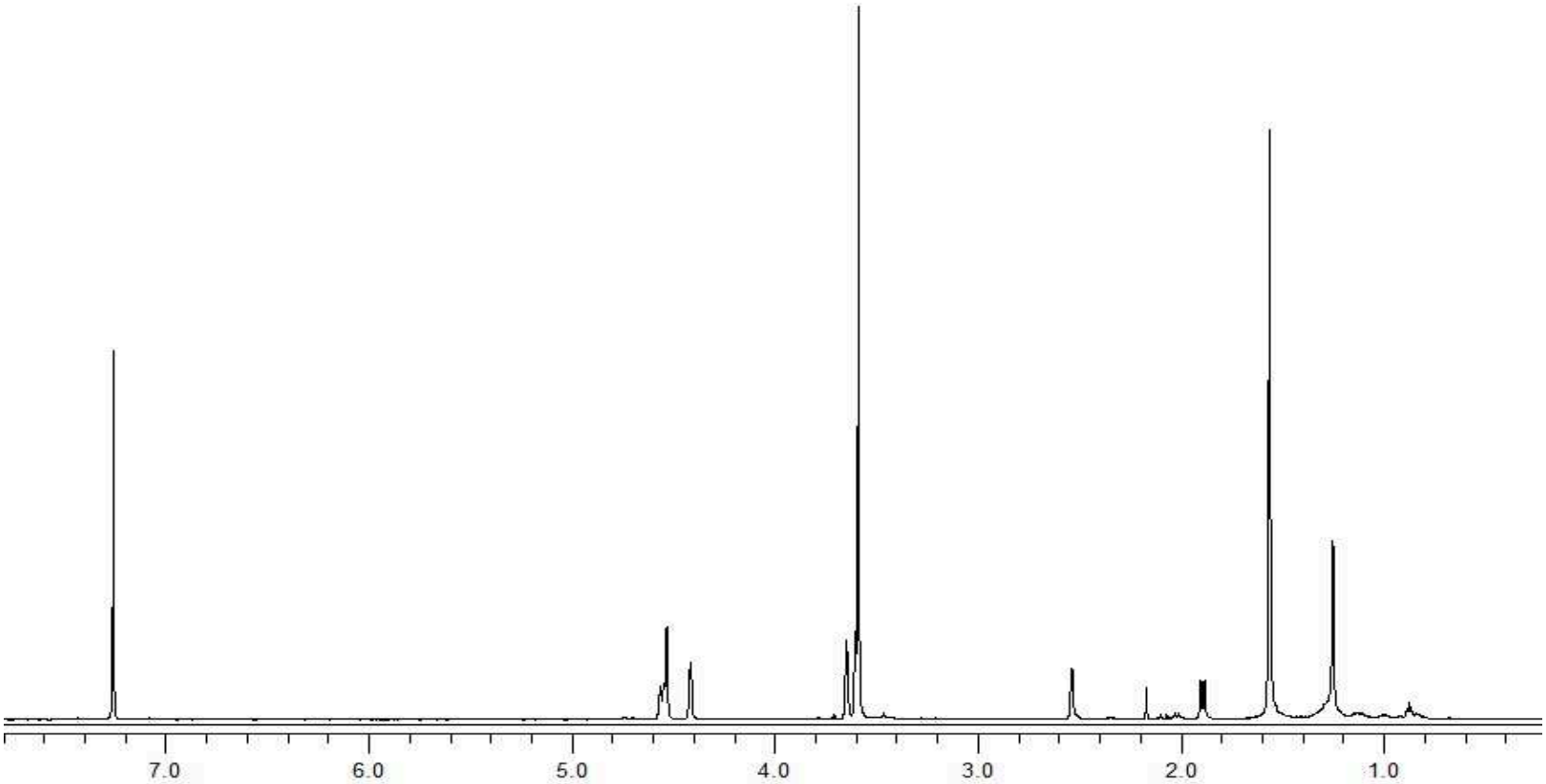

Figure 48. ^{1}H NMR spectrum of 2,*O*-dihydrosphaeropsidone (**49**), recorded in $CDCl_3$ at 600 MHz.

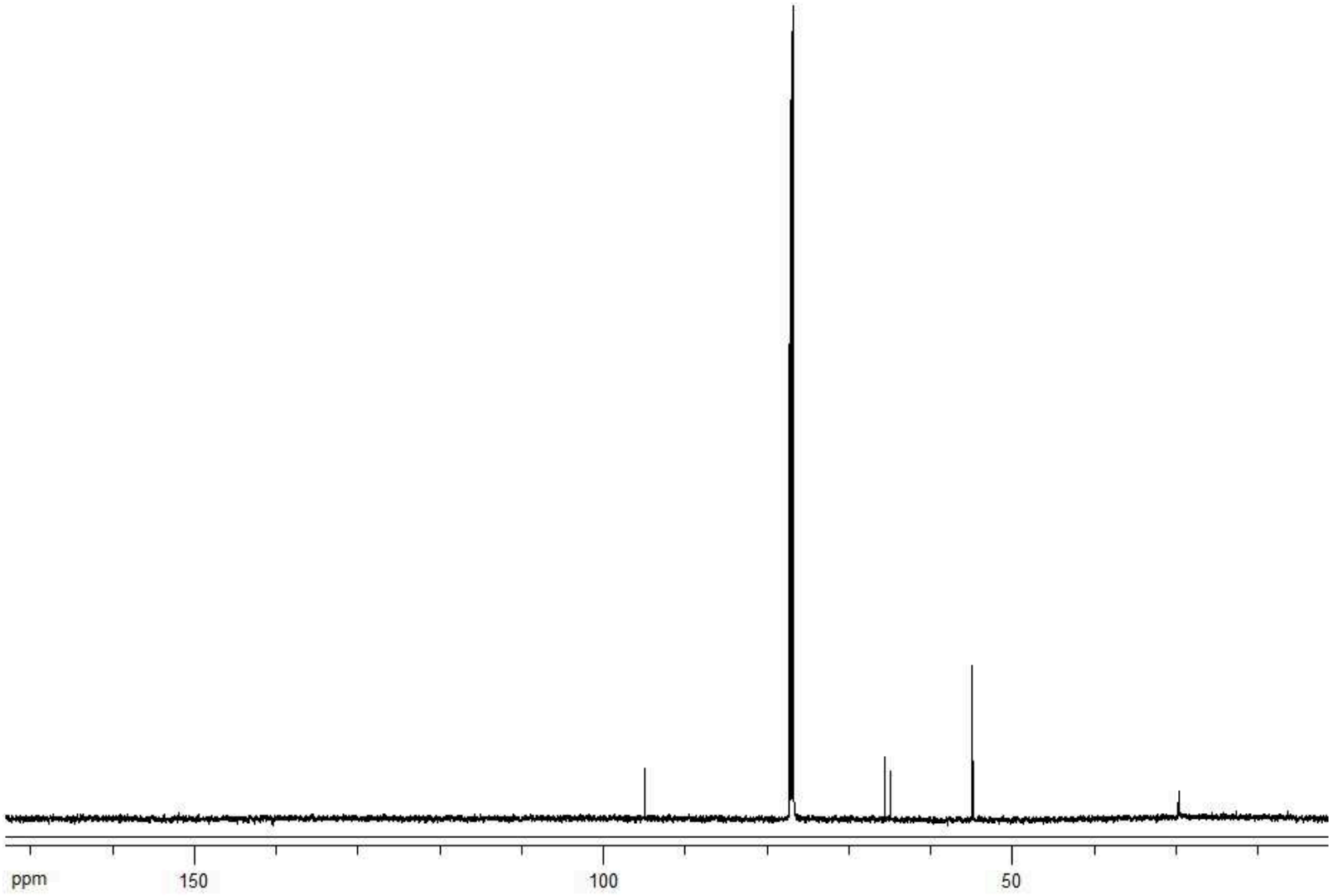

Figure 49. ^{13}C NMR spectrum of 2,*O*-dihydrosphaeropsidone (**49**), recorded in $CDCl_3$ at 150 MHz.

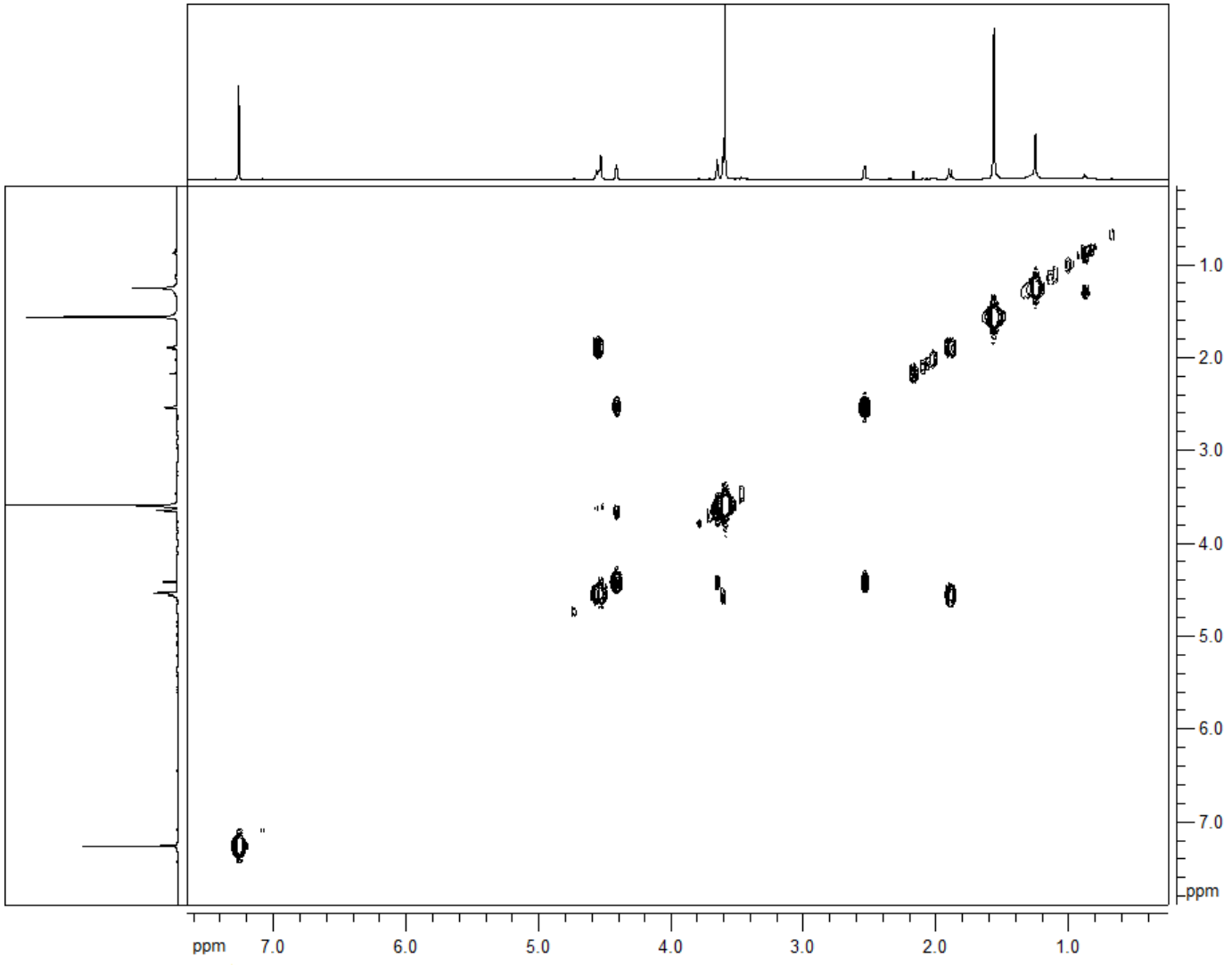

Figure 50. COSY spectrum of 2,*O*-dihydrosphaeropsidone (**49**), recorded in $CDCl_3$ at 600 MHz.

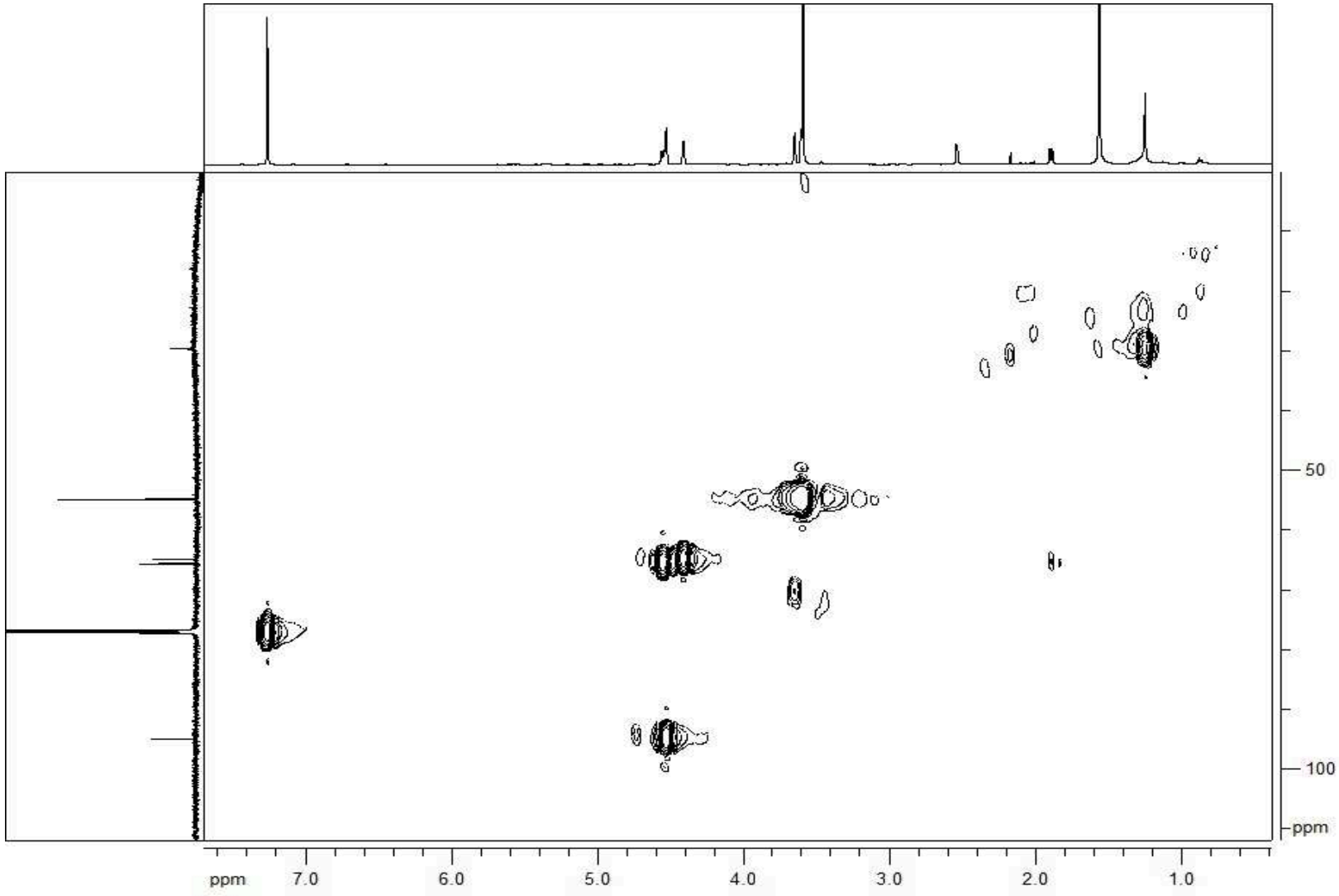

Figure 51. HSQC spectrum of 2,*O*-dihydrosphaeropsidone (**49**), recorded in $CDCl_3$ at 600 MHz.

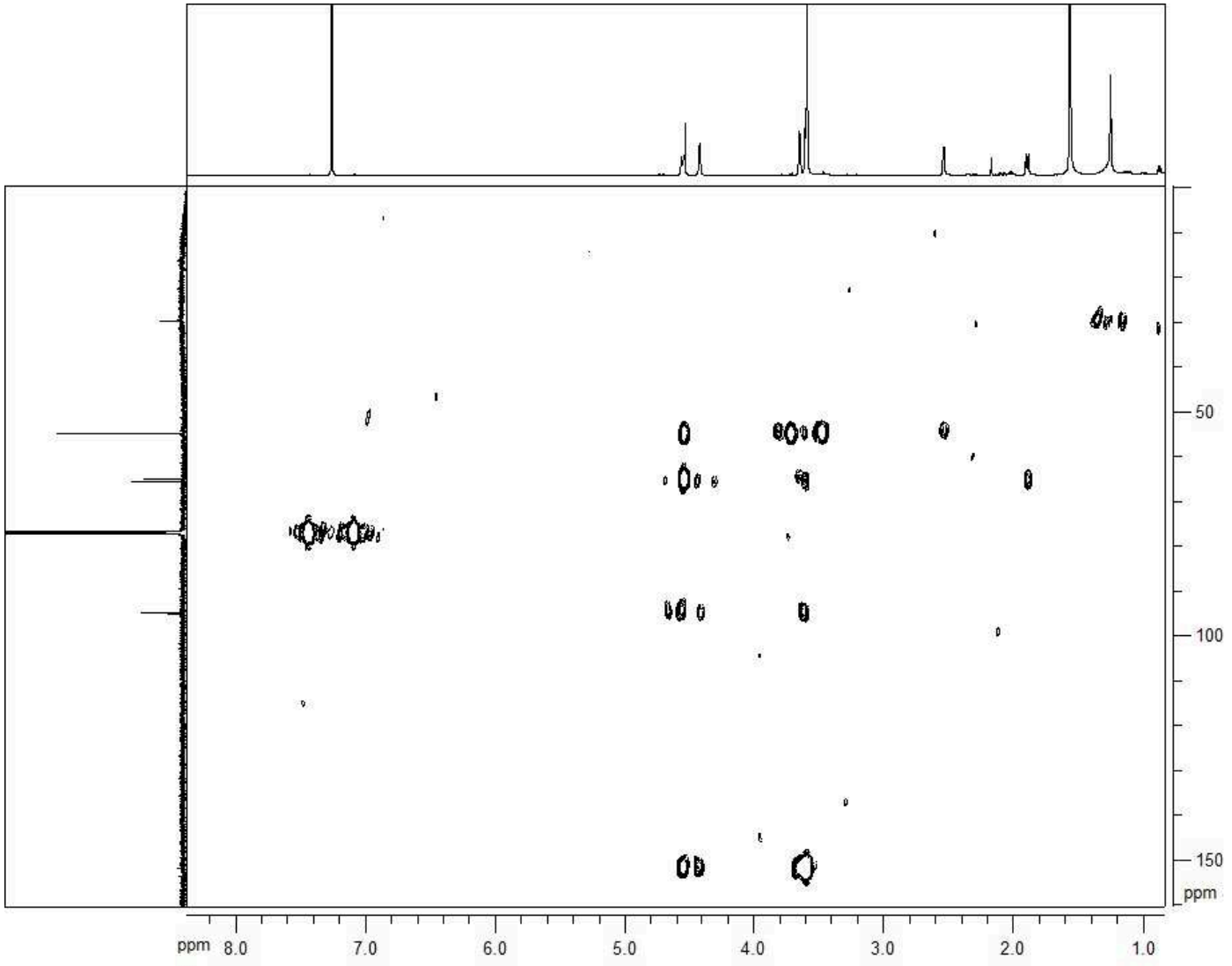

Figure 52. HMBC spectrum of 2,*O*-dihydrosphaeropsidone (**49**), recorded in $CDCl_3$ at 600 MHz.

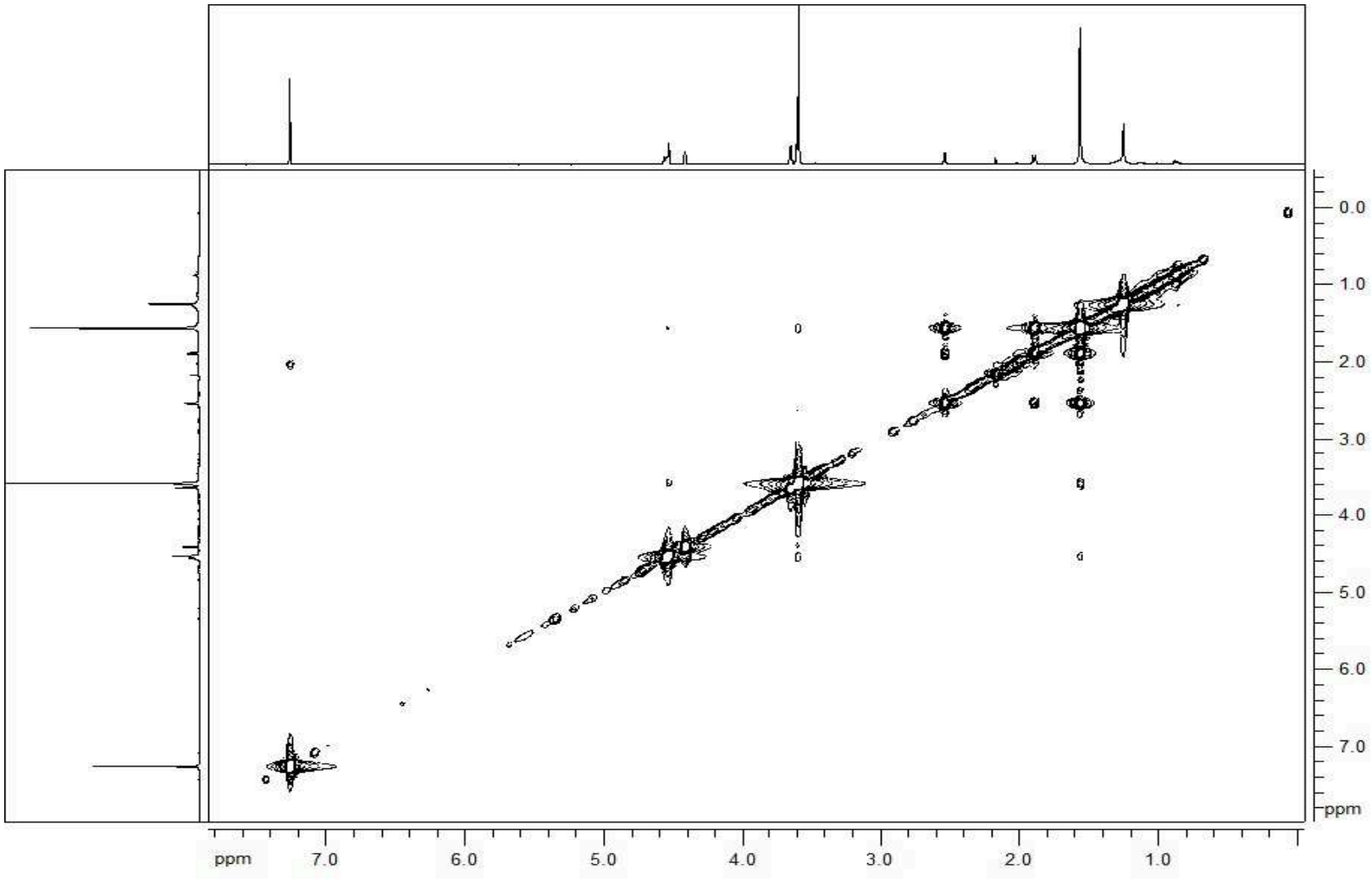

Figure 53. NOESY spectrum of 2,*O*-dihydrosphaeropsidone (**49**), recorded in $CDCl_3$ at 600 MHz.

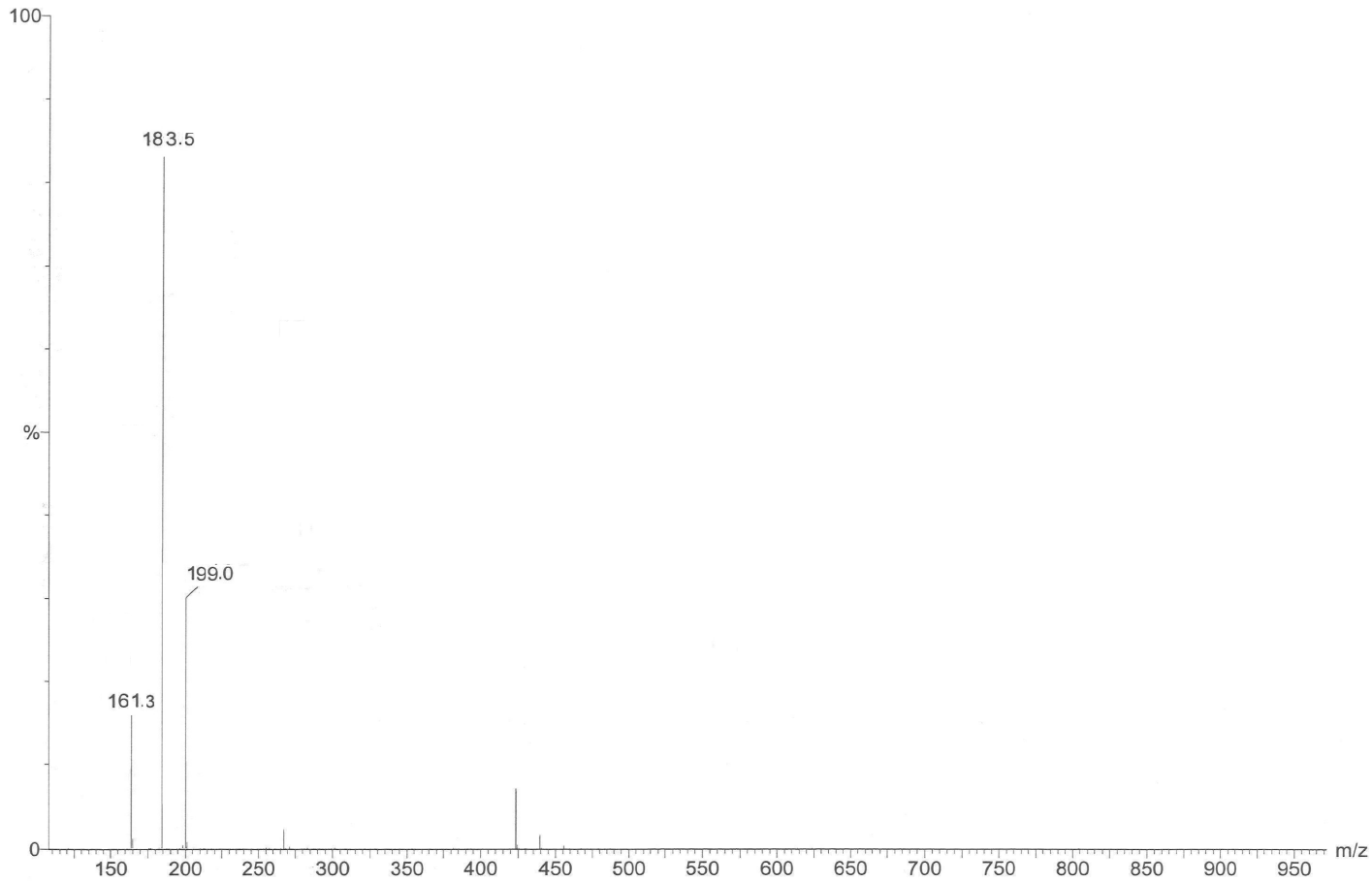

Figure 54. ESI MS spectrum of 2,4-dihydroxy-5-metoxycycloexanone (**50)**, recorded in positive modality.

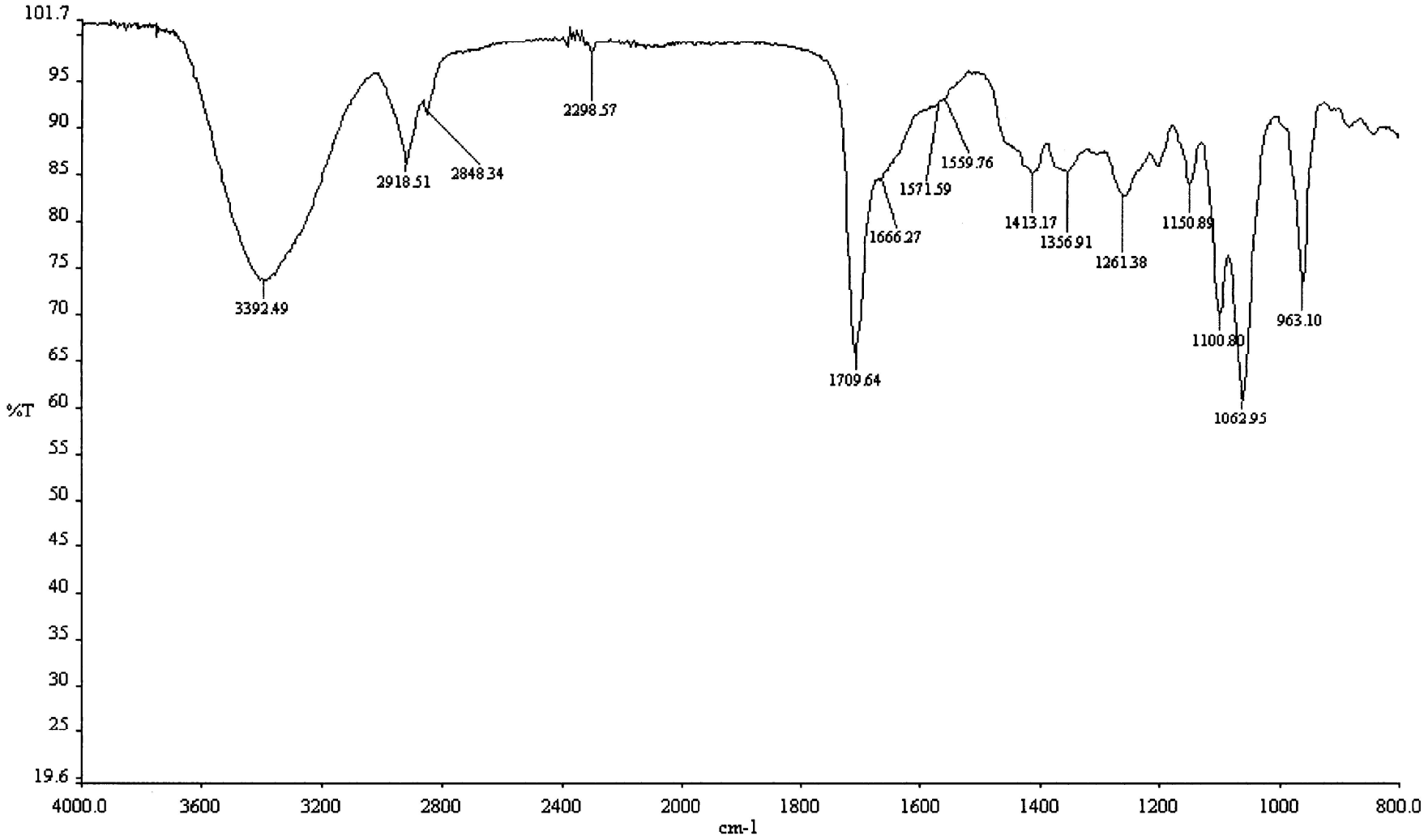

Figure 55. IR spectrum of 2,4-dihydroxy-5-metoxycycloexanone (**50**), recorded as glassy film.

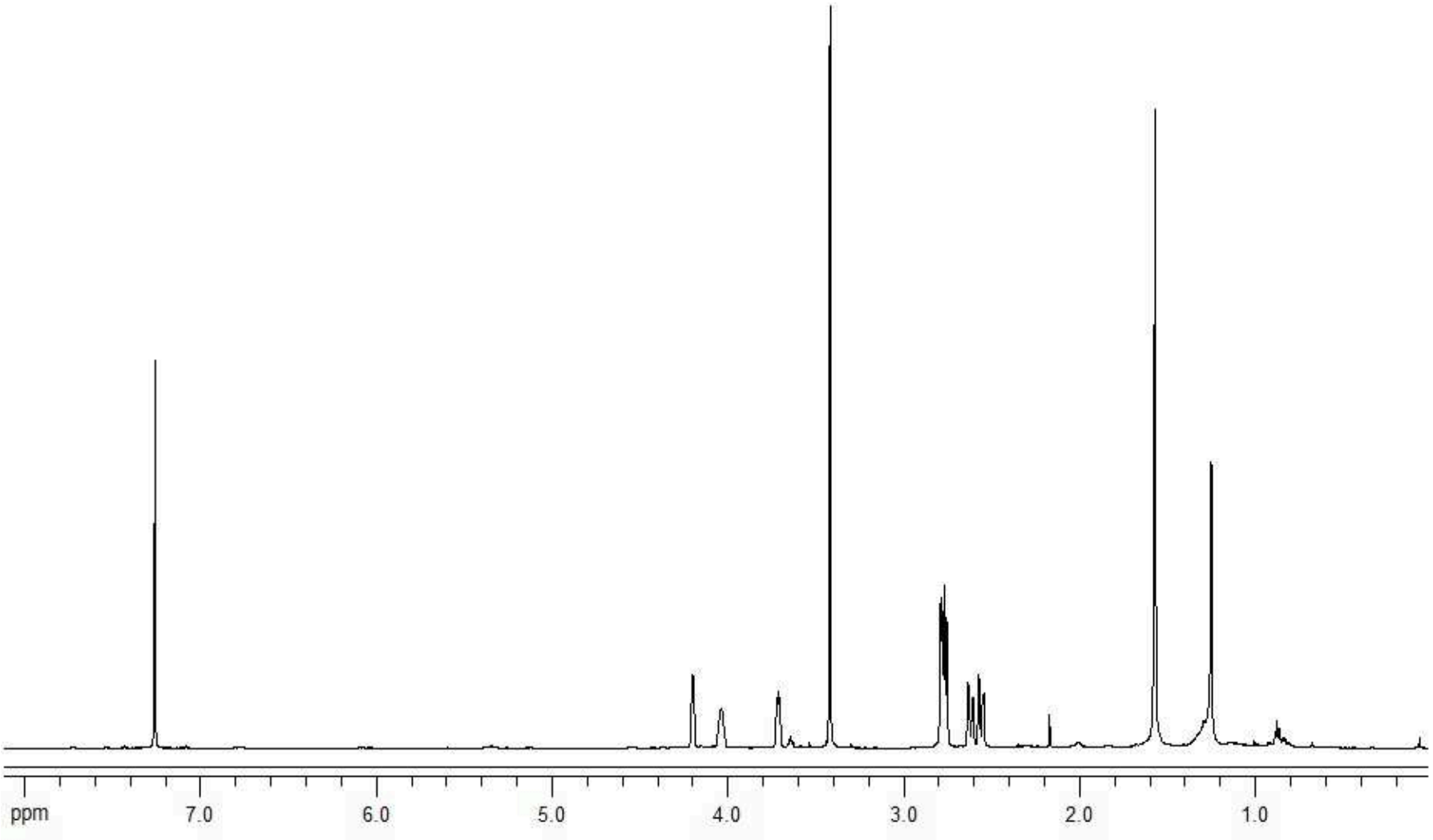

Figure 56. ^{1}H NMR spectrum of 2,4-dihydroxy-5-metoxycycloexanone (**50**), recorded in $CDCl_3$ at 600 MHz.

at δ 2.62 and 2.55 due to H_3 C-3 were also observed. The structure of this derivative was determined by extensive NMR (^{13}C, COSY, HSQC, HMBC and NOESY, Fig. 57-61, respectively), and MS spectra. The configuration was deduced, as for **49**, by the coupling observed in the ^{1}H NMR and NOESY spectra. In particular, considering that **49** assumes a half-chair conformation, the configuration at C-4 was assigned by considering the mechanism of reaction but essentially by the absence of any coupling in the NOESY spectrum between the methoxy protons and H-5, while as expected coupling was observed between H-4 and both H_2-3, between H-1 and both H_2-6 and H-5 and H-6. These results together with the values measured in the ^{1}H NMR spectrum for the coupling constants (4.8 and 4.0 Hz) between H-4 with both H_2-3 and the absence of its coupling with H-5, showed that H-4 was α-pseudoaxial oriented and its geminal methoxy group β-pseudoequatorial (Pretsch *et al.*, 2000). Similarly, the low values observed for the coupling between both H-1 and H-5 with H_2-6 placed H-1 and H-5 both α-pseudoequatorial, and consequently their geminal hydroxy groups both β-pseudoaxial (Pretsch *et al.*, 2000). This stereochemistry is also in agreement with a Dreiding model of **50**. Derivative **50** showed both the reduction of the olefinic double bond and the selective reductive opening of the epoxy ring, resulting in the 2,4-dihydroxy-5-methoxycyclohexanone which should assume a half-chair conformation.

Acetylation of episphaeropsidone **23** (Scheme 4) yielded the corresponding 5-*O*-acetyl derivative (**51**), which is the 5-epimer of **45**, and the triacetyl derivative (**52**). The latter, following acetylation of the C-5 hydroxy group as in **51**, was probably generated by cleavage of the epoxy ring via nucleophilic attack of the acetoxy group at the less-hindered C-1 from the α-side and subsequent acetylation of the resulting anionic oxygen at C-6. The configuration of **52**, deduced from the coupling constants confirmed such a hypothesized reaction mechanism. The ESI MS spectrum of **51** (Fig. 62) showed the potassium and

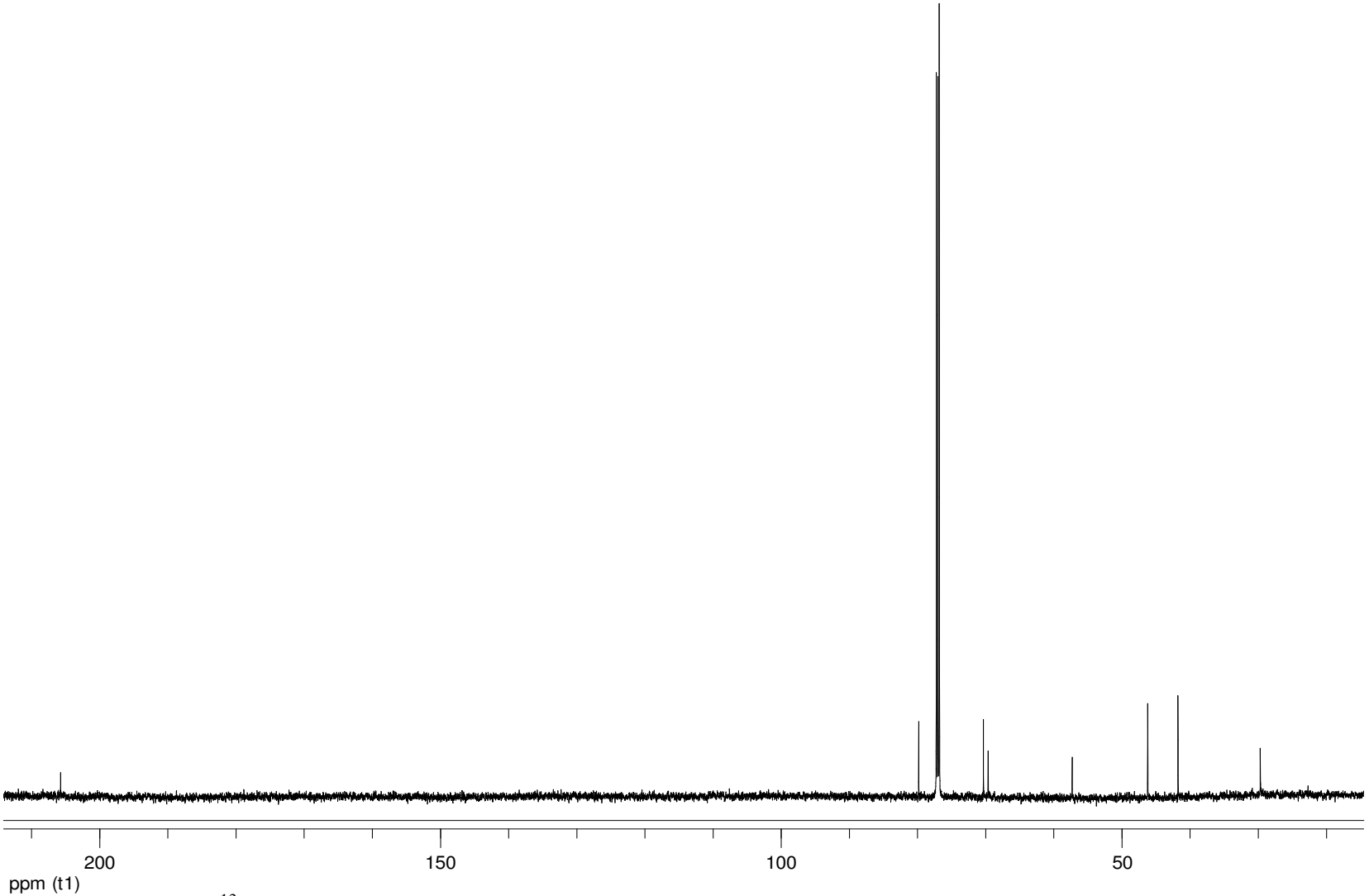

Figure 57. ^{13}C NMR spectrum of 2,4-dihydroxy-5-metoxycycloexanone (**50**), recorded in $CDCl_3$ at 150 MHz.

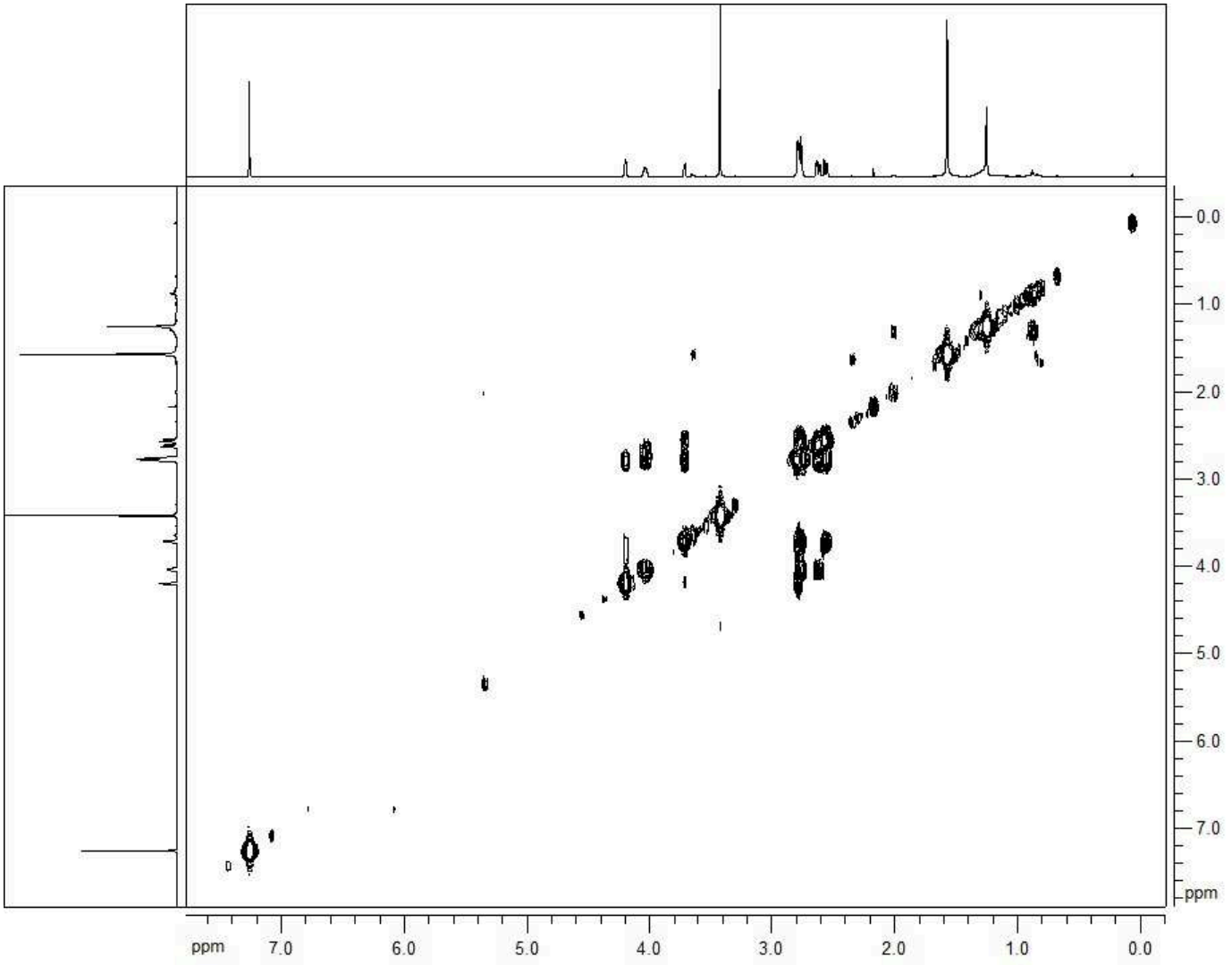

Figure 58. COSY spectrum of 2,4-dihydroxy-5-metoxycycloexanone (**50)**, recorded in $CDCl_3$ at 600 MHz.

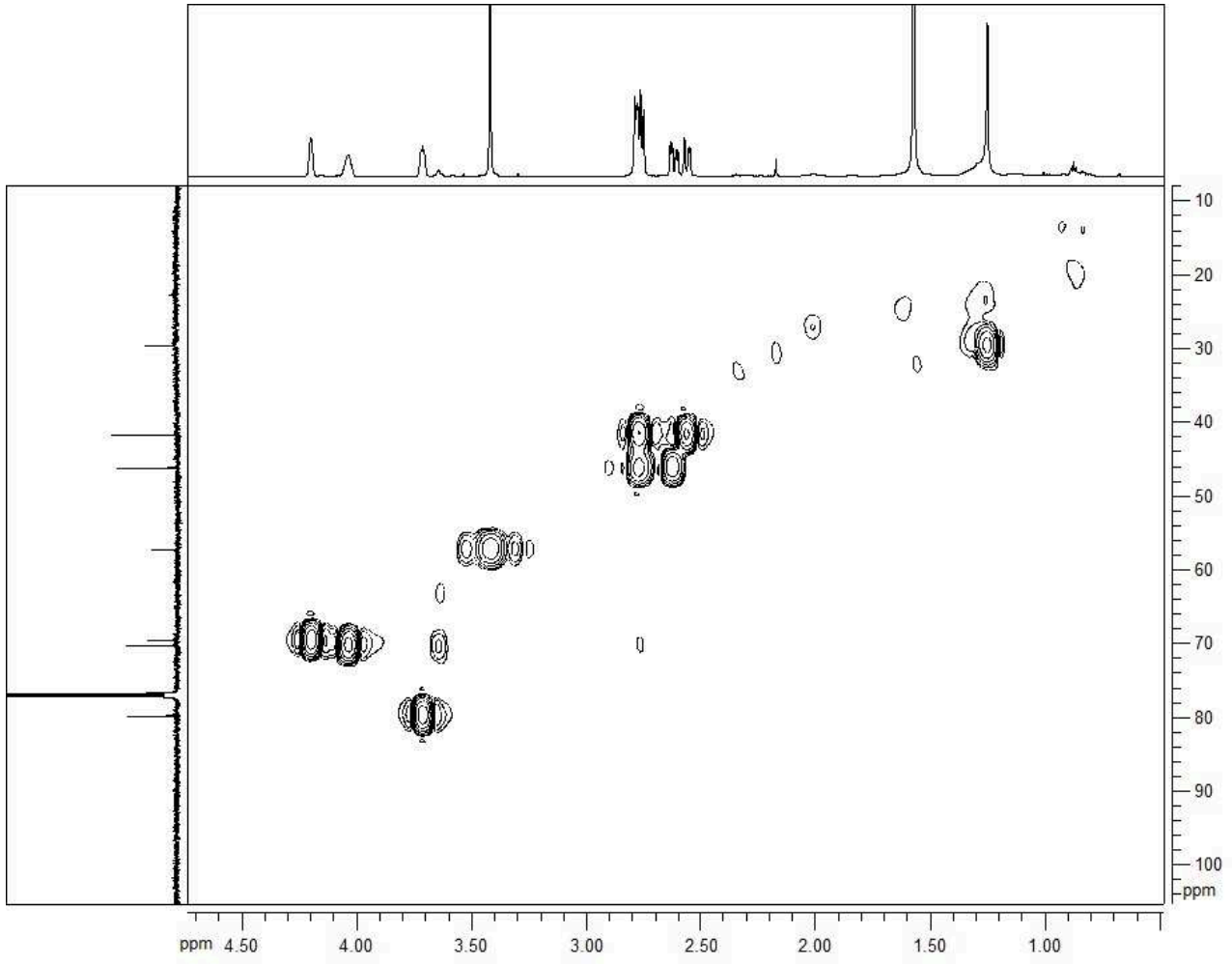

Figure 59. HSQC spectrum of 2,4-dihydroxy-5-metoxycycloexanone (**50**), recorded in $CDCl_3$ at 600 MHz.

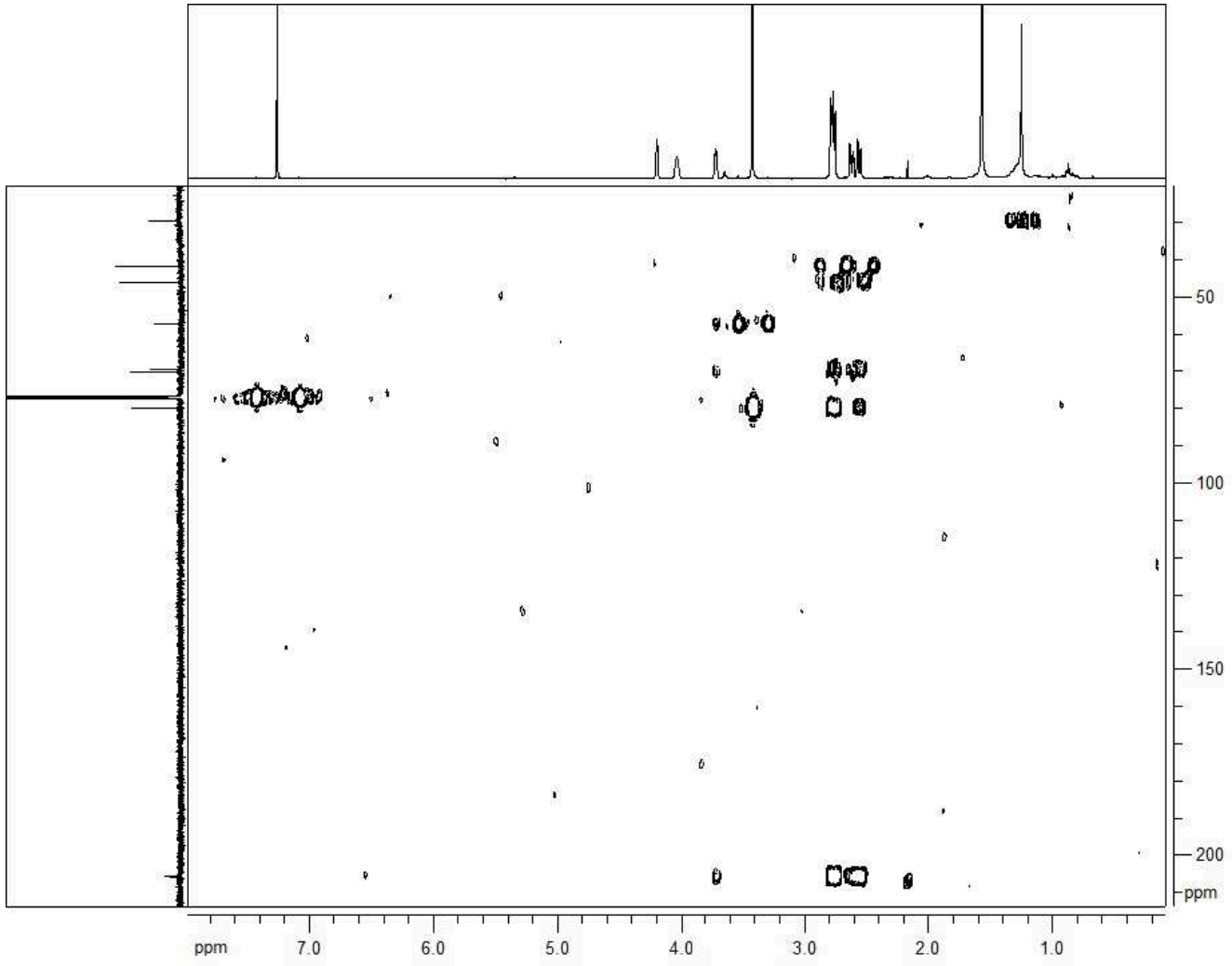

Figure 60. HMBC spectrum of 2,4-dihydroxy-5-metoxycycloexanone (**50**), recorded in $CDCl_3$ at 600 MHz.

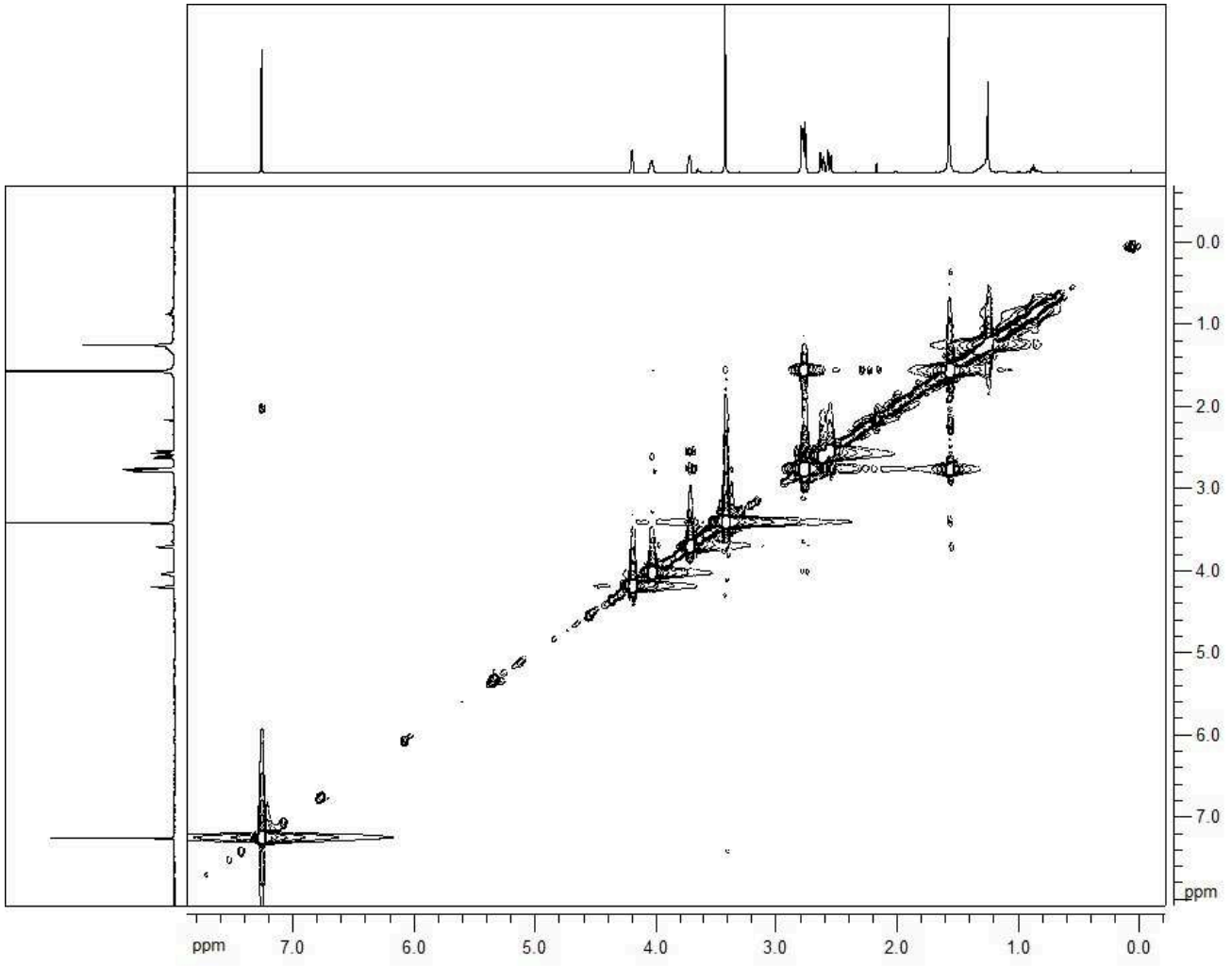

Figure 61. NOESY spectrum of 2,4-dihydroxy-5-metoxycycloexanone (**50)**, recorded in $CDCl_3$ at 600 MHz.

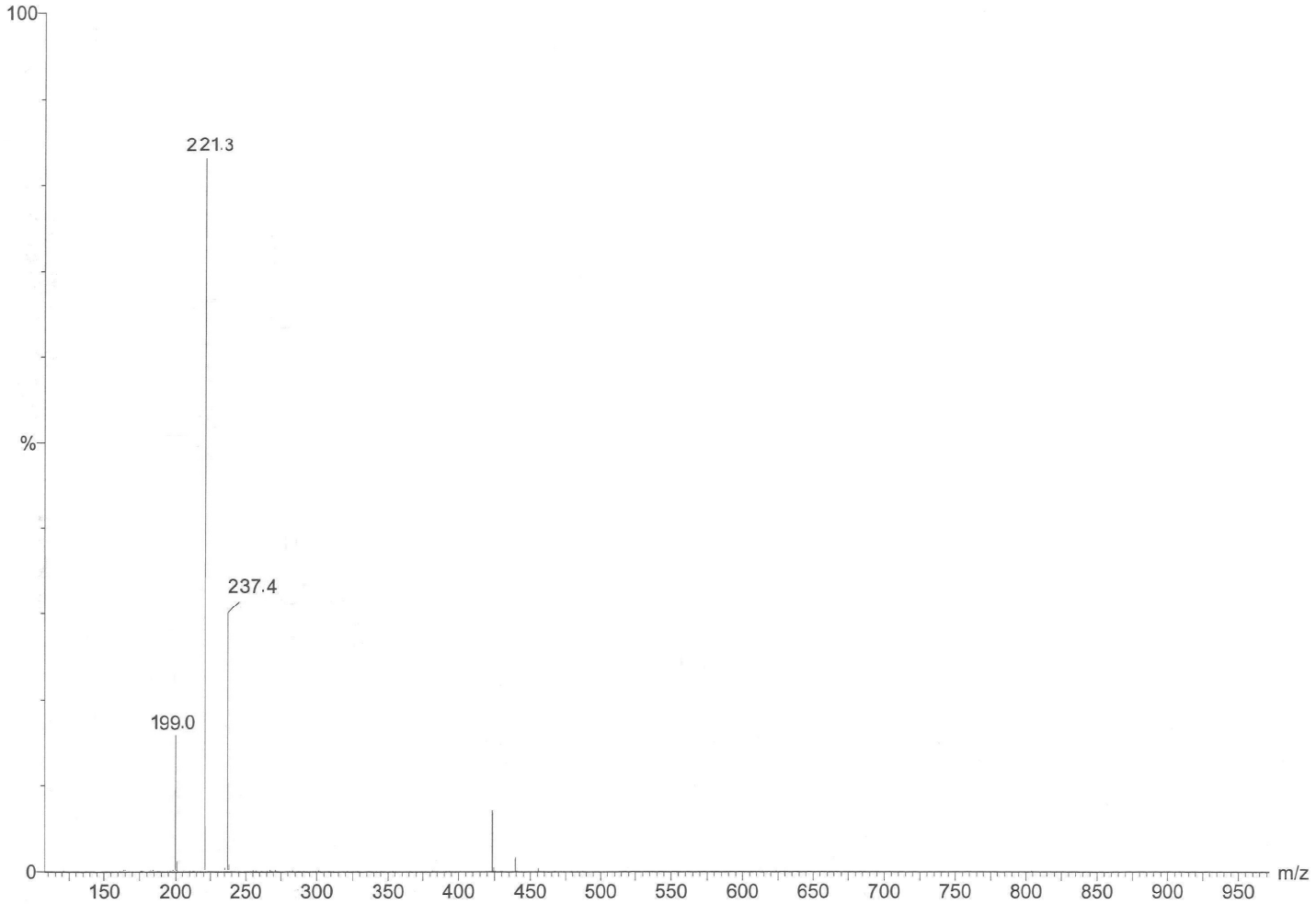

Figure 62. ESI MS spectrum of 5,*O*-acetylepisphaeropsidone (**51**), recorded in positive modality.

sodium clusters and the pseudomolecular ions at *m/z* 237, 221 and 199. As expected, the IR (Fig. 63) and the UV (Fig. 64) spectra of **51** were very similar to those of **45**. The ^{1}H-NMR spectrum (Fig. 65) differed from that of **23** only for the singlet of MeCO at δ 2.17 and the downfield shift (Δδ: 1.24) of the proton H-5 resonating as doublet at δ 5.91 (Pretsch *et al.*, 2000).

The ESI MS spectrum of **52** (Fig. 66) showed the potassium and sodium clusters and the pseudomolecular ions at *m/z* 339, 323 and 301. The IR (Fig. 67) and the UV (Fig. 68) spectra of **52** were very similar to those of **46**. The ^{1}H NMR spectrum (Fig. 69) of **52** differed from **51** for the presence of two singlets of the further acetyl groups at δ 2.12 and 2.07 and for the downfield shifts (Δδ: 2.29 and 1.99) of H-1 and H-6.

5.6. Phytotoxic and antifungal activities of sphaeropsidones and their derivatives

The phytotoxic and antifungal activities of the eight derivatives (**45-52**, Scheme 3 and 4, Pag. 112-113) and of episphaeropsidone (**23**), proposed to be a naturally modified analogue of **22**, were evaluated in comparison to sphaeropsidone (**22**). Furthermore, other two natural analogues of sphaeropsidone, as well as chlorosphaeropsidone (**24**) and its 6-epimer (**25**), were also bio-assayed in comparison to **22** and **23**. As described in the Experimental section, two bioassays were used to investigate the phytotoxic activity.

In the leaf-puncture bioassay, the phytotoxicity was evaluated for *Quercus ilex*, *Q. Rubra*, *Q. suber*, and tomato (*Lycopersicun esculentum* var. Marmade) leaves. The toxicity data in Fig. 70 show that both sphaeropsidone (**22**) and its epimer (**23**), at the concentration used, had a remarkable toxicity causing necrotic lesions to leaves of all species tested. Among the sphaeropsidone (**22**) derivatives, only compounds **47** and **48** retained phytotoxicity to different extents, whereas a significant decrease and/or a complete loss of activity was observed for the derivatives **24**, **25**, **45**, **46, 49, 50** and **52**. In particular, the

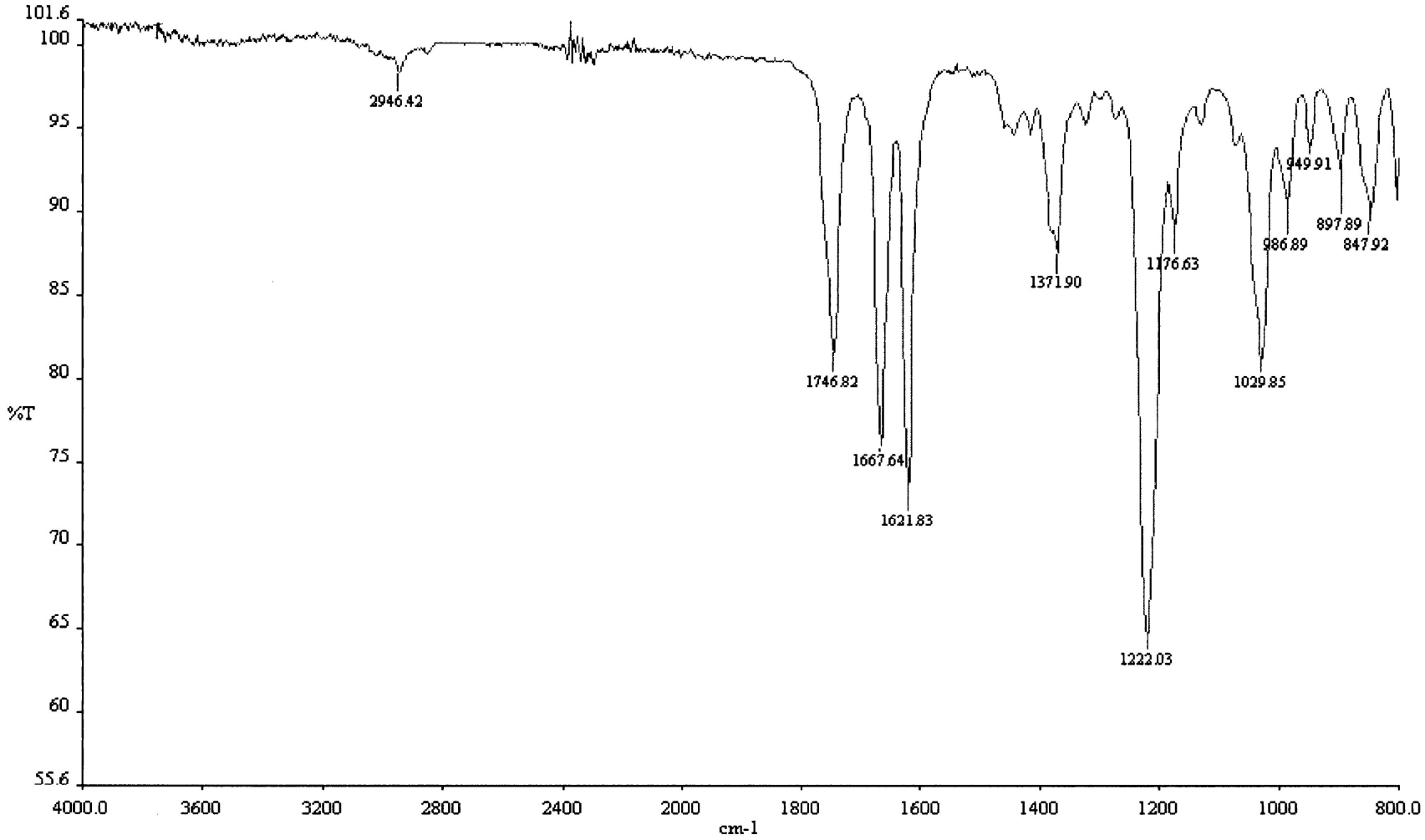

Figure 63. IR spectrum of 5,*O*-acetylepisphaeropsidone (**51**), recorded as glassy film.

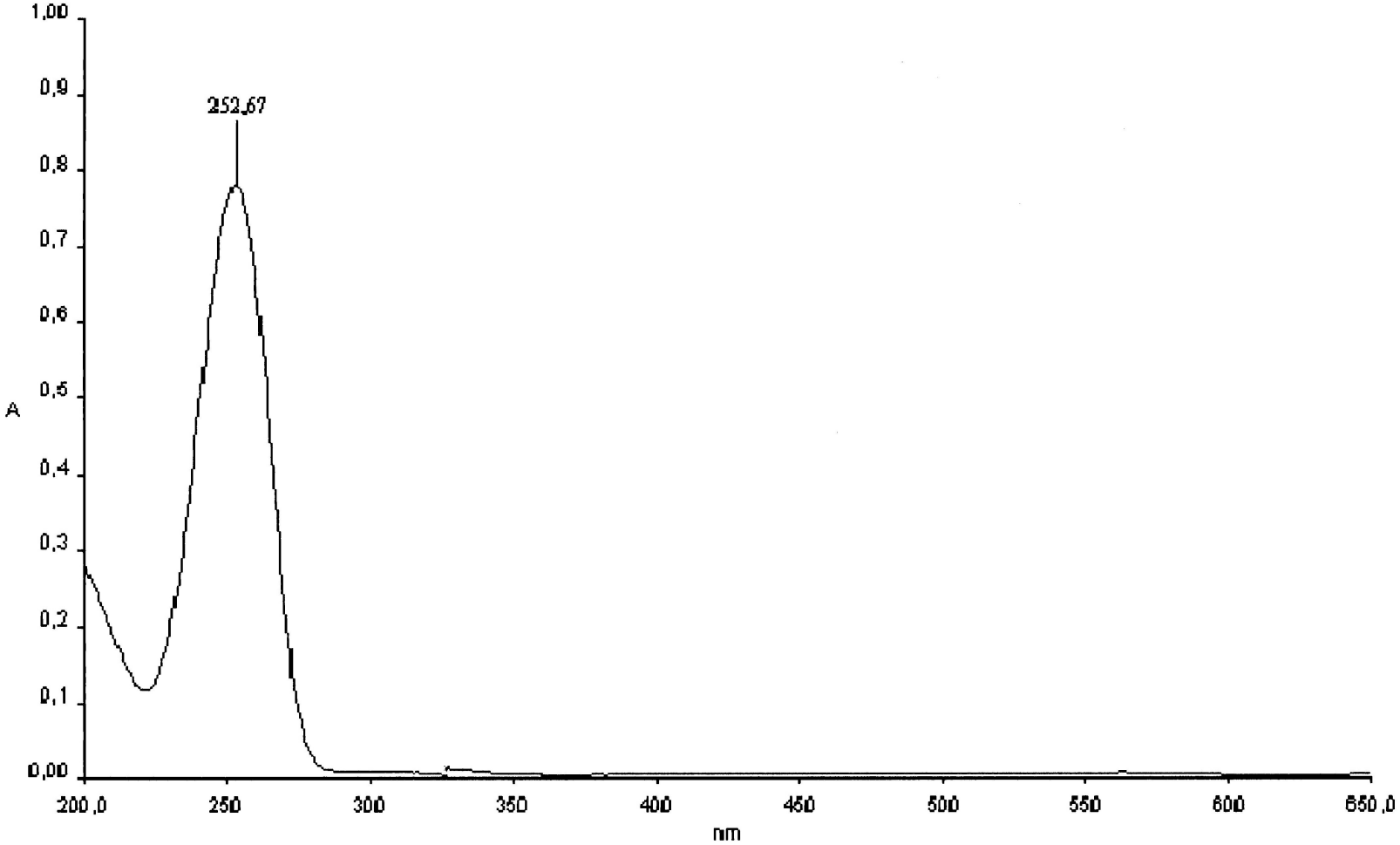

Figure 64. UV spectrum of 5,*O*-acetylepisphaeropsidone (**51**), recorded in MeCN solution.

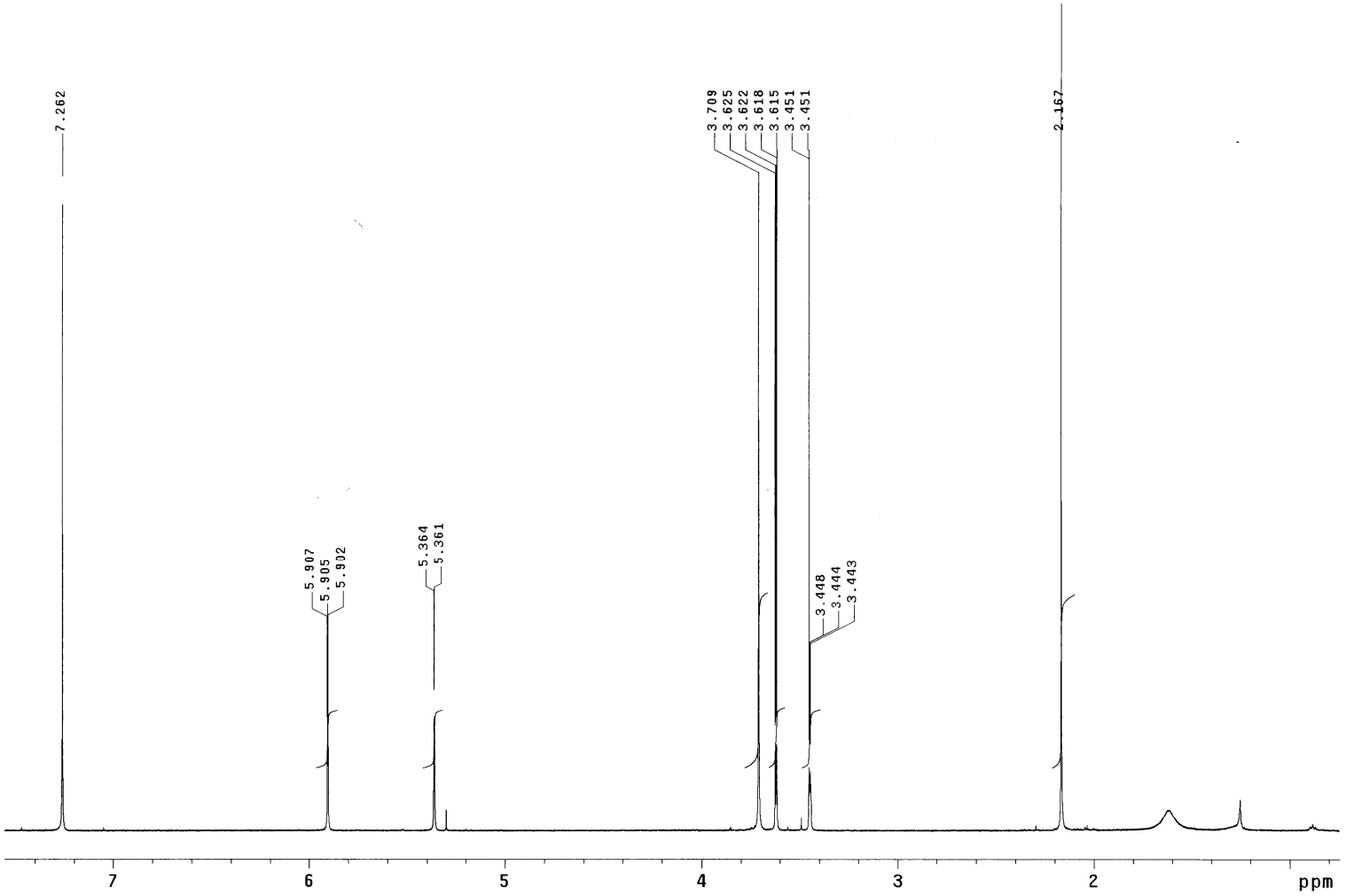

Figure 65. ^{1}H NMR spectrum of 5,*O*-acetylepisphaeropsidone (**51**), recorded in $CDCl_3$ at 600 MHz.

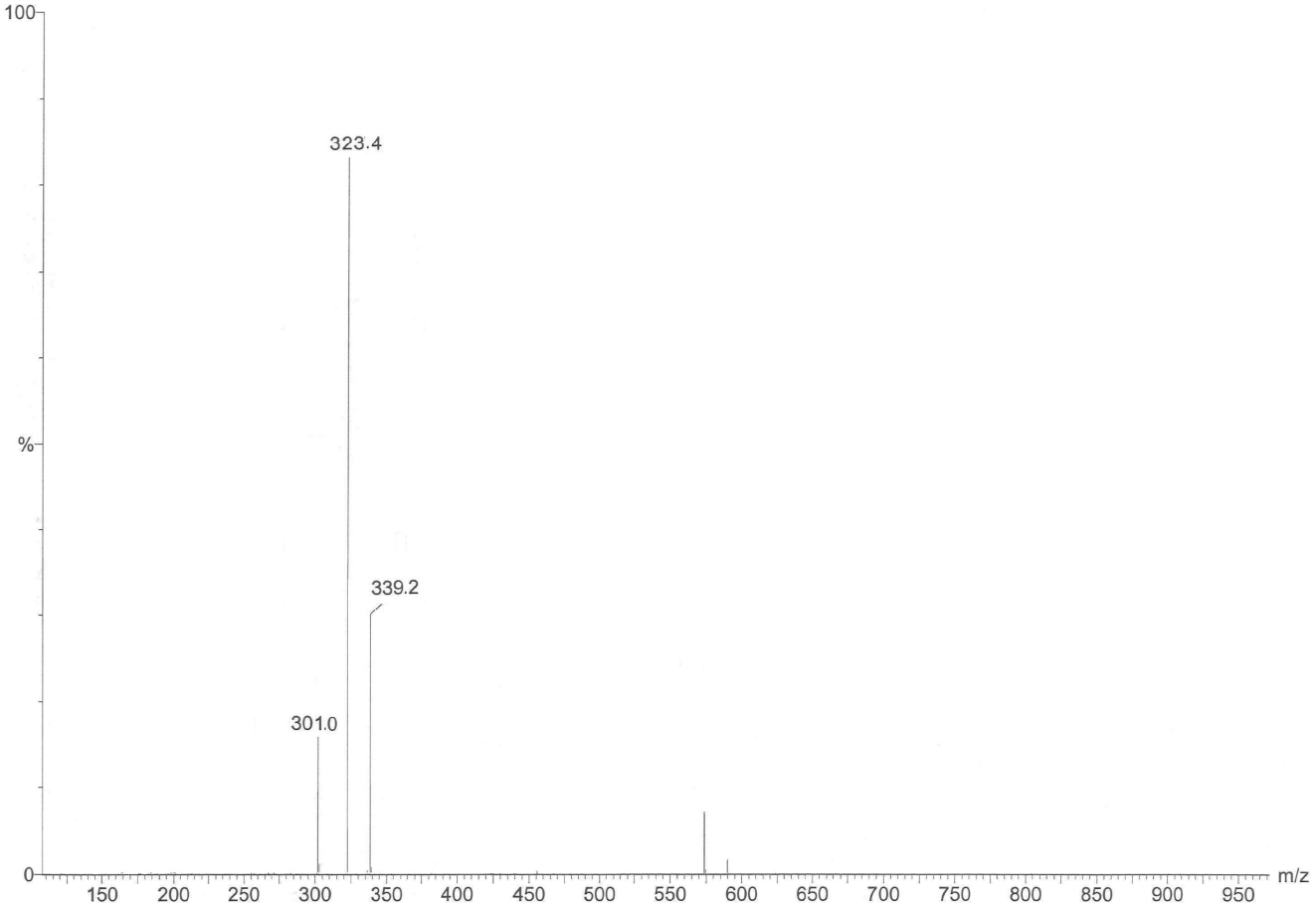

Figure 66. ESI MS spectrum of 4,5,6-triacetoxy-3-methoxycyclohex-2-enone (**52**), recorded in positive modality.

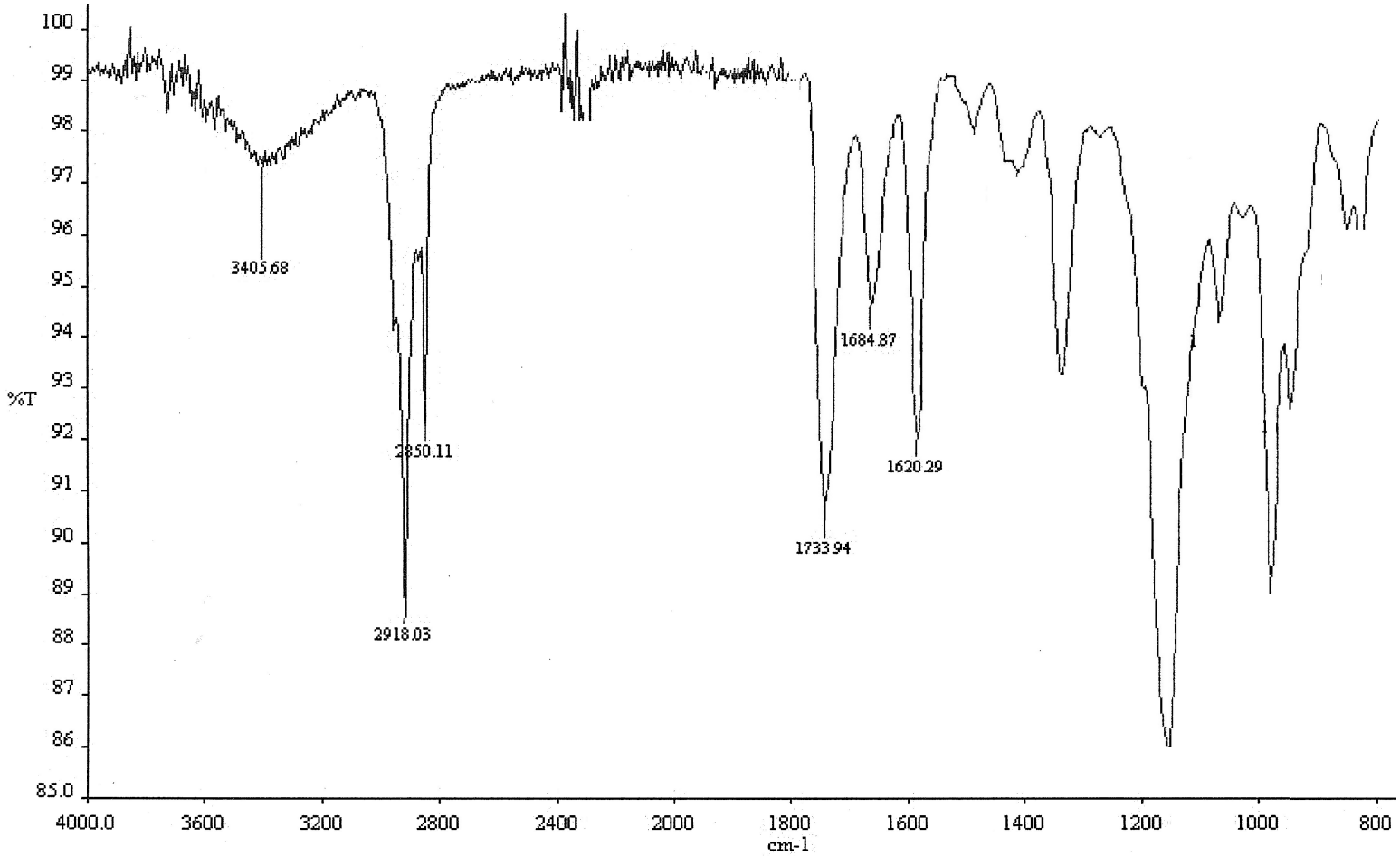

Figure 67. IR spectrum of 4,5,6-triacetoxy-3-methoxycyclohex-2-enone (**52**), recorded as glassy film.

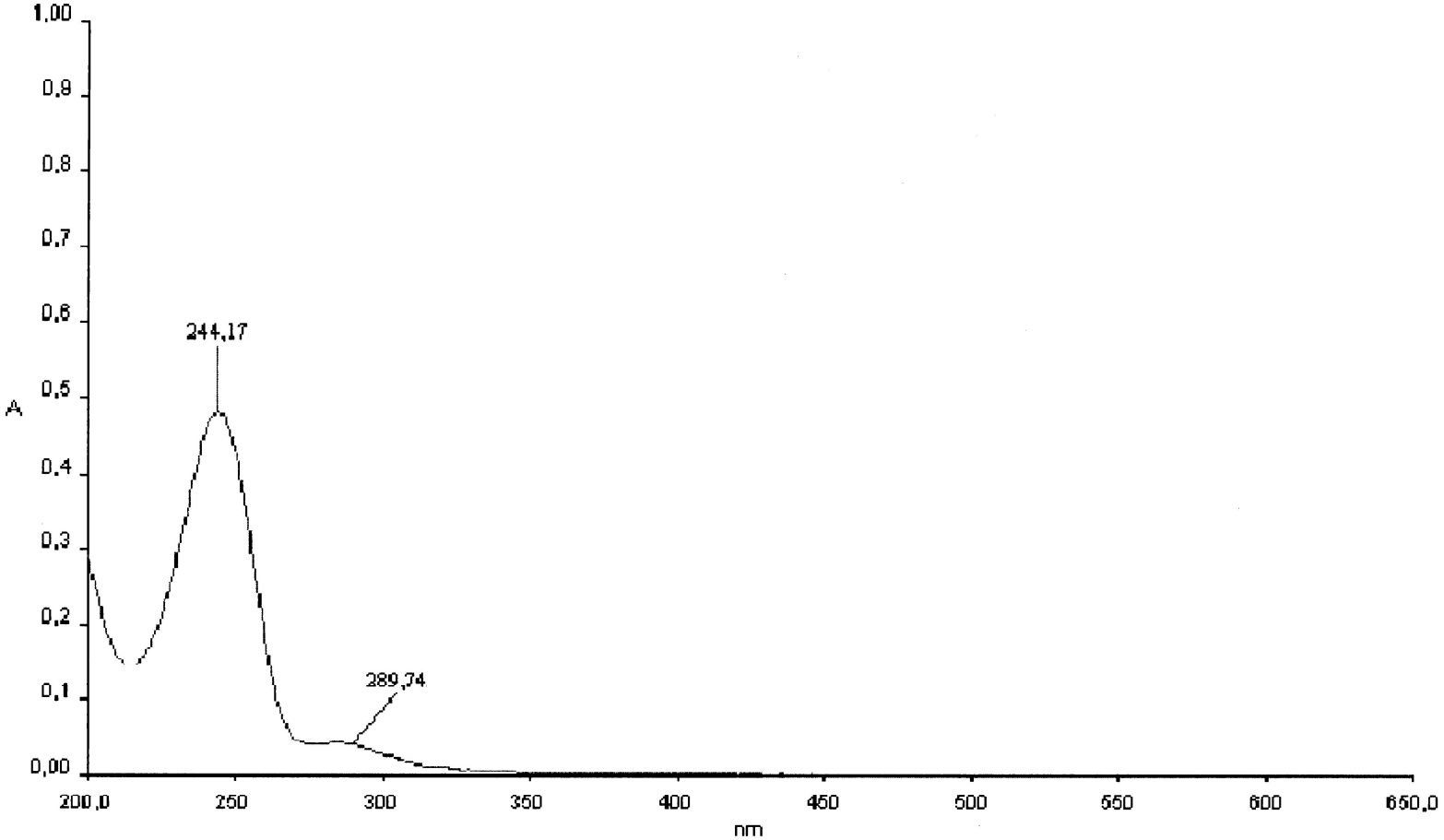

Figure 68. UV spectrum of 4,5,6-triacetoxy-3-methoxycyclohex-2-enone (**52**), recorded in MeCN solution.

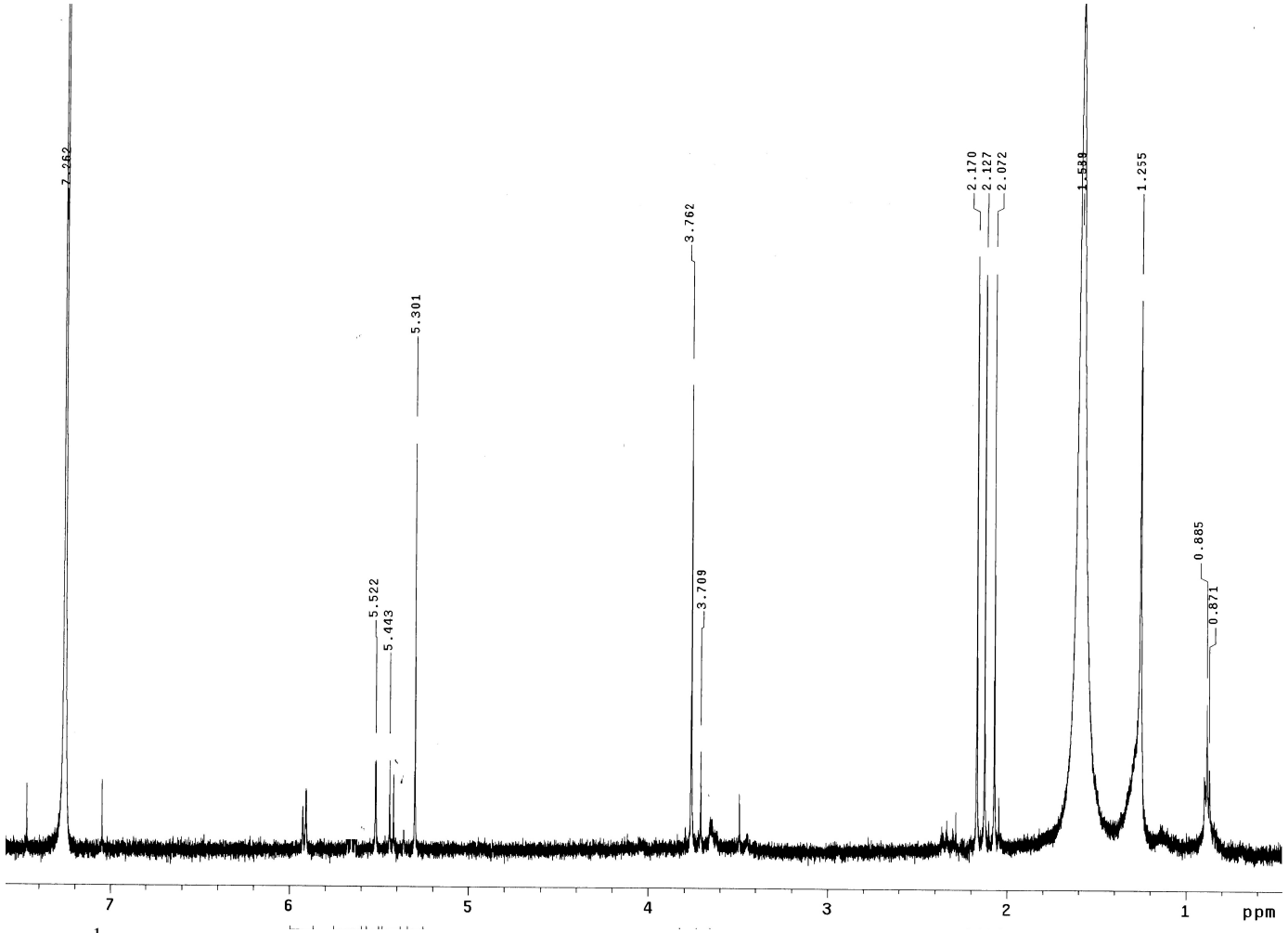

Figure 69. ^{1}H NMR spectrum of 4,5,6-triacetoxy-3-methoxycyclohex-2-enone (**52**), recorded in $CDCl_3$ at 600 MHz.

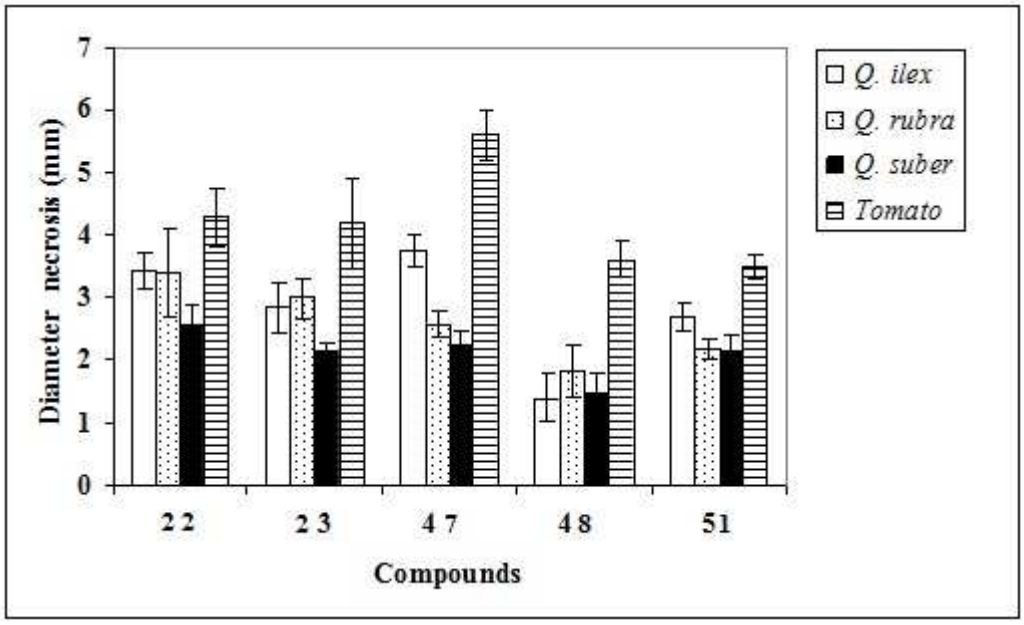

Figure 70. Phytotoxicity of sphaeropsidones (**22**, **23**) and their derivatives **47, 48** and **51** evaluated at 0.4 mg/ml on four plant species using a leaf puncture assay.

1,4-dione derivative (**47)** showed the same strong activity as that of **22** on all tested plant species. The derivative **48** was moderately toxic (necrosis diameter < 2 mm for all species tested except for tomato leaves). Compound **51**, the monoacetyl derivative of episphaeropsidone (**23**) exhibited a moderate decrease in phytotoxicity in comparison to **23**, whereas its triacetyl derivative (**52**) was inactive in the bioassay.

In the tomato cuttings bioassay, the compounds **22**, **23**, **47** and **51** were active. The cuttings treated with 0.1 mg/ml sphaeropsidone (**22**) and derivative **47** showed complete wilting in leaves and stems within 48 h of application. Furthermore, symptoms of phytotoxicity (stewing on stem) were also observed with derivative **47** at a concentration of 0.025 mg/ml. At the same concentration, sphaeropsidone (**22**) and its epimer (**23**) were inactive. Episphaeropsidone (**23**) appeared to be less toxic than **22** in this bioassay. The tomato cuttings showed wilting symptoms (first only on the stem) after four days at a concentration of 0.1 mg/ml. Derivative **51** showed stewing on the stem at 0.1 mg/ml. None of the other compounds caused any visible symptoms in this bioassay even at the highest concentration used.

These results allowed us to speculate on the structure-activity relationships and on some structural features determining the phytotoxic activity showed by each dimedone methyl ether. The epoxy ring seems to be somehow associated with the activity, even if it is not alone sufficient to produce the phytotoxic effects. The marked decrease and/or the complete lack of activity for derivatives **24**, **25**, **46**, **50** and **52** supports this result. Considering that some compounds having the epoxy ring were inactive it is reasonable to suppose that other features of the compound could be important.

The oxidation of the C-5 allylic hydroxy group leading to **47** seems to enhance, albeit slightly, the bioactivity of **22,** whereas the stereoselective epoxy ring opening obtained by converting **22** into the corresponding bromohydrin (**48**) reduces the bioactivity

of **22**. The activity of **47** can probably be ascribed to its quinonoid nature, and thus to its greater reactivity with nucleophiles compared to the α,β-unsaturated carbonyl group of **22**. The persistent, although reduced, toxicity of **48** is probably due to its conversion *in vivo* into **1** by an S_N2 nucleophilic oxirane-forming process via the C-6 OH group and bromide ion being a good leaving group. This probably did not occur in **24** as the chloride ion is a poor nucleofuge compared to the bromide ion. However, in this case it generated an α-oxirane ring. On the other hand, **25** is not suitable for an S_N2 nucleophilic substitution.

Both the reduction of the C-2 carbonyl group (**49**) and the reduction of the olefinic double bond with the selective reductive opening of the epoxy ring (**50**) led to a complete loss of activity. The lack of toxicity exhibited by derivative **49** underlines the important role of the C-2 carbonyl group in the biological activity.

Furthermore, not all the compounds (see derivatives **24**, **25**, **45**, **49** and **52**) preserving the olefinic Δ^3 double bond were active. This result could suggest that this feature is probably not essential for activity. However, compounds **24**, **25**, **45**, **49** and **52** also showed the opening of the oxirane ring and/or the modification of other structural features important for toxicity.

A marked loss of activity was observed with the conversion, by acetylation, of **22** in derivatives **45** and **46**. It is interesting to note that the 5-*O*-acetylsphaeropsidone (**45**) was inactive compared to its epimer (**51**), indicating the importance of the absolute configuration at this position for the interaction of the molecule with its corresponding target site. The activity of 5-*O*-acetylepisphaeropsidone is probably due to its hydrolysis *in vivo* into **23**, which occurs more easily compared to that of **45** into **22** since the acetyl group in **51** is located at the less hindered α-side opposite to the epoxy group.

Similar SAR trends were also observed for antifungal activity and the structural requirements for sphaeropsidone (**22**) seem to be the same as those needed for its

phytotoxicity. Sphaeropsidones **22** and **23**, their natural analogues **24** and **25** and derivatives **45**-**52** were assayed on five fungal species belonging to the genus *Phytophthora* (Table 4), which are destructive pathogens of forest trees and shrubs. As shown in Table 5, all fungal species were highly sensitive to sphaeropsidone (**22**) at 0.2 mg/plug. At the lowest concentration assayed (0.05 mg/plug), **22** was still active against all fungi with the exception of *P. gonapodydes* which was inhibited by less than 25%. Episphaeropsidone (**23**) had a weaker effect compared to sphaeropsidone (**22**) emphasizing once more the role of the absolute configuration at C-5 in the expression of bioactivities.

The results showed that most of the modifications made to **22** led to a loss of toxicity toward fungal species tested. Among the natural analogues (**24** and **25**) and derivatives **45-52**, compounds **24**, **25**, **46**, **49**, **50**, and **52** were pratically ineffective against all fungi tested even at the highest concentration assayed. Compound **45** inhibited less than 50% the mycelial growth of *P. nicotianae*, *P. cinnamomi*, *P. gonapodydes*, and *P. cambivora* at 0.2 mg/plug; it was more active against *P. pseudosyringae* at 0.2 mg/plug (100% inhibition). Derivative **47** completely inhibited the mycelial growth of fungi assayed even at the lowest concentration except for *P. gonapodydes*. Derivative **48** displayed a significant activity toward *P. pseudosyringae*. Compound **51** caused a marked reduction of mycelial growth of all fungi except for *P. gonapodydes* even at the lowest concentration. It is interesting to highlight that the only structural change in **22** resulting in an increase of its bioactivity was the oxidation of the C-5 allylic hydroxy group.

In brief, the C-5 hydroxy group, the epoxy ring, and the C-2 carbonyl group, along with the C-5 absolute configuration, could be pointed out as important structural features. In fact, modifications of the C-5 hydroxy group, such as acetylation, the reduction of the C-2 carbonyl group, and opening of the epoxy ring led to compounds which were much less active and/or inactive in comparison to **22**. The role of the α,β-double bond remains to

Table 4. Isolates and hosts of the *Phytophthora* species used in antifungal assay.

Species	Strains	Host
P. cambivora	Ph 041	Sweet chestnut
P. cinnamomi	Ph 001	Olm oak
P. gonapodydes	Ph 038	Sweet chestnut
P. nicotianae	Ph 002	Mirtle
P. pseudosyringae	Ph 043	Sweet chestnut

Table 5. Percentage growth inhibition by sphaeropsidones (**22**, **23**) and their naturalal analogues **24** and **25** and derivatives **45**-**52** tested on five plant pathogenic fungi belonging to genus *Phytophthora* after 4-7 days of treatment.

		Fungal species				
Compound	Concentration (mg/plug)	*P. cambivora*	*P. cinnamomi*	*P. gonapodydes*	*P. nicotianae*	*P. pseudosyringae*
	0.2	100.0	100.0	100.0	100.0	100.0
22	0.1	64.1	73.3	50.5	79.8	100.0
	0.05	48.9	64.5	24.1	61.5	64.2
	0.2	70.5	72.8	82.6	61.8	100.0
23	0.1	41.3	39.8	10.7	43.1	39.9
	0.05	27.3	21.1	n.i.	25.1	22.4
	0.2	n.i.	20.3	n.i.	n.i.	12.3
24	0.1	nt	nt	nt	nt	nt
	0.05	nt	nt	nt	nt	nt
	0.2	10.4	23.3	n.i.	14.1	13.4
25	0.1	nt	nt	nt	nt	nt
	0.05	nt	nt	nt	nt	nt
	0.2	26.1	49.7	24.1	33.9	100.0
45	0.1	nt	nt	nt	nt	23.1
	0.05	nt	nt	nt	nt	11.9
	0.2	13.7	28.0	15.9	16.5	15.8
46	0.1	nt	nt	nt	nt	nt
	0.05	nt	nt	nt	nt	nt
	0.2	100.0	100.0	100.0	100.0	100.0
47	0.1	100.0	100.0	100.0	100.0	100.0
	0.05	100.0	100.0	12.9	100.0	100.0
	0.2	44.2	61.5	21.8	53.2	74.6
48	0.1	nt	nt	nt	nt	62.7
	0.05	nt	nt	nt	nt	39.9
	0.2	n.i.	n.i.	n.i..	n.i.	n.i.
49	0.1	nt	nt	nt	nt	nt
	0.05	nt	nt	nt	nt	nt
	0.2	n.i.	n.i.	n.i.	n.i.	n.i.
50	0.1	nt	nt	nt	nt	nt
	0.05	nt	nt	nt	nt	nt
	0.2	100.0	100.0	100.0	100.0	100.0
51	0.1	82.5	100.00	57.2	100.0	100.0
	0.05	30.0	57.7	14.8	57.2	42.9
	0.2	n.i.	20.8	n.i.	16.5	n.i.
52	0.1	nt	nt	nt	nt	nt
	0.05	nt	nt	nt	nt	nt
Mefenoxam	0.2	84.1	100.0	47.0	100.0	100.0
	0.1	81.9	100.0	43.3	100.0	100.0
	0.05	78.3	100.0	37.6	100.0	100.0

be defined by preparing a derivative with only one modification in **22**. Finally, among the synthesized derivatives, compound **47** was found more effective than **22** in inhibiting mycelial growth of invasive pathogens on a global scale such as *Phytophthora* species. Its antifungal activity *in vitro* (Table 5) was shown to be similar to the synthetic fungicide (mefenoxam) commonly employed for control of diseases caused by oomycetes (Erwin and Ribeiro, 1996). This encourages to continue studies aimed at generating further compounds which are suitable for development of alternative strategies for management of these pathogens, also in light of the development of resistance in *Phytophthora* species to the phenylamides.

5.7. Hemisynthesis and chemical characterization of sphaeropsidins A-C derivatives

To investigate the potential antibacterial activity of sphaeropsidins against several bacterial rice pathogens and identify which structural features are essential for this biological activity 14 derivatives were prepared by chemical transformation of the functionalities present in sphaeropsidines A, B and C (**16**-**18**, Fig. 3, Pag. 26), as described in the Experimental section.

The structural features of **16** and those of the **17** and **18** provide evidence for considering these two latter as a naturally modified analogues of **16**.

The spectroscopic and physical data of the 7 known derivates (**26**-**30** and **32**-**33**, Fig. 5, Pag. 32) were identical to those previously reported (Evidente *et al.*, 1997; Sparapano *et al.*, 2004). The structures assigned to the 7 new derivatives (**55**-**59**, Scheme 5) of sphaeropsidins A and B (**16-17**) were determined by comparing their UV, IR, ^{1}H and ^{13}C NMR, and EI or ESI MS spectra with those of **16** and **17**, respectively.

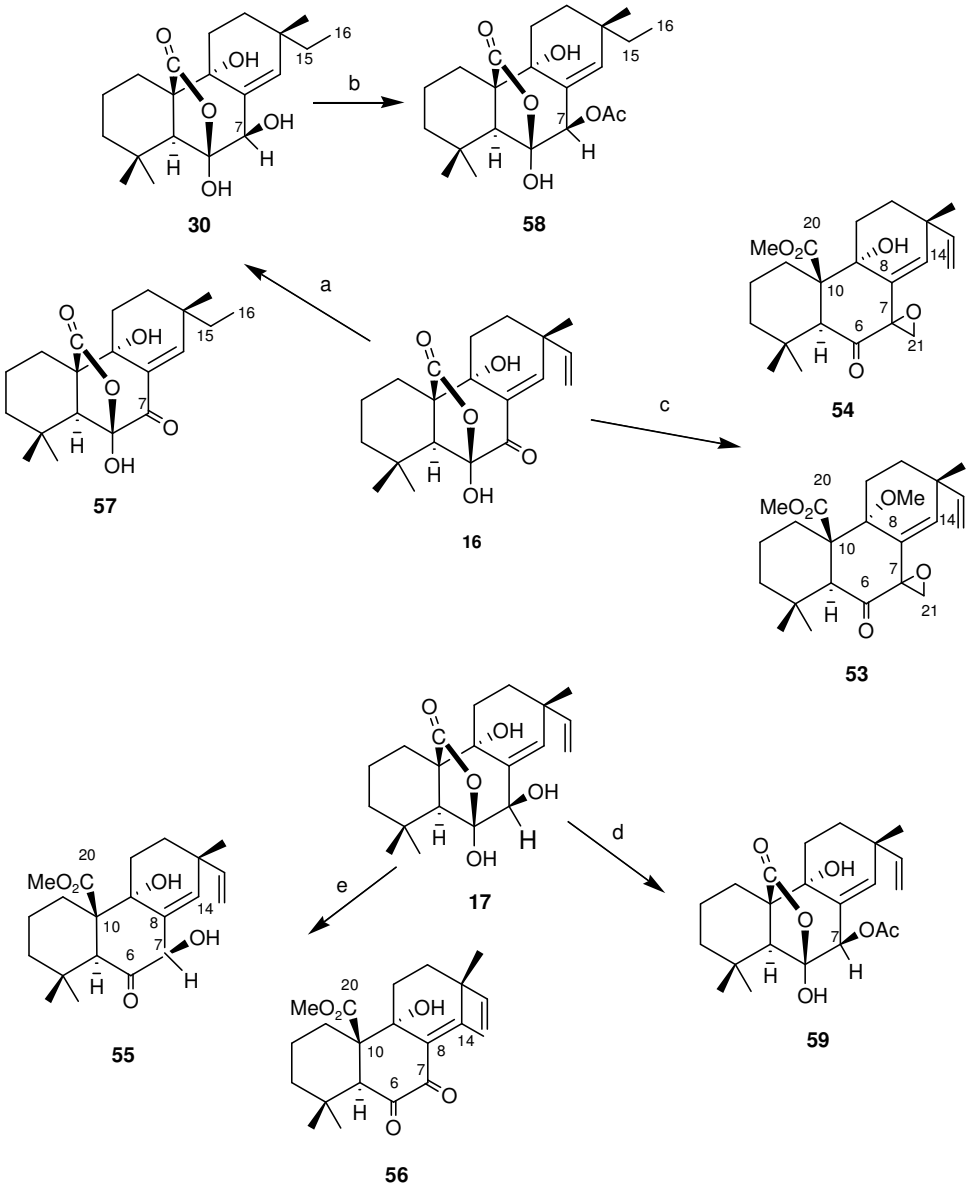

[a]Reagents and conditions: (a) H_2, PtO_2, MeOH, rt, 15 h; (b) Ac_2O, pyridine, 25 °C, 3 h; (c) CH_2N_2, MeOH, rt, 24 h; (d) Ac_2O, pyridine, rt, 4 h; (e) CH_2N_2, MeOH, rt, 4 h.

Scheme 5. Hemisynthesis of sphaeropsidins A-B (**16**-**17**) derivatives (**30**, **53**-**59**).[a]

By acetylation, sphaeropsidin A (**16**) was converted into the 6-*O*-acetyl derivative (**26**, Fig. 5) while with the Fritz and Schenk reagent, used to acetylate the hindered C-9 hydroxy group, **16** was converted into the 6-*O*-acetyl-14-acetoxy derivative (**29**, Fig. 5).

The catalytic hydrogenation of **16** generated the derivatives **30** and **57** (Fig. 5 and Scheme 5), saturation of the C-13 vinyl group for **57**, additionally the reduction of the C-7 carbonyl group for **30**.

The ESI MS spectrum of **57** (Fig. 71) showed the potassium and sodium clusters and the pseudomolecular ion at *m/z* 387, 371 and 349. The IR (Fig. 72) and the UV (Fig. 73) spectra were very similar to that of **16** while the ^{1}H NMR (Fig. 74) differed essentially for the absence of the proton of the vinyl group at C-13 and for the presence of the signal of the ethyl group attached to the same carbon appearing as a quartet and a triplet (J= 7.5 Hz) at δ 1.36 and 0.88 for CH_2-15 and Me-16.

Acetylation of **30** gave the corresponding 7-*O*-acetyl derivative (**58**, Scheme 5). The ESI MS spectrum of **58** (Fig. 75) showed the potassium and sodium clusters and the pseudomolecular ions at *m/z* 431, 415 and 393. The IR (Fig. 76) and UV spectra were very similar to those of **30**. The ^{1}H NMR (Fig. 77) differed from that of **30**, for the downfield shift of H-7 (Δδ: 0.99) appearing as a broad singlet at δ 5.24 and for the presence of the singlet of the acetyl group at δ 2.28.

By reaction with diazomethane, sphaeropsidin A (**16**) was converted into the known derivative **32** (Fig. 5) and into the new compounds **53** and **54** (Scheme 5). All these three derivatives showed the opening of the hemiketal lactone ring, the conversion of the carboxy group into the corresponding methyl ester, and the C-6 hemiketal group into the corresponding carbonyl group. The C-7 carbonyl group in the methyl ester of **16** has susceptible to methylene insertion by diazomethane to generate the corresponding 1,1-disubstitued oxirane ring in **53** and **54**.

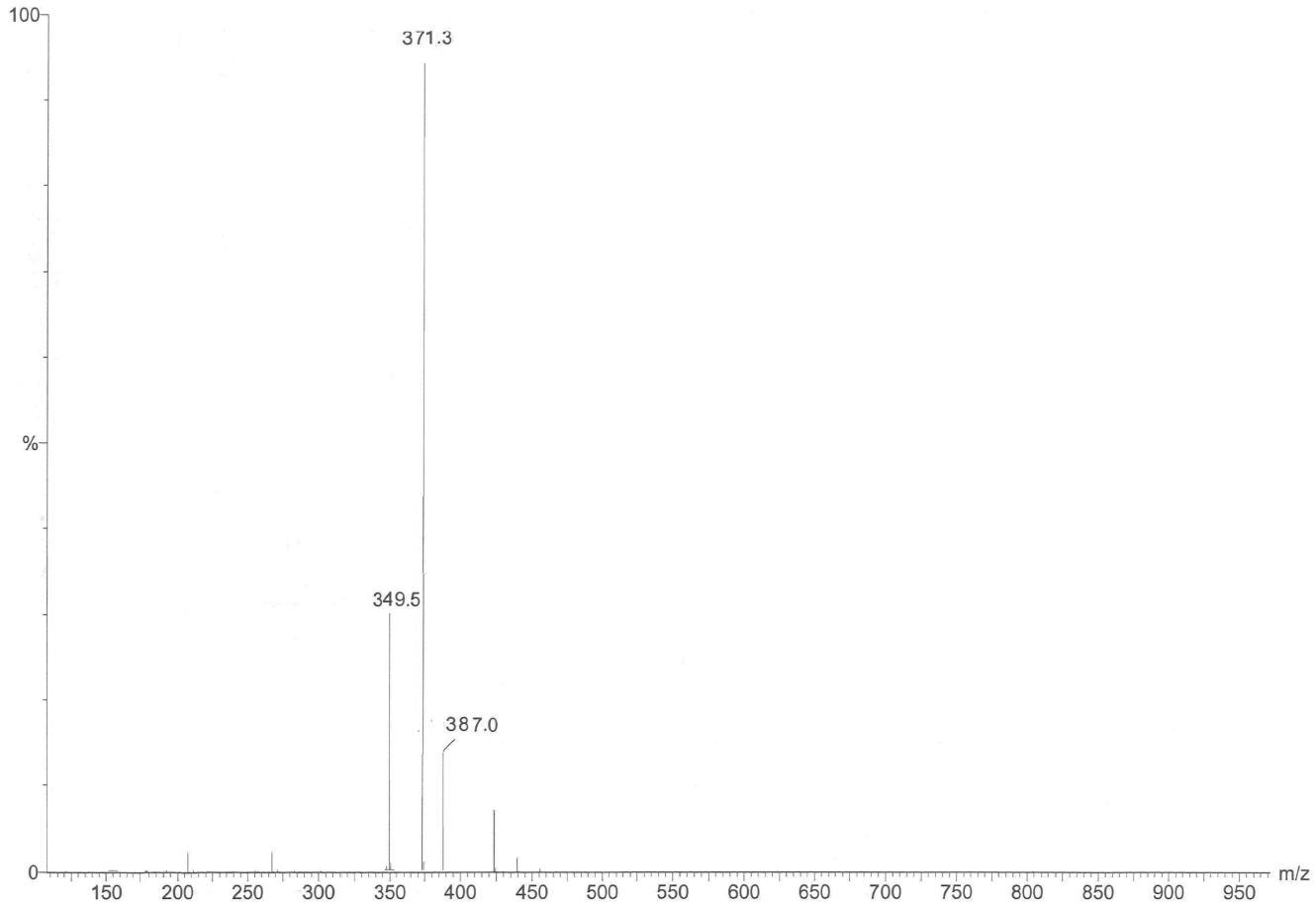

Figure 71. ESI MS spectrum of 15,16-dihydrosphaeropsidin A (**57**), recorded in positive modality.

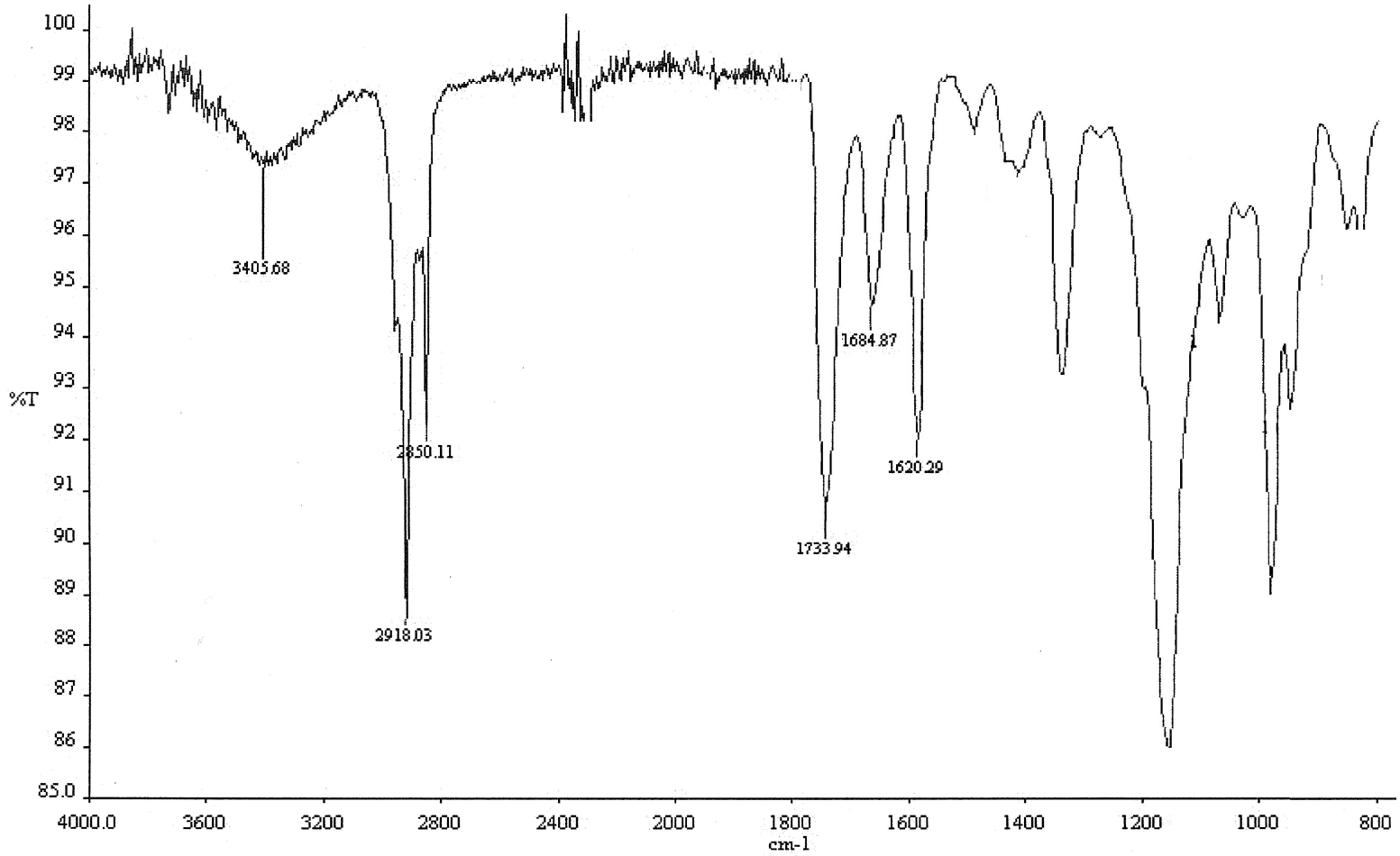

Figure 72. IR spectrum of 15,16-dihydrosphaeropsidin A (**57**), recorded as glassy film.

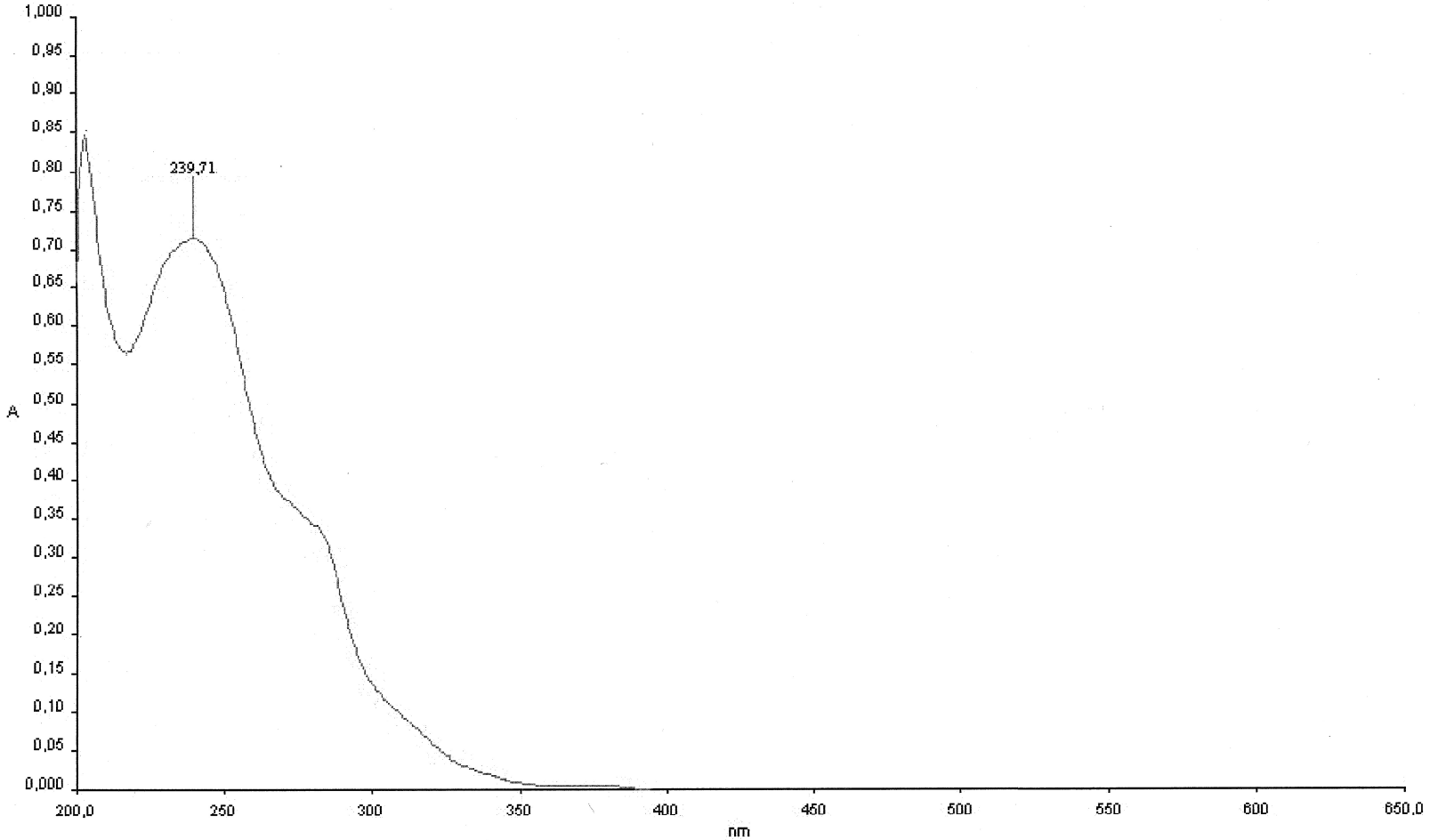

Figure 73. UV spectrum of 15,16-dihydrosphaeropsidin A (**57**), recorded in MeCN solution.

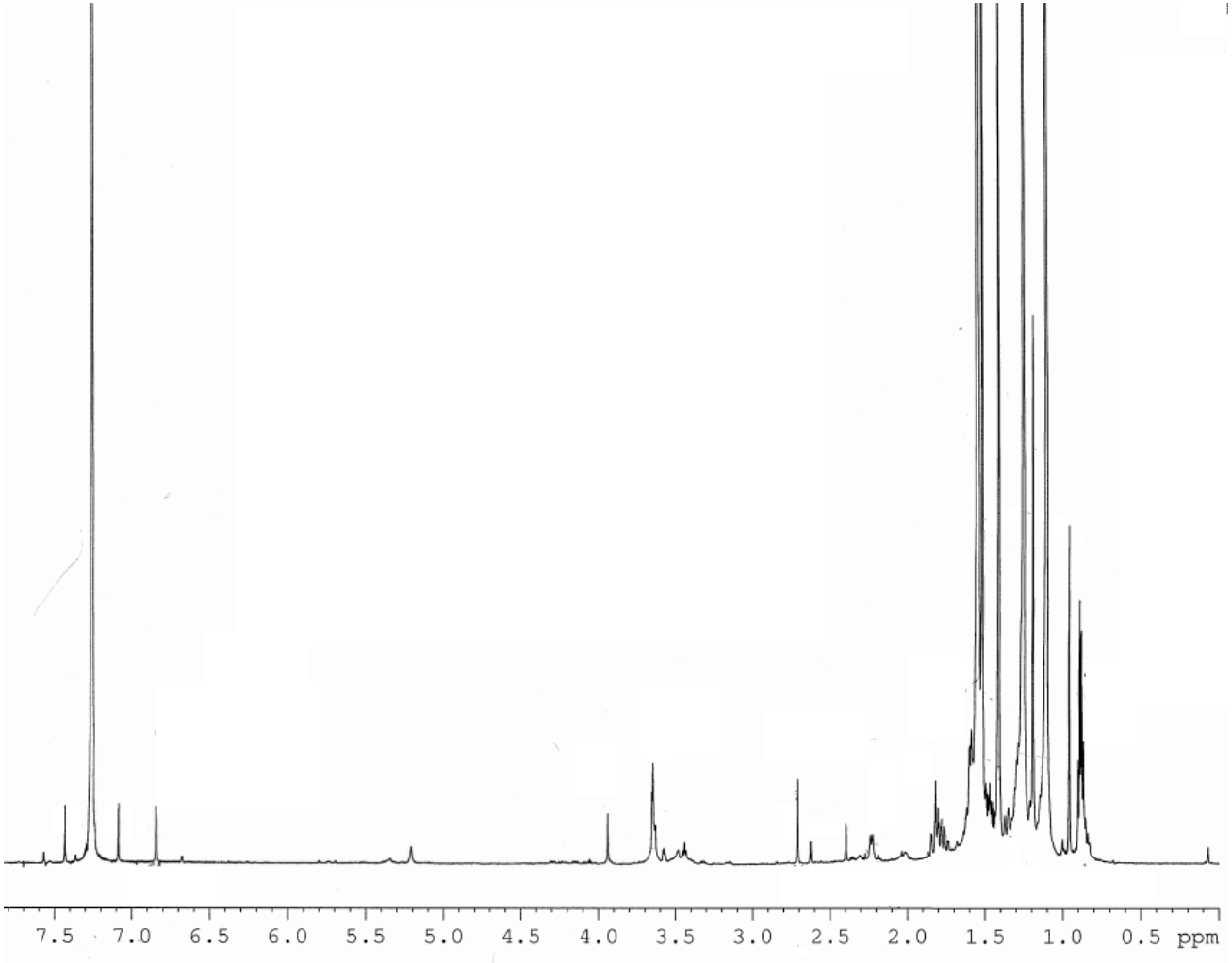

Figure 74. ^{1}H NMR spectrum of 15,16-dihydrosphaeropsidin A (**57**), recorded in $CDCl_3$ at 600 MHz.

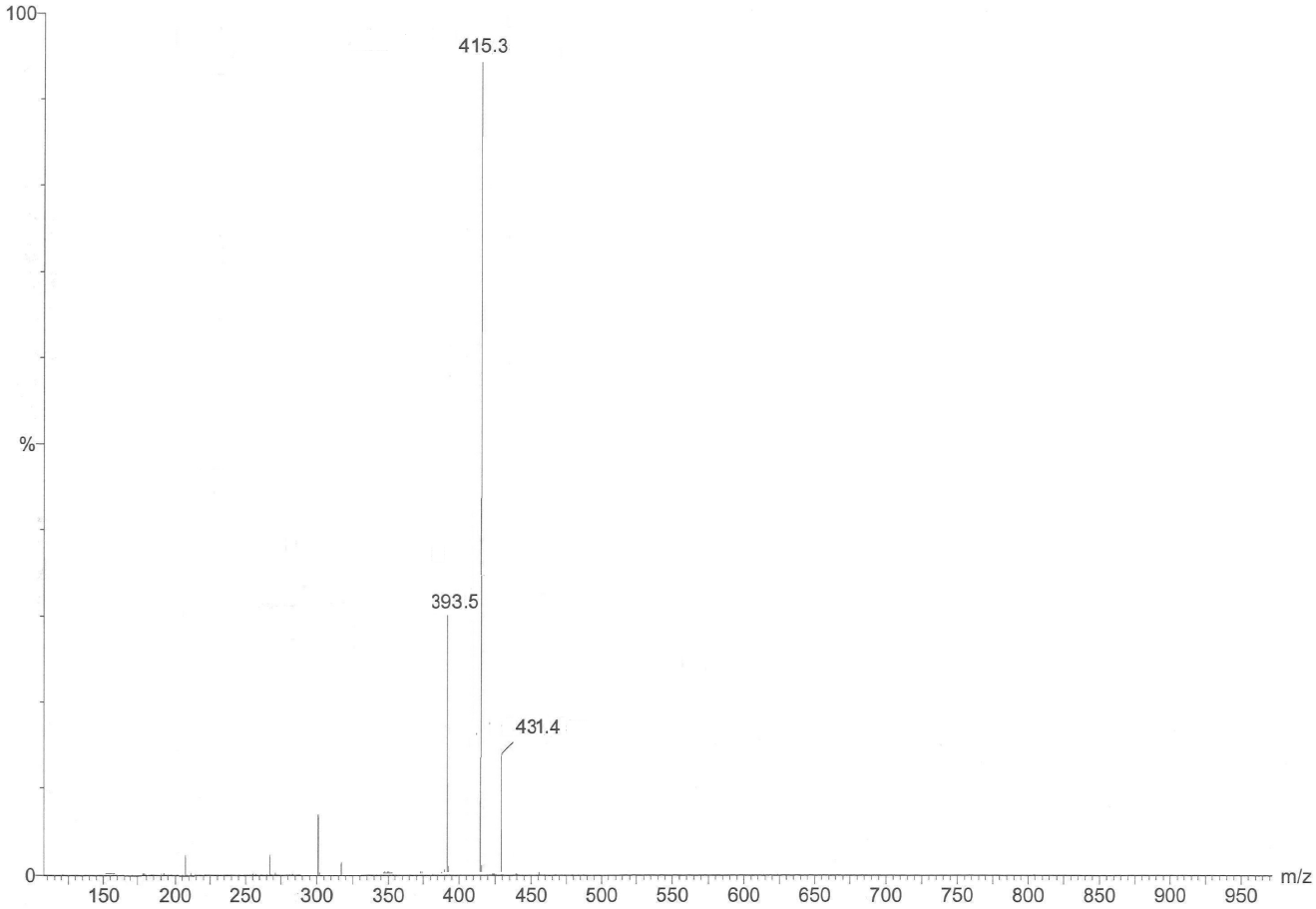

Figure 75. ESI MS spectrum of 7-*O*-acetyl-7,*O*,15,16-tetrahydrosphaeropsidin A (**58**), recorded in positive modality.

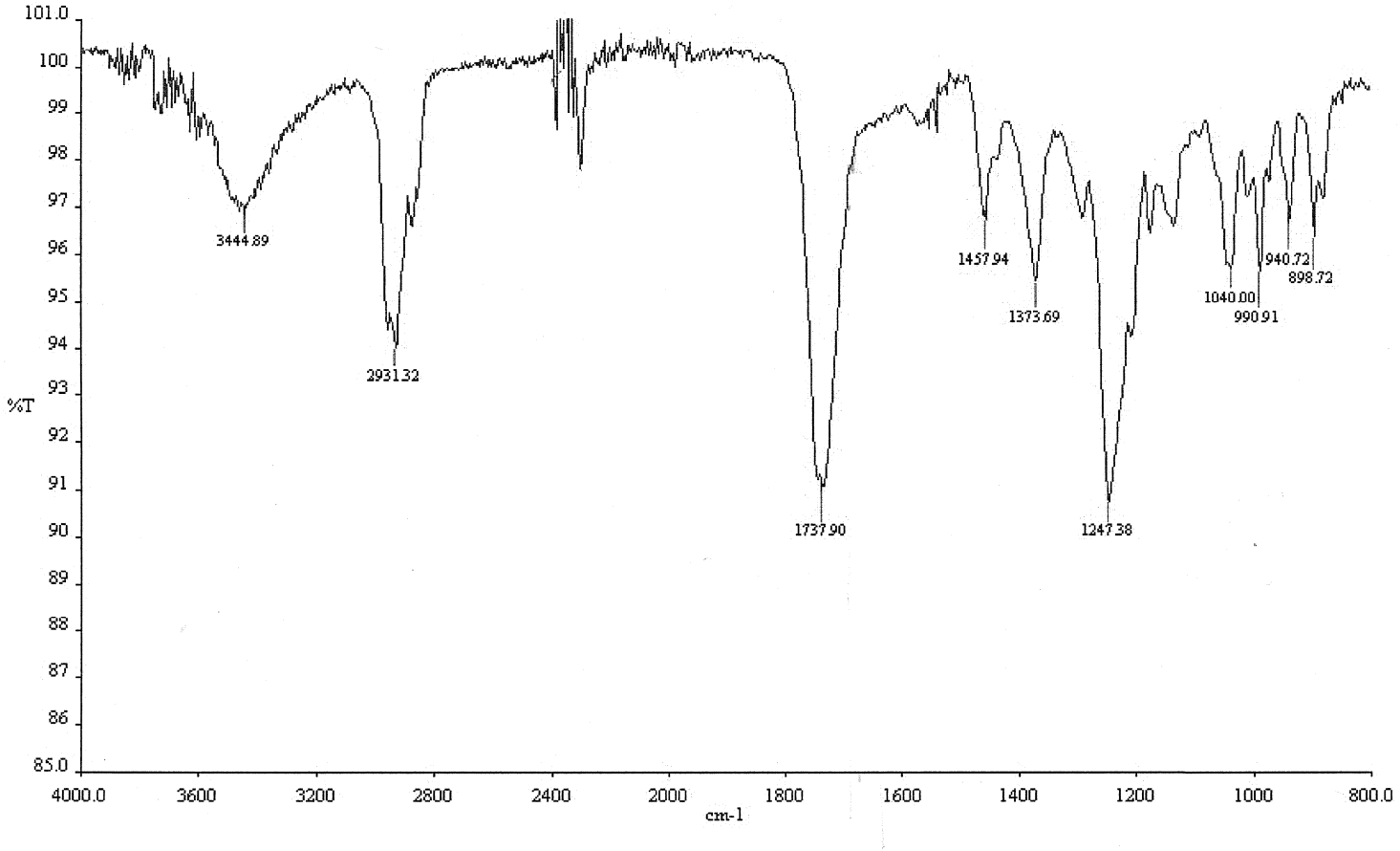

Figure 76. IR spectrum of 7-*O*-acetyl-7,*O*,15,16-tetrahydrosphaeropsidin A (**58**), recorded as glassy film.

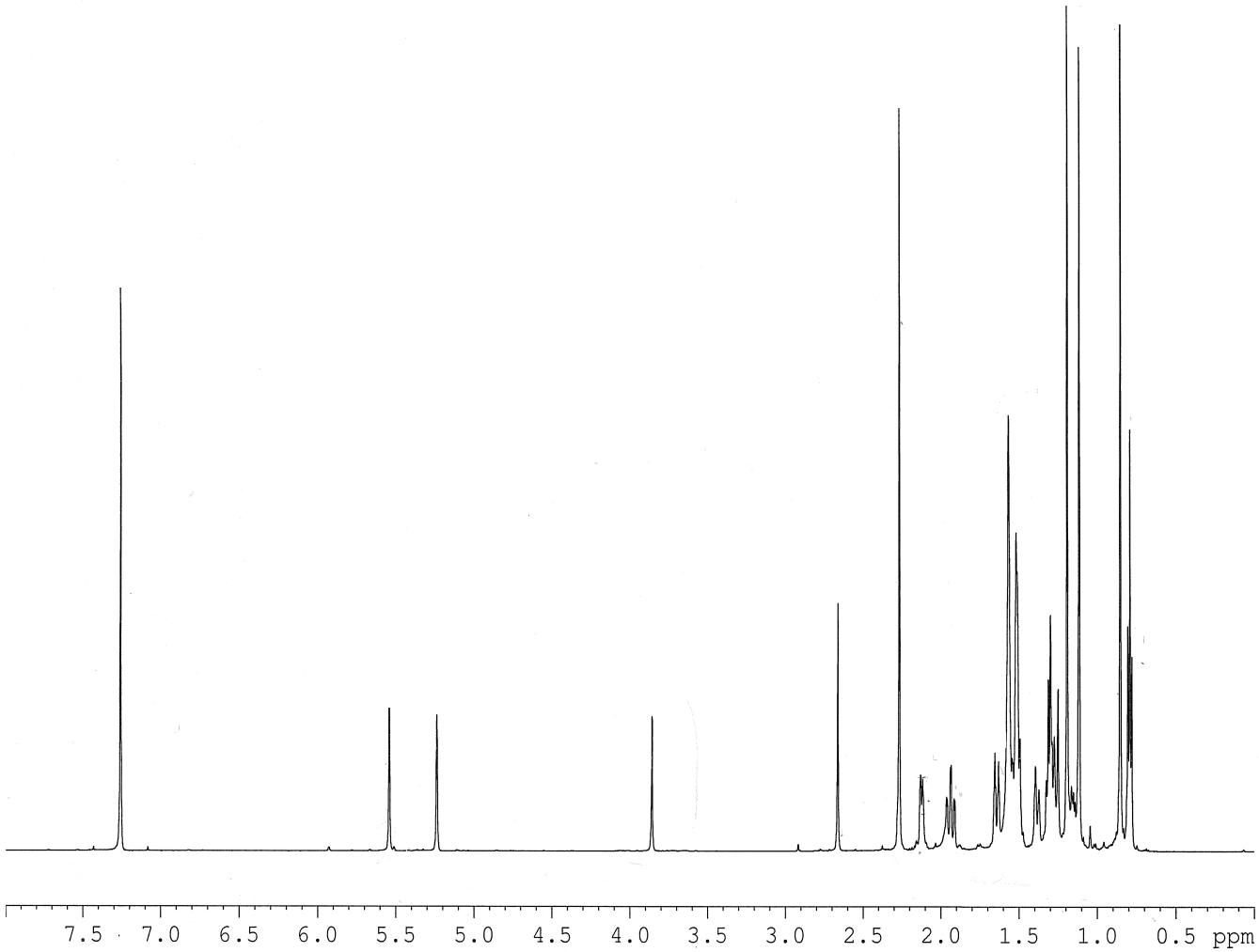

Figure 77. ^{1}H NMR spectrum of 7-*O*-acetyl-7,*O*,15,16-tetrahydrosphaeropsidin A (**58**), recorded in $CDCl_3$ at 600 MHz.

The IR (Fig. 78) and UV spectra of **53**, compared to that of **16**, showed the absence of the hydroxyl group and no absorption maximum due to a conjugated carbonyl group, respectively. The ^{1}H-NMR (Fig. 79 and Table 3), differed from that of **16**, essentially for the singlets of the ester and ether metoxy groups at δ 3.47 and 3.62, respectively, and for two doublets (J= 6.2 Hz) due to the protons of the metylene group (H_2-C-21) of the 2,2 disubstitute oxirane ring at δ 2.78 and 2.47. The C(8)-C(14) double bond was similarly susceptible to methylene insertion to generate **32**. Because of steric hindrance, the presence of the C-9 *O*-methyl group in **53** may be explained as resulting from solvolysis (MeOH) of the allylic hydroxyl group. The structure of **53** was supported by the fragmentation ions observed in the EI MS spectrum at *m/z* 374, 356, and 342 which are generated from the molecular ion at 388 by the loss of CH_2, CH_3OH and both, respectively.

The ESIMS spectrum of **54** (Fig. 80) showed the potassium and sodium clusters and the pseudomolecular ions at *m/z* 413, 397 and 375. The IR spectrum (Fig. 81), differed from that of **53**, for the presence of hydroxyl group band while its ^{1}H NMR differed only for the presence of the ester metoxy group as singlet at δ 3.46.

Acetylation of sphaeropsidin B (**17**) gave the 7-*O*-acetyl derivative (**59**, Scheme 5), preserving the hemiketal hydroxy group at C-6 and showing the acetylation of the hydroxyl group at C-7. The ESIMS spectrum of **59** (Fig. 82) showed the potassium and sodium clusters and the pseudomolecular ions at *m/z* 429, 413 and 391. The IR spectrum (Fig. 83), comparing to that of **17**, showed the presence of a further carbonyl group due to the acetyl group wile its ^{1}H NMR (Fig. 84) differed from that of **17** for the downfield shift of H-7 (Δδ: 1.33) resonating as singlet at δ 5.55 and for the presence of the same acetyl group appearing as singlet at δ 2.27.

Treatment of **17** with diazomethane yielded the new derivatives **55** and **56** (Scheme 5), which, like the sphaeropsidin A derivatives **32**, **53** and **54** showed opening of the

Table 3. ^{1}H NMR data of derivatives of sphaeropsidins A (**53** and **54**) and B (**55** and **56**).

	53	**54**	**55**	**56**
Position	δ_H, *J* (Hz)	δ_H, *J* (Hz)	δ_H, *J* (Hz)	δ_H, *J* (Hz)
1	2.28 br d (11.0)	2.28 br d (11.0)	2.29 br d (11.6)	2.36 br d (12.6)
1’	1.56 m	1.60 m	1.65 m	1.56 m
2	1.56 m	1.60 m	1.65 m	1.56 m
2’	1.56 m	1.60 m	1.65 m	1.56 m
3	1.56 m	1.80 m	1.84 m	1.70 m
3’	1.56 m	1.60 m	1.65 m	1.56 m
5	3.02 s	3.85 s	2.94 s	3.13 s
7			4.70 br s	
11	1.38 m	1.38 m	1.32 m	1.41 m
11’	1.29 m	1.29 m	1.24 m	1.28 m
12	1.78 m	1.80 m	1.80 m	2.15 m
12’	1.56 m	1.60 m	1.65 m	1.56 m
14	5.17 br s	5.17 br s	5.85 br s	5.85 br s
15	5.70 dd (17.4, 10.5)	5.70 dd (17.4, 10.5)	5.82 dd (17.4, 10.6)	5.82 dd (17.5,10.7)
16	5.00 dd(17.4, 1.5)	4.91 dd (17.4,1.5)	5.01 dd (17.4, 1.5)	5.04 dd (17.5, 1.5)
16’	4.99 dd (10.5, 1.5)	4.88 dd (10.5, 1.5)	4.98 dd (10.6, 1.5)	5.01 dd (10.7, 1.5)
17	0.87 s	0.87 s	0.90 s	0.87 s
18	1.15 s	1.15 s	1.14 s	1.25 s
19	1.02	1.02 s	0.95 s	0.97 s
21	2.78 d (6.2)	2.78 d (6.2)		
21’	2.47 d (6.2)	2.47 d (6.2)		
OMe	3.62 s	3.46 s	3.54 s	3.70 s
OMe	3.47 s			
Me-C=C				1.34 s

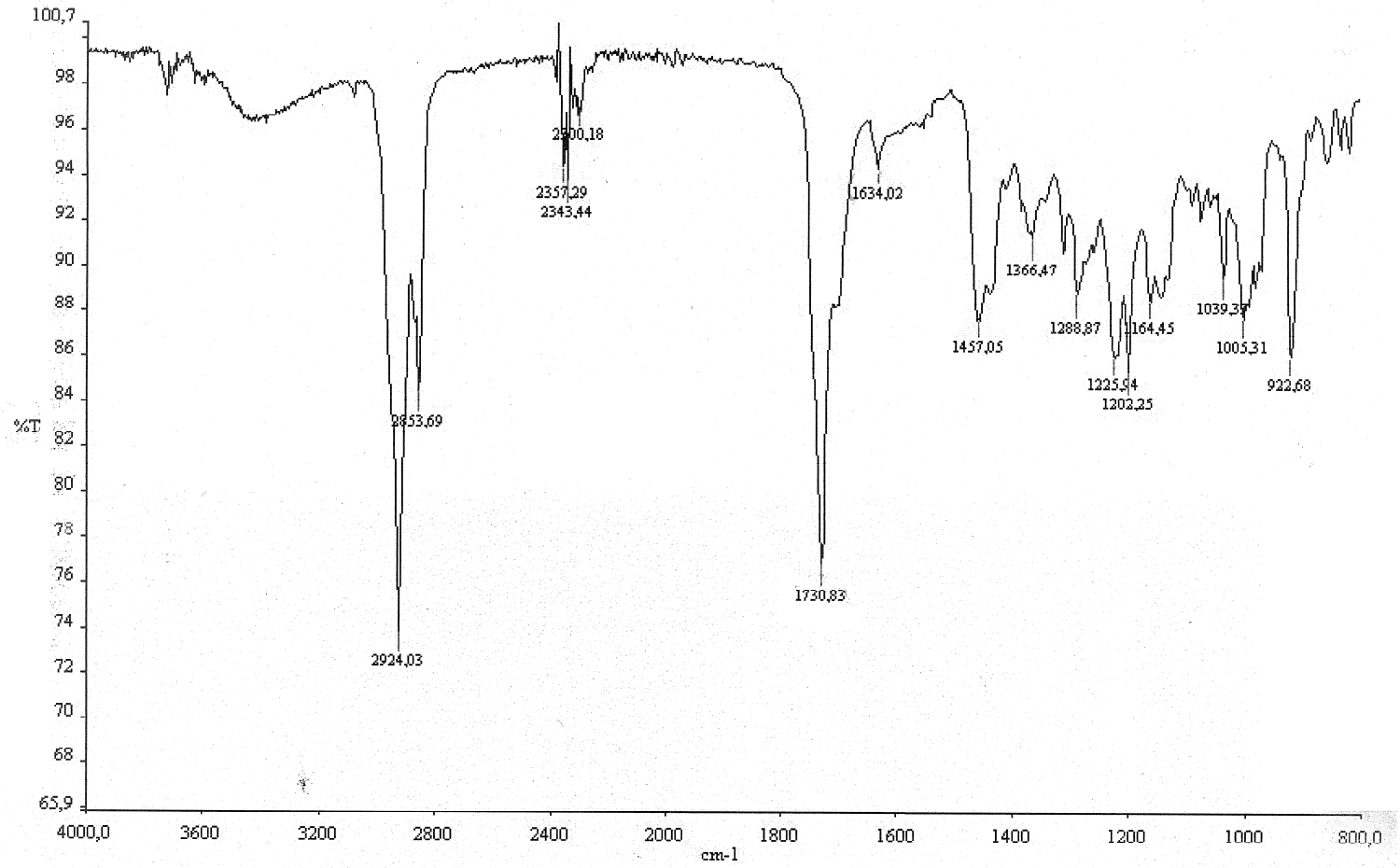

Figure 78. IR spectrum of 7,*O*-methylen-9,*O*-methyl-sphaeropsidin A methyl ester (**53**), recorded as glassy film.

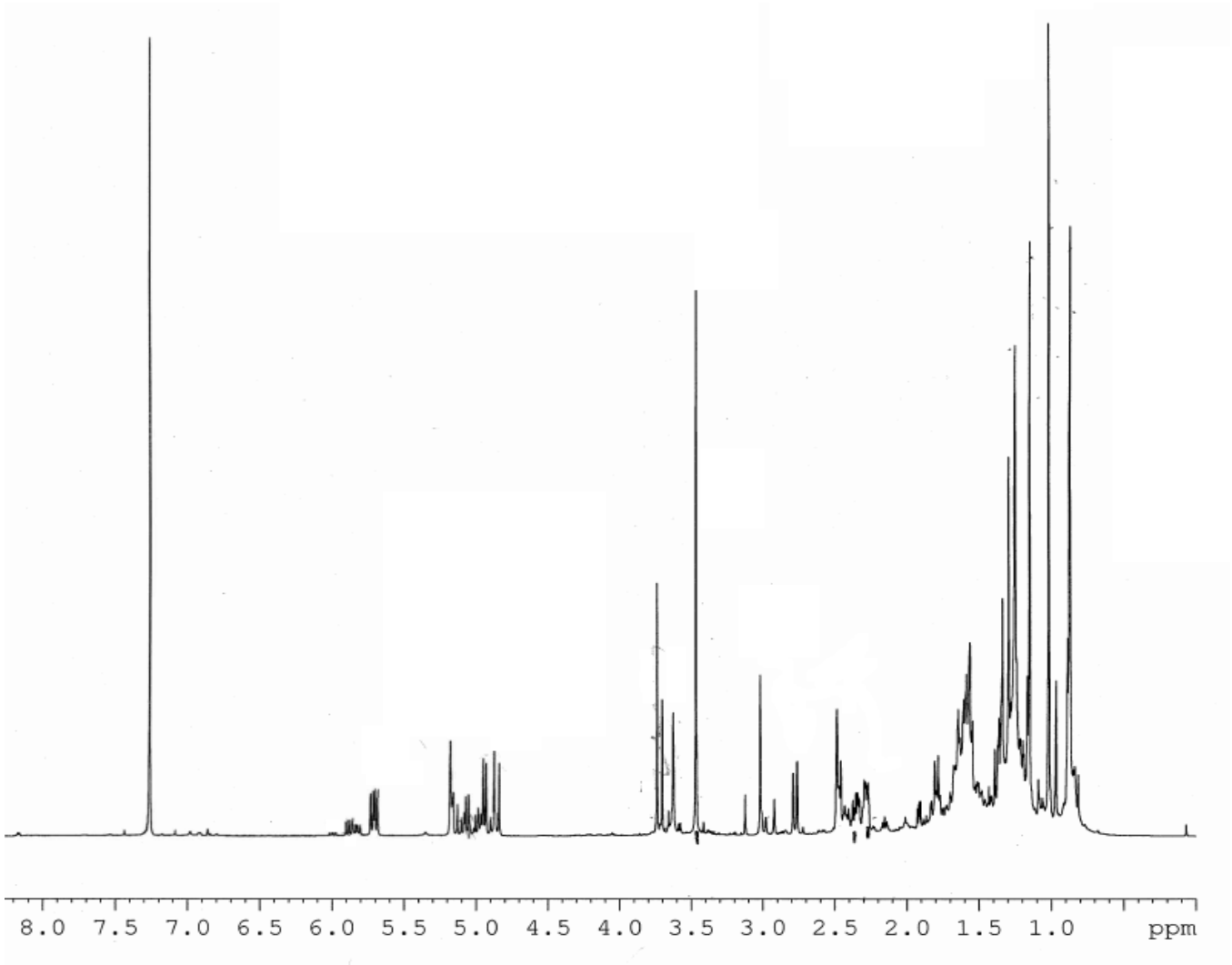

Figure 79. ^{1}H NMR spectrum of 7,*O*-methylen-9,*O*-methyl-sphaeropsidin A methyl ester (**53**), recorded in $CDCl_3$ at 600 MHz.

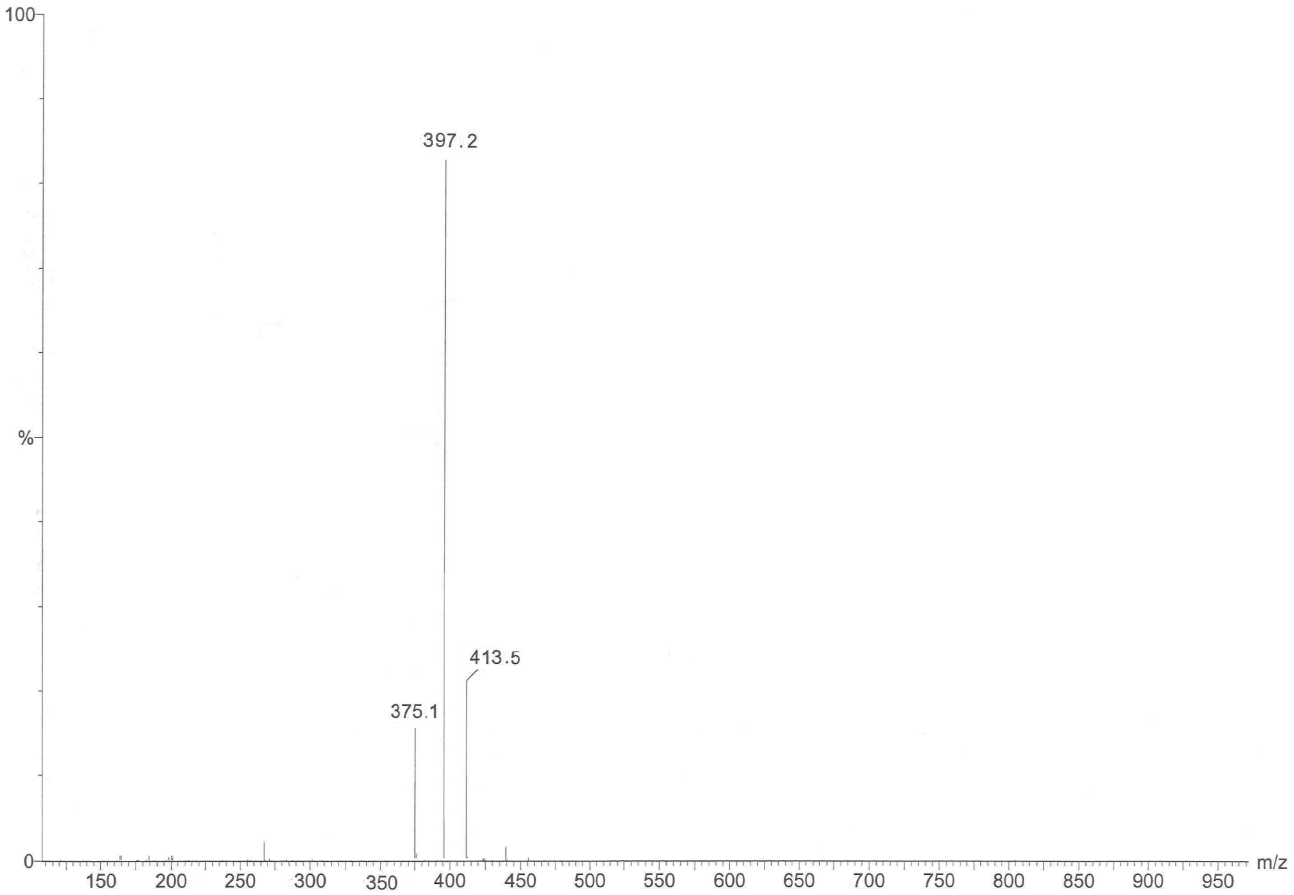

Figure 80. ESI MS spectrum of 7,*O*-methylen-sphaeropsidin A methyl ester (**54**), recorded in positive modality.

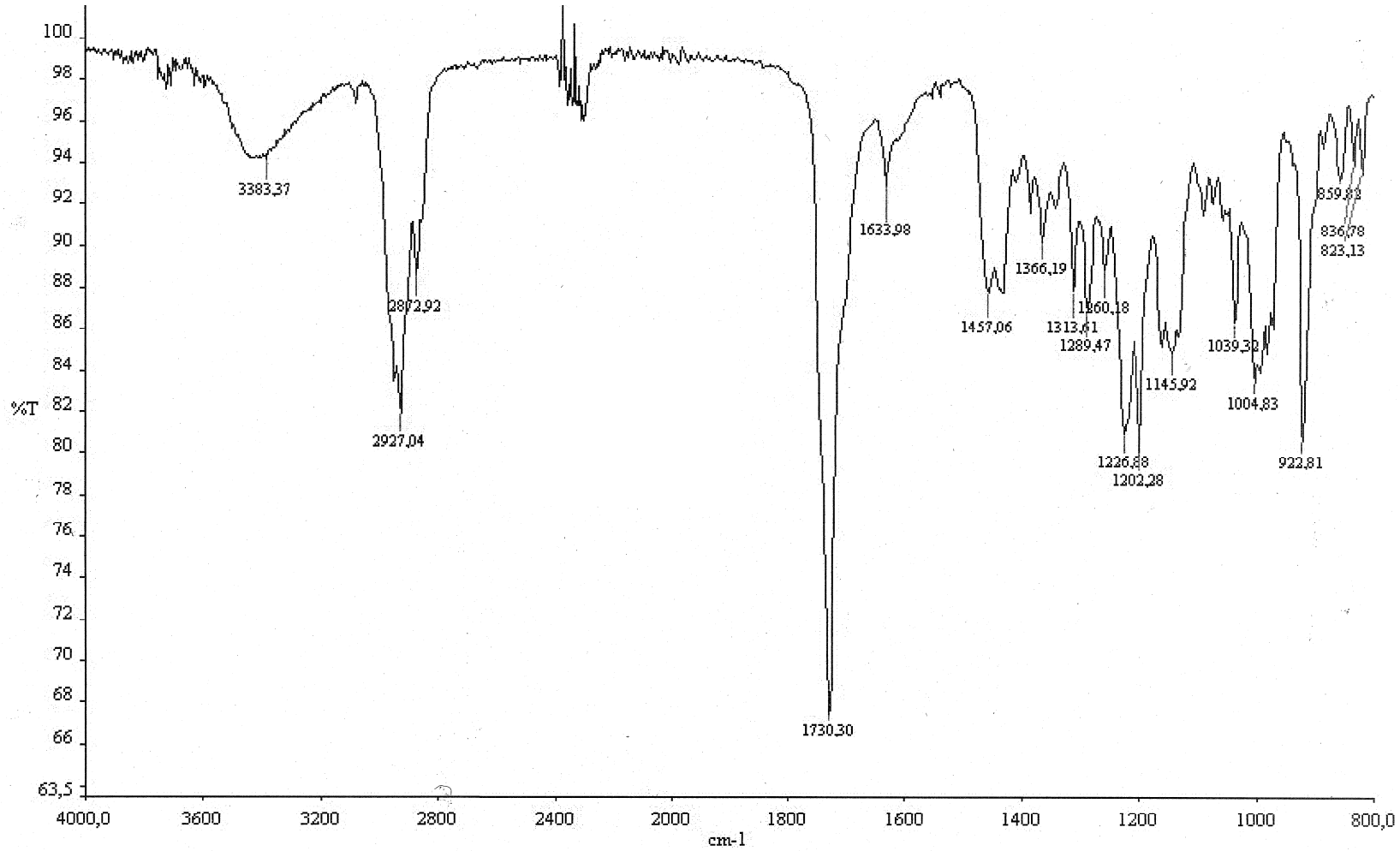

Figure 81. IR spectrum of 7,*O*-methylen-sphaeropsidin A methyl ester (**54**), recorded as glassy film.

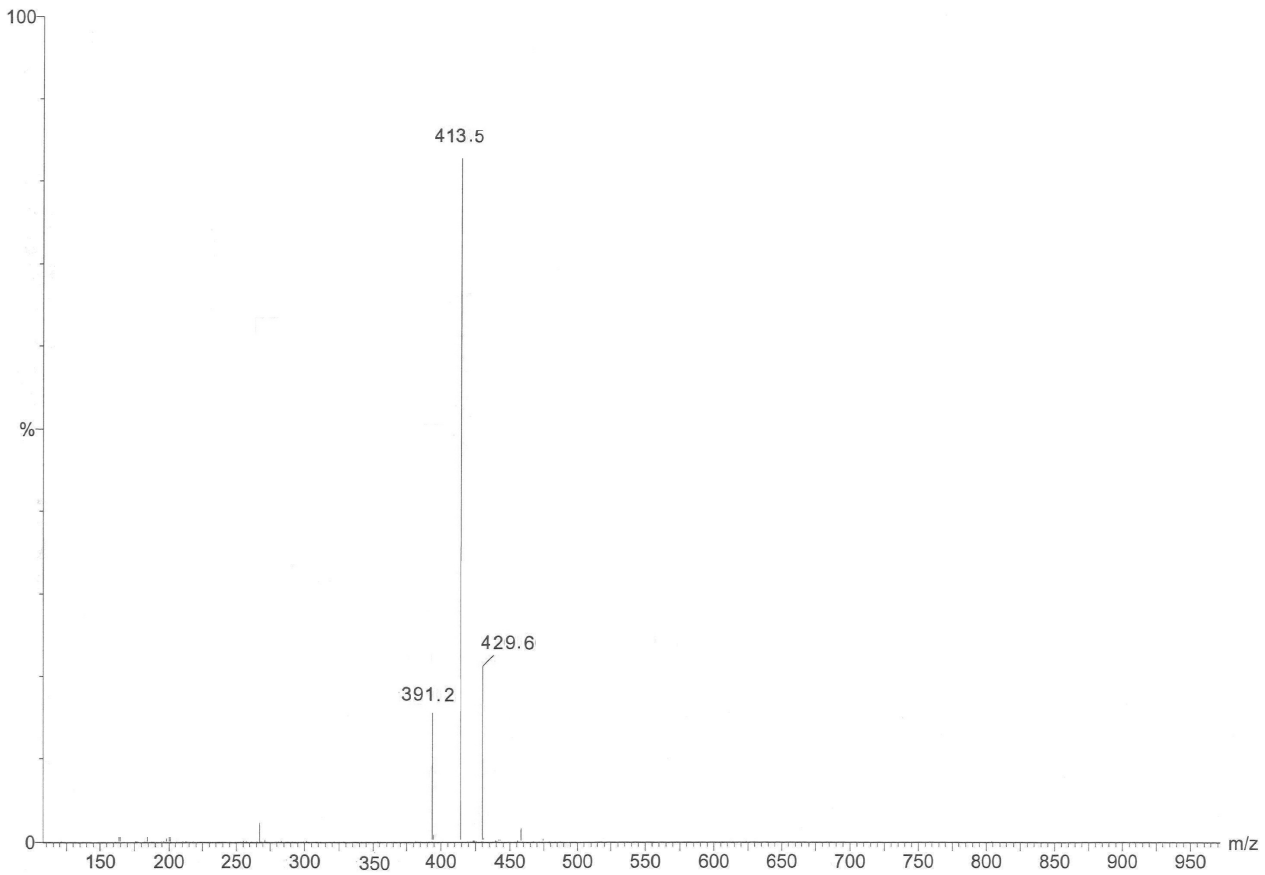

Figure 82. ESI MS spectrum of 7,*O*-acetylsphaeropsidin B (**59**), recorded in positive modality.

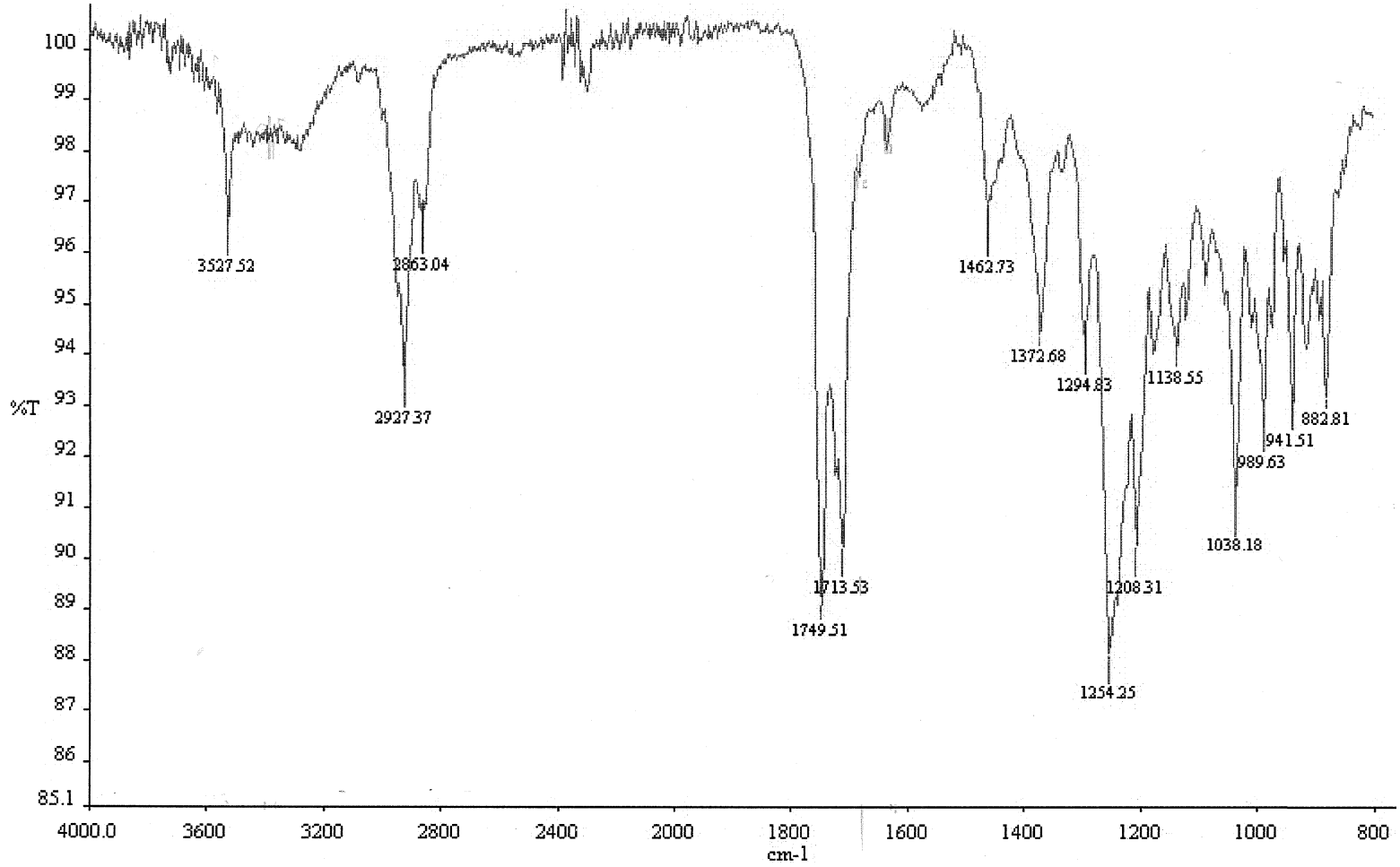

Figure 83. IR spectrum of 7,*O*-acetylsphaeropsidin B (**59**), recorded as glassy film.

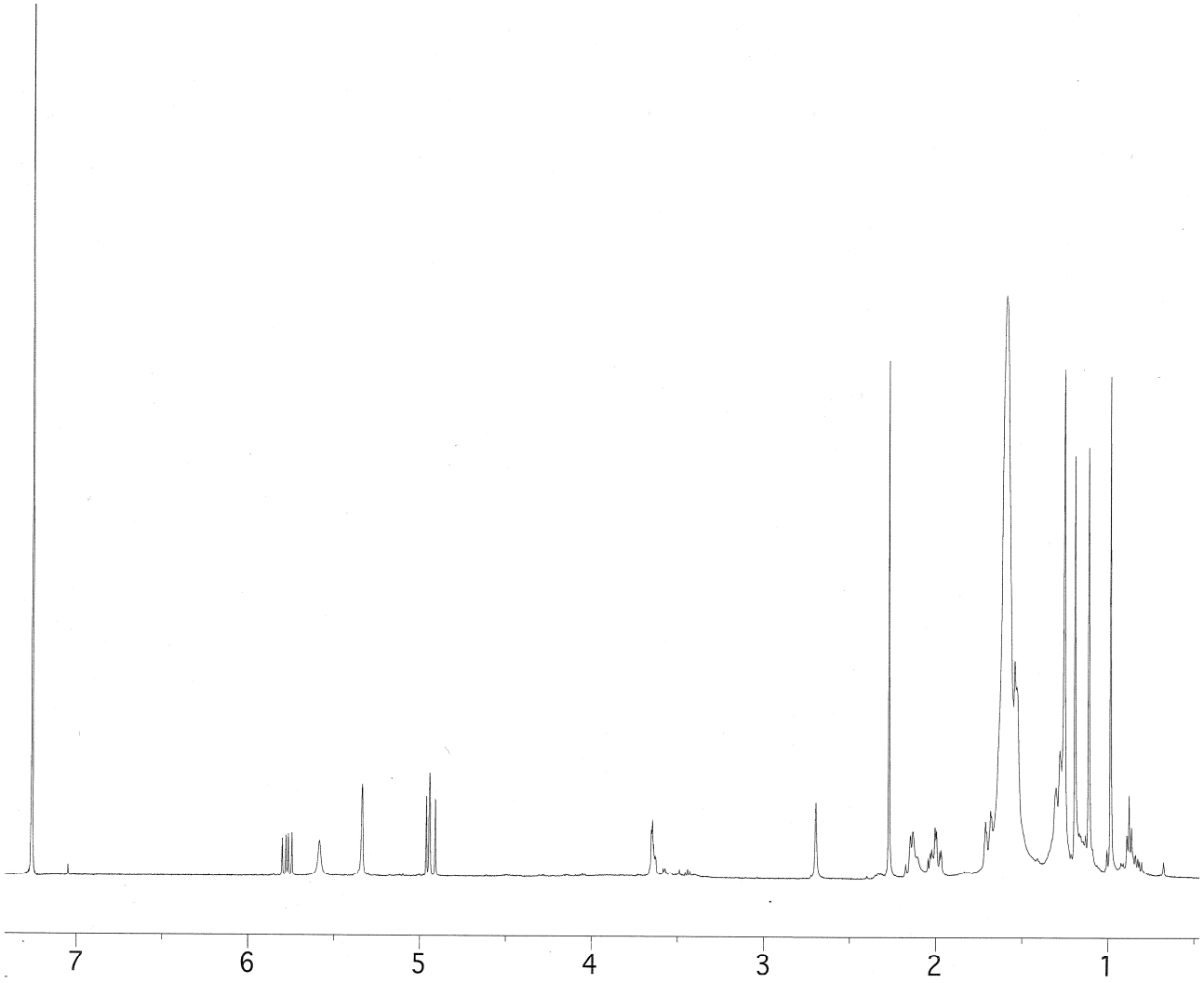

Figure 84. ^{1}H NMR spectrum of 7,*O*-acetylsphaeropsidin B (**59**), recorded in $CDCl_3$ at 600 MHz.

hemiketal lactone and the conversions of the carboxy group into the corresponding methyl ester, and the C-6 hemiketal functionality into the corresponding carbonyl group. Furthermore, derivative **17** also showed the methylene insertion into the olefinic C(14)-H bond generating the corresponding vinylic methyl group.

The ESIMS spectrum of **55** showed the potassium and sodium clusters ions at *m/z* 385 and 363. The IR spectrum (Fig. 85) was very similar to that of **17**, while its ^{1}H NMR (Fig. 86) spectrum differed from that of the parent compound only for the presence of the ester methoxy group appearing as singlet at δ 3.54.

The ESIMS spectrum of **56** showed the potassium and sodium clusters and the pseudomolecular ions at *m/z* 413, 397 and 375. The IR spectrum was very similar to that of **55** while the UV spectrum showed a significant adsorption due to an extended conjugated system involving the two carbonyl at C-6 and C-7 and the double bond between C-8 and C-14. The ^{1}H NMR (Fig. 87) compared to that of **55**, showed the absence of the proton H-7 and the presence of the vinylic methyl group observed at δ 1.34.

Compound **17**, in turn, was converted by $NaIO_4$ oxidation into the oxidized derivative **33** (Fig. 5), which showed marked modification of the B-ring, while the A and C rings appeared practically unaltered. In particular, derivative **33** exhibited the opening of the hemiketal lactone producing a carboxylic group at C-10, and the cleavage of the C-6-C-7 bond. C-6 was oxidized into a hydroxycarbonyl group, which formed a γ-lactone functionality with the C-9 hydroxy group, while the carbonyl group at C-7 appeared as a formyl group conjugated with the C-8-C-14 double bond. These noteworthy structural modifications resulted in substantial disruption of the tricyclic pimarane system. Treatment of sphaeropsidin C (**18**) with diazomethane afforded corresponding methyl ester **28** (Scheme 5), while stereoselective reduction with $NaBH_4$, as was observed in the

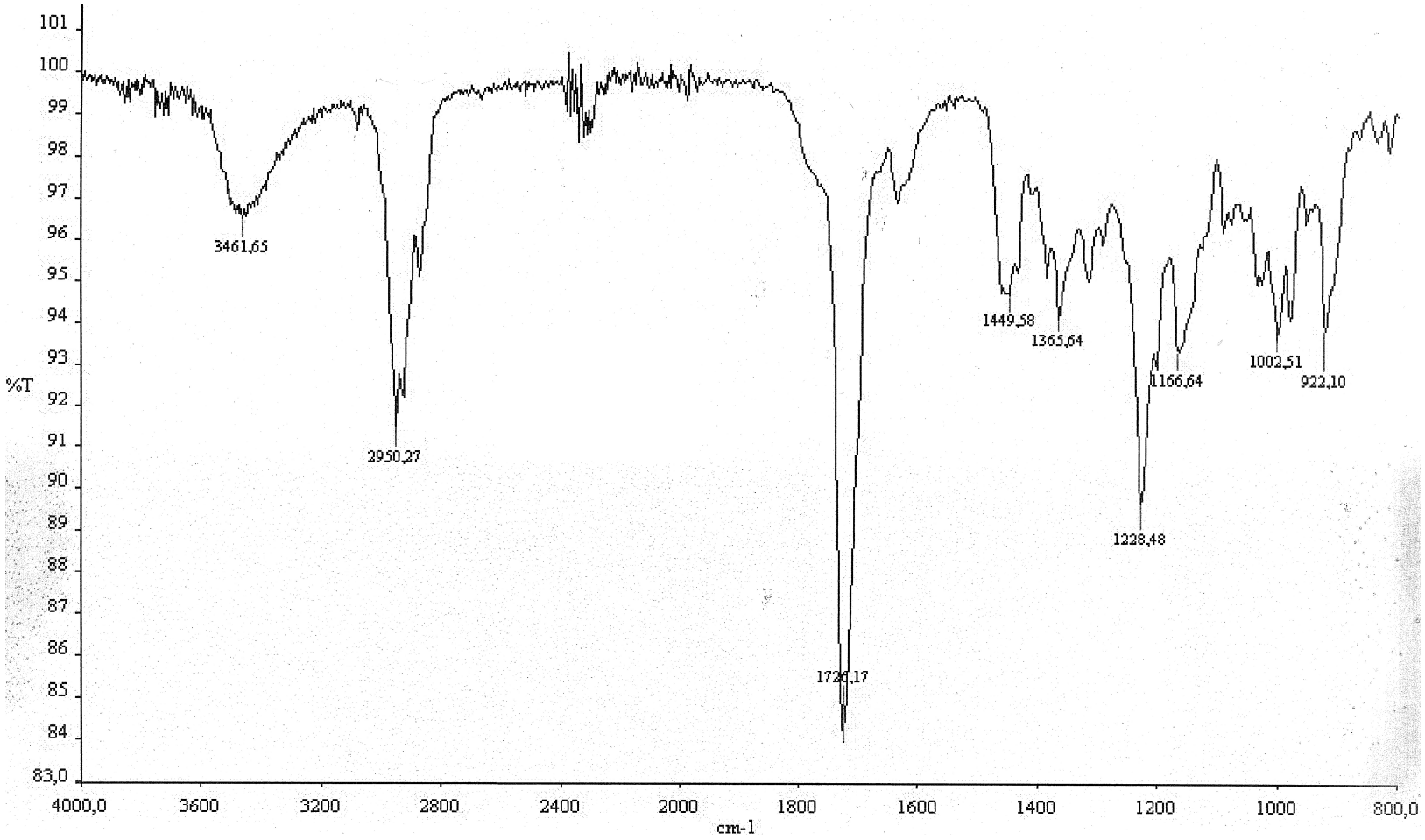

Figure 85. IR spectrum of sphaeropsidin B methyl ester (**55**), recorded as glassy film.

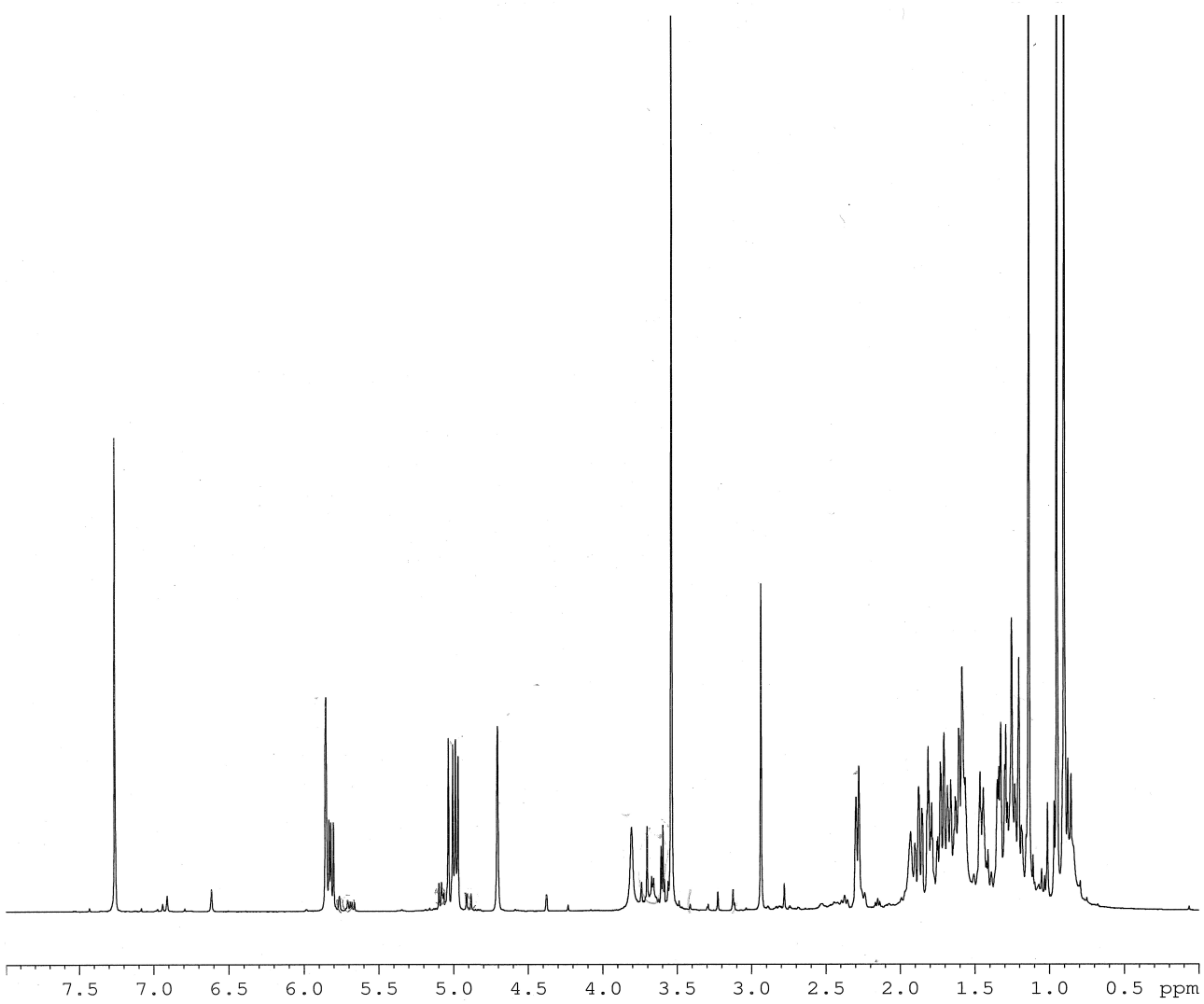

Figure 86. ^{1}H NMR spectrum of sphaeropsidin B methyl ester (**55**), recorded in $CDCl_3$ at 600 MHz.

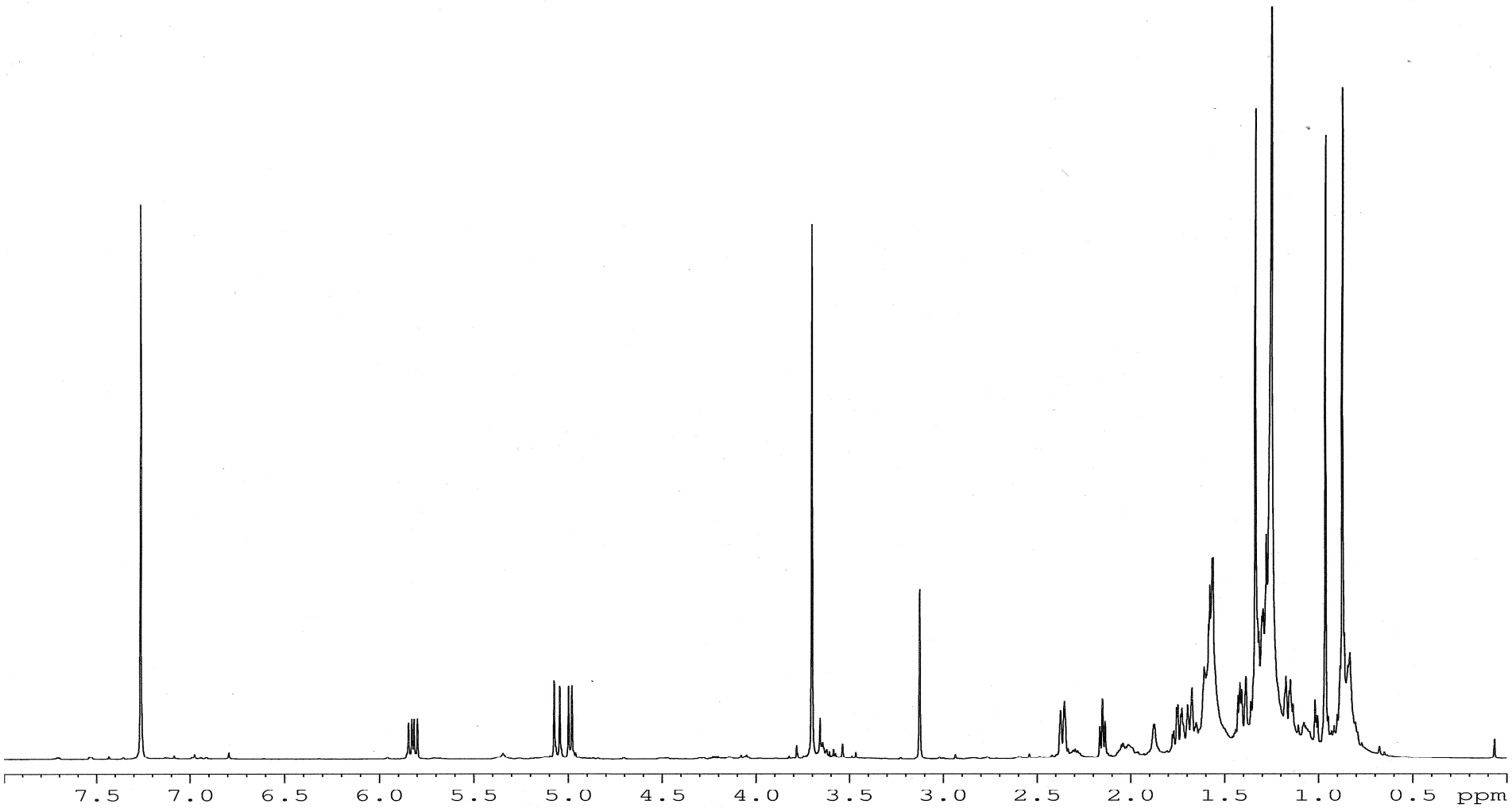

Figure 87. ^{1}H NMR spectrum of 14-methyl-7,*O*-didehydro-sphaeropsidin B methyl ester(**56**), recorded in $CDCl_3$ at 600 MHz.

conversion of **16** into **17**, was reduced into 7-hydroxy derivative **27** (Scheme 5) (Evidente *et al*., 1996 and 1997).

5.9. Antibacterial activity of sphaeropsidins their derivatives against several rice bacterial pathogens

The derivatives (**26**-**30**, **32**-**33** and **53**-**59**, Fig. 5 and Scheme 5, Pag. 32 and 160, respectively), in comparison to the natural sphaeropsidins A-C (**16**-**18**), were assayed for their antibacterial activity against *Burkholderia glumae*, *Pseudomonas fuscovaginae*, and *Xanthomonas oryzae* pv. *oryzae*, by growing the three pathogens in top agar media and exposing them to 25 and 100 μg of sphaeropsidin A pipetted into a well. The growth inhibition zone around the well was taken as a measure to assess the antibacterial activity.

On *B. glumae* and *P. fuscovaginae,* sphaeropsidin A (**16**) showed weak antagonistic activity, while sphaeropsidin B and C (**17**-**18**) and derivatives **26**-**30**, **32-33** and **53-59**) were inactive. On *Xoo* on the other hand **16** displayed strong antibacterial activity (Fig. 88). Table 6 and Fig. 88 depict the results using **17** and **18**, which appear to be naturally modified analogues of **16,** and of derivatives **26**-**30**, **32-33** and **53-59** compared with that of sphaeropsidin A. Interestingly, only the monoacetyl derivative **26** of sphaeropsidin A showed the same strong activity of **16,** while the diacetyl- (**29**) and dihydro- (**57**) derivatives of sphaeropsidin A showed a reduced activity and all natural and hemisynthesized compounds were practically inactive. When ampicillin was used as a positive control, the activity of compounds **16** and **26** were, respectively, 49 and 39 % of the activity of ampicillin (Table 7). In order to confirm these results and collect more information about the bacteriostatic or bactericidal activity of the sphaeropsidins, the growth inhibition experiment was performed also in liquid medium and *Xoo* growth measured after 6 and 24 h from the inoculation. The result obtained on Petri dishes was

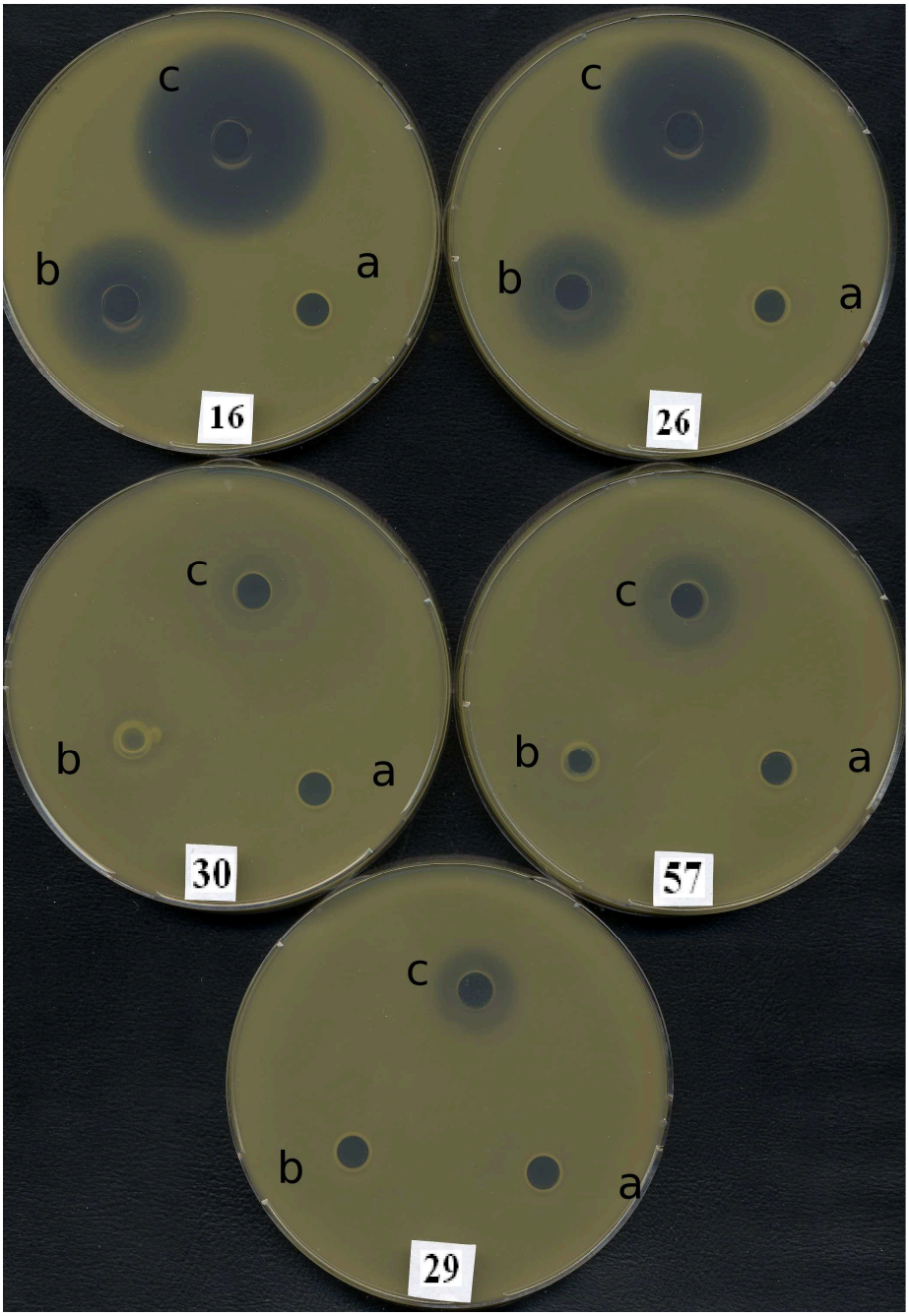

Figure 88. Petri dishes showing the growth inhibition of *Xanthomonas oryzae* pv. *oryzae* by sphaeropsidin A (**16**) and derivatives (**26**, **29**, **30** and **57**). On each Petri dish: (a) negative control (50 µl of DMSO); (b) and (c) 25 µg and 100 µg of sphaeropsidin A or its derivatives.

Table 6. Growth inhibition by sphaeropsidins (**16**-**18**) and their derivatives (**26-30**, **32-33** and **53-59**) on *Xanthomonas oryzae* pv. *oryzae.*

Compound	Inhibition diameter (mm)[a]	Concentration (M)[b]	Inhibition diameter (mm)	Concentration (M)
16	18.3	$1.5\ 10^{-3}$	25.5	$6.0\ 10^{-3}$
17	ni[c]	$1.5\ 10^{-3}$	ni	$6.0\ 10^{-3}$
18	ni	$1.5\ 10^{-3}$	ni	$6.0\ 10^{-3}$
26	15.8	$1.3\ 10^{-3}$	20.7	$5.2\ 10^{-3}$
59	ni	$1.0\ 10^{-3}$	ni	$4.0\ 10^{-3}$
27	ni	$1.5\ 10^{-3}$	ni	$6.0\ 10^{-3}$
28	ni	$1.5\ 10^{-3}$	ni	$6.0\ 10^{-3}$
30	ni	$1.5\ 10^{-3}$	8.9	$6.0\ 10^{-3}$
58	ni	$1.3\ 0^{-3}$	ni	$5.2\ 10^{-3}$
57	ni	$1.5\ 10^{-3}$	11.6	$6.0\ 10^{-3}$
29	ni	$0.5\ 10^{-3}$	15.3	$2.0\ 10^{-3}$
32	ni	$1.3\ 0^{-3}$	ni	$5.2\ 10^{-3}$
33	ni	$1.5\ 10^{-3}$	ni	$6.0\ 10^{-3}$
53	ni	$1.3\ 10^{-3}$	ni	$5.2\ 10^{-3}$
54	ni	$1.3\ 10^{-3}$	ni	$5.2\ 10^{-3}$
55	ni	$1.4\ 10^{-3}$	ni	$5.6\ 10^{-3}$
56	ni	$1.4\ 10^{-3}$	ni	$5.6\ 10^{-3}$

[a]The inhibition of growth around the wells was measured in mm (4 mm-well diameter included)

[b]Amount assayed in 50 µL of DMSO. The negative control was represented by 50 µL of DMSO

[c]ni=no inhibition

Table 7. Inhibition of *Xanthomonas oryzae* pv. *oryzae* growth in Petri dish assay using sphaeropsidin A (**16**) and derivatives **26**, **29**, **30** and **57**. [a]

Compound	Concentration (M)	Zone of inhibition diameter (mm)	% inhibition[b]
16	$6.0\ 10^{-3}$	25.5 ± 7.0	49.0
26	$5.2\ 10^{-3}$	20.7 ± 5.6	39.8
29	$2.0\ 10^{-3}$	15.3 ± 2.5	29.4
30	$6.0\ 10^{-3}$	n.d.	n.d.
57	$6.0\ 10^{-3}$	11.6 ± 2.1	22.3
Ampicillin	$5.7\ 10^{-3}$	52.0 ± 4.0	100

[a]The experiment was repeated three times and the standard deviation calculated. The compounds not reported in this table were unable to inhibit the growth.

[b]The percentage of inhibition is calculated considering the inhibition zone given by Ampicillin (positive control) as 100%.

[c]n.d.=not detected

confirmed except for compound **30** whose activity was not detected in liquid culture. Moreover, the results suggested that compounds **16** and **26** have also bactericidal activity because the CFU/mL after 24 h is lower than after 6 h (Fig. 89 and 90).

This result could be explained since according to a known lethal mechanism (Hassal, 1990), **26** was probably *in vivo* hydrolysed to **16**. This result also agrees with a reduced activity observed testing the diacetyl derivative **29** in which probably the same mechanism operates, *i.e.*, hydrolysis of the C-6 acetyl group. However, it could be that the C-14 acetyl group was not hydrolysed as well while a role could be played by the shift of the double bond from C-8-C-14 to C-8-C-9, which also affects the stereochemistry of the B/C ring junction and, hence, the conformational freedom of the two rings. This derivative lacks of the C-9 hydroxy group, which is modified as *O*-methyl ether in derivative **53**. Also important for the activity appeared to be the presence of a C-7 carbonyl group as shown by the total loss of the activity of sphaeropsidin B and its 7-*O*-acetyl derivative (**59**).

Very important for the activity appeared to be the presence of the hemiketal lactone functionality as shown by the inactivity of sphaeropsidin C and its derivatives **27** and **28**, with the latter also showing the reduction of the C-7 carbonyl group as in **17** and **59**, while in **28** the carboxy group was converted into the corresponding methyl ester. As expected the derivatives having the latter structural modification showed total loss of activity as the three (**32**, **53** and **54**) and the two (**55** and **56**) derivatives obtained, respectively, by reaction of sphaeropsidin A and B with diazomethane. The derivatives **53** and **54** also showed the conversion of the C-7 carbonyl group into the corresponding 1,1-disubstituted oxirane ring, confirming the importance of this structural feature for the activity. Compounds **32** and **56** showed different modifications of the C-8-C-14 double bond, which is converted into the corresponding cyclopropane ring and C-14 methyl derivative,

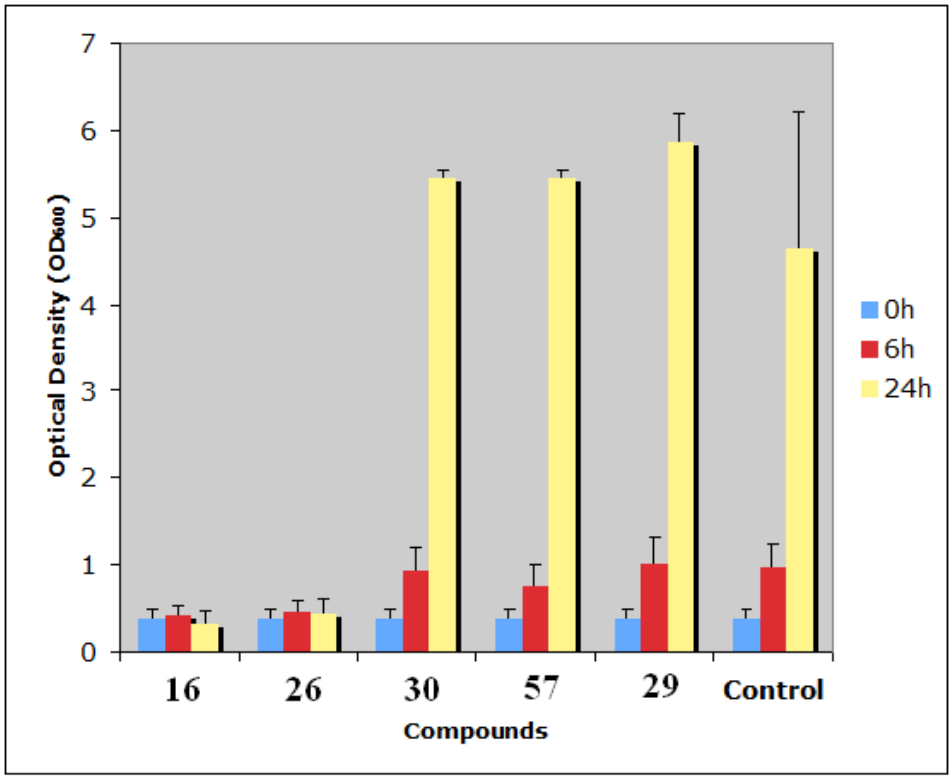

Figure 89. Growth inhibition of *Xanthomonas oryzae* pv. *oryzae* by sphaeropsidin A (**16**) and derivatives (**26**, **29**, **30** and **57**) calculated by measuring the optical density of the cultures after 6 and 24 hours from a dilution of an overnight culture (initial OD_{600} = 0.4). The compounds were tested in a concentration range of 0.5-1.5 10^{-4} M. The experiment was repeated three times and the standard deviation calculated. The control is a *Xoo* culture grown without any spheropsidin derivative.

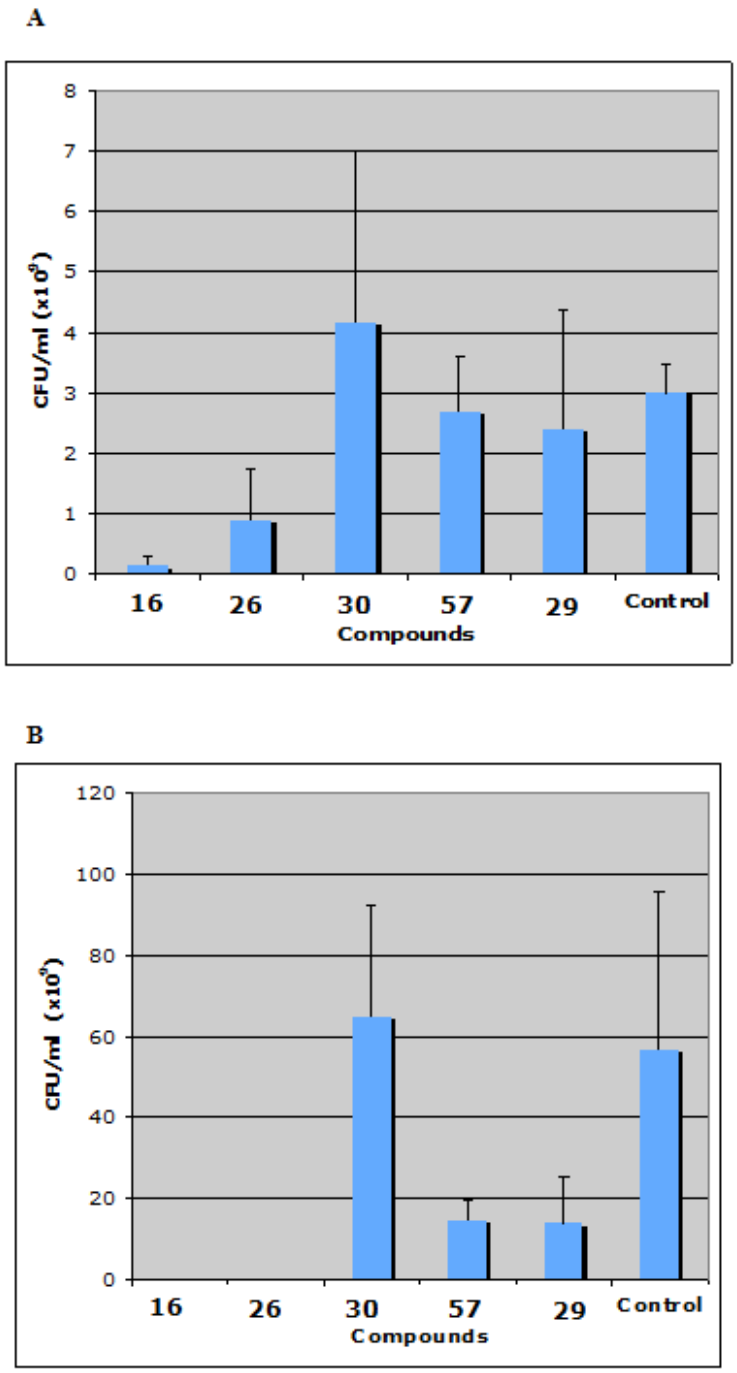

Figure 90. Growth inhibition of *Xanthomonas oryzae* pv. *oryzae* by sphaeropsidin A (**16**) and derivatives (**26**, **29**, **30** and **57**) estimated by measuring the colony forming unit (CFU/mL) after 6h (A) and 24h (B). The compounds were tested in a concentration range of 0.5-1.5 10^{-4} M. The experiment was repeated three times and the standard deviation calculated. The control is a *Xoo* culture grown without any spheropsidin derivative.

respectively. As described above for derivative **29** the structural modification of the C-8-C-14 double bond could affect the activity.

The vinyl group at C-13 appeared to impart activity as shown by the reduced activity of derivative **57** of sphaeropsidin A, which differs from **16** by saturation of the C-13 vinyl group. As expected, the tetrahydroderivative **30** of **16**, as well as its acetyl derivative (**58**) showed total loss of the activity as it also possess a reduced C-7 carbonyl group at C-7 as in **17**, **27,** and **59**. The same result was observed testing derivative **33** in which the B ring modification resulted in substantial disruption of the tricyclic pimarane system.

The results described above for the SAR studies agreed with those obtained assaying the three natural sphaeropsidins A-C, as well as the minor sphaeropsidins D-F, and some (seven) of the cited derivatives of **16**-**18** testing their phytotoxicity against both hosts (three species of cypress) and non hosts (tomato and mung bean) (Sparapano *et al.*, 2004).

They also agreed with the results obtained by testing the antimycotic activity of same the sphaeropsidins and derivatives against fungi pathogens for forestry (*Seiridium cardinale*, *S. cupressi* and *S. unicorne*) and agriculture (*Botrytis cinerea*, *Fusarium oxysporum*, *Penicilllium expansus*, *Verticillium dahliae*, and *Phomopsis amygdali*) (Sparapano *et al.*, 2004).

The *in vitro* antibacterial data indicated which specific structural features are related to toxic properties of sphaeropsidines, *i.e.* as the presence of the C-7 carbonyl group and the hemiketal lactone. The vinyl group at C-13, the C ring double bond and/or the C-9 tertiary hydroxy, as well as the pimarane structural feature are important for the activity. The antibacterial activity displayed by sphaeropsidin A and derivatives against *Xoo* could make these compounds potentially useful for practical application in agriculture (Evidente *et al.*, 2011).

5.10. Anticancer activity of sphaeropsidins A-C and their derivatives

The natural sphaeropsidins A-C (**16**-**18**) and the hemisynthetic derivatives (**26**-**30**, **32**-**33** and **53**-**59**, Fig. 5 and Scheme 5, Pag. 5 and 160, respectively) were also assayed for their *in vitro* anticancer activities against five human and one mouse cancer cell lines (Table 8) because only a preliminary anticancer activity of **16** was reported (Wang *et al.*, 2011). The IC_{50} *in vitro* growth-inhibitory concentrations of these latter compounds were determined using the MTT colorimetric assay and cisplatin, carboplatin, etoposide (VP16) and temozolomide, used to treat a large set of human cancers, were included as reference compounds.

Sphaeropsidin A (**16**) was the most active compound out of the 13 investigated (Table 8). In addition, compound **16** revealed itself as active as cisplatin and etoposide, while more active than carboplatin and temozolomide, which are four drugs largely employed to treat a large variety of human cancers. **26** and **57**, displayed similar *in vitro* anticancer activity compared to **16** (Table 8), indicating that acetylating the hemiketal hydroxyl group at C-6 on **16** did not modify **16**-induced growth inhibition activity in cancer cells, a feature that could be associated with the hydrolysis of **26** into **16**. Furthermore, the vinyl group at C-13, which was saturated in **57**, does not affect the *in vitro* anticancer activity of **16**. The hemiketal hydroxyl and the vinyl groups at C-6 and C-13, respectively, therefore do not seem to participate in **16**-induced cancer cell growth inhibition. The activity of **16** and **26** agrees with the results previously published by Wang *et al.*, 2011, although they tested them on seven different tumor cell lines. In contrast, the acetylation of C-14, which determines the shift of the double bond from C(8)–C(14) to C(8)–C(9) with consequent dehydroxylation of C-9 (**29**), the reduction of the ketone group at C-7 (**30**) or the acetylation of the hydroxyl group at C-7 (**58**) on **16** skeleton led to

Table 8. IC_{50} *in vitro* growth-inhibitory concentrations (µM) of natural (**16**-**18**) and hemisynthetic derivatives of sphaeropsidins A-C (**26**-**30**, **32**-**33** and **57**-**59**) established by the MTT colorimetric assay.

Compounds			IC_{50} *in vitro* growth inhibitory concentrations (µM) (MTT colorimetric assay)						
			A549 (NSCLC)	**OE21 (esophageal)**	**Hs683 (glioma)**	**U373 (glioma)**	**SKMEL28 (melanoma)**	**B16F10 (melanoma)**	**Mean ± SEM**
16	Sphaeropsidin A (SphA)	Exp-1	4	1	3	2	7	3	3.3 ± 0.8
		Exp-2	1	0.3	n.d.	0.4	2	0.4	0.8 ± 0.3
26	6-O-acetyl sphaeropsidin A		2	1	3	1	3	2	2.0 ± 0.4
29	6-*O*-Acetyl-14-acetyloxy-9-dehydroxy-$\Delta^{8,9}$-sphaeropsidin A		27	9	20	6	30	8	16 ± 4
30	7,*O*-15,16-Tetrahydro sphaeropsidin A		74	62	90	81	> 100	99	> 84 ± 6
58	7-*O*-Acetyl-7,*O*-15,16-tetrahydrosphaeropsidin A		>100	74	>100	>100	>100	>100	> 96 ± 4
57	15,16-Dihydrosphaeropsidin A		3	2	3	3	2	2	2.5 ± 0.2
17	Sphaeropsidin B		> 100	78	> 100	> 100	> 100	> 100	> 96 ± 4
59	7-*O*-Acetyl sphaeropsidin B		>100	77	>100	>100	>100	97	> 96 ± 4
33	Oxidized derivative of sphaeropsidin B		26	78	9	61	> 100	30	> 51 ± 14
18	Sphaeropsidin C		45	57	65	71	> 100	17	> 59 ± 11
28	Methyl ester of sphaeropsidin C		69	71	73	57	> 100	32	> 67 ± 9
27	7,*O*-Dihydro sphaeropsidin C		81	68	82	76	70	48	71 ± 5
32	8,14-Methylensphaeropsidin C methyl ester		> 100	75	> 100	> 100	> 100	87	> 94 ± 4
	Cisplatin		0.5	n.d.	0.5	0.4	1.6	1.9	1.0 ± 0.3
	Carboplatin		11	n.d.	20	19	149	44	48 ± 26
	VP16		3.2	n.d.	3.2	30.5	1.6	0.04	8 ± 6
	Temozolomide		611	n.d.	763	676	905	234	630 ± 112

marked losses in cancer cell growth inhibition (Table 8). These data suggest that the double bond located between C(8)–C(14) and/or the tertiary hydroxyl group at C-9 as well as the ketone group at C-7 are important features to impart **16**-mediated *in vitro* anticancer activity.

Sphaeropsidin B (**17**) and C (**18**) appeared to be less active than **16**, and the various semisynthetic derivatives of **17** (**33** and **59**) and of **18** (**27**, **28** and **32**) did not restore in vitro anticancer activity relative to **16** (Table 8). This confirms that the ketone group at C-7, which is reduced in **17**, and the hemiketal lactone ring located between C-6 and C-10 (open in **18**) are essential for maintaining the *in vitro* anticancer activity of **16**. As expected, similar results were observed with the acetyl derivative of **17** (**59**), which was probably hydrolyzed into **17** and the three derivatives of **18** (**27**, **28** and **32**). In fact, these latter undergo opening of the hemiketal lactone ring as well as esterification of the carboxyl group generated at C-10 in **28** and **32**. The latter also showed conversion of the C(8)–C(14) double bond into a cyclopropane ring and its lack of anticancer activity confirmed the importance of this structural feature for the activity of **16**, as already observed in **29**. Derivative **27** also showed the reduction of the ketone group at C-7 as already observed in **17**, **30**, **58** and **59**.

Also these results are essentially in agreement with those obtained in analogous SAR studies carried out to evaluate phytotoxic and the antibacterial activities of sphaeropsidins and some of therir derivatives (Sparapano *et al.*, 2004; Evidente *et al.*, 2011). However, in both previous SAR studies, the vinyl group at C-13 also seemed to play a role in the antipathogenic activity. We made use of quantitative videomicroscopy (Delbrouck *et al*., 2002) to analyze the type of in vitro growth inhibitory effects induced by **16** in cancer cells, i.e. cytotoxic versus cytostatic. The pictures in Fig. 91 morphologically illustrate that sphaeropsidin A exerts cytotoxic effects on mouse melanoma B16F10 cells

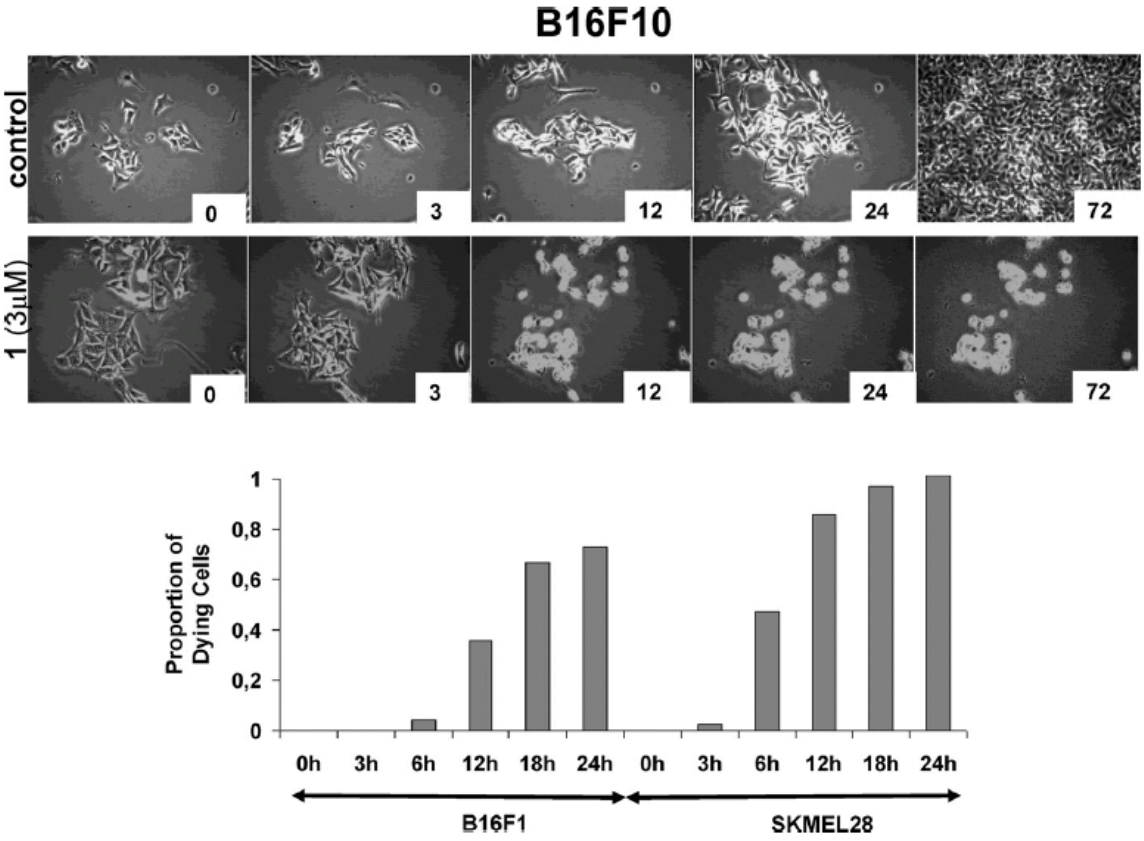

Figure 91. Illustration of the B16F10 mouse melanoma cells treated with **16** or left untreated over time.

and the same feature was observed with respect to human SKMEL-28 melanoma cells. The bottom of Fig. 91 reports the percentages of cell killing by **16** based on the morphological criteria described in the top of the figure. Thus, *in vitro* growth inhibitory effects of sphaeropsidin A relate to cytotoxic effects, at least in B16F10 and SKMEL-28 melanoma cells. From these results sphaeropsindin A is considered a potential anticancer natural product and further new studies are in progress to evaluate the *in vivo* application of this compound.

5.11. Taxonomic implications of secondary metabolites in *Botryosphaeriaceae*

The results reported in this thesis, provide further important useful insights regards to taxonomic purpose.

Diplodia species belonging to *Botryosphaeriaceae* family which are well known as cosmopolitan pathogens, saprophytes and endophytes and occur on a wide range of hosts (Slippers and Wingfield, 2007). The taxonomy of genera and species in the *Botryosphaeriaceae* has been confused for a long time. The identification of these fungi has been based on morphological comparison of the anamorph structures for many years due to the fact that teleomorph states are rarely found in nature. Recently, DNA based molecular techniques have proven to be a powerful tool for identification as well as classification purpose of species of the *Botryosphaeriaceae* (Crous *et al.*, 2006; Phillips *et al.*, 2008).

What would be the value of some phenotypic characteristics such as metabolite profiling in the classification and identification of genera and species in this fungal family? Several isolates of botryosphaeriaceous fungi are known for producing secondary bioactive metabolites, which are probably involved in the that disease they cause, but, to our knowledge, no studies have been reported on metabolites production for classification and

identification purpose. In this respect the data reported in this thesis allow us to make some considerations. *D. africana* produce sphaeropsidin A as well as other species of *Diplodia* such as *D. corticola* and *D. cupressi* (Evidente *et. al*, 1996; Maddau *et al.*, 2006), but this metabolite is not produced, for example, by *D. pinea*. Furthermore, (3*R*,4R)-4-hydroxymellein and (3*R*,4*S*)-4-hydroxymellein were also found in different strains of *D. corticola* and *D. pinea* (Cabras *et al.*, 2006; Maddau *et al*., 2006) but they, along with *R*-(-)-mellein, were never detected in *D. cupressi*. Then, can the presence or absence of these metabolites help to discriminate between species such as *D. africana* and *D. cupressi* or other species of *Diplodia*? Episphaeropsidone occurs in *D. africana* and *D. cupressi*, while it is not detected in *D. corticola* and *D. pinea*. On the other hand, oxysporone occurs as main metabolite in the liquid culture of *D. africana* but it is never detected in any other species of *Diplodia*. Previously, the phytotoxic metabolite diplopyrone was isolated from *D. corticola* (Evidente *et al.*, 2003) but it was not detected in any other species of *Diplodia* thus far. Is it unreasonable to suppose that some metabolites such as oxysporone, diplopyrone or (3*R*,4*R*)-4-hydroxymellein and (3*R*,4*S*)-4-hydroxymellein can be used as biomarkers for species recognition? We think not, even if with great caution. Further investigations should be carried out in order to develop an unbiased method for metabolite profiles in standardized conditions and to infer some taxonomic implications.

6. CONCLUSIONS

i) From the liquid culture of *D. africana*, a fungal pathogen involved in branch dieback of *Phoenicean juniper* in Italy, two new phytotoxic dihydrofuropyran-2-ones, named afritoxinones A and B, were isolated and characterized.

Six others known metabolites were isolated and identified as oxysporone, sphaeropsidin A, episphaeropsidone, *R*-(-)-mellein, (3*R*,4R)-4-hydroxymellein and (3*R*,4*S*)-4-hydroxymellein.

The phytotoxic activity of afritoxinones A and B and oxysporone was evaluated on host and non-host plant and the taxonomic implications of secondary metabolites in *Botryosphaeriaceae* family studies was discussed.

ii) From the liquid culture of *D. cupressi*, the causal agent of a canker disease of cypress in the Mediterranean area, two phytotoxic dimedone methyl ethers, sphaeropsidone and episphaeropsidone and three phytotoxic unrearranged pimarane diterpenes, sphaeropsidins A-C, were isolated. The relative configuration of sphaeropsidones was confirmed by an X-ray structural analysis.

iii) Eight derivatives obtained by chemical modifications and two natural analogues of sphaeropsidones were assayed for phytotoxic and antifungal activities, and a structure-activity relationship was examined. The hydroxy group at C-5, the absolute C-5 configuration, the epoxy group, and the C-2 carbonyl group appear to be structural features important in conferring biological activity. The conversion of sphaeropsidone into the corresponding 1,4-dione derivative led to a compound showing greater antifungal activity, against five fungal pathogenic species belonging to the genus *Phytophtora*, than its precursor. This finding could be useful in devising new natural fungicides for practical application in agriculture.

iv) Sphaeropsidins A-C and fourteen hemisynthetic derivitaves obtained by chemical modification were assayed for antibacterial activity against *Xanthomonas oryzae* pv. *oryzae* (*Xoo*), *Pseudomonas fuscovaginae*, and *Burkholderia glumae*, the causal agents of severe bacterial rice diseases. The results of structure-activity relationships study showed that structural features important to impart this antibacterial activity are the presence of the C-7 carbonyl group and the hemiketalic lactone functionality. The C-13 vinyl group, the double bond of ring C and/or the tertiary C-9 hydroxyl group, as well as the pimarane arrangement of the tricylic carbon skeleton were also important for the antibacterial activity. The antibacterial activity displayed by sphaeropsidine A and derivatives against *Xoo* could make these compounds potentially useful for practical application in agriculture.

7. REFERENCES

Achenbach, H., Mühlenfeld, A., Weber, B., Kohn, W. and Brillinger, G.U. (1982). Stoffwechselprodukte von Mickroorganismen. XXVII. Cyclopaldsäure und 3-*O*-Methyl-cyclopolsäure, zwei antibiotisch wirksame Substanzen aus *Aspergillus duricaulis*. *Zeitschrift für Naturforschung*, 37b: 1091-1097.

Adesogan, E.K. and Alo, B.J. (1979). Oxysporone, a new metabolite from *Fusarium oxysporum*. *Phytochemistry,* 18: 1886-1887.

Akatsuka, T., Kodama, O., Kato, H., Kono, Y. and Takeuchi, S. (1983). 3-Hydroxy-7-oxo-sandaraco-pimaradiene (orylzalexin A), a new phytoalexin isolated from rice blast leaves. *Agric. Biol. Chem.,* 47: 445-447.

Akatsuka, T., Kodama, O., Sekido, H., Kono, Y. and Takeuchi, S. (1985). Novel phytoalexins (oryzalexins A, B and C) isolated from rice blast leves infected with *Pyricularia oryzae*. Part I: isolation, characterization and biological activities of orylzalexins. *Agric. Biol. Chem.*, 49: 1689-1694.

Aldridge, D.C., Galt, S., Giles, D. and Turner, W.B. (1971). Metabolites of *Lasiodiplodia theobromae*. *J. Chem. Soc.*, 1623-1627.

Allen, F.H., Kennard, O., Watson , D.G., Brammer, L., Orpen, A.G. and Taylor R. (1987). Tables of bond lengths determined by *X*-ray and neutron diffraction. Part 1. Bond lengths in organic compounds. *J. Chem. Soc. Perkin Trans.* 2: S1-S19.

Alves, A., Correia, A. and Phillips, A.J.L., (2006). Multi-gene genealogies and morphological data support *Diplodia cupressi* sp. nov., previously recognized as *D. pinea* f. sp. *cupressi*, as a distinct species. *Fungal Divers*., 23: 1–15.

Anderson, J.R. and Edwards, R.L. (1983). Metabolites of the higher fungi. Part 21. 3-Methyl-3,4-dihydroisocoumarins and related compounds from the Ascomycete family Xylariaceae. *J. Chem. Soc. Perkin Trans.,* 1: 2185-2192.

Ballio, A., Castiglione Morelli, M.A., Evidente, A., Graniti, A., Randazzo, G. and Sparapano, L., (1991). Seiricardine A, a phytotoxic sesquiterpene from three *Seiridium* species pathogenic for cypress. *Phytochemistry*, 30: 131-136.

Ballio, A., Evidente, A., Graniti, A., Randazzo, G. and Sparapano, L. (1988). Seiricuprolide, a new phytotoxic macrolide from a strain of *Seiridium cupressi* infecting cypress. *Phytochemistry*, 27: 3117-3121.

Ballio, A. and Graniti, A. (1991). Phytotoxins and their involvement in plant diseases. *Experientia,* 47: 751-864.

Barthelet, J. and Vinot, M. (1944). Notes sur les maladies des cultures méridionales. *Annales des Epiphyties,* 10: 18-20.

Batoko, H., Flamand, M.C., Boutry, M., Kinet, J.M. and Maraite, H. (1997). Biological effects of *Pseudomonas fuscovaginae* toxins on rice cells. *Devol. Plant Pathol.*, 9: 215-229.

Behr, S., Hegeman, K., Schimanski, H., Froehlich, R. and Haufe, G. (2004). Synthesis of γ-lactones from cycloocta-1,5-diene. Starting materials for natural product synthesis. *Eur. J. Org. Chem.,* 18: 3884-3892.

Berger, S. and Braun, S. (2004). 200 and More Basic NMR Experiments: a Practical Course, first ed. (Wiley-VCH ed.), Weinheim, Germany.

Biswas, B., Sarkar, D. and Venkateswaran, R.V., (2008). Total synthesis of alboatrin, a phytotoxic metabolite from *Verticillium alboatrum*. *Tetrahedron*, 64: 3212-3216.

Brasier, C.M. (1996). *Phytophthora cinnamomi* and oak decline in southern Europe. Environmental constraints including climate change. *Ann. For. Sci*., 53: 347-358.

Brasier, C.M., Robredo, F. and Ferraz, J.F.P. (1993). Evidence for *Phytophthora cinnamomi* involvement in Iberian oak decline. *Plant Pathol.*, 42: 140-145.

Bernstein, J., Davis, R.E., Shimoni, L. and Chang, N-L. (1995). Patterns in Hydrogen Bonding: Functionality and Graph Set Analysis in Crystals. *Angew Chem. Int. Ed. Ingl.*, 34: 1555-1573.

Breitmaier, E. and Voelter, W. (1987). Carbon-13 NMR Spectroscopy, VCH, Weinheim, pp. 183-280.

Brown, R.C.D., Hughes, R.M., Keily, J. and Kenney, A. (2000). Diastereoselective synthesis of tetrahydrofuran containing fragments by the permanganate oxidation of 1,5,9-trienes. *Chem. Commun.*, 175-1738.

Cabras, A., Mannoni, M.A., Serra, S., Andolfi, A., Fiore, M. and Evidente, A. (2006). Occurrence, isolation and biological activity of phytotoxic metabolites produced *in vitro* by *Sphaeropsis sapinea*, pathogenic fungus of *Pinus radiata*. *Eur. J. Plant Pathol.,* 115: 187–193.

Cakir, S.P. and Mead, K.T. (2004). Stereoselective approach to C-aryl pyranosides synthesis which addressed the problems of C7-substitution in blepharocalyxin. *Eur. J. Org. Chem.* 69: 2203-2205.

Camarda, I. and Valsecchi, F. (2008). Alberi e arbusti spontanei della Sardegna. (Delfino C., ed.), Sassari, Italy.

Carpinella, M.C., Ferrayoli, C.G. and Palacios, S.M. (2005). Antifungal synergistic effect of Scopoletin, a hydroxycoumarin isolated from *Melia azedarach* L. fruits. *J. Agric. and Food Chem.*, 53: 2922-2927.

Carreno, M.C., Merino, E., Ribagorda, M., Somoza, A. and Urbano, A. (2007). Enantioselective synthesis of natural polyoxygenated cyclohexanes and

cyclohexenes from [(*p*-tolylsulfinyl)methyl]-*p*-quinols. *Chem. Eur. J.*, 13: 1064-1077.

Cartwright, D., Langcake, P., Pryce R.J. and Leworthy, D.P. (1977). Chemical activation of host defence as a basis for crop protection. *Nature,* 267: 511-512.

Clough, S., Raggatt, M.E., Simpson, T.J., Wilis, L.C., Whiting, A. and Wrigley, S.K. (2000). Structure elucidation and synthesis of (4*S*,5*S*,6*Z*,8*E*)-5-hydroxydeca-6,8-dien-4-olide [(*S*,*S*)-sapinofuranone B]-a novel γ -lactone metabolite of *Acremonium strictum*. *J. Chem. Soc. Perkin Trans.* 1: 2475-2481.

Cole, R.J. and Cox, R.H. (1981). Handbook of Toxic Fungal Metabolites. New York: Academic Press, pp. 264-343, 755.

Creppy, E.E., Chiarappa, P., Baudrimont, I., Borracci, P., Moukha, S. and Carratù, M.R. (2004). Synergistic effects of fumonisin B1 and ochratoxin A: are *in vitro* cytotoxicity data predictive of *in vivo* acute toxicity. *Toxicology*, 201: 115-123.

Crous, P.W., Slippers, B., Wingfield, M.J., Rheeder, J., Marasas, W.F.O., Phillips, A.J.L., Alves, A., Burgess, T., Barber, P. and Groenewald, J.Z. (2006). Phylogenetic lineages in the *Botryosphaeriaceae*. *Stud. Mycol.* 55: 235-253.

Damm, U., Crous, P.W. and Furie, P.H. (2007). *Botryosphaeriaceae* as potential pathogens of *Prunus* species in South Africa, with descriptions of *Diplodia africana* and *Lasiodiplodia plurivora* sp. nov. *Mycologia*, 99: 664–680.

Dawe, R.D., Molinski, T.F. and Turner, J.V. (1984). Dilithium tetrabromonickelate (II) as a source of soft nucleophilic bromide : Reaction with epoxides**.** *Tetrahedron*, 25: 2061-2064.

Dean, F.M. (1963). Naturally Occurring Oxygen Ring Compounds. London: Butterworths, pp. 53-81, 82-134, 553.

Delbrouck, C., Doyen, I., Belot, N., Decaestecker, C., Ghanooni, R., de Lavareille, A., Kaltner, H., Choufani, G., Danguy, A., Vandenhoven, G., Gabius, H.J., Hassid, S. and Kiss, R. (2002). Galectin-1 is overexpressed in nasal polyps under budesonide and inhibits eosinophil migration. *Lab. Invest.*, 82: 147–158.

Devescovi, G., Bigirimana, J., Degrassi, G., Cabrio, L., Li Puma, J.J., Kim, J., Hwang, I. and Venturi, V. (2007). Involvement of a quorum-sensing-regulated lipase secreted by a clinical isolate of *Burkholderia glumae* in severe disease symptoms in rice. *Appl Environ Microbiol*, 73: 4950-4958.

Devys, M. and Barbier, M. (1992). Isolation of the new (-)-(3*R*,4*S*)-4-hydroxymellein from the fungus *Septoria nodorum* Berk. *Zeitschrift fuer Naturforschung*, 47c: 779-881.

Dickinson, J.M. (1993). Microbial pyran-2-ones and dihydropyran-2-ones. *Nat. Prod. Rep*., 10: 71-98.

Ellestad, G.A., Kunstmann, M.P., Mirando, P. and Morton, G.O. (1972). Structures of fungal diterpene antibiotics LL-S491β and γ. *J. Amer. Chem. Soc.*, 94: 6206-6208.

Erwin, D.C. and Ribeiro, O.K. (1996). Phytophthora Diseases Worldwide, first ed., APS Press, St. Paul, Minn.

Evidente, A. (1997). Bioactive metabolites from phytopathogenic fungi and bacteria, In: Recent Research Developments in Phytochemistry. (Pandalai, S.G. ed.), Trivandrum (India): Research Signpost; pp. 255-292.

Evidente, A., Andolfi, A., Cimmino, A. and Abouzeied, A.M. (2010a). Phytotoxins produced by fungi responsible of forestall plant disease. In: Sustainable Agriculture: Technology, Planning and Management. (Salazar, A., Rios, I., eds.), New York: Nova Science Publishers Inc.; pp 177-234.

Evidente, A., Andolfi, A., Fiore, M., Spanu, E., Franceschini, A. and Maddau, L. (2007). Diplofuranones, A and B, two further new 4-monosubstituted 3(3H)-

dihydrofuranones produced by *Diplodia corticola*, a fungus pathogen of cork oak. *Arkivoc*, 7: 318-328.

Evidente, A., Andolfi, A., Fiore, M., Spanu, E., Maddau, L., Franceschini, A., Marras, F. and Motta, A. (2006b). Diplobifuranylones A and B, 5'-monosubstituted tetrahydro-*2H*-bifuranyl-5-ones produced by *Diplopia corticola*, a fungus pathogen of cork oak. *J. Nat. Prod.*, 69: 671-674.

Evidente, A., Andolfi, A., Maddau, L., Franceschini, A. and Marras, F. (2005). Biscopyran, a phytotoxic hexasubstituted pyranpyran produced by *Biscognauxia mediterranea*, a fungus pathogen of cork oak. *J. Nat. Prod.*, 68: 568-571.

Evidente, A., Capretti, P., Giordano, F. and Surico, G. (1992). Identification and phytotoxicity of nitropropionic acid produced *in vitro* by *Melanconis thelebola*. *Experientia*, 48: 1169-1172.

Evidente, A., Fiore, M., Bruno G., Sparapano, L. and Motta A. (2006a). Chemical and biological characterization of sapinopyridione, a phytotoxic 3,3,6-trisubstituted-2,4-pyridione produced by *Sphaeropsis sapinea*, a toxigenic pathogen of native and exotic conifers, and its derivatives. *Phytochemistry*, 67: 1019-1028.

Evidente, A., Maddau, L., Spanu, E., Franceschini, A., Lazzaroni, S. and Motta, A. (2003b) Diplopyrone, a new phytotoxic tetrahydropyranpyran-2-one produced by *Diplodia mutila*, a fungus pathogen of cork oak. *J. Nat. Prod.*, 66: 313-315.

Evidente, A. and Motta, A. (2001). Phytotoxins from fungi pathogenic for agrarian, forestal and weedy plants. In: Bioactive Compounds from Natural Sources. (Tringali C. ed.) London, (UK): Taylor and Francis, pp. 473-525.

Evidente, A. and Motta, A. (2002). Bioactive metabolites from phytopathogenic bacteria and plants. In: Studies in Natural Products Chemistry. (Atta-ur-Rahman, ed.), Amsterdam: Elsevier Science; 26; pp. 581–628.

Evidente, A., Motta, A. and Sparapano, L. (1993). Seiricardines B and C, phytotoxic sesquiterpenes from three species of *Seiridium* pathogenic for cypress. *Phytochemistry*, 33: 69-78.

Evidente, A., Punzo, B., Andolfi, A., Cimmino, A., Melck, D. and Luque, J. (2010b). Lipophilic phytotoxins produced by *Neofusicoccum parvum*, a grapevine canker agent. *Phytopathol. Mediterr*. 49: 74-79.

Evidente, A., Randazzo, G. and Ballio, A. (1986). Structure determination of seiridin and isoseiridin, phytotoxic butenolides from culture filtrate of *Seiridium cardinale*. *J. Nat. Prod.*, 49: 593-601.

Evidente, A. and Sparapano, L. (1994). 7'-Hydroxyseiridin and 7'-hydroxyisoseiridin, two new phytotoxic $\Delta^{\alpha,\beta}$-butenolides from three species of *Seiridium* pathogenic to cypress. *J. .Nat. Prod.*, 57: 1720-1725.

Evidente, A., Sparapano, L., Andolfi, A., Bruno, G., Giordano, F. and Motta, A. (2000). Chlorosphaeropsidone and epichlorosphaeropsidone, two new chlorinated dimedone methyl ethers isolated from liquid cultures of *Sphaeropsis sapinea* f. sp. *cupressi*. *Phytopatol. Medit.*, 39: 299-309.

Evidente, A., Sparapano, L., Andolfi, A., Bruno, G. and Motta, A. (2003a). Sphaeropsidin F, a new pimarane diterpene produced in vitro by the cypress pathogen *Sphaeropsis sapinea* f. sp. *cupressi*. *Aust. J. Chem.*, 56: 615-619.

Evidente, A., Sparapano, L., Bruno, G. and Motta, A. (2002). Sphaeropsidins D and E, two other pimarane diterpenes, produced in vitro by the plant pathogenic fungus *Sphaeropsis sapinea* f.s. *cupressi*. *Phytochemistry*, 59: 817-823.

Evidente, A., Sparapano, L., Fierro, O., Bruno, G., Giordano, F. and Motta, A. (1998). Sphaeropsidone and episphaeropsidone, phytotoxic dimedone methyl ethers produced

by *Sphaeropsis sapinea* f. sp. *cupressi* grown in liquid culture. *Phytochemistry*, 48**:** 1139-1143.

Evidente, A., Sparapano, L., Fierro, O., Bruno, G. and Motta, A. (1999). Sapinofuranones A and B, two new 2(3H)-dihydrofuranones produced by *Sphaeropsis sapinea,* a common pathogen of conifers. *J. Nat. Prod.*, 62: 253-256.

Evidente, A., Sparapano, L., Giordano, F., Fierro, O. and Motta, A. (1997). Sphaeropsidines B and C, phytotoxic pimarane diterpenes from *Sphaeropsis sapinea* f. sp. *cupressi* and *Diplodia mutila*. *Phytochemistry*, 45: 705-713.

Evidente, A., Sparapano, L., Motta, A., Giordano, F., Fierro, O. and Frisullo, S. (1996). A phytotoxic pimarane diterpene of *Sphaeropsis sapinea* f. sp. *cupressi*, the pathogen of a canker disease of cypress. *Phytochemistry*, 42: 1541-1546.

Evidente, A., Venturi, V., Masi, M., Degrassi, G., Cimmino, A., Maddau, L. and Andolfi, A. (2011). *In vitro* antibacterial activity of sphaeropsidins and chemical derivatives towards *Xanthomanas oryzae* pv. *orizae* the causal agent of rice bacterial blight. *J. Nat. Prod.* 74: 2520–2525.

Farrugia, L.J. (1997). *ORTEP*-3 for Windows - a version of *ORTEP*-III with a Graphical User Interface (GUI). *J. Appl. Cryst.*, 30: 565.

Ferluga, S., Bigirimana, J. and Venturi, V. (2007). A LuxR homologue of *Xanthomonas oryzae* pv. *oryzae* is required for optimal rice virulence. *Mol Plant Pathol* 8: 529-38

Fex, T. and Wickberg, B. (1981). Structure and synthesis of the methyl ester of 3,4-anhydroshikimic acid, isolated from a *Chalara* sp. *Acta Chemica Scandinavica*, B35: 91-95.

Flynn, P.H. and Gleason, M.L. (1993). Isolation of *Botryosphaeria stevensii*, cause of *Botryosphaeria canker*, from rocky mountain juniper in Iowa. *Plant Dis.*, 77: 210.

Flematti, G.R., Goddard-Borger, E.D., Merritt, D.J., Ghisalberti, E.L., Dixon, K.W. and Trengove, R.D. (2007). Preparation of 2*H*-furo[2,3-c]pyran-2-one derivatives and evaluation of their germination-promoting activity. *J. Agric. Food Chem.* 55: 2189-2194.

Franceschini, A., Corda, P., Maddau, L. and Marras, F. (1999). Observations sur *Diplodia mutila*, pathogène du chêneliège en Sardaigne. *IOBC Bulletin*, 22: 5-12.

Franceschini, A., Maddau, L and Marras, F. (2002). Incidence d'endophytes fongiques impliqués dans le dépérissement du chêne-liège. *IOBC/wprs Bulletin*, 25: 29-36.

Frisullo, S., Bruno, G., Lops, F. and Sparapano, L. (1997). Morphological, physiological and pathogenic studies on *Sphaeropsis sapinea*, *S. sapinea* f. sp. *cupressi* and *Diplodia mutila*. Proceed. 10th Cong. Medit. Phytopathol. Union, Montpellier, 201-205.

Fritz, J.S. and Schenk, G.H. (1959). Acid-catalized acetylation of organic hydroxyl groups. *Anal. Chem.*, 31: 1808-1812.

Garson, M.J., Staunton, J. and Jones, P.G. (1984). New polyketide metabolites from *Aspergillus melleus*: structural and stereochemical studies. *J. Chem. Soc. Perkin Trans*., 1: 1021-1026.

Graniti, A. (1985). *Seiridium cardinale* and other cypress cankers. *EPPO Bulletin*, 17: 479-486.

Graniti, A. (1998). Cypress canker: a pandemic in progress. *Ann. Rev. of Phytopathol.*, 36: 91-114.

Graniti, A., Durbin, R.D. and Ballio, A. (1989). Phytotoxins and Plant Pathogenesis. NATO ASI Series, Series H, Vol 27, Springer-Verlag, Berlin.

Graniti, A. and Frisullo, S. (1987). Fungi associated with cypress canker disease in the Mediterranean area. *Proceed. 7th Cong. Mediter. Phytopathol. Union*, pp. 211-213.

Graniti, A., Sparapano, L. and Evidente, A. (1992). Cyclopaldic acid, a major phytotoxic metabolite of *Seiridium cupressi*, the pathogen of a canker disease of cypress. *Plant Pathology*, 41, 563-568.

Grasso, V. and Raddi, P. (1979). Seminario: Il Cipresso: malattie e difesa. Firenze, Italia: CEE-AGRIMED; 23-24 Settembre, pp- 275.

Grotenbreg, G.M., Tuin, A.W., Witte, M.D., Leeuwenburgh, M.A., Van Boom, J.H., Van der Marel, G.A., Overkleeft, H.S. and Overhand, M. (2004). An expeditious route towards pyranopyran sugar amino acids. *Synlett.*, 5: 904-906.

Hachiro, O. (1988). Role of phytotoxins in pine wilt disease. *Journal of Nematol.*, 20: 245-251.

Ham, J.H., Melanson, R.A. and Rushn, M.C. (2011). *Burkholderia glumae***:** next major pathogen of rice?. *Mol. Plant Pathol.,* 12: 329–339

Hansen, M., and Lewis, K.J. (1997). Compendium of Conifer Diseases. American Phytopathological Society, St. Paul, Minn.

Hershernhorn, J., Park, S.H., Stierle, A. and Strobel, G.A. (1992). *Fusarium avenaceum* as a novel pathogen of spotted knapweed and its phytotoxins, acetamido-butenolide and enniatin B. *Develop. Plant Sci.*, 86: 155-160.

Hassal, K.A. (1990). Biochemistry and Uses of Pesticides; Weinheim: Verlag Chemie; pp. 58, 72, 304, 429 and 497.

Hikino, H., Aota, K., Maebaayashi, Y. and Takemoto, T. (1966). Structure of cyperolone. *Chem. Pharm. Bulletin,* 14: 1439-1441.

King, E.O., Ward, M.K. and Raney, D.E. (1954). Two simple media for the demonstration of pyocyanin and fluorescein. *J. Lab Clin Med* 44: 301-307.

Kis, Z., Closse, A., Sigg, H.P., Hruban, L. and Snatzke, G. (1970). Die struktur von panepoxydon und verwandten pilzmetaboliten. *Helv. Chim. Acta*, 53: 1577-1597.

Kono, Y., Takeuchi, S., Kodama, O. and Akatsuka T. (1984). Absolute configuration of oryzalexin A and structures of its related phytoalexin isolated from rice blast leaves infected with *Pyricularia oryzae*. *Agric. Biol. Chem.,* 48: 253-255.

Kozikowski, A.P. and Lee, J. (1990). A synthesis approach to the cis-fused marine pyranopyrans, (3*E*)- and (3*Z*)-dactomylene. X-ray structure of a rare organomercurial. *J. Org. Chem.,* 55: 863-870.

Lamari, L. (2002). Assess: Image analysis Software for plant disease quantification. APS Press, St. Paul, MN.

Langstrom, B.O., Solheim, H., Hellqvist, C. and Krokene, P. (2001). Host resistance in defoliated pine: effects of single and mass inoculations using bark beetle-associated blue-stain fungi. *Agric. and Forest Entomol.,* 3: 211-216.

Leeuwenburgh, M.A., Overkleeft, H.S., Van der Marel, G.A. and Van Boom, J.H. (1977). A novel approach towards *cis*- and *trans*-fused pyranopyrans based on ring-closing metathesis reaction of carbohydrate derivatives. *Synlett.*, 11: 1263-1264.

Linaldeddu, B.T., Scanu, B., Maddau, L. and Franceschini, A., (2011). *Diplodia africana* causing dieback on Juniperus phoenicea: a new host and first report in the northern hemisphere. *Phytopatholog. Mediterr*. 50: 473–477.

Luque J., Parladè, J. and Pera, J. (2001). El decaimiento del alcornoques en Cataluna: sıntomas y hongos asociados. *Investigacion Agraria: Sistemas y Recursos Forestales*, 10: 271–289.

Madar, Z., Solel, Z. and Kimchi, M. (1989). Effect of water stress in cypress on the development of canker by *Diplodia pinea* f. sp. *cupressi* and *Seiridium cardinale*. *Plant Disease*, 73: 484-486.

Madar, Z., Solel, Z. and Kimchi, M. (1991). *Pestalotiopsis* canker of cypres in Israel. *Phytoparasitica*, 19: 79-81.

Maddau, L., Ferracane, R., Franceschini, A., and Cabras, A. (2002). Proceeding book of the National Congress "L'endofitismo di funghi e batteri patogeni in piante arboree e arbustive"; Sassari-Tempio Pausania, Italy, pp 361-368.

Maddau, L., Spanu, E., Franceschini, A., Marras, F., Andolfi, A., Fiore, M. and Evidente, A. (2006). Phytotoxic metabolites produced by fungi involved in cork oak decline. Proceedings 12th Congress Mediterranean Phytopathological Union, Rhodes Island, Hellas, 341-342.

Manitto, P. (1981). Biosynthesis of Natural Products, Chicester: Ellis Harwood, pp. 208, 213-222 and 237-255.

Mano, H. and Morisaki, H. (2008). Endophytic bacteria in the rice plant. *Microbes Environ.,* 23: 109-117.

Marras, F., Franceschini, A. and Maddau, L. (1995). Les principales maladies du chêne-liège (*Quercus suber* L.) en Sardaigne (Italie). *IOBC/wprs Bulletin*, 18 : 8-13.

Mattiuzzo, M., Bertani, I., Ferluga, S., Cabrio, L., Bigirimana, J., Guarnaccia, C., Pongor, S., Maraite, H. and Venturi, V**.** (2011). The plant pathogen *Pseudomonas fuscovaginae* contains two conserved quorum sensing systems involved in virulence and negatively regulated by RsaL and the novel regulator RsaM. *Environ Microbiol.,* 13: 145-162.

McCrindle, R. and Overton, K.H. (1969). The Diterpenoids, Sesterterpenoids and Triterpenoids. In: Rodd's Chemistry of Carbon Compounds. (Coffey S. ed.), Amsterdam: Elsevier; pp. 369-403.

Mennucci, B., Claps, M., Evidente A. and Rosini, C. (2007). Absolute configuration of natural cyclohexene oxides by time dependent density functional theory calculation of the optical rotation: the absolute configuration of (-)-sphaeropsidone and (-)-*epi*-sphaeropsidone revised. *J. Org. Chem.*, 72: 6680-6691.

Miller, M.W. (1968). The structure of terremutin. *Tetrahedron,* 24: 4839-4851.

Mirocha, C.J., DeVay, J.E. and Wilson, E.E. (1961). Role of fumaric acid in the hull rot disease of almond. *Phytopathology*, 51: 851-860.

Moreno-Manas, M. and Pleixats, R. (1992). In Advances in Heterocyclic Chemistry. (Katritzky, A.R., ed.), San Diego, CA: Academic Press, 53, pp. 1-84.

Nagasawa, H., Suzuki, A. and Tamura, S. (1978). Isolation and structure of (+)deoxyepiepoxydon and (+)epiepxydon, phytotoxic fungal metabolites. *Agri. Biol. Chem.,* 42: 1303-1304.

Nagata, T. and Ando, Y. (1989). Oxysporone, a phytotoxin isolated from tea gray blight fungus *Pestalotia longiseta*. *Agric. Biol. Chem.* 53: 2811.

Nakanishi, K. and Solomon, P.H., (1977). Infrared Absorption Spectroscopy, second ed., Holden Day, Oakland, pp. 17-44.

Noyes, R.D. and Hancock, J.G. (1981). Role of oxalic acid in the *Sclerotinia* wilt of sunflower, *Physiol. Plant Pathol.*, 18: 123-132.

Phillips, A.J.L., Alves, A., Pennycook, S.R., Johnston, P.R., Ramaley, A., Akulov, A. and Crous, P.W. (2008). Resolving the phylogenetic and taxonomic status of dark-spored teleomorph genera in the *Botryosphaeriaceae*. *Persoonia* 21 29-55.

Pinon, J. and Manion, P.D. (1991). *Hypoxylon mammatum* and its toxins-recent advances in understanding their relationships with canker disease of poplar. *Eur. J. For. Path.*, 21: 202-209.

Pretsch, E., Bühlmann, P. and Affolter, C., (2000). Structure Determination of Organic Compounds – Tables of Spectral Data. Springer-Verlag, Berlin, pp. 161-243.

Ren , X.G., Huang, J.R., Xiang, J.G., Chen, Z., Wu, W.J., Li, B.W. and Pen, F. (1993). Researches on the control technique of rice bacterial leaf strak. *J. Hunan. Agric. College,* 19: 591-599.

Richards, J.H. and Hendrikson, J.B. (1964). The Biosynthesis of Terpenes, Steroids and Acetogenins, Amsterdam: Benjamin, W.A. Inc., pp. 1-4, 16-26, 35, 151.

Roy, N.K. and Dureja, P. (1998). New ecofriendly pesticides for integrated pest management. *Pesticides World,* 3: 16-21 .

Sakamura, S., Nabeta, K., Yamada, S. and Ichihara, A. (1975). Minor constituents from *Phyllostica* sp. and their correlation with epoxydon (phyllosinol). *Agric. Biol. Chem.,* 39: 403-407.

Scala, F., Evidente, A., Coppola, L., Capasso, R. and Zoina, A. (1996). Identification and phytotoxicity of 3-methylthiopropanoic and *trans*-3-methylthiopropenoic acids produced in culture by *Xanthomonas campestris* pv. *Vitians. J. Phytopathol*., 144: 325-329.

Scott, A.I. (1964). Interpretation of the Ultraviolet Spectra of Natural Compounds. Pergamon Press, Oxford.

Sekido, H. and Akatsuka, T. (1987). Mode of action of orylzalexin D against *Pyricularia oryzae. Agric. Biol. Chem.,* 51: 1967-1971.

Sheldrick, G.M. (2008). A short history of SHELX. *Acta Cryst.*, A64: 112

Shen, G.B. and Zhou, M.G. (2002). Resistance monitorino of *Xanthomonas oryzae* pv. *oryze* to saikuzuo. *Plant Prot.,* 28: 9-11.

Slippers, B. and Wingfield, M.J. (2007). *Botryosphaeriaceae* as endophytes and latent pathogens of woody plants. Diversity, ecology and impact. *Fungal Biol. Rev.* 21: 90-106.

Solel, Z., Madar, Z., Kimchi, M. and Golan, Y. (1987). Diplodia canker of cypress. *Can. J. Plant Pathol.*, 9: 115-118.

Sparapano, L. and Evidente, A. (1995a). Studies on structure-activity relationship of seiridins, phytotoxins produced by three species of Seiridium. *Natural Toxins*, 3: 166-173.

Sparapano, L. and Evidente A. (1995b). Biological activity of cyclopaldic acid, a major toxin of *Seiridium cupressi*, its six derivatives and iso-cyclopaldic acid. *Natural Toxins*, 3: 156-165.

Sparapano, L., Bruno, G., Fierro, O. and Evidente, A. (2004). Studies on structure-activity relationships of sphaeropsidins A-F, phytotoxins produced by *Sphaeropsis sapinea* f. sp. *cupressi*. *Phytochemistry,* 65: 189-198.

Sparapano, L., Evidente, A., Ballio, A., Graniti, A. and Randazzo, G. (1986). New phytotoxic butenolides produced by *Seiridium cardinale*, the pathogen of cypress canker disease. *Experientia*, 42: 627-628.

Stadler, M., Wollweber, H., Muhlbauer, A., Asakawa, Y., Hashimoto, T., Rogers, J.D., Ju Yu-ming, Wetzstein, H.G., and Tichy, H.V. (2001). Molecular chemotaxonomy of Daldinia and other Xylariaceae. *Mycol. Res.*, 105: 1191-1205.

Stanosz, G.R. and Moorman, G.W. (1997). Branch dieback of savin juniper in Pennsylvania caused by *Diplodia mutila*. *Plant Dis.,* 81: 111.

Strobel, G.A. (1982). Phytotoxins. *Ann. Rev. of Biochem.*, 51: 309-333.

Swart, W.J. and Wingfield, M.J. (1991). Biology and control of *Sphaeropsis sapinea* on *Pinus* species in South Africa. *Plant Dis.*, 75: 761-766.

Swart, W.J., Wingfield, M.J. and Grant, W.S. (1993). Comparison of *Sphaeropsis sapinea* and *Sphaeropsis sapinea* f. sp. *cupressi*. *Mycol Res.*, 97: 1253-1260.

Tabacchi, R. (1994). Secondary phytotoxic metabolites from phytopathogenic fungi – structure, synthesis and activity. *Pure Appl. Chem.*, 66: 2299-2302.

Tezuka, T., Miyamoto, R., Mukai, T., Kabuto, C. and Kitahara, Y. (1972). Novel photochemical rearrangement of aryl-6,7-dioxabicyclo[3.2.2]nona-3,8-dien-2-one into tricyclic lactone. *J. A. Chem. Soc.* 94: 9280-9282.

Thomson, R.H. (1985). The Chemistry of Natural Products. Glasgow: Blackie; pp. 107-153.

Tisserat, N.A., Rossman, A.Y. and Nus, A., (1988). A canker disease of rocky mountain juniper caused by *Botryosphaeria stevensii*. *Plant Dis.,* 72: 699–701.

Trinh, C., Gevaert, L., Kohout, L., Van Staden, J. and Verschaeve, L. (2010). Genotoxicity evaluation of two kinds of smoke-water and 3,7-dimethyl-*2H*-furo[2,3-*c*]pyran-2-one. *Appl. Toxicol.* 30: 596-602.

Turner, W.B. and Aldridge, D.C. (1983). Fungal Metabolites II. London: Academic Press, pp. 228-280, 370-383,398-399, 468-484, 505, 530-532, 631.

Tuzi, A., Andolfi, A., Maddau, L., Masi, M. and Evidente, A. (2012). Structure and sterochemical assigment of spheropopsidone, a phytotoxin from *Diplodia cupressi*. *J. of Struct. Chem.*, 53: 786-792.

Upadhyay, R.K. and Mukerji, K.G. (1997). Toxins in Plant Disease Development and Evolving Biotechnology, New Delhi: Oxford & IBH Publishing Co. Pvt. Ltd.; pp. 167.

van Goietsenoven, G., Hutton, J., Becker, J.P., Lallemand, B., Lefranc, F., Pirker, C., Vandenbussche, G., Van Antwerpen, P., Evidente, A., Berger, W., Prevost, M., Pelletier, J., Kiss, R., Kinzy, T.G., Kornienko, A. and Mathieu, V. (2010). Targeting of eEF1A with Amaryllidaceae isocarbostyrils as a strategy to combat melanomas. *FASEB J.*, 24: 4575–4584.

Venkatasubbaiah, P., van Dyke, C.G. and Chilton, W.S. (1991). Phytotoxins produced by *Pestalotiopsis oenotherae*, a pathogen of evening primrose. *Phytochemistry*, 30: 1471-1474.

Vurro, M., Bottalico, A., Capasso, R. and Evidente, A. (1997). Cytochalasins from phytopathogenic *Ascochita* and *Phoma* species. In: Toxins in Plants Disease Development and Evolving Biotechnology (Upahyay R.K. and Mukerji K.G. eds.), New Delhi: Oxford & IBH publishing Co. Pvt. Ltd.; pp. 127-147.

Wagener, W.W. (1939). The canker of *Cupressus* induced by *Coryneum cardinale* n. sp. *J. Agric. Res.*, 58: 1-46**.**

Wang, X-N., Bashyal, B.P., Wijeratne, E.M.K., U'Ren, J.M., Liu, M.X., Gunatilaka, M.K., Arnold, A.E. and Gunatilaka, A.A.L. (2011). Smardaesidins A-G, isopimarane and 20-norisopimarane diterpenoids from *Smardae* sp., a fungal endophyte of the moss *Ceratodon purpureus*. *J. Nat. Prod.,* 74: 2052-2061.

Wang, W.X., Gu, J.T., Xia, J. and Vichia, K.A. (1998). Research on the resistances of *Xanthomonas oryzae* pv. *oryzae* to bactericides under laboratory conditions. *Acta Phytophylactica Sin,* 25: 171-174.

Whalley, A.J.S. and Edwards, R.L. (1995). Secondary metabolites and systematic arrangement within the Xylariaceae. *Can J. Bot.*, 73: 5802-5810

Xenopoulos, S. (1987). A new for Greece pathogen causing the cypress canker disease. *Dasike Eurena*, 2: 85-94.

Xu, Y., Zhu, X-F., Zhou., M-G., Kuang, J., Zhang, Y., Shang, Y. and Wang, J-X. (2010). Status of streptomycin resistance development in *Xanthomonas oryzae* pv. *oryzae* and *Xanthomonas oryzae* pv. *oryzicola* in China and their resistance characters. *J. Phytopathol.,* 158: 601-608.

Xue, Y.H. (2002). Control effect of several biotic pesticides against diseased rice Jiangxi. *Plant Prot,* 25: 68-71.

Zhang, Y.L., Ge, H.M., Li, F., Song, Y.C. and Tan, R.X. (2008). New phytotoxic metabolites from *Pestalotiopsis* HC02, a fungus residing in *Chondracris rosee* gut. *Chem. Biodiver.* 5: 2402-2407.